Provenance changes and glauconite formation in the Broken River to Iron Creek/Waipara Greensand Formations marks the Late Cretaceous – Eocene Transgression

A thesis
Submitted in partial fulfilment
of the requirement for the degree
of
Master of Science in Geology
In the
University of Canterbury
By
David Kapoutsos

UNIVERSITY OF CANTERBURY
Te Whare Wānanga o Waitaha
CHRISTCHURCH NEW ZEALAND

University of Canterbury
2005

Geological Sciences
University of Canterbury NZ

ABSTRACT

Detailed provenance analysis and glauconite morphology of the Broken River and Iron Creek/Waipara Formations and other correlatives were conducted at 6 localities: the Mandamus-Dove River area, Waipara River, Avoca-Iron Creek, Castle Hill Basin, Malvern and Mt Somers. The basal Broken River Formation is a fluvial boulder conglomerate interbedded with sandstones, mudstones and coal dated as Haumurian (Late Cretaceous) by pollen. The transgression is marked by a gradual drowning of the fluvial conglomerates with minor glauconite appearing in the beds immediately overlying the conglomerates in all localities. The estuarine-marginal marine / lower shoreface succession of the Broken River Formation contains minor nascent micaceous glauconite. This increases in the overlying Iron Creek / Waipara Formations to 30-60% glauconite composed of nascent-micaceous to evolved/mature glauconity types characteristic of lower shoreface / foreshore to shallow shelf depositional setting. Up section, evolved mature glaucony dominates, in some beds formed in situ (autochthonous) and in other beds transported from nearby (parautochthonous) to line foresets. An extremely low sedimentation rate is necessary to form the evolved / mature type of glauconite. The age of the greensands is Teurian to Whaingaroan (Late Paleocene-Late Eocene). Overall the glauconite analysis indicates extremely low sedimentation rates with autochthonous / parautochthonous glaucony formation in nearshore marine settings, possibly even estuary environments.

Clast counts from the basal conglomerates indicate derivation from local sources such as the underlying Torlesse greywackes (Pahau and Rakaia Terranes) and/or the Mandamus Igneous Complex. Sandstone composition indicates the addition of more distal sources. Quartzose sandstones plot in the interior craton province in QFL plots for both Broken River and Iron Creek/Waipara Greensand Formations. Sandstone lithics are probably derived from the underlying Torlesse greywacke. Alkali feldspar dominates over plagioclase indicating a probable plutonic felsic source. SEM-cathodoluminescence on quartz grains indicates a bimodal metamorphic to plutonic quartz grains with minor volcanic input. Plutonic grains are identified by healed microcracks, and are possibly derived from Western Province plutonic suites such as the Karamea and Separation Point Batholiths. Polycrystalline/dark CL quartz grains indicate a relatively high grade metamorphic source such as the Otago/Haast Schist while dark CL monocrystalline quartz grains indicate a low to medium metamorphic grade source such as the Alpine Schist. Volcanic quartz is zoned with straight extinction and was most likely derived from the Cretaceous Mount Somers Volcanics Group.

Overall the provenance suggests local derivation of sediments when coarse fluvial deposition occurred followed by more distal derivation once transported in the nearshore marine setting.

TABLE OF CONTENTS

LIST OF FIGURES

Chapter Four.

LIST OF APPENDICES

CHAPTER ONE
INTRODUCTION

The formation of sedimentary basins are controlled by the interaction of multiple factors, such as the size of source areas providing the detritus, the accommodation space necessary to host the detritus, the role of subsidence which in turn is related to tectonic influences, sea level rises, tectonic or eustatic and the process of uplift and exhumation in relation to erosion and transport of sediments or merely the process of runoff and erosion. Source rock composition, climate, relief, slope, vegetation and characteristics of the depositional environment all play important roles in controlling the composition of fluvial sands (Blatt 1967). Furthermore provenance analysis of siliciclastic sediment and rock provides valuable information on the evolution of the sediment sources and the development of sedimentary basins necessary to reconstruct depositional environments and tectonic settings. Other factors such as sedimentation rates are important in tracing the evolution of basins. The analysis of the Broken River Formation, the Iron Creek Formation and their regional correlatives in this thesis will indicate if similar trends occur at each location in depositional environments, sedimentation rates and provenance with or without minor local variations.

The aim of this research is to carry out provenance analysis of the Broken River - Iron Creek Formations and their correlative members and formations, of the Canterbury region in South Island as well as studying glauconite morphology from the Iron Creek Formation in terms of providing sedimentation rates and revising depositional settings. The Broken River Formation, part of the Eyre Group, generally records the onset of a marine transgression (Field & Browne, 1989) from terrestrial to marginal marine settings. The formation consists of terrestrial coal measures, which locally include subaerial pebbly sediment gravity flow deposits, fluvial deposits followed by several units of fluviodeltaic and estuary deposits. The Late Paleocene - Early Eocene to Late Eocene glauconitic quartz sandstones and glaucarenites of the Iron Creek Formation/Waipara Greensand were deposited under shallow marine conditions and are also considered part of the larger Eyre Group by Brown and Field (1985).

1.1 Research Questions

In terms of analysing the Broken River –Iron Creek Formations and locally correlative units, several questions need to be answered. The first aspect of looking at the formations is what the composition, sedimentology and glauconite morphology can tell us about rich glauconitic successions in terms of depositional setting and sedimentation. Can the glauconite morphology identify sediment reworking and tell something about sedimentation rate? In addition what significant refinements can be made to the interpretation of depositional environment based on glauconite morphology? Glaucony can be used as an indicator of low sedimentation rate in glauconite rich successions. Maturity of glaucony mostly reflects the time of residence of the green grains at the sea bottom before burial (Odin & Matter 1981); as a consequence, glauconies at various stages of evolution are generally related to breaks of sedimentation of different importance (Amorosi 1997).

What is the provenance of conglomerates within the formations, in addition the depositional setting? In assessing quartz rich sandstones of the formations what is the likely provenance? A detailed provenance analysis using various techniques will reveal changes in sediment source areas through time, leading to a better understanding of changes in the paleoenvironment and tectonic setting. Thus a major question that needs to be explored is whether the sediment source is local or regional? In a preliminary study (Bernet & Bassett, 2005) the Broken River Formation quartz arenites have a bi-modal grain size distribution of well rounded coarse sand to granule sized quartz grains and fine sand grains at Mandamus, North Canterbury. The coarse fraction, which is well rounded, consists of a mixture of poly- and monocrystalline quartz (Bernet and Bassett, 2005). There is a striking relation between grain size and certain quartz types in preliminary study, with plutonic quartz grains dominating the medium to fine fraction and metamorphic/recrystallized quartz dominating the very coarse to coarse fraction based on the SEM-CL/optical microscopy provenance technique (Bernet & Bassett, 2005). This study proposes to apply the same technique to an expanded area of research to include the entire geographic extent of the Broken River Formation and Iron Creek Formation/Waipara Greensand. Given preliminary studies in exploring the entirety of the formation, is there a difference between grain size, rounding and quartz types at local and regional level? When, where and how were the rounded grains formed?

Traditionally provenance analysis for siliciclastic or quartzose sandstones was confined to standard QFL techniques such as analysis of quartz, feldspar and lithic components as devised by McBride (1963), Dickinson (1983) and other authors. The advent of provenance analysis on quartz devised by Seyedolali et al (1997) and Kwon and Boggs (2002) provided greater constraints on provenance of quartz and quartzose rich sandstones than previously known. In recent research, Bernet and Bassett (2005) embellished the possibilities of quartz provenance by devising the direct grain to grain comparison of cathodoluminescence of quartz and petrographic analysis using the combined scanning electron microscope – cathodoluminescence (SEM-CL) and optical microscopy on quartz, hence the SEM-CL/optical microscopy provenance technique. Through this technique, information was retrieved allowing the distinction of several quartz types much more easily than with conventional microscopy or colour CL analysis (Bernet & Bassett 2005). Features obtained by both techniques on the same grain were able to distinguish between plutonic, volcanic, and metamorphic quartz in coarse to medium grained sand or sandstone (Bernet & Bassett 2005). Therefore a strong connection could be made between the sedimentary rocks and their source area as well as the evolution of source over a period of time.

A major component of this research will be the use of standard petrographic and combined SEM-CL/optical microscopy provenance of quartz on the sandstones.

1.2 Source Areas

The relationship between source and sink is important, therefore the source areas are analysed in relationship to the tectonic setting. The mid Cretaceous period immediately post-dates the last compressional movements of the Rangitata 2 orogeny and includes the extensional tectonic events that occurred prior to the rifting of New Zealand from Antarctica (Field and Brown 1989). Early Cretaceous peneplanation was interrupted by late Early Cretaceous graben and half graben formation and the development of distinct basins and highs over most of the area. This episode was followed by calc alkaline volcanism in the mid-Late Cretaceous (Field & Brown 1989). During the Late Cretaceous rifting was concentrated on mid-ocean ridges in the Tasman and Southern Seas and New Zealand became a stable platform during the Paleocene and Eocene (Field & Brown 1989).

The basement of the New Zealand continent consists of terranes that formed adjacent to the Gondwana margin. The geological units now make up a series of discrete fault-bounded terranes which, prior to the development of the Alpine fault in the mid-Cenozoic, formed north to northwest trending curvilinear belts (Bradshaw 1989). The terranes of New Zealand are divided into two major groups, the Western and the Eastern Provinces (fig. 1.1). The former comprises mainly Early Paleozoic and Late Mesozoic granitoids, and the latter comprises volcanic arc, forearc and accretionary rocks of the younger Permian to Cretaceous convergent margin (Bradshaw 1989). The Eastern Province consists of an assemblage of accreted allochthonous terranes such as the Rakaia, Pahau, Haast, Esk Head Melange, Caples Terrane, Matai, Murihiku and Brook Street Terranes making up almost all of Northern Island and the eastern part of the South Island (Wandres & Bradshaw 2005).

The Torlesse Superterrane (Wandres et al. 2004a) consists of three belts, the Rakaia and Pahau Terranes and the Esk Head Melange (Bradshaw 1989). The Permian to Late Triassic Rakaia Terrane is an accretionary complex that comprises an enormous volume of very fine quartzofeldspathic sandstones alternating with argillite and mudstones with subsidiary conglomerates plus minor oceanic assemblages (Campbell & Warren 1965, Wandres et al. 2004a).

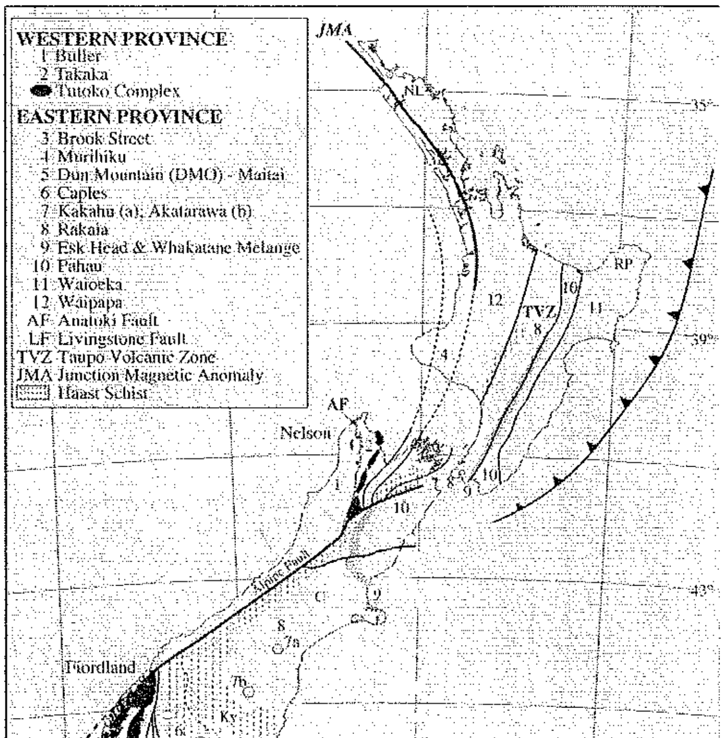

Figure 1.1: Simplified tectonostratigraphic terrane map of New Zealand (from Wandres & Bradshaw 2005).

The Rakaia Terrane forms most of the eastern province from North Otago to North Canterbury. The Pahau Terrane is Late Jurassic to Early Cretaceous and it is composed of recycled older Rakaia Terrane material based on petrography and geochemistry (Wandres 2004b). The Pahau Terrane forms the north eastern province from North Canterbury to Marlborough (fig. 1.1). The thin band of the Esk Head Melange (Bradshaw 1973) contains Late Triassic and Early Jurassic sediments that were scraped from oceanic crust (Silbering et al. 1988 in Field). The rocks of the Esk Head Melange are strongly deformed and are fine grained.

The Haast Schist consists of metamorphosed mainly biotite zone, greenschist facies overprinting alternating sandstone and mudstone beds (Field & Brown 1989). To the north it grades into the quartz feldspathic Torlesse Superterrane (Bradshaw 1989). Shelley (1975) produced a metamorphic map of the South Island with the Haast Schist described as a higher metamorphic grade, a greenschist biotite zone while a strand paralleling the present day Alpine fault was described as a greenschist chlorite zone. Near the Alpine fault the Haast Schist is referred to informally as Alpine Schist (Grindley 1963). In addition Wandres and Bradshaw (2005) mentioned the Haast Schist including the Otago, Marlborough Schist and Alpine providing a metamorphic overprint for the Caples terrane. The Haast Schist a Late Triassic –Early Jurassic age for Schist metamorphism, with younger ages (to 115 Ma) represents either long continued exhumation or a second stage of metamorphism (Adams & Graham 1997). Initial metamorphism and deformation of the Otago/Haast Schist has been attributed to the amalgamation of the Caples and the Rakaia terranes, while the present broad arc of schistose rocks has been explained as a core complex exhumed from beneath low angle ductile shear zones (Forster & Lister 2003).

The Permian Brook Street terrane of the Eastern Province is composed of basic/intermediate arc volcanic related sediments (Bradshaw 1989). The Murihiku and Caples terranes are Triassic – Jurassic and Permo-Triassic respectively, they are in turn composed of volcaniclastic arenites, mudstones, tuffs and metavolcanics, chert and volcaniclastic sandstone, and mudstones (Bradshaw 1989).

The Western Province is composed of two terranes, the Buller and the Takaka terranes and various intrusive complexes of different ages. The Takaka terrane of the Western Province is Cambrian-Devonian and is composed of volcano-clastics and limestone; the Bullet Terrane is Cambro-Ordivician, composed of Greenland Group quartzite and quartz rich turgidities with black shales (Coombs et al. 1976). The intrusives are the older Karamea Suite – Paleozoic granites which form a present day north - south trending belt and the Cretaceous granites including the Rahu, Separation Point Suite of the Tukoko Complex (Wandres & Bradshaw 2005) and the Hohonu Batholith (Muir et al 1997).

The Tukoko Complex comprises of the Separation Point Batholith and Darran Suite intrusives (Wandres & Bradshaw 2005) and is considered as a magmatic belt which formed adjacent to the edge of the Western Province (Wandres & Bradshaw 2005). Source rock areas of the Western and Eastern Provinces evolved and were juxtaposed during the Cretaceous. The Cretaceous tectonic evolution of the New Zealand region involves convergence and arc magmatism, collision and crustal thickening, while the Tukoko Complex (Separation Point Batholith) suggests docking of Western and Eastern Provinces and transcurrent faulting of those provinces which preceded separation from the Gondwana margin (Kimbrough et al. 1993, Bradshaw 1989).

The Karamea Batholith in the Buller Terrane of the South Island forms part of an extensive Mid – Late Devonian belt of magmatic activity, along or close to the Paleo – Pacific margin of Gondwana (Muir et al 1996). The rocks forming the Karamea Batholith are a high – K calcalkaline suite ranging from metaluminous to peraluminous. The northern two thirds of the batholith and smaller bodies to the south are coarsely crystalline, porphyritic biotite granite (syenogranite-monzogranite), termed the Karamea granite, containing large, pink, prismatic alkali feldspar megacrysts (30-40mm in length) in a groundmass of quartz, oligoclase, microcline, biotite and muscovite with accessory apatite, zircon and iron oxide (Muir et al. 1996). Granitic rocks and related diorites make up approximately 50% of the total area of the Western Province (Muir et al. 1996).

The Early Cretaceous Separation Point Batholith (118 Ma) of the South Island represents the final magmatic stage of an extensive arc system located on the SW Pacific margin of Gondwana during the Mesozoic, and it consists of Na-rich, alkali-calcic diorite to biotite – hornblende monzogranite (Muir et al 1996). The batholith is composed of elongate segments with a total length of 120 km and with a width of 10 km. In addition, it comprises mainly quartz (15-20%), plagioclase (30-35%), orthoclase (30-35%), microcline (5-10%), biotite (5-10%) and hornblende (2-3%) (Muir et al. 1995). The Early Cretaceous Western Fiordland Orthogneiss matches compositionally and isotopically the Separation Point Batholith, and is regarded as its lower crustal equivalent. The orthogneiss has been exhumed as a metamorphic core by late Mesozoic crustal extension and Cenozoic movements on the Alpine Fault (Muir et al. 1996).

The Mount Somers Volcanics consists of Cretaceous calc-alkaline volcanic rocks which range through a continuum from high-alumina basalt to rhyolite (Tappenden 2003). The Mount Somers Rhyolite covers a large area including Mount Somers peak comprising a sequence of coalesced domes and is composed of quartz bipyramids and subhedral sanidine phenocrysts (Oliver & Keene 1989). In addition the Alford Rhyolite is a black basal pitchstone with bipyramidal quartz and sanidine phenocrysts in a devitrified glass groundmass (Oliver & Keene 1989). Van der Lingen (1988) described the presence of quartz crystals in pyroclastic flows and in clay horizons. The Mandamus Igneous Complex is largely composed of syenite, trachyte, microsyenite, trachybasalt, alkali microgabro and syenodiorites (Tappenden 2003; Sevon 1969). Coarse graben-fill deposits were accompanied by alkaline and calc alkaline volcanism at the Mandamus River, in central Canterbury and in the southeast of the region (Bradshaw 1989, Field & Brown 1989). The Late Cretaceous Volcanics forming a north –east south-west trending linear belt were erupted during the Late Cretaceous (95-85 Ma) as a response to the thinning crust and ridge collision according to Bradshaw (1989).

1.3 Study Area

The Canterbury Basin is largely a passive continental margin basin resting on basement rocks of Triassic (Rakaia – Pahau Terranes) to Cretaceous age (Mount Somers Volcanic Group) and includes the basal Monro Conglomerate - Broken River Formations (Late Cretaceous – Paleocene) including the Stour Coal Measures - Blondin Sand Members, and the correlative Iron Creek Formation, Conway Formation, Loburn Mudstone, Waipara Greensand, Homebush Sandstone (Late Paleocene –Late Eocene). The sequence is largely transgressive culminating in the main glaucarenite phase during the Late Paleocene – Eocene. The areas studied in this research include in North Canterbury the Mandamus area in the NE, the Waipara River area in the east, the Castle Hill Basin and Avoca-Iron Creek in the west and the Malvern and Mount Somers areas in the south (fig. 1.2). Each locality largely consists of basal conglomerates, coal measures and carbonaceous quartz rich sandstones followed by glauconitic sandstones and mudstones. However, the nomenclature includes a myriad of local formation names which reflect largely the transgressive sequence from basal coal measures to glauconitic sandstones.

1.4 Stratigraphy

Despite a relatively simple transgressive stratigraphy of basal conglomerates, and quartzose coal measures to glauconitic quartz arenites, there are multiple formation names reflecting subtle differences between localities. The plethora of formation names given by different authors to mark the local characteristics thus masks the correlation of regional geology. Brown and Field (1985) and Andrews et al (1987) correlated the different formations in the regional sense. However, in this research it is important to correlate the different localities studied herein with respect to their sedimentary structures and composition. The various formations are the basal Monro Conglomerate, the Broken River Formation and the Stour Coal Measures corresponding to the quartzose coal measure sequence and the Blondin Sand Member-Charteris Bay Sandstone- Iron Creek Greensand Members of the Iron Creek Formation and the Waipara Greensand for the glauconitic and glaucarenite sandstones as well as the Homebush Sandstone Formation. Overall water deepens to the east and north with more proximal subaerial deposits to the west and south.

1.4.1 Coal Measures

The rocks of the Monro Conglomerate and Broken River Formation consist largely of basal conglomerates, coal and carbonaceous sandstones – siltstones and are easily correlated over the Canterbury region. The Monro Conglomerate is the oldest formation overlying unconformably Torlesse Supergroup rocks. The Monro Conglomerate is a brown to light grey, conglomerate interbedded with pebbly sandstones and rests unconformably on the Mt. Misery Volcanics of the Mt. Somers Volcanics Group and Torlesse Supergroup sediments in the Malvern area (fig. 1.3). The conglomerate contains rhyolite clasts derived from the underlying Mt Somers Volcanics Group, mudstones, carbonaceous sandstones and thin lenses of dirty coal (Mathews 1989). The sequence is Piripauan (Mid-Late Cretaceous) and it grades into the overlying Broken River Formation.

The Broken River Formation is a transgressive sequence of Upper Cretaceous to Lower Tertiary sedimentary rocks deposited unconformably on Mesozoic basement. In most areas, the Broken River Formation rests on Torlesse Supergroup rocks while in some areas it rests on mid-Cretaceous calcalkaline volcanics (Mt Somers Volcanics and Mandamus Igneous Complex). The Formation is interpreted as non-marine to marginal marine at the base, becoming fully marine towards the top (Browne & Field, 1985). Haumurian ages are indicated by micro and macrofossil evidence for the great majority of the formation (Browne & Field, 1985). The formation outcrops in various areas from North to South Canterbury in isolated exposures due to erosion or coverage from younger deposits. The formation consists of terrestrial coal measures, which locally include subaerial volcanic-pebbly gravity flow deposits (Van Der Lingen, 1988; Sevon, 1969), fluvial deposits followed by several units of marginal marine quartz rich sandstones with minor glauconite and siltstones from shoreface to estuarine deposits. The Broken River Formation is easily correlated over the Canterbury region between Mandamus, Waipara River, Castle Hill Basin – Avoca/Iron Creek, Malvern and Mount Somers (fig. 1.3).

At Mount Somers the Broken River Formation includes the Stour Coal Measures Member and the Blondin Sand Member (Oliver and Keene 1989). The Stour Coal Measures consist of kaolin clay and coal measures, with coal of low grade lignite to sub-bituminous rank grading up into silica sand with thin carbonaceous clay beds. The age of the coal measures are Haumurian to Teurian based on pollen assemblages (Oliver & Keene 1989).The Stour Coal Measures Member is most likely correlative to the Broken River Formation from the other areas (fig 1.3). The overlying Blondin Sand Member is most likely part of a different formation and correlative to other formations as described below.

1.4.2 Greensands

The overlying glauconitic sandstones have different formation names by area as studied in this research. The Conway Formation overlies the Broken River Formation and is Teurian (Paleocene) in age at Waipara River and Malvern. It consists of light grey to dark grey, silty fine sandstone and is jarositic with large spherical concretions and glauconite increasing up section. It grades into the overlying Loburn Mudstone at Waipara River (Brown & Field 1985) which is comprised of dark grey, brown-purple, soft to moderately indurated, calcareous, jarositic burrowed sandy mudstone that is slightly glauconitic (Brown & Field 1985). Microfossil evidence indicates the formation is Teurian (Webb 1971). The Waipara Greensand Formation's type area occurs at the Waipara River area and consists of alternating, centimetre to decimetre bedded, slightly jarositic, richly glauconitic (>50% of the rock), moderately sorted, medium to fine, quartzose sandstone (Brown & Field 1985). The Waipara Greensand

Formation has a Teurian to Waipawan (Paleocene to Early Eocene) age (Brown & Field 1989).

The Iron Creek Formation was defined initially by Gage (1970) as Iron Creek Greensand for glauconitic sandy sediments overlying the Broken River Formation in the Iron Creek/Castle Hill area. McLennan (1981) and McLennan and Bradshaw (1984) separated the Iron Creek Greensand into two members, the lower Avoca Sand Member and the upper Greensand Member. McLennan (1981) recognised that the upper part of Gage's Iron Creek Greensand was distinctly more glauconitic (>50%) than the lower part (5-30% with an average of 10-15%) and for this reason subdivided the formation into two members. Browne and Field (1985) adopted the classification for its regional stratigraphic and sedimentologic similarities to Charteris Bay Sandstone. Browne and Field (1985) modified the informal stratigraphy of McLennan and Bradshaw (1984) and the Iron Creek Formation was split into the lower Charteris Bay Sandstone Member and the upper Iron Creek Greensand Member.

The Iron Creek Formation at Castle Hill and Avoca-Iron Creek consists of the lower Charteris Bay Sandstone which is a light grey to light yellow, friable to poorly indurated, massive, and glauconitic (15-30%), well sorted, cross bedded, medium to fine, silica-cemented sandstone (Brown & Field 1989). The age is poorly constrained, however Browne and Field (1985) place the upper 10 meters as early Teurian (microflora) and the base is Haumurian (macrofauna). The moderate to well sorted nature of the sediment, the presence at Castle Hill Basin of ophiomorpha, and cross stratification and at Avoca of trough cross stratification, suggest a shallow marine, high energy environment (Browne & Field, 1985). The bimodal current directions described by McLennan (1981) correspond to a near shore, marginal marine setting influenced by tidal currents. The Blondin Sand Member of the Broken River Formation at Mount Somers is described as friable sandstone with nearly pure quartz with local iron stained horizons and minor glauconite (Oliver & Keene 1989). The sand is cross bedded on a centimetre to metre scale with quartzite pebbles indicating reworking in a shallow marine environment, while the age of the unit is Waipawan to Bortonian (Late Paleocene- Mid Eocene).The Blondin Sand Member is most likely correlative to the Charteris Bay Sandstone.

The Iron Creek Greensand Member was defined by Browne and Field (1985) to include only the highly glauconitic upper part of Gage's (1970) formation with glauconite comprising over 50% of the lithology. The Member consists of dark green-grey green to olive-green, moderately to poorly indurated, bioturbated, muddy, very fine to fine, glauconite sandstone. Gage (1970) infers an Eocene age based on Whaingaroan foraminifera at the top. The greensand is shallow marine deposited under a slow sedimentation rate.

The Homebush Sandstone Formation at Mount Somers is described as a yellow glauconitic (>50% glauconite) sand with quartz pebbles and glauconitic beds of quartz sand while its Bortonian to Whaingaroan (Mid Eocene – Early Oligocene) age is based solely on stratigraphic relationships (Oliver & Keene 1989, Brown & Field 1985).

1.4.3 Correlations

Overall the Monro Conglomerate and the Broken River Formation is correlative through out all the locations with basal conglomerates carbonaceous sands and coal measures and it is correlative to the Stour Coal Measures Member at Mount Somers (fig. 1.3). In turn the overlying glauconitic sandstones of the Charteris Bay Sandstone are correlative with the Conway Formation/Loburn Mudstone Formation at Waipara River and Malvern, also correlative with the Blondin Sand Member at Mount Somers, while the glaucarenites of the Iron Creek Greensand and Waipara Greensand are correlative.

The Blondin Sand Member of the Broken River Formation is most likely correlative to the Charteris Bay Sandstone Member in the north since it is dated at Waipawan to Bortonian (Early Eocene-Late Eocene) (Oliver & Keene 1989). In addition, the unit is cross stratified with mud drapes and *Ophiomorpha nodosa* trace fossils similar to the cross stratified Charteris Bay Sandstone Member of the Iron Creek Formation at Castle Hill (fig. 1.3). The Charteris Bay Sandstone at Castle Hill Basin and Avoca-Iron Creek is most likely correlative with the Conway Formation and Loburn Mudstone in the east at Waipara River and Malvern according to Brown and Field (1985) (fig. 1.3).

Up section the Iron Creek Greensand at Castle Hill Basin – Avoca/Iron Creek locations is most likely correlative to the Waipara Greensand Formation at Waipara River since Gage (1970) refers to the Iron Creek Greensand as the inland equivalent of the Waipara Greensand. The Homebush Sandstone is difficult to correlate with other formations; however it is much younger than the Charteris Bay Sandstone Member of the Iron Creek Formation and the Blondin Sand Member. It is possible the

Homebush Sandstone is diachronous and correlative laterally with the Charteris Bay Sandstone or with the upper Iron Creek Greensand, unless it is not correlative at all.

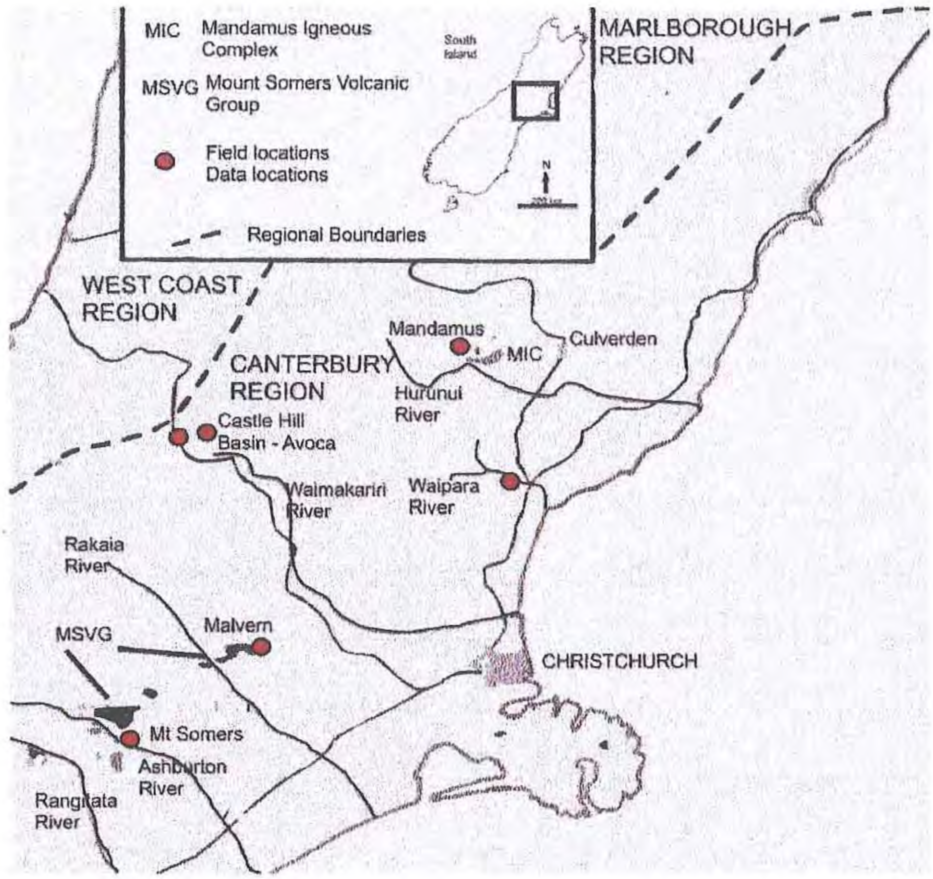

Figure 1.2: Field locations of data collections for the Broken River and Iron Creek Formations in the Canterbury region.

1.5 Methods

The questions posed in the beginning will be addressed in this thesis. At first a regional correlation of all localities will be attempted based on the sedimentology-sedimentary structures and composition of the Broken River and Iron Creek Formations. In addition glauconite content and type will be used in assisting the correlation of units between geographic locations. Paleoenvironment depositional settings will be established based on stratigraphy, sedimentary structures, and composition. A significant element of this research is the estimation of sedimentation rates using glauconite morphology-maturity. SEM-CL/optical microscopy provenance technique will form the major core of this study based on the quartz rich sandstones,

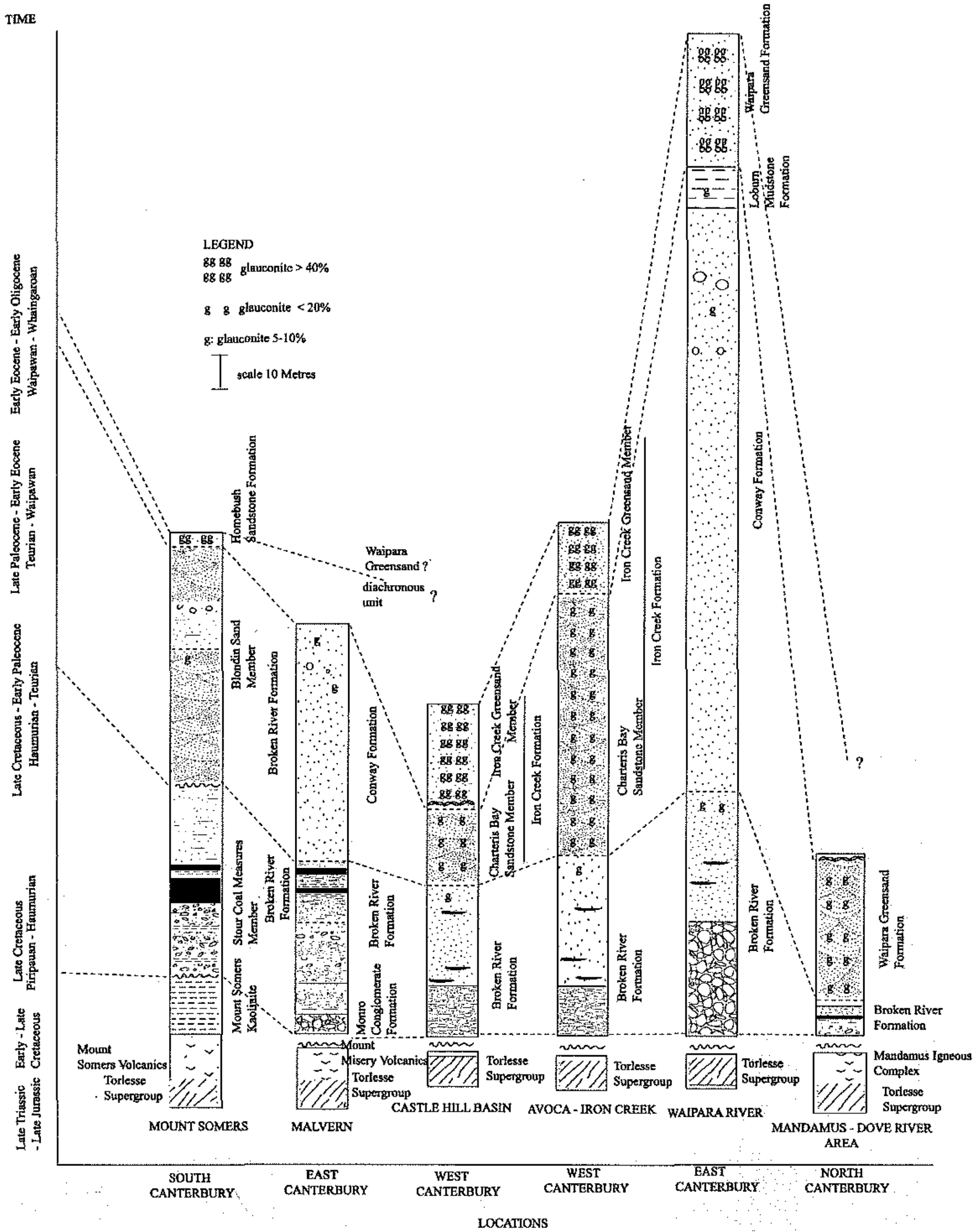

Figure 1.3: : Stratigraphic successions between formations and members of the Monro Conglomerate, Broken River Formation – Stour Coal Measures, Iron Creek Formation – Conway Formation – Blondin Sand Member, Loburn Mudstone, Waipara Greensand and Homebush Sandstone at localities studied in this research. Diagonal lines correlate the ages to the formations (Modified from Brown and Field (1989) including results from this research).

combined with conventional arenite provenance point counting techniques and conglomerate clast counts. Furthermore the object is to identify the different types of quartz and identify likely sources. The quartz source types will be used to identify local versus regional provenance. Based on the morphology of grains it may be possible to identify if sediment recycling has occurred and identify the number of sources. Finally the object is to integrate all the data into the regional geologic setting describing the transgression during the Late Cretaceous to Late Eocene.

1.6 Thesis Structure

The second chapter describes the methods used in this research and the reasoning behind the techniques used, as well as the analytical methodology of those techniques. The thesis is then divided into chapters where data have been collected from each region. Chapters 3 to 8 include the Mandamus, Waipara River, Castle Hill Basin, Avoca-Iron Creek, Malvern and Mount Somers locations. The locations divided into chapters include previous work and stratigraphy, revisions to the stratigraphy and depositional environment from this research as well as data and interpretations from glauconite morphology-maturity and provenance. The final chapter 9 presents the regional interpretation and includes the assimilation of all data into a regional paleoenvironment and tectonic setting based on depositional environments, sedimentation rates and provenance data.

CHAPTER TWO
METHODS

2.1 Introduction

The main aim of this thesis is to establish a local and regional depositional environment for the Broken River Formation and Iron Creek formations with particular emphasis on provenance, sedimentation indicators and paleoenvironment-tectonic setting. In order to establish a provenance for the formations in question, the methods employed were those that could be applied to the analysis of quartz rich sedimentary rocks.

The formations in this study required stratigraphic logging and sampling as an aid to place the provenance in its stratigraphic context. Since the dominant succesion of the formations was composed of quartz rich sandstones (subarkose-arenittes) a viable method was essential. Standard microscopy and QFL analysis techniques on sandstone composition were employed. However, the integrated SEM-CL/Optical microscopy technique on quartz was employed as the primary tool in this research. Since glauconite mineral was a main component of the sandstones within the Iron Creek Formation an additional method employed was petrographic analysis of glauconite grains and correlation with sedimentological data as a tool in deciphering sedimentation rate indicators.

All these techniques with emphasis on SEM-CL/optical microscopy of quartz were employed with the objective of detecting variations in sediment character by exploring multiple facets. The ultimate motive for the selection of these methods is the linkage of quartz types and formations to specific source areas.

2.2 Measured Sections

Initial fieldwork involved logging stratigraphic sections of the Broken River and Iron Creek Formations and other correlative formations. Stratigraphic sections were logged from locations where the Broken River Formation overlies the Torlesse Supergroup basement grading into the overlying Iron Creek Formation or where the Iron Creek Formation is overlain by the Porter Group rocks. Data was collected such as bedding thickness, structure, texture, and composition; the nature of sedimentary contacts; and clast counts of conglomerates. Stratigraphic sections were measured from a minimum of 10-20cm intervals up to metre intervals at most locations. Where complete measured sections were not feasible due to incomplete exposure, detailed descriptions of each sample were substituted.

2.3 Paleocurrents

Paleocurrent measurements were taken to establish sediment transport directions in these formations, paleocurrents were taken mostly from low angle and parallel crossbeds and minor heringbone crossbeds. Azimuth compass directions and dip angle of crossbeds as well as bedding were recorded in the field and consequently bedding was restored to horizontal using a stereographic projection to provide with the original azimuth paleocurrent directions. Subsequently this data was drafted on commercial drafting programs such as Adobe Illustrator and Grapher version 5.

2.4 Conglomerate Clast Counts

Data were also obtained concerning structure texture and composition of conglomerates with emphasis on interpreting depositional environment and provenance. 100 clasts were counted on the conglomerates with a grid spacing of 10 cm apart to estimate average composition and provenance. Composition and texture of individual clasts were recorded as well as the structure texture and composition of matrix. Conglomerates containing an assortment of single clasts types were labelled as monomictic while conglomerates containing an assortment of many kinds of clasts were labelled as polymictic conglomerates based on Boggs (1995) terminology. Conglomerates that are rich in clasts that touch and form a supporting framework are called clast-supported conglomerates (Boggs 1995). Conglomerates that consist of sparse clasts in mud/sand matrix were labelled matrix-supported conglomerates based on Boggs (1995) terminology.

2.5 Sandstone Composition Analysis

2.5.1 Thin Section Description Data acquisition

Samples required for petrographic thin sections were collected from widespread geographic and stratigraphic locations. Sandstone samples were prepared for thin sections and subsequently polished for SEM-CL analysis. Sandstone samples ranged in grain size from fine sand (< 250 microns), medium grain size (< 500 microns) to coarse sand (<1000 microns) based on the Udden-Wentworth scale (Lewis & McConchie 1994). Occasional samples were very coarse grained and some minor samples were very fine to fine grained (<250 – 125 microns). Most of the samples collected for compositional point counts, optical petrography and cathodoluminescence were medium to coarse sand sized.

Thin sections were described for all minerals and fossil components. All these components were part of the 300 grain point count framework. Calcite was described into their respective components such as: fine micritic-matrix, sparry calcite-cement and individual calcite crystals. Micas and the variety of muscovite were described and counted as well as glauconite grains. Quartz feldspars and lithics were described and subsequently counted.

2.5.2 QFL Point Counts

Samples were point counted with 300 grains for each thin section independent of the grains used in the optical/SEM-CL analysis. The quartz, feldspars and lithics were recalculated to 100 percent to provide a QFL composition and provenance, following the technique of Mcbride (1963). A Nikon Optiphot2-Pol polarizing microscope equipped with an automatic James Swift Prior Model "F" point counter was used for point counting.

Feldspars were first described as plagioclase or alkali feldspar by obtaining optical axis interference figures for each crystal and then including them as the total feldspar component for QFL. Alkali feldspar was identified based on its optical axis described for its different varieties where possible. Orthoclase was identified by its optical axis interference figure noted as being biaxial negative with a large 2V angle. Orthoclase and microcline appear to be by far the most abundant potassium feldspars in sandstones (Boggs 1992). Plagioclase was distinguished through optical interference figures; however the distinction between albite and unzoned plagioclase was done clearly on the presence or absence of twinning.

Lithics described and point counted were sedimentary lithics, chert lithics, volcanic lithics and plutonic lithics and subsequently totalled for QFL composition based on Dickinson et al (1983). Igneous lithics were distinguished into volcanic and plutonic based on the presence of aphanitic texture and in the latter case based on presence of felspars and quartz crystal framework within the lithoclast as described by Dickinson et al (1983). For QFL classification all lithics were grouped together while the variations in lithics were listed in the appendices. Polycrystalline quartz was distinguished from monocrystalline quartz as a grain containing 2-3 or more crystal units based on the technique of Basu et al (1975). The polycrystalline quartz grains were listed separately in the point counts from monocrystalline quartz and then included as one in the total QFL classification. Subsequently this data was entered into tables. Quartz, feldspar and lithics were recalculated to 100 percent for each thin section ignoring the other components, entered in separate tables, and drafted into QFL ternary plots.

2.6 Glauconite Analysis

2.6.1 Background

Glauconite can be used as a paleoenvironmental indicator and as a sedimentation indicator when present in basins. Glauconitic minerals are relatively common authigenic constituents of marine sediments, and are good indicators of low sedimentation rate (Pasquini et al. 2004).

In the broad mineralogical sense, glauconite is a hydrated Fe and K-rich clay, fundamentally of the illite type (Pasquini et al. 2004). The original host grain replaced by the glauconitic mineral may have been composed of clay minerals, calcite, mica, quartz, feldspar, heavy minerals (Odin & Fullagar 1988).

The most abundant form is the glauconitic mineral fecal pellet. It has been amply documented that filter feeding organisms in the shallow – water marine realm remove vast quantities of clay and silt-sized material from the water column and produce pelletized clay aggregates (Chafetz & Reid 2000).

Glauconite to form requires low sedimentation rate hence no significant input of detritus which would inhibit growth. According to Odin and Fullagar (1988) the prerequisites influencing the habit of glaucony is a suitable substrate, the presence, origin and size of the pores in which forms the authigenic phase characterizing the facies, the size of the substrate and the stage of evolution of the glauconized material.

Evolution begins and proceeds close to the water sediment interface and the mechanism proceeds more efficiently where the sediment is in granular form (Odin & Fullagar 1988). Glauconite in the common granular form occurs in different morphologies depicting its early stage and its later evolved stage. Odin and Fullager (1988), describe an earlier nascent stage – morphology through a slightly evolved, evolved and a highly evolved stage (Fig. 2.1).

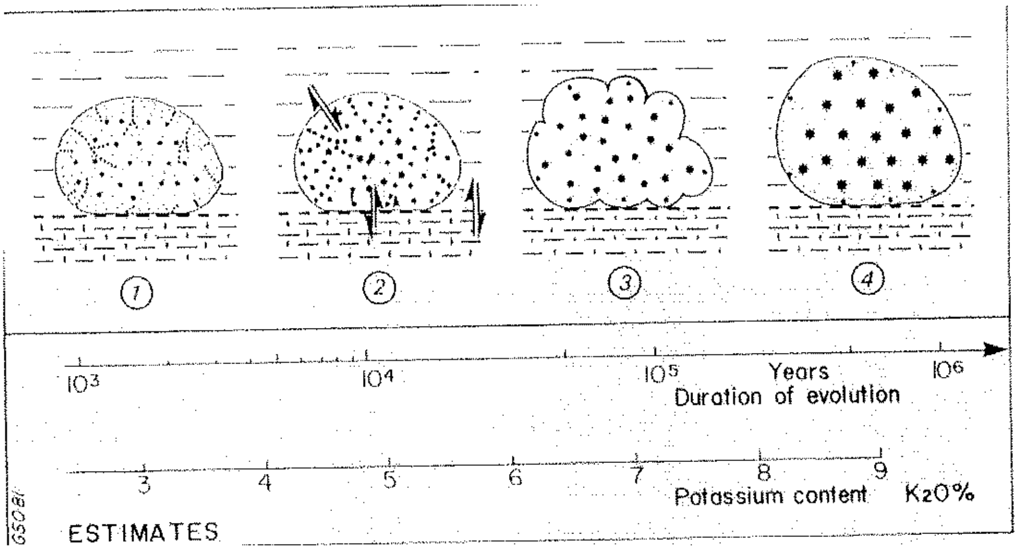

Figure 2.1: Glauconitization of a granular substrate: 1) nascent stage; 2) slightly – evolved stage; 3) evolved stage; 4) highly – evolved stage. Stars represent glauconitic minerals. The grain (about 5 mm in diameter) is shown at the boundary between sea – water and sediment. After this evolution, the glauconitic minerals do not evolve anymore at the sea – water/ sediment interface and the green grain is relict (From Odin and Fullagar 1988).

According to Odin and Fullagar (1988) the development of new minerals imparts a green colouration to the grains, at the nascent stage the main green clay is iron – rich and characteristic of the glauconitic mineral family K contents are in the order of 2-4%. The minerals of the substrate become progressively destroyed as glauconitization proceeds (Odin & Fullagar 1988). Micas and quartz are much more stable and remnants of these materials are commonly found in ancient glauconies (Odin and Fullagar 1988). At the slightly evolved stage pores form which in turn are filled with authigenic clays and K content increases. With continuing evolution the initial textures of the grains are obscured and cracks appear on the surface of the grains, this stage is the evolved (Odin and Fullagar 1988). The highly evolved stage is typical of filled cracks imparting a smooth aspect to the grains and an overall increase in K content.

Fibroradiated Rims

A feature studied in glauconites is that of fibroradiated rims which coat the external surface of the glauconite grains. Most commonly, the authigenic rims occur as concentric coatings of radially oriented crystals on glauconitic mineral pellets (Chafetz & Reid 2000). In case studies it has been shown that fibroradiated rims of glauconitic minerals average about 10μm thick, and range from those that completely envelope the grains, to those that only partially coat grains (Chafetz & Reid 2000). The glauconitic mineral pellets formed as the result of replacement-precipitation of a host mineral (Odin & Fullagar 1988) whereas the rims formed by precipitation of glauconitic minerals in the free spaces surrounding pellets (Chafetz & Reid 2000). Chafetz and Reid (2000) ascertain that glauconitic mineral rims, and by reasonable analogy, the glauconitic mineral pellets must have formed at or immediately below the sea floor.

According to Chafetz and Reid (2000) the presence of rims indicates a period where precipitation and maturation was facilitated at low sedimentation rate without significant clastic input.

The evolution process of glauconites may be halted at any stage of the above continuum if the environment becomes unsuitable. Two main factors appear to be involved sea-level change and burial (Odin & Fullagar 1988). McConchie and Lewis (1978) described that glauconite forms originally at the sediment – water interface, thus implying a marine setting. A paleodepth range between 60 and 550 m and an open marine environment are considered as ideal for glauconitization (Odin & Fullager 1988). These are generally low-energy settings in which accumulation of sediment is relatively slow (Pasquini et al. 2004). This interpretation occurs mostly for modern deposits however there are numerous ancient deposits which show a shallow marine environment, quite commonly glauconitic grains are found in shallower storm-dominated deposits as the result of transport and reworking processes (Amorosi 1997). Chafetz and Reid (2000) have found autochtonous glauconitic minerals formed under shallow – water to tidal-flat conditions, in a high energy environment.

Given the presence of glauconites in shallow water settings Amorosi (1997) compared sedimentological, petrographic and stratigraphic data and differentiated between autochthonous, parautochthonous and allochthonous (Amorosi 1997; Figs. 2.2, 2.3). Autochthonous glauconite is formed on site, allochthonous glauconite is formed at a distant source and then transported to the site of deposition, while parautochthonous glauconite is sourced and transported locally. These terms were employed in this study based on the spatial and temporal characteristics of the deposits.

2.6.2 This study

A study on glauconite from the Iron Creek Formation – Waipara Greensand and correlative members and formations had the purpose of establishing the spatial and temporal characteristics of glauconite and in turn establishing a slow versus fast rate of sedimentation based on the sedimentological and petrographic data. The study was focused on studying and recording the morphological and textural data as an aid to maturity of glaucony, hence revealing the mode of formation, depositional environment and sedimentation rates.

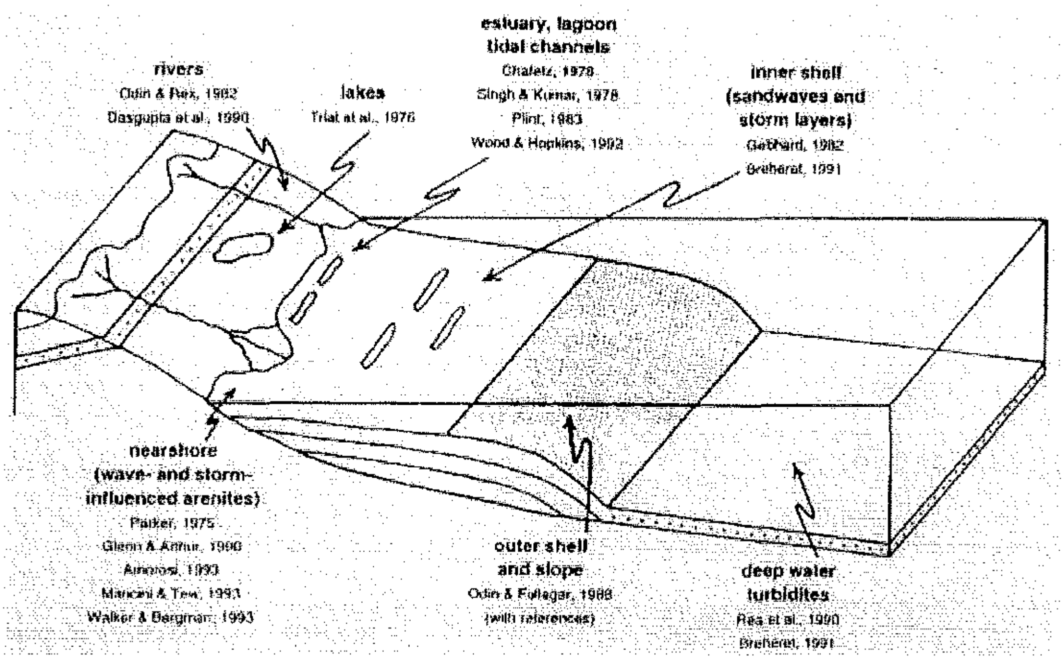

Figure 2.2: The occurrence of allochthonous glaucony in various environments, as the result of transport and reworking processes, based on selected examples from the literature. Autochthonous glaucony (grey tone) is mostly restricted to outer-shelf and slope environments (From Amorosi 1997).

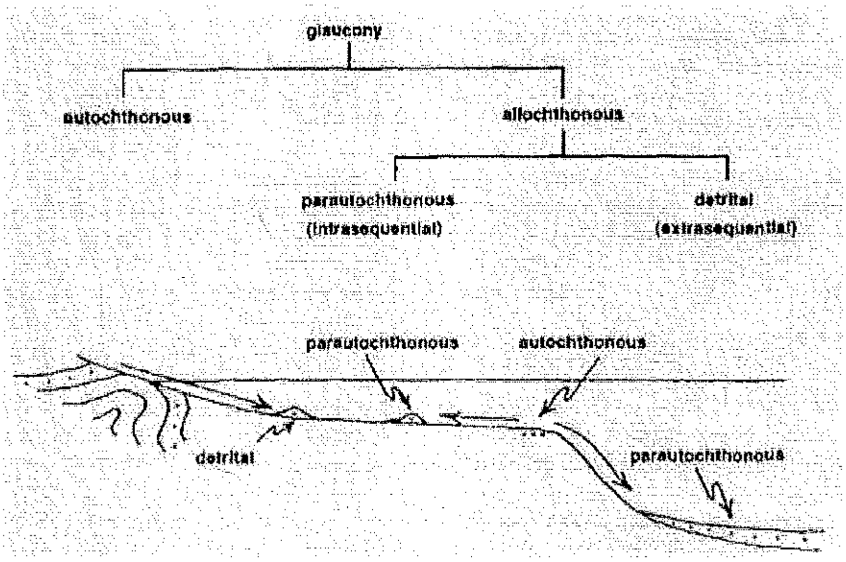

Figure 2.3: Classification scheme of glaucony based on spatial and temporal characteristics (From Amorosi 1997).

2.6.2 Analytical methodology of Glauconite morphology

The glauconite morphology/maturity index used herein involved isolating glauconite grains in petrographic point counts and recording texture, grain size, sorting, grain roundness, and other morphological features such as cracks and authigenic minerals such as micas. The establishment of maturity index and type of glauconite was done following the terminology of Odin and Fullagar (1988) for granular glauconite: 1) nascent stage, 2) slightly evolved stage, 3) evolved stage 4) highly evolved stage (Fig). For the purpose of this study the terminology was modified, morphological names such as: micaceous - glauconite, nascent glauconite, and evolved-mature glauconite were used.

Glauconite grains were counted for the properties mentioned above in the framework of petrographic point counts. Grains were described from rock thin sections using an optical petrographic microscope in plane and cross-polarized light. Subsequently loose sand samples were disaggregated with HCL 1% in water or dry and glauconite grains were selected by handpicking using a reflected light optical microscope. Individual glauconite grains were mounted and used in a Scanning Electron Microscope (SEM) to quantify morphological features such as roundness and cracks whereas possible. Samples in the SEM were worked at magnifications of 100-650 x with an average working distance of 18mm, an average scan speed of 19.6 seconds and a beam current of 50 pA.

Subsequently petrographic data and glauconite content was correlated with sedimentological data (sedimentary structures) to establish spatial and temporal relationships, environment of formation and deposition as an aid for sedimentation rate and tectonic setting. Chemical analysis was not done on the samples as it is not purpose of this project; however McConhie and Lewis (1980) gathered such data from Cretaceous and Eocene glauconites within the South Island.

2.7 Quartz Analysis

Quartz is the most abundant mineral in the earth's crust, because it occurs in plutonic, volcanic and metamorphic rocks. Because quartz resists disintegration and decomposition, there is more quartz than other rock-forming minerals in sediments (Prothero & Schwab 1999). Given the prevalence of monocrystalline quartz grains in sandstone, many efforts have been made to discriminate varieties of quartz derived from a particular provenance (Prothero & Schwab 1999).

2.7.1 Optical Microscopy Techniques

Blatt and Christie (1963) examined the use of undulatory extinction and polycrystallinity for the determination of provenance of arenites. The use of undulatory extinction and polycrystallinity was re-evaluated by Basu et al. (1975). Blatt and Christie (1963) recognised quartz from extrusive rocks to have a higher frequency of straight extinction compared to metamorphic quartz grains with higher undulose extinction. Basu et al. (1975) re-evaluated the use of polycrystallinity and undulatory extinction applied to modern and ancient sandstones and concluded that plutonic quartz had a higher frequency of non-undulatory quartz and low polycrystallinity. While high-rank metamorphic and low-rank metamorphic quartz had progressive lower non-undulose extinction and progressive abundant polycrystalline grains > 3 crystals according to Basu et al. (1975). Young (1976) described a generalized quartz deformation continuum of features visible with an optical microscope starting from nonundulose quartz to undulose, polygonized, elongated-crenulated quartz to recrystalized quartz mosaic leading to polygonal-polyhedral quartz grains with increasing deformation rate. Young (1976) interpreted the continuum of deformation to reflect a continuum in metamorphic grade corresponding from low grade and medium to high grade metamorphism. Thus a provenance based on quartz deformational textures was feasible at a certain extent.

Provenance based entirely on petrographic methods was insufficient to provide a source without limitations. Blatt and Christie (1963) recognised their ability to distinguish between populations of plutonic and metamorphic quartz would obviously improve if they could supplement observation of undulosity with observation of other genetically significant properties of quartz.

2.7.2 Cathodoluminescence Techniques

2.7.2.1 Background

Cathodoluminescence (CL) of detrital quartz adds to the plethora of methods used in provenance, such as sedimentary petrography, geochemistry, isotopes and heavy minerals.

Cathodoluminescence is the light given off by a material when it is struck by an electron beam (Garlick 1966; Marshall 1988). Cathodoluminescence generally depends on crystal structure, defects and the concentration and interaction of various trace elements (Leverenz 1968). In comparison to optical petrography of detrital quartz, CL can give much more information regarding complex growth histories within a grain, deformation effects and metamorphic overprints.

The CL technique is divided in two types; cold cathode optical microscope and hot cathode cathodoluminescence. In cold cathode microscopic equipment, the electrons are generated by an electric discharge between two electrodes under a low gas pressure (Marshall 1988). The former technique is cheaper, and samples are uncoated. However, the disadvantages include low spatial resolution (only within 2 cm), instability due to the variation in gas pressure, and damage of the surface from the electron bombardment. The hot cathode technique involves an electron gun associated with a scanning electron microscope (SEM) with the electrons generated by heating a filament (2000-3000 °C) (Pagel et al. 2000). The advantages include high magnification, good spatial resolution and coupling with an EDS for mineral identifications where necessary. The disadvantages are that samples require coating (C, Al, N, and Au), a high vacuum is necessary, and certain minerals produce high luminescence (calcite, sericite) (Pagel et al. 2000).

Cathodoluminescence produces distinctive shades of grey and black and features and fabrics not visible in standard petrography. These fabrics and CL intensity variations are visible in most minerals. The several underlying factors for the changes in CL luminosity in minerals and in particular quartz have been proposed from various authors. Possible contributory factors include: the presence of minor chemical impurities (e.g. Al, Na, and Oh) acting either directly changing CL characteristics as a result of chemical variation, or indirectly causing defects in the crystal lattice; trapped electron hole pairs; or oxygen vacancies (D'Lemos et al. 1997; Zinkernagel 1978).

The intensity of quartz CL is weak compared to the CL of feldspars, carbonates and many other minerals (Marshall 1988). However the CL of quartz is consistent in producing results. The dull luminescence of quartz is of great significance, for by employing the best luminescence petrographic techniques it is often possible to distinguish secondary optically continuous quartz from the detrital grains by contrasts in the luminescence (Sippel 1968). Most examples of quartz from igneous and metamorphic rocks show CL (Marshall 1988). In normal petrographic practice such features can only be distinguished where inclusions, liquid or solid, either rim the detrital grain, thus outlining it, or are present in considerably different density in the detrital and secondary quartz (Sippel 1968). CL can identify the presence of healed microfractured or the recrystalized areas of crystals (Pagel et al. 2000).

In contrast, the luminescence technique frequently reveals apparently complete separation. In these cases, it is possible to see the shape, size and degree of rounding of the detrital grains, as well as the quantity and disposition of secondary quartz overgrowths (Sippel 1968).

CL textures in quartz grains are not only useful for identifying the lithological provenance of some grains, but also the predepositional deformational history of some grains (Reed & Milliken 2003).

2.7.2.2 SEM-CL applied to provenance

Quartz grain provenance by CL was initially addressed based on CL colour by Zinkernagel, (1978) and Gotze et al. (2001). Field (1989) used CL colour of quartz on sedimentary successions from Canterbury. Cathodoluminescence colour of quartz was evaluated by Boggs et al. (2002) and proved to be unreliable due to a significant overlap of colour between volcanic and plutonic quartz. Thus alone colour is subjective, although it can provide clues about differences of CL in healed microcracks in plutonic quartz grains as studied by Sprunt and Nur (1979).

The recent development of CL involves the usage of the monochromatic SEM-CL techniques for quartz provenance analysis (Milliken 1994; Seyedolali et al. 1997; Kwon & Boggs 2002; Bernet & Bassett 2005). Seyedolali et al. (1997) observed certain CL characteristics and features unique to quartz from plutonic, volcanic, metamorphic and shock-deformed rocks, thus setting the basis for provenance analysis of quartz.

Quartz grains studied by SEM-CL display a variety of features owing to variation in luminescence intensity within different parts of grains (differential CL) (Seyedolali et al. 1997). These features show up as various shades of grey, ranging from black (weak or no CL response) to white (strong CL response) (Seyedolali et al. 1997). Seyedolali et al. (1997) identified zoning, healed fractures, complex shears, planar features (shocked- quartz), dark CL streaks, patches, mottled CL texture and homogeneous (nondifferential) CL. The SEM-CL fabric-analysis technique provides a rapid method for distinguishing quartz from a variety of source rocks (Seyedolali et al. 1997).

2.7.3 The Integrated Optical Microscopy/SEM-Cathodoluminescence Technique

2.7.3.1 Background

The use of CL on its own leads to an identification of source type but has limitations. Kwon and Boggs (2002) studied the same Tertiary sandstone applying both SEM-CL and QFL petrography on the samples. They showed that while there was good agreement in some categories, others did not agree well. Thus although they used both methods (petrographic and CL) they used them independently.

The SEM-CL technique as noted above is more powerful in conjuction with optical petrography. Therefore a technique that combines both CL and optical petrography on the same grain is essential.

The integration of monochromatic SEM-CL with optical microscopy analysis on each individual quartz grain is a new technique to interpret provenance of quartz rich sediments (Bernet & Bassett, 2005). The combination of information gained from SEM-CL response and texture with information from optical microscopy allows distinction of different quartz types much more easily than with conventional microscopy or CL colour analysis (Bernet & Bassett 2005).

Ettmuller (2003) applied the integrated SEM-CL/optical microscopy to sedimentary rocks from the Paparoa Trough, South Island, New Zealand and revealed compatible trends between undulosity-polycrystallinity and CL features and characteristics indicative of certain quartz types from plutonic, volcanic and metamorphic quartz thus supporting the integrated method as a powerful technique in provenance analysis.

2.7.3.2 Analytical methodology of the integrated technique

The integrated SEM-CL/Optical petrography technique used herein involves the direct point counting and comparison of quartz grains using the diagnostic features from each technique to assign a type of quartz. The starting point is identifying and marking areas of interest under a conventional optical microscope on polished thin sections. Subsequently, the thin section is examined in a scanning electron microscope (SEM), here a Leica stereoscan 440 equipped with an Oxford MonoCL cathodoluminescence detector.

Images are acquired during the SEM-CL session to compare with thin sections under standard petrographic microscope. Digital monochromatic images are taken from the circled areas of interest at 300pA to 2.0 nA beam current and 15 to 25 kV acceleration voltage at an average working distance of 19 to 22mm from the encircled areas of interest. Images are taken at 4096 – 8192 pixel average corresponding to 5-10 minutes of scanning time. Imaging problems associated with carbonate minerals on SEM – Cathodoluminescence were prevented by removing carbonate minerals by acid etching, a technique used by Reed and Milliken (2003) and with a long scaning time as mentioned before.

The images are then compared directly with features from optical petrography by viewing the images in a commercial photo editing program, placing a grid over the image, and identifying the same quartz in both techniques. Petrographic analysis of single quartz grains was undertaken by locating individual grains, numbered in the SEM-CL images, on the corresponding thin section using the microscope as developed by Bernet and Bassett (2005).

Standard optical petrography was performed on a binocular Nikon microscope using planar and cross-polarized transmitted light. From every sandstone thin section a total of 105 quartz grains were counted and the following characteristics were identified based on Bernet and Bassett's (2005) methodology:

1) Extinction characteristics straight, weak undulose and strong undulose extinction were discriminated. Undulatory extinction describes the uneven extinction positions within a grain that has been plastically deformed heterogeneously (Shelley 1993). Quartz grains with weak undulose extinction are distinquished from grains with strong undulose extinction in that the latter show clear extinction boundaries, which might be related to slightly different orientations between subgrains (Shelley 1993).
2) Polycrystallinity quartz grains consisting of three or less crystals were distinguished from grains containing more than three crystals according to the approach taken by Basu et al. (1975).
3) Grain roundness, rounded, subrounded to subangular and angular.
4) Grain shape: elongate, platy and spherical.
5) Grain size <2000 microns – very coarse sand, <1000 microns – coarse sand, <500 microns – medium sand, <250 microns – fine sand and <125 microns- very fine sand.

Further data concerning the presence or absence of diagenetic overgrowths and petrographic textures of polycrystalline quartz based largely on deformation features were obtained from each quartz grain following the technique of Young (1976).

2.7.3.3 SEM-CL/Optical characteristics of quartz

The following descriptions of diagnostic characteristics of quartz types are based on Bernet and Bassett (2005).

Plutonic quartz

Black, irregularly shaped streaks or bands and large (10-100µm), black patches characterize many plutonic quartz grains (Seyedolali et al.; figure 2.4, 1997), but overall plutonic grains have relatively bright CL. Typical plutonic quartz is characterized by large crystals containing primary healed and rarely open microcracks, fluid inclusion trails, and non-undulose to weak undulose extinction (Bernet & Bassett 2005). Rarely, plutonic crystals may show concentric zoning. Fluid inclusion trails and extinction can be easily seen with an optical microscope but the microcracks are primarily visible with CL (Bernet & Bassett 2005). Cracking and healing in quartz during crystallization is much more abundant and common in granitic and related rocks than previously thought (Sprunt & Nur 1979). Sprunt and Nur (1979) used CL colour to show differences in CL between the entire grain and the healed microcracks. Sprunt and Nur (1979) interpreted the domains of CL in granitic and pegmatitic quartz as relatively lower-temperature quartz deposited in the pre-existing high-temperature CL of quartz.

Figure 2.4: Two individual quartz grains in CL imaging depict healed microcracks characteristic of plutonic quartz source, and characteristic of weak to straight extinction in standard microscopy. (From Castle Hill Basin - this thesis).

Volcanic quartz

Volcanic quartz appears as pristine crystals in thin sections under an optical microscope, showing non-undulose extinction and commonly idiomorphic or hypidiomorphic crystal shape (Bernet & Bassett 2005; figure 2.5, 2005). Much quartz of volcanic, origin is characterized by the presence of distinct, concentric zoning, resembling in pattern the compositional zoning common in plagioclase (Seyedolali et al. 1997). Volcanic quartz crystals may also contain melt inclusions, embayments and large open cracks, which are visible with an optical microscope, but can also be seen with the SEM-CL (Bernet & Bassett 2005). Compositional zoning in minerals implies that complete equilibrium was not reached during crystallization, and it happens most frequently during rapid volcanic crystallization (Shelley 1993).

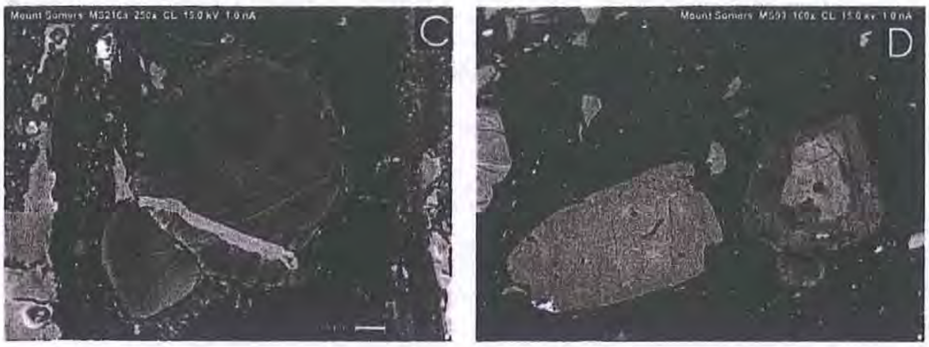

Figure 2.5: CL images of volcanic quartz grains with characteristic CL zoning and Hypidiomorphic crystal shape, otherwise these grains depict straight extinction in standard optical microscopy. (From Bernet & Bassett 2005)

Metamorphic quartz

Metamorphic quartz is part of a continuum from deformed quartz to metamorphosed quartz of low to high grade metamorphism. Young (1976) described a generalized quartz deformation continuum of features visible with an optical microscope starting from nonundulose quartz to undulose, polygonized, elongated-crenulated quartz to recrystalized quartz mosaic leading to polygonal-polyhedral quartz grains with increasing deformation rate. Bernet and Bassett (2005) attempted to add CL characteristics to this continuum of metamorphic grades, however more work needs to be done in this area. The following descriptions draw heavily on the optical microscopy with a minor contribution from SEM-CL since most recrystallized quartz dark CL intensity.

Figure 2.6: Left image is SEM-CL image depicting dark CL, image on the right is an optical micrograph of the same quartz grain depicting polycrystallinity and high metamorphic grade (from Mandamus, this thesis).

Brittle deformation of quartz grains occurs under non- to very low- or low-grade metamorphic conditions (<300-400°C) and is formed during burial, or local or regional tectonic deformation (Bernet & Bassett 2005). As a result, primary CL and optical features are preserved overprinted with undulose extinction. Grains will retain bright CL luminosity and primary CL features such as healed microcracks and zoning but will have weak to strong undulose extinction under the optical microscope.

The onset of ductile deformation with increasing metamorphic grade (400-700°C) is marked by the occurrence of deformation lamellae, deformation bands and medium to strong undulose extinction in quartz (Passchier & Trouw 1996). Deformation lamellae can be examined with both SEM-CL and optical petrographic techniques, while deformation bands and undulose extinction are only visible with an optical microscope (Bernet & Bassett 2005). Undulosity increases with increasing rate of deformation. Increasing deformation will lead to stronger undulose extinction and quartz crystals with strong undulose extinction tend to develop inhomogeneous, patchy or mottled CL texture (Bernet & Bassett 2005). However patchy CL is not only characteristic of metamorphic quartz, many plutonic quartz grains can also have patchy CL (Seyedolali et al. 1997). Therefore in general the CL response from metamorphic quartz grains is mottled and/or dark.

Increasing metamorphism leads to polygonization and recrystallization of quartz. Recrystallized quartz grains usually depict polygonal-polyhedral grains viewed under the microscope and moderate-dark CL to completely black CL. Young (1976) and Winkler (1974) assign high grade metamorphism to recrystallized quartz grains. Bernet and Bassett (2005) in their study conclude that from 95% of quartz grains recrystallized under medium to high grade metamorphic conditions appear very dark to black in SEM-CL images and the disappearance of previously acquired textural features such as zoning and microcracks is the rule.

Quartz from veins shows similar characteristics to recrystallized, high grade metamorphic quartz (Bernet & Bassett 2005). The striking characteristic of vein quartz is oscillatory narrowly spaced, concentric zoning with sharp corners. Vein quartz was grouped in metamorphic quartz for the purpose of source types; however it was noted when it was obvious.

For the assignation of quartz types to quartz grains based on their optical petrographic and CL features the steps taken were outlined in Bernet and Bassett (2005), (fig.2.7; appendix 6). Grains with visible metamorphic fabrics have been placed under a metamorphic grade based on Young's (1976) continuum from deformed to low grade, medium grade and high grade metamorphic. Clear boundaries of metamorphic grade are not always possible because of the continuum, however inferences have been made about the metamorphic grade and the grains that exhibit weak-strong undulose extinction and dark and/or mottled CL have been labelled metamorphic (fig. 2.6).

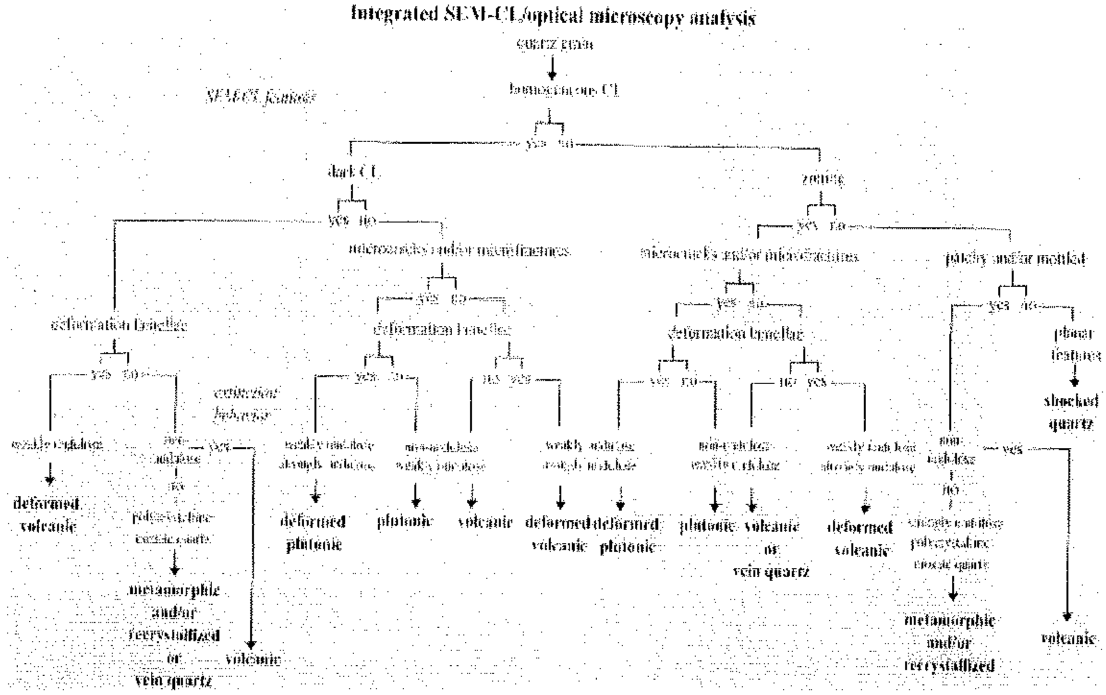

Figure 2.7: Flow chart showing steps to identify quartz type on the basis of a combination of CL and petrographic characteristics and features (From Bernet & Bassett 2005).

2.8 Summary

Sedimentological data, petrographic data, QFL point counts, glauconite morphological features and the integrated SEM-CL/Optical microscopy of quartz provided valuable information in deciphering depositional environments, correlations spatial and regional, while providing sedimentation rate indications and provenance indicators. Petrographic data and QFL employed together with the newly developed integrated SEM-CL/optical microscopy technique on quartz supplemented each other thus providing an integration of data sets.

CHAPTER THREE

MANDAMUS AREA

3.1 Regional - Geologic Setting & Previous Work

The Mandamus area is located in northern Canterbury in the Mandamus-Pahau district. The Mandamus area is situated about 20 km inland from the township of Culverden (fig. 3.1). A sequence of Tertiary sedimentary rocks preserved in a syncline lies between the Mandamus and Dove Rivers which drain into the Huruni River to the south and bound by the Hurunui Peak towards the east. The Mandamus River area is bound by the Mandamus Igneous Complex to the south east.

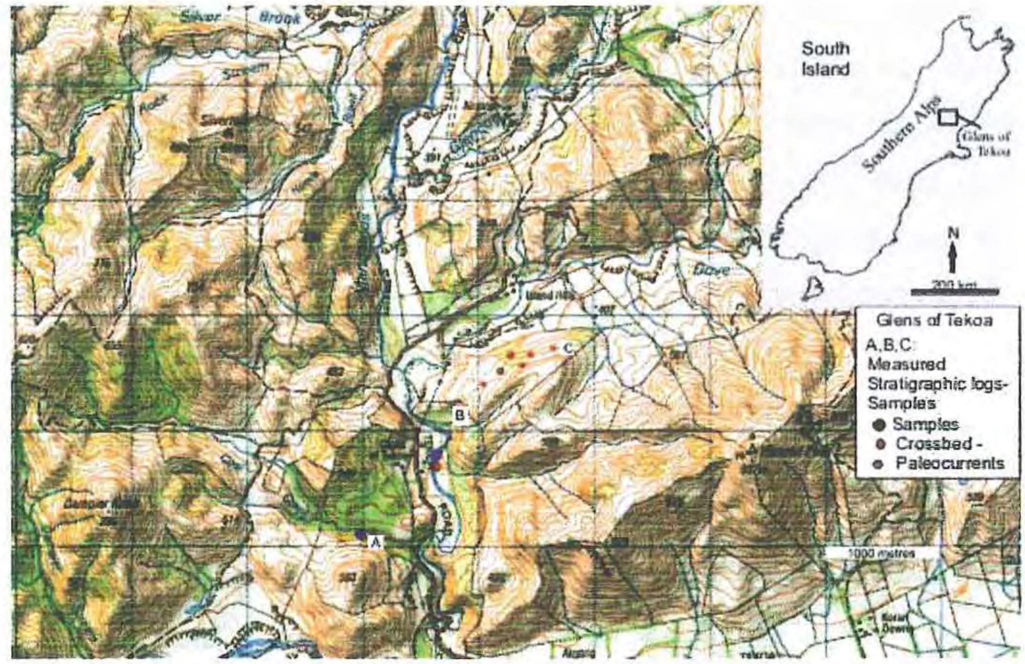

Figure 3.1: Topographic map of the Mandamus outlining locations of measured stratigraphic sections, sample locations and the locations where crossbed-paleocurrent measurements where taken.

The previous work in the area was done by Haast (1871), Hutton (1877) and Speight (1918) and revised by Mason (1949). Mason (1949) mapped about seventy-five square miles in the Mandamus Survey District and discussed the Mandamus Igneous Intrusives. Sevon (1969) did a sedimentological study of the Tertiary sediments of the Mandamus – Dove River on a smaller scale. Sevon (1969) described the sequence including the interbedded coal-conglomerates which unconformably overlie the Torlesse basement and the overlying glauconitic sandstone as Coal Creek Formation based on the exposure in the Coal Creek locality and in the Mandamus River. Brown and Field (1985) made reference to the Tertiary sequence in the

Mandamus area but without particular detail. However, they are named the basal conglomerates Tertiary sequence as the Broken River Formation and the glauconitic sandstones overlying the basal conglomerates as the Waipara Greensand.

3.2 Stratigraphy

The Mandamus Dove area is characterized by a succession of Tertiary sediments that uncomformably overlie greywacke-argillite Torlesse Supergroup of Late Jurassic metamorphosed to pumpellyite-prehnite facies and the Mandamus Igneous Complex (Fig.3.2). The overlying Tertiary sequence is characterized by basal conglomerates and coal of the Broken River Formation, Paleocene to Early Eocene overlain by glauconitic sandstones of the Iron Creek Greensand (Early Eocene to Late Eocene). The sequence is followed by the Tekoa Tuff (Early Oligocene) and by the Flaxdown Limestone (Mid-Late Oligocene) Members of the Omihi Formation. At the top of the sequence is the Pahau Siltstone Member of the Waikari Formation. This sequence reflects a transition from terrestrial to marine sedimentary rocks in a transgressive sequence from the Paleocene to the Late Oligocene.

The Torlesse basement was intruded during the Cretaceous by the Mandamus Igneous Complex (MIC) (Tappenden 2003). The igneous complex has ages of 97 Ma (Weaver & Pankhurst 1991) and Tappenden (2003) revised that age to 98 Ma. The Tertiary sequence was subsequently deformed and a south –west plunging syncline formed as the result of regional thrust faults developing during the Late Miocene.

The Torlesse basement is separated from the overlying Broken River Formation by a strong angular unconformity (Fig.3.2).

3.2.1 Basement Rocks – Torlesse Supergroup

The Torlesse Supergroup – makes up the Pahau terrane which underlies the Tertiary sequence at the Mandamus River. Rocks of the Torlesse Supergroup are the oldest exposed in the study area. According to Sevon (1969) two types of sequences occur in rocks of this group. The first type comprises 6 to 24 cm thick beds of greywacke grading upward into argillite. The second type is massive greywacke beds up to 1 m thick separated by ½ to 20 cm thick beds of argillite. Some massive beds have closely spaced parallel laminations in their upper part and some of the graded beds have cross lamina in the upper part. Colour varies from medium grey to olive grey to brownish grey with lighter shades of these colours produced by weathering (Sevon 1969).

3.2.2 Mandamus Igneous Complex Intrusives

The Mandamus Igneous Intrusives that occur in the Mandamus – Dove River area were first studied by Mason (1951). The main body of igneous intrusive is a large mass of syenite which outcrops south-east of the Tertiary rocks. The syenite is generally very coarsely crystalline and heavily altered (Tappenden 2003). The trachytes are generally pale grey in colour and commonly heavily hydrothermally altered. The igneous geology in the Mandamus field area is dominated by a syenite plutonic complex with a carapace of trachytic and mafic lava flows and lahar deposits.

In some exposures this syenite is cut by dikes of melanocratic biotite hornblende microsyenite and biotite gabbro (Sevon 1969; Tappenden 2003). Numerous sills from the syenites plutonic complex occur in the greywacke rocks and range from 0.3 m to several tens of metres thick. Identified sill rocks are: hornblende trachyte, melanocratic hornblende microsyenite, trachyte and trachybasalt (Sevon 1969). Younger alkaline mafic and intermediate dykes cut both greywacke and syenite plutonic complex (Tappenden 2003).

Syenite is the most voluminous rock type in the Mandamus Igneous Complex (MIC) and intrudes both the lava carapace and the Torlesse basement. Numerous trachytic and trachybasalts intrude the Torlesse basement while in small volumes syenodiorites, and alkali microgabbro also occur (Tappenden 2003).

3.2.3 Broken River Formation

The distribution and thickness of the Broken River Formation is confined to thin slivers unconformably overlying Torlesse basement. Brown and Field (1985) referred to the Broken River Formation thinning to the northwest while Sevon (1969) recorded 7 meters in the Mandamus area. Characteristic deposits of Broken River Formation are thin basal boulder conglomerates with coal beds and lenses. The age of the Broken River Formation is Haumurian (Late Cretaceous) based on a pollen sample yielding a Haumurian age (Late Cretaceous) above a coal seam (Sevon 1969) in the Coal Creek locality.

3.2.4 Waipara Greensand

The conglomerates of the Broken River Formation are overlain by glauconitic sandstones. Sevon (1969) had described the basal conglomerates and the greensands as Coal Creek Formation while Brown and Field (1985) revised the nomenclature by renaming approximately 40 metres of greensand at Mandamus as Waipara Greensand.

Sevon (1969) presented a Mangaorapan-Heretaungan (Eocene) age for the formation based on foraminifera.

For the Mandamus field area this study focuses on the Tertiary sequence encompassing the Broken River Formation and Waipara Greensand.

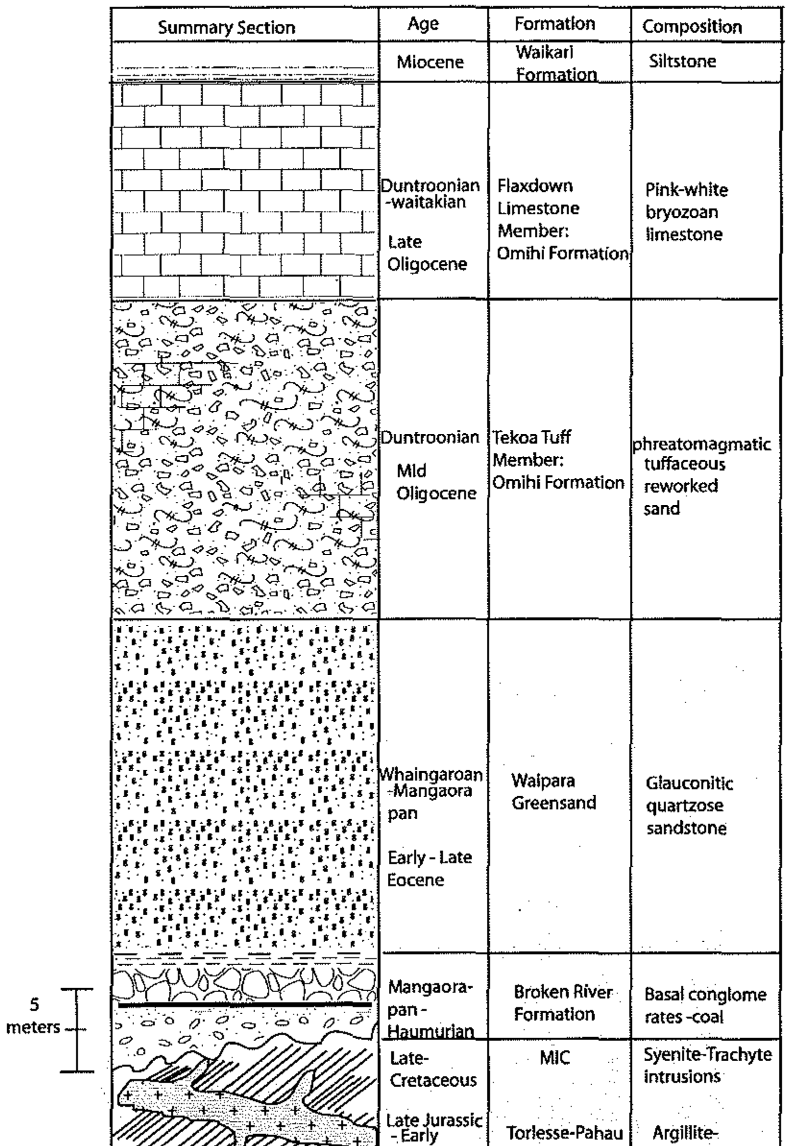

Figure 3.2: Summary stratigraphic column of the Island Hills area.

3.3 Sedimentary Descriptions

3.3.1 Broken River Formation

The Broken River Formation occurs mainly in the Coal Creek a small tributary of the Mandamus River (Fig. 3.1) where it is 7 metres thick (Fig. 3.3); the outcrop is vertical due to the south-west plunging syncline. The exposure at Coal Creek was measured on 20 centimetres to 1metre intervals recording sedimentary structures texture and composition (appendix 1 Fig.1.1) while taking in consideration the vertical bedding orientation.

The exposure at Coal Creek is characterized by a basal unconformity with the underlying Torlesse basement. The lower bed consists of a basal conglomerate which is 3 metres thick. The conglomerate is matrix supported and polymictic (appendix 1 Fig.1.1). It is massive, poorly sorted with clasts rounded to subrounded to occasionally sub-angular; matrix is medium-fine sand. The clasts are predominantly greywacke and white sandstone. Sparse pyritized concretions occur within the conglomerate. The conglomerate is overlain by a 60cm grey sandy siltstone characterized by jarosite staining, while the contact with the conglomerate is gradational. The siltstone bed grades into an overlying coal seam. A petrographic study of a coal sample from the seam gave a vitrinite reflectance of 0.45 corresponding to a low rank sub-bituminous variety. The coal petrography shows high percentage of ash (detrital minerals such as quartz) and other major components. Framboidal pyrite is also present in the coal which results from bacterial action. The coal seam is 40 cm thick with rare pyrite nodules, jarosite staining and peat material at the top of the seam.

The upper conglomerate rests sharply on top of the coal bed and is 2.5 metres thick. It is massive, poorly sorted, clast supported, polymict conglomerate while the matrix is moderately sorted, coarse to fine sand (appendix 1 Fig. 1.1). Clasts are composed predominantly of trachyte, microsyenite and at a lesser extent syenite ranging from 15cm to as large as 90cm boulders.

3.3.2 Waipara Greesand

Waipara Greensand glauconitic sandstones outcrop in Coal Creek and cliffs around the syncline. The basal contact with the upper conglomerate of the Broken River Formation occurs only in Coal Creek where (appendix 1 Fig. 1.1) a moderately indurated, green to cream coloured glauconitic mudstone grades into the overlying glauconitic greensand. Despite its glauconite content no glauconite analysis was done on the thin siltstone due to its muddy grain size. The contact of the Waipara Greensand with the Broken River Formation's conglomerates is sharp without displaying any significant break in sedimentation or erosion. Higher in the section in Coal Creek, exposures of poorly sorted, calcareous cemented, glauconitic, cross bedded quartz sandstones dominate in close lateral proximity to the section measured in Coal Creek (fig. 3.4).

A continuous exposure of the Waipara Greensand occurs in the Mandamus River (locality B, Fig. 3.1). The sequence is characterized by grey-green massive, poorly-to moderately sorted, fine-medium, glauconitic quartz sandstones with intermittent calcareous cemented layers (fig. 3.5 & appendix 1 fig. 1.2), (Appendix 1). The type section defined by Sevon (1969) of the Waipara Greensand consists of 20 metres of friable, rhythmically alternating massive and, faintly laminated sandstone with granule layers and coarse sandstones (appendix 1 Fig. 1.2).

Figure 3.3: Exposure of Broken River Formation basal conglomerates interbedded with coal at the Coal Creek locality. A lower, matrix supported polymictic and an upper clast supported polymictic conglomerate above the coal seam towards the right of the figure.

Some burrowing activity is evident in the section. Burrows are typically 1- 4 cm in length and occur as vertical and horizontal (appendix 1 Fig. 1.2). Granule layers are common with disarticulated shells and sharks teeth. The granule layers are predominantly quartzose with occasional polycrystalline granules, while occasional minor laminations and hummocky cross stratified layers occur.

At locality C on the north-western limb of the syncline (fig. 3.1) an exposure of Waipara Greensand occurs (appendix 1 fig. 1.3). The section consists of 11.5 metres of poorly sorted quartz rich sandstone with minor glauconite. The stratigraphic section reveals a poorly sorted, massive, very fine to medium grained calcareous sandstone with shell beds and calcareous cemented lenses. Rip up clast granule layers and articulated ostrea and gastropod shells occur while further up section are shell beds of ostrea and oyster shells. The tabular cemented layers tend to be coarser grained with few fines and associated with pebbly clasts and/or shells and sharks teeth.

Large cross bedded foresets occur within the Mandamus area, predominantly in Coal Creek in the Mandamus River but also on the western north-western limb of the syncline (Fig. 3.1). Cross bed paleocurrents were measured in the field and then restored to true azimuth direction using sterographic projection. Most paleocurrents flowed from the south while some sets of paleocurrents from Coal Creek flowed from the north. Some minor paleocurrents flowed from a north-east direction (Fig. 3.6). The cross bed foresets occur within sets of 20cm-50cm to large as 1.5 metres.

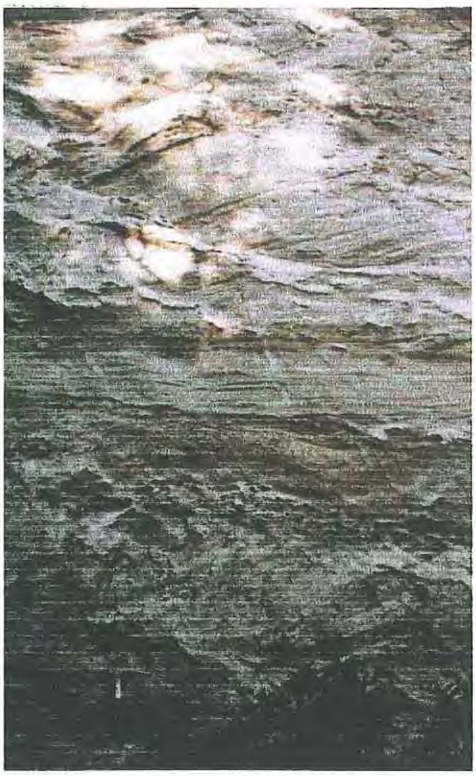

Figure 3.4: Large scale cross bed foresets of the Waipara Greensand at Coal Creek

Figure 3.5: Tabular calcareous cemented sandstone of the Waipara Greensand at section B, Mandamus River.

3.4 Interpretations of Depositional Settings

3.4.1 Broken River Formation

The basal conglomerate overlying the Torlesse basement is interpreted as a debris flow previously modified by fluvial action. The deposit is dominantly a poorly sorted, matrix supported conglomerate without imbricated clasts or bedding (appendix 1 Fig. 1.1) indicating debris flow. The deposit's rounded and subrounded clasts are accounted for by fluvial interaction. The greywacke-argillite clasts are interpreted to have been sourced from the pre-unconformity Torlesse-Pahau basement.

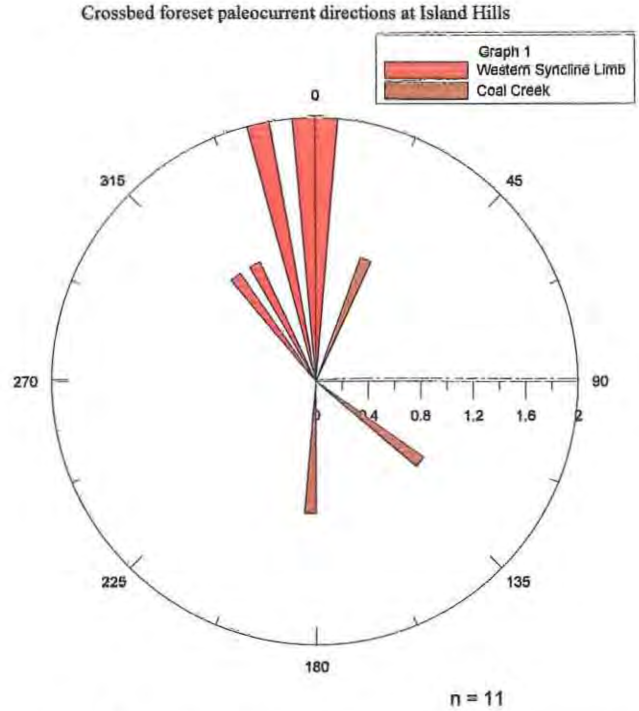

Figure 3.6: Restored azimuth cross bed foreset paleocurrents of the Waipara Greensand

Following this episode a quiescent period is marked by deposition of first mudstone then peat formation in isolated interdistributary settings necessary for formation of peat without any significant detrital input at that period. The coal likely represents accumulation of material in an abandoned channel. The composition of the coal based on high ash content and high sulphur as well as the vitrinite reflectance indicates a clastic environment with the supply of detritus in an alluvial setting. Framboidal pyrite (high organic sulphur) and pyrite concretions present is an indicator for saline water associated with a marine transgression however its formation is post depositional as saline fluids percolate from the overlying transgressive deposits of the Waipara Greensand.

The sharp contact of the coal seam with the overlying clast supported conglomerate is interpreted to represent deposition by a braided river which would account for the clasts as large as 90cm. The clasts of the conglomerates were sourced from pre-unconformity basement rocks and igneous intrusives suggesting that they were locally derived and subjected to short transport. A MIC (Mandamus Igneous Complex) provenance and a Torlesse basement source have been proposed for the clasts in the second conglomerate. The overall setting is perhaps distal alluvial fan to braided river to account for debris flow and fluvial conglomerate plus the formation of coal. Overall gradual erosion of hills is followed by marine transgression.

3.4.2 Waipara Greensand

The basal succession of the Waipara Greensand is characteristic of mudstone and siltstones interpreted as paralic deposits; however no structures or fossils indicate either a paralic or estuary type deposit, in contrast the presence of glauconite indicates an estuary or marginal marine-submarine depression. The absence of structures indicating a foreshore environment may be attributed to the presence of a local disconformity of the Waipara Greensand with underlying Broken River Formation, however this not overemphasized. In contrast the presence of glauconitc sandstones analysed further later indicate low sedimentation rate, therefore no significant break in sedimentation or erosion. The sandstones of the Waipara Greensand contain, 15-20% glauconite, and 7% marine fossils, 40% carbonate only for certain beds; therefore it is interpreted to be a marginal marine setting. Exposures of large cross bedded tabular foresets are interpreted as a shallow marine environment indicative of a foreshore setting. The presence of burrowed laminar sandstones marks a small shift towards a lower shoreface environment, above by a fair weather wave base. Coarse grained granule beds with disarticulated shells and sharks teeth are influenced by storm conditions. Fluctuations between fair weather and storm wave conditions are interpreted by the alternations of burrowed sands and hummocky cross stratified layers, while the shell beds up section mark large storm events.

Paleocurrent directions (fig. 3.6) indicate major south and south/south-east sources and minor north/north-east sources. The north and south directions are interpreted as currents produced from longshore drift while the north-east and south-east directions are interpreted as waves. This reflects a shallow marine-near shore environment where the glauconite and carbonates content increase up section during the transgression.

3.5 Glaucony as Sedimentation Indicator

3.5.1 Descriptions of Glauconite

The arenites within the Waipara Greensand at the Mandamus range in glauconite from 13 to 20% (appendices 1, 2, 4). Glauconite fecal pellets in granular form are the predominant form of glauconitic minerals. The pellets are generally medium to coarse with some very coarse. Samples from fine grained beds have fine glauconite grains. In the Mandamus Dove River area three varieties of glauconite have been observed; micaceous glauconite, nascent glauconite and evolved/mature glauconite. Glauconites are concentrated within parallel crossbeds within the Coal

Creek and Mandamus River while glauconite is concentrated in layers and laminations at the type section. However, at some beds in the Waipara Greensand glauconite occurs randomly.

The glauconitic minerals range from micaceous glauconites, expanded books of mica in which glauconitic minerals have grown between the sheets (fig. 3.10) and precipitates in intraskeletal cavities replacement of fossils (bryozoa) (fig. 3.9). The nascent variety is pale green with indistinct irregular boundaries (figs. 3.11, 3.12). The evolved/mature glauconite with a deep emerald green colour that is common at Mandamus described by Odin and Fullagar (1988) as highly evolved K rich glauconite.

The glauconite grains contain a high abundance of nascent and micaceous glauconite at sample localities such as Coal Creek (fig. 3.11) while at the Mandamus River higher in the section within the Mandamus River bed (fig. 3.1) the grains are well rounded indicating mature/evolved grains while some appear squashed and abraded by compaction at a post-maturity stage (figs. 3.14 & 3.15). Type B glauconite always appears as rounded pellets, sometimes deformed against adjacent grains (McConchie & Lewis 1978). Triplehorn (1966) gave a definition for type B grains as generally rounded, unbroken spheroidal, ovoidal and lobate grains. At the stratigraphic section B (Fig. 3.1), well rounded evolved/mature glauconies are also dominant but some are fragmented by detrital grains indenting those (figs. 3.16, 3.17, 3.18).

The texture of fibroradiated rims is evident in some glauconite grains in the Waipara Greensand especially in the basal sequence at Coal Creek (fig. 3.13). The fibroradiated rims coat the exterior of the glauconite grain. The presence of the rims (fig. 3.13) clearly indicate a period where precipitation and maturation was facilitated by a low sedimentation rate without significant clast input hence the fibroradiated rims being the progenitor of sedimentation.

The succesion at Coal Creek above the Broken River Formation (figs. 3.4, 3.11) is dominated by 24% glauconite; the nature of the glauconite is nascent followed by a high micaceous glauconite (fig.3.19) component which in turns marks an authigenic phase of dissolution-precipitation around a host mineral. The sequence up section is characterized by the nascent glauconite component being replaced by an increasing evolved/mature component (fig. 3.19).

At the Mandamus River bed (fig 3.1; (blue circle)) beneath the type section glauconite reaches 14%, glaucarenites contain a high frequency of evolved glauconies per sample with periodic increases in nascent glaucony. At the designated section B (appendix 1 fig.1.2), glauconite ranges from 8 to 22% and shows a rapid increase in evolved/mature glauconite in stratigraphic younger beds (fig. 3.19). The presence of minor micaceous glauconites and nascent glauconites marks a second authigenic phase. The general trend for the Mandamus glauconitic sandstones is an abundance of nascent and micaceous glauconite with low numbers of evolved/mature glauconite at the base of the Waipara Greensand while up section this trend reverses and an increase of evolved mature glauconite occurs at the expense of nascent and micaceous glauconite (Fig. 3.19). The nascent glauconite resembles closely the Type A glauconite described by McConchie and Lewis (1978, 1980) and the evolved/mature glauconite resembles the Type B glauconite.

3.5.2 Glauconite Interpretation

The Waipara Greensand is interpreted to have formed in shallow-water environments. The basal succession above Broken River conglomerates displays no evidence of unconformable contact just a gradual transgression. A large time span between the Broken River Formation at Haumurian times (Late Cretaceous) and the Waipara Greensand at Mangaorapan - Whaingaroan times (Early Eocene Late Eocene) indicating a slow sedimentation rate overall.

Stratigraphic, sedimentological and petrographic relationships negate the possibility that the glauconite grains are allochthonous. The Mesozoic basement and Cretaceous Igneous intrusives do not contain glauconitic minerals. Thus glauconite minerals could not have been derived by erosion of older basement rocks. Similar examples from other geographic regions of the world have been observed and interpreted (Chafetz & Reid 2000; Pasquini et al. 2004; Amorosi 1997).

The glauconitic sandstones at Mandamus contain a random distribution of poorly sorted nascent glauconite pellets in the basal succession of Coal Creek in lithological homogeneous succession. Amorosi (1997) interprets lithologically homogeneous successions with non selective spatial distribution of glaucony is likely to reflect an autochthonous origin of grains. In that case a low sedimentation rate is interpreted and an autochthonous origin. Other localities in Coal Creek and in the Mandamus River of the Waipara Greensand contain coarse evolved/mature glauconite grains within cross bedded sandstones. The glauconite grains that have been abraded and indented by quartz grains but retained the original well rounded mature nature are interpreted as parautochthonous. The alternation of glaucony-rich and glaucony-free layers can readily be assumed to indicate allochthonous origin of glaucony (Amorosi 1997). However, the evolved/mature glauconite grains when agitated in water disaggregate with relative ease. Glauconite grains would need to have been transported from the source to the locus of deposition locally before they displayed the inevitability of dissagregation. A parautochthonous origin is likely for the cross bedded sequence that display high energy conditions and hence compacted glaucony grains. Amorosi (1997) discusses that the association of glaucony with high-energy and/or reworked deposits should not necessarily be regarded as diagnostic for an allochthonous origin of grains. In transgressive successions, glauconitization commonly post – dates coarse-grained sedimentation in nearshore areas (Amorosi 1997).

The presence of nascent glauconite grains in fine detrital sands(tidal estuarine environments) with fibroradiated rims are interpreted as clearly pre-dating clastic input, the increase up the stratigraphic section of evolved/mature grains in coarse cross bedded sands (foreshore environment) which show well rounded grains indented by detrital grains are interpreted to mark pre-clastic input conditions. While evolved glauconites in alternating quiescent conditions (lower shoreface) all point towards glauconitization that post-dated coarse grained sedimentation. Overall the morphology of the grains indicates low sedimentation.

The glauconites are interpreted as autochthonous-parautochthonous hence a low sedimentation rate is proposed for the Waipara Greensand at Mandamus thus accounting for the large time-span from Broken River Formation deposits and pre-Waipara Greensand deposits.

3.6 Provenance

3.6.1 Clast Counts

The clast counts performed on the Broken River Formation conglomerates suggest multiple sources for the lower conglomerate (fig. 3.7, A). The clast count revealed that 59% of the clasts are greywacke-argillite, clasts indicative of a Torlesse Supergroup basement source, while 27% are white, fine quartzose friable sandstone clasts, indicative of a possible local source. The non indurated state of the clasts suggests they were probably derived locally from a pre-Broken River Formation source. The Monro conglomerate which occurs at the southeastern Harper Hills (southern Malvern) could have accounted for the quartzose fine sandstone clasts. The Monro Conglomerate is pre-Haumurian and its thickest occurrence is at the Harper Hills area (Andrews 1987). According to Andrews (1987) and Mathews (1989) the clasts are predominantly rhyolite derived with quartzose grit and sandstone. The Monro Conglomerate is possible a source for the white sandstone clasts. The rest of the clasts are mudstones and siltstones, 5 and 6% respectively.

The upper conglomerate above the coal bed is also of polymictic composition (fig.3.7, B) with 58% of the clasts composed of trachyte similar to the underlying Mandamus Igneous Complex. The other 14% and 9% of the clasts are microsyenite and syenite composition indicating erosion of the hypabyssal part of the Mandamus Complex source. A small percentage is altered volcanic clasts possibly basalt clasts, from dikes in the Torlesse while the remaining 16% is of greywacke clasts indicating a Torlesse basement. A Mandamus Igneous complex source is suggested for the upper conglomerate based on the clast composition with a remaining Torlesse basement source.

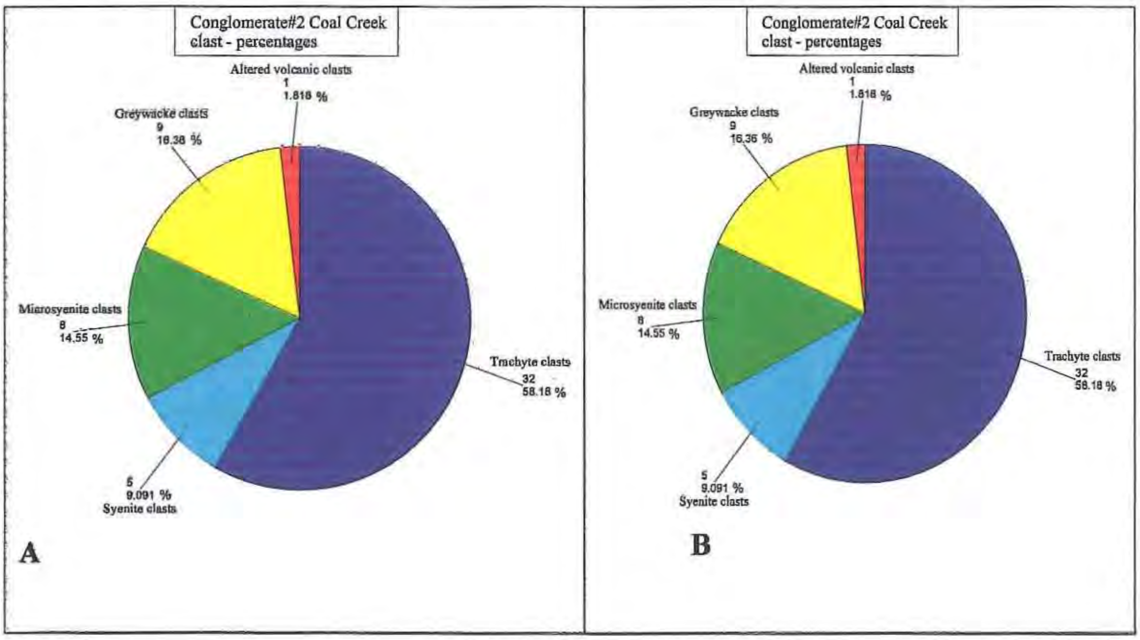

Figure 3.7: Pie diagrams depicting source types for the conglomerates at Coal Creek. **A)** Basal conglomerate polymictic, matrix supported, multiple source predominantly greywacke-white sandstone clasts. **B)** Clast supported polymictic conglomerate predominant source types volcanic and greywacke clasts.

3.6.2 Sandstone Composition

Compositionally the Waipara Greensand is subarkosic arenite. The samples have minimal lithic components. The samples have an average of 15-20% glauconite

(Appendices 1, 2 ,4), (see glauconite section for detail). Sparry calcite cement and micrite matrix is common in some samples. Some other intragranular allochems are echinoderms, foraminifera and bryozoa (Appendix 1, figs. 3.8 & 3.9). Feldspars are generally alkali feldspar and minor plagioclase (Appendix 1, see QFL composition section). Accessory minerals are muscovite, chert, and calcite matrix and cement (micrite and sparite). Calcite matrix ranges from 2-30% in the arenites and reaches up to 49% within the tabular cemented sandstones. Micas are minor 1.4% and are confined to the muscovite variety.

The Waipara Greensand subarkosic arenites are bimodal with well rounded coarse sand to granule size quartz grains in the basal Waipara Greensand and a mode of subangular to angular fine sand up section. The basal Waipara Greensand in Coal Creek and Mandamus River display a higher proportion of polycrystalline (figs. 3.20 & 3.22), coarse and granule quartz grains with higher degree of rounding compared to the arenites up section which display higher degree of subangular-angular grains. Occasional coarse arenites occur up section, however at lesser degree than at the base of the formation. Overall there is bimodal distribution of coarse to granule sand and fine sand.

The petrographic samples from the Waipara Greensand were conventionally point counted at 300 grains in total (appendix 2). The quartz, feldspar and lithic components were recalculated and normalized to 100% ignoring the other minerals and matrix (appendix 3). The arenite samples collected from Coal Creek and Mandamus River within the Waipara Greensand are compositionally subarkose (Fig 3.27, A); lithic component is minor. The subarkose arenites, plot in an interior craton tectonic setting (fig. 3.27; A).

The feldspars are dominated by 97-100% Alkali type, orthoclase and some microcline feldspar with minor plagioclase (appendices 2, 3). Orthoclase was identified by its optical axis interference figure noted as being biaxial negative with a large 2V angle. In general orthoclase and microcline appear to be by far the most abundant potassium feldspars in sandstones (Boggs 1992).

Plagioclase occurs in the Waipara Greensand, however to a lesser degree than its alkali feldspar counterpart. Plagioclase was distinguished through optical interference figures; however the distinction between albite and unzoned plagioclase was done clearly on the presence or absence of twinning. The lithic components are at 1-7% dominated by sedimentary lithoclasts.

Alkali feldspars are essential constituents of several rocks such as felsic igneous rocks, pegmatites and many felsic and intermediate gneisses and are the most common framework grains in sands and sandstone after quartz (Shelley 1985; Boggs 1992). They are especially abundant in syenites, granites, granodiorites and their volcanic equivalents (Shelley 1985). Shelley (1985) describes that in felsic plutonic rocks and high grade metamorphic rocks, the alkali feldspars are usually orthoclase and microcline while in volcanic rocks sanidine and anorthoclase is common. Therefore a felsic plutonic and/or high grade metamorphic source is likely while a granitic source is also possible. Plagioclase occurs commonly in volcanic and metamorphic rocks and is abundant in igneous rocks (Shelley 1985).The minor percentages of plagioclase source of felsic/plutonic and/or metamorphic rocks are likely. The Mandamus Igneous Complex is the most likely source.

Muscovite is common in regionally metamorphosed rocks, especially those derived from pelitic sediments (Shelley 1985). Muscovite occurs also in granites and pegmatites (Boggs 1992). Since the detrital muscovites are minor and confined to finer grain sizes a general interpretation of low grade metamorphic or granitic source is made.

Lithics or rock fragments provide source type lithologies, however the presence of minor lithics are confined to sedimentary ones thus being fine sandstone and chert. The minor occurrence of those sedimentary lithics is interpreted as reworking from the underlying fine grained greywacke-argillite Torlesse basement. This interpretation is most likely given the Torlesse conglomerate clasts in Coal Creek.

In summary QFL indicates a local source from the underlying Torlesse Group and Mandamus Igneous Complex with a possible minor plutonic or metamorphic source.

3.6.3 Quartz Provenance (SEM-CL)

The integrated SEM-CL/optical microscopy provenance technique of quartz was applied to the Waipara Greensand's glauconitic subarkose arenites. 105 selected quartz grains were analyzed with integrated SEM-CL/optical analysis in each sample following the technique devised by Bernet and Bassett (2005). Detrital quartz was compared for its CL and optical properties (appendices 5, 6) as described in chapter 2.

The Mandamus area was sampled from the Coal Creek and Mandamus River localities (Fig. 3.1; (locations A, B& blue circles)), for SEM-CL/Optical analysis. The same samples used in petrographic point counts were also used in CL analysis.

About 38% of the grains are plutonic in the basal sequence while that component increases to 41% in the finer sands up section which are angular.

Grains with strong undulose extinction and black-dark CL and/or polycrystalline were interpreted as metamorphic. The samples within the basal Formation in Coal Creek and Mandamus River display a higher percentage of metamorphic grains. In fact ~ 58% of the quartz grains are of metamorphic origin. The majority of metamorphic grains are coarse to very coarse, well rounded and polycrystalline in the basal sequence appearing black in SEM-CL images (figs. 3.21-3.22, 3.23-3.24). The majority of polycrystalline grains are polygonized and polyhedral while grains displaying abundant crenulated quartz are also present. The polygonized metamorphic quartz was identified as merely deformed low grade quartz whereas the recrystallized and crenulated quartz was identified as high grade metamorphic quartz. Up section, the metamorphic quartz grains at 53% slightly decrease at the expense of plutonic grains (appendix 5, figs. 5.1-5.2; fig. 3.25); while further upsection the metamorphic component increases relative to the plutonic one (appendix 5 figs 5.3-5.4; fig. 3.25).

The volcanic quartz component is at a minimum compared with the plutonic and metamorphic components. At the base of the sequence volcanic quartz is at about 3.8% while up section it is 13% (Fig. 3.25).

The data obtained from the SEM-CL/optical microscopy technique reveal that there is a strong bimodality of plutonic versus metamorphic grains (Fig. 3.25), with the metamorphic source type being the dominant one. The volcanic type is very low.

Samples have well rounded polycrystalline-metamorphic quartz grains at the base of the section displaying textural maturity with significant percentage of angular plutonic grains. Bernet and Bassett (2005) in a preliminary study interpret the well rounded polycrystalline grains as transported by longshore currents and the more angular quartz grains transported by fluvial processes.

The evidence of coarse well rounded metamorphic grains within cross bedded sandstones clearly indicates long distance transport by longshore currents while the angular plutonic grains indicate transport by rivers. Quartz sand when transported in shallow marine environments becomes very well rounded through reworking by waves on the shoreface while texturally immature sands are characteristic of fluvial conditions (Chandler 1988). According to Moss (1972) granitic quartz displays fragmentation under fluvial conditions.

Bernet and Bassett (2005) suggested that there is a striking relation between certain quartz types and grain rounding and/or grain size, with plutonic quartz grains dominating the medium to fine fraction and metamorphic quartz dominating the very coarse to coarse fraction. That initial estimate is partially confirmed by the trends of quartz types (Fig. 3.26). Samples CC4b, CC3 and MGS1 are coarse to very coarse with higher metamorphic grains to angular plutonic grains. However a significant percentage of medium and coarse plutonic grains which are subrounded-subangular also occur in the samples; while in samples tpgs-11 and tpgs-15 high metamorphics compared to plutonics occur in finer grain sizes. Therefore this trend should not be over interpreted.

The dominance of deformed plutonic grains displaying strong undulose and polygonized, characteristics (appendix 6) are interpreted to mark deformation by mild regional metamorphism or by regional deformational events. Therefore the plutonic grains with polygonized and strong undulose characteristics are indicative of lower levels of deformation. The dominance of well rounded polycrystalline metamorphic quartz grains displaying recrystallized quartz and in some cases crenulated grains are indicative of low to high grade metamorphism. Although the metamorphic quartz is determined by the combined SEM-CL/optical microscopy, the grade of metamorphism is established by the structures and textures of the grains in conventional microscopy. Lower grade rocks are characterized by a diversity of crystal sizes polygonized to recrystallized (50µm-500µm) while high grade rocks have slightly larger crystal sizes (Young 1976).

The trends of the quartz types depict overall a bimodality of metamorphic versus plutonic with a minor volcanic quartz type which is evident through out the succession (fig. 3.25). The provenance of quartz is dominantly metamorphic and plutonic with a minor volcanic source.

The metamorphic source is more likely regional than local because the Torlesse basement is too fine grained to produce large polycrystalline quartz grains. Bernet and Bassett (2005), while suggesting distant plutonic or metamorphic sources make alternate suggestions of local derivation of plutonic quartz from the Mandamus Igneous Complex syenite-trachytes.

The volcanic grains are a minor constituent hence they are more likely derived from the distant Mount Somers Volcanics than the local intrusives because trachytes are compositionally low in quartz. Shelley (1993) describes a quartz-bearing syenite as a plutonic rock transitional between syenite and granite with quartz being from 5 – 20%. The same occurs for trachyte, hence the interpretation that the local igneous intrusives play a minor to insignificant source for a volcanic source type or for a plutonic source.

The plutonic quartz signature is interpreted to have been derived from a distant plutonic suite provenance, likely a western granitic source (Karamea Batholith, Separation Point Batholith) while the metamorphic quartz is either derived from a metamorphic terrane such as the southern Otago/Haast Schist by southern longshore drift or by a western quartzite source. A minor volcanic source type is the distant Mount Somers Volcanic field (fig. 3.27, B). In comparison the QFL suggests at least some local source for the sedimentary lithics and for the alkali feldspar, in this case a regional source and local minor source are possible.

3.7 Summary of Results for Mandamus Area

The Mandamus area, North Canterbury, consists of a Late Cretaceous -Tertiary sequence that overlies Late Cretaceous intrusives of the Mandamus Igneous province and Torlesse basement which is Early to Late Jurassic. The basal sequence consists of interbedded conglomerates with coal of the Broken River Formation at Haumurian age (Late Cretaceous) which overlies unconformably Torlesse basement. The Broken River formation consists of a lower, poorly sorted, matrix supported polymictic conglomerate interpreted as a debris flow succeeded by peat deposition and coal formation; followed by fluvial activity, braided river setting and deposition of a clast supported polymictic conglomerate. Thus the succession reflects an alluvial-fluvial terrestrial depositional environment succeeded sharply by the shallow marine near shore sequence – Waipara Greensand.

The Waipara Greensand reflects sedimentation that began with a marine transgression in the Eocene. The Tertiary succession begins with thin mudstone-siltstone layers that indicate a possible estuarine setting followed by glauconitic, fine-medium quartzose sandstones with occasional coarse sands and quartz granules. The glauconitic sandstones are cross bedded to massive and laminated succeeded by shell beds. Thus the Waipara Greensand marks a foreshore to lower shoreface setting occasionally affected by storm events. Paleocurrents reflect south-south east with minor north and north east directions indicative of longshore drift and minor waves.

The abundance of glauconite and especially the transition of nascent and micaceous glauconite to mature/evolved glauconite upsection within lower shoreface to foreshore conditions challenged the traditional view of glauconite formation in deep marine settings. The abundance of evolved mature glauconite marks an autochthonous – parautochtonous mode of formation for glauconite hence a low to medium sedimentation rate for the Waipara Greensand for the area. The glauconite content and the carbonate matrix indicated a shallow marine depositional setting.

Provenance from clast counts for the Broken River Formation conglomerates show a local source of Torlesse Basement for the greywacke clasts and a secondary possible Monro Conglomerate regional source for the quartzose sandstone clasts. The upper conglomerate shows also a local provenance of the Mandamus Igneous Complex for the trachyte and microsyenite-syenite clasts while a small percentage of greywacke clasts show a local provenance from Torlessse.

Provenance of QFL components indicates a subarkose arenite typical of a craton interior setting. The dominance of alkali feldspar indicated a local felsic igneous source while an alternative metamorphic and/or plutonic regional source was possible. The minor presence of sedimentary lithics indicated subsequently a minor provenance contribution from the fined grained Torlesse Basement. Plagioclase feldspar at a lesser degree indicated a similar source while a minor muscovite percentage indicated a granitic/pegmatitic source however a metamorphic provenance was also possible.

The application of the SEM-CL/Optical microscopy technique on quartz provenance for the Waipara Greensand revealed a strong bimodality of metamorphic to plutonic quartz types and a minimal volcanic quartz type. This provides a strong metamorphic terrane source more likely the Otago/Haast Schist or Alpine Schist which accounts for polycrystalline highly metamorphosed quartz grains being transported from the source areas by longshore currents and a granitic suite possibly the western Karamea Batholith or Separation Point Batholith as a source for the plutonic quartz grains delivered perhaps by fluvial drainage. The minor volcanic quartz type is indicative of a distant volcanic field more likely the Mount Somers Volcanics rather than the local Mandamus Igneous Province.

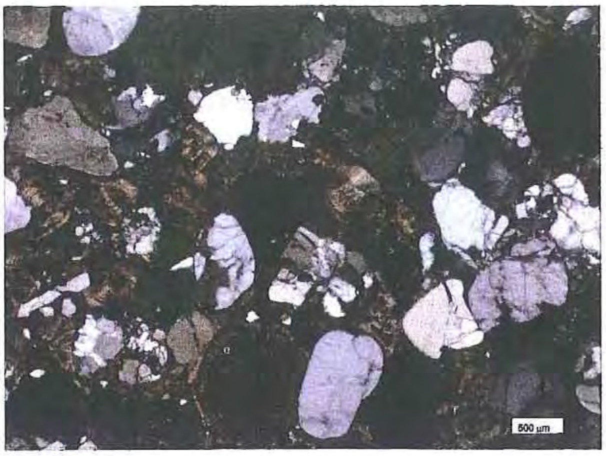

Figure 3.8: optical micrograph of intragranular allochems, (e = echinoderms, f = foraminifera).

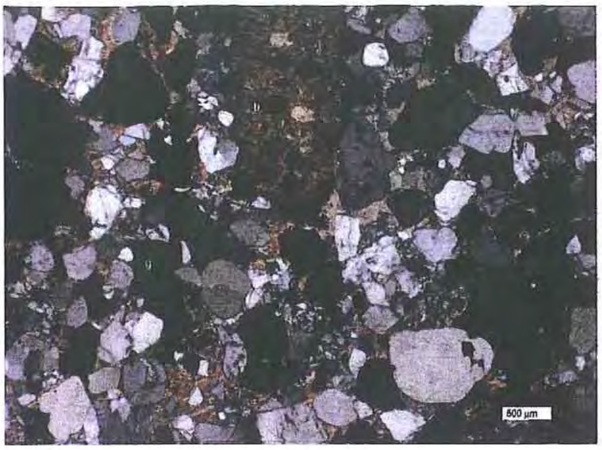

Figure 3.9: optical micrograph of intragranular Allochems, (b = bryozoa, g = glauconite).

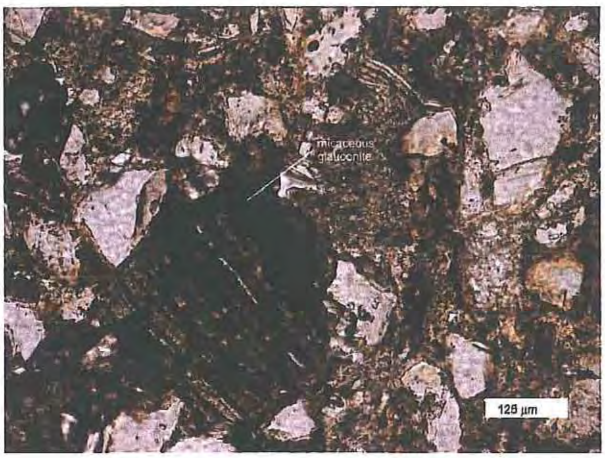

Figure 3.10: optical micrograph (plane polarized light) of micaceous glauconite variety in sample cc1b (Expanded "book" of mica).

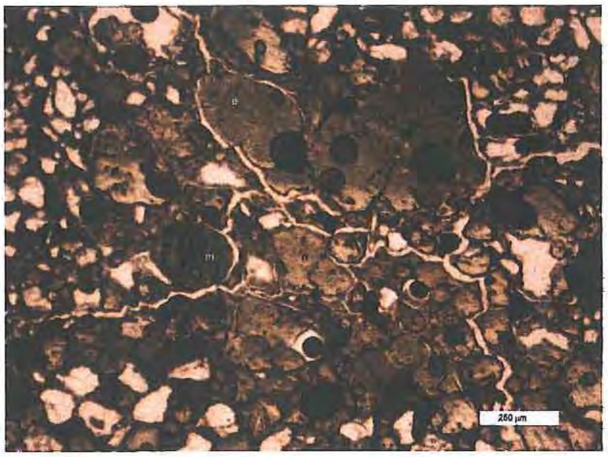

Figure 3.11: optical micrograph (plane polarized light) of glauconite types in Coal Creek sample cc1b, (m= glauconite, n = nascent – pale green, e = evolved /mature).

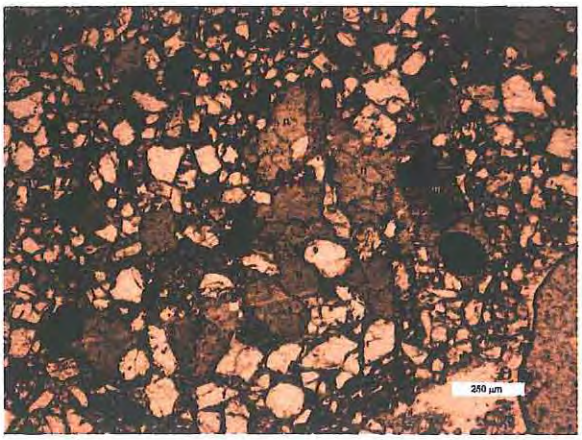

Figure 3.12: optical micrograph (plane polarized light) of glauconite in sample cc1b (n = nascent glauconite, m = micaceous glauconite, e = evolved glauconite).

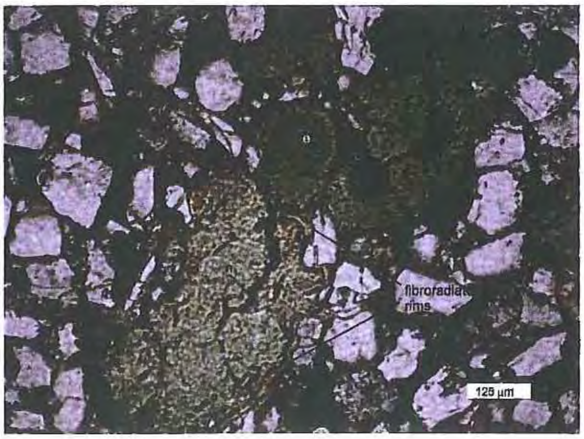

Figure 3.13: optical micrograph of glauconite grain displaying fibroradiated rims around (yellow lines), e = Evolved, n = nascent, (sample ccb1 = Coal Creek).

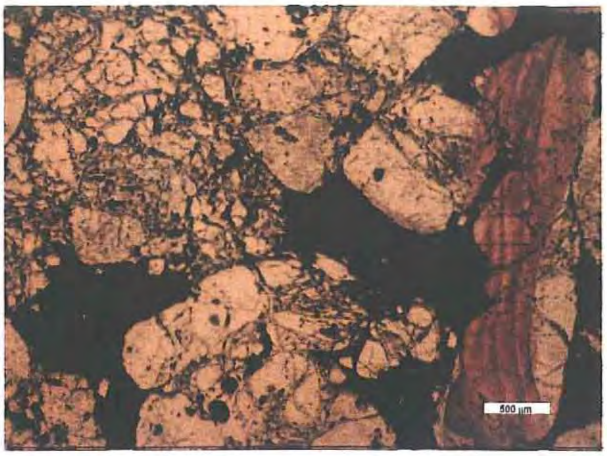

Figure 3.14: Sample MGS1, optical micrograph polarized light) of glauconite. (e = evolved/mature Glauconite).

Figure 3.15: SEM micrograph of glaucony grain from sample MGS1 depicting evolved/mature glaucony Indented by detrital grains.

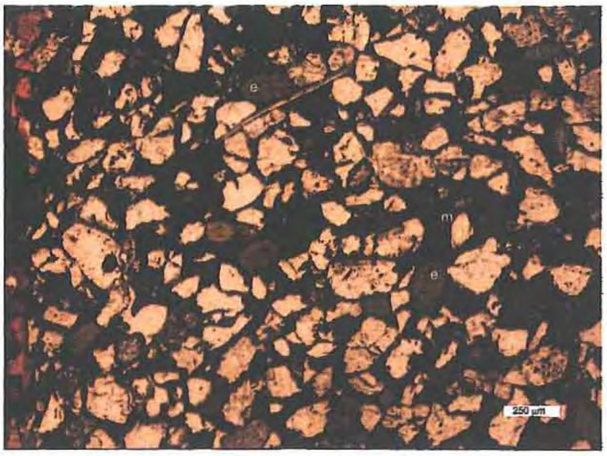

Figure 3.16: Sample TPGS1, optical micrograph polarized light) glauconite grains display Evolved/mature well rounded (e = evolved, m = Micaceous glauconite).

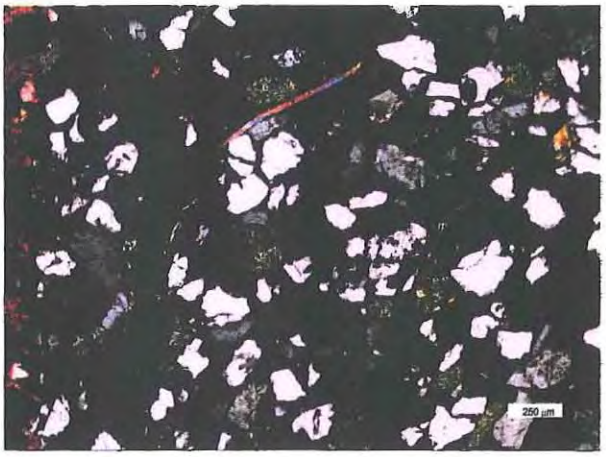

Figure 3.17: Sample TPGS1, (cross polarized (plane

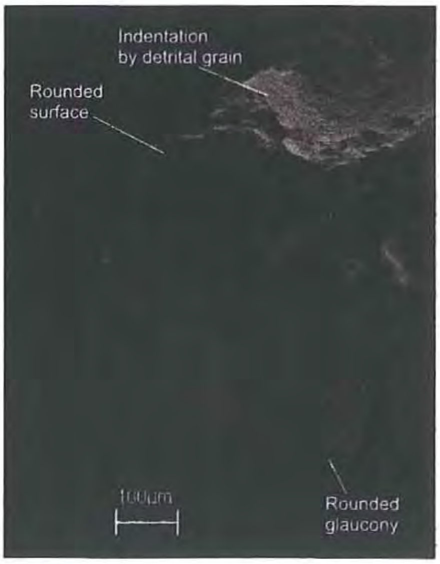

Figure 3.18: SEM micrograph of single glaucony grain displaying abrasion and indentation by detrital grains.

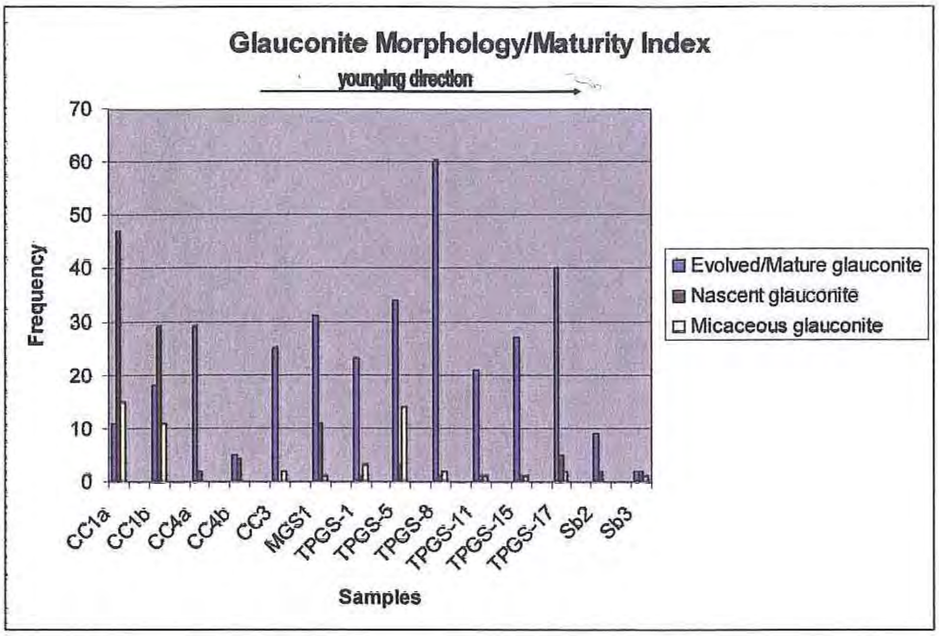

Figure 3.19: Frequency of glauconite grains displaying nascent stage, evolved/mature glauconite and micaceous glauconite. Evolved-mature glauconite increases up section at the expense of decreasing nascent glauconite up section. The sharp rise of micaceous glauconite represents a second growth episode.

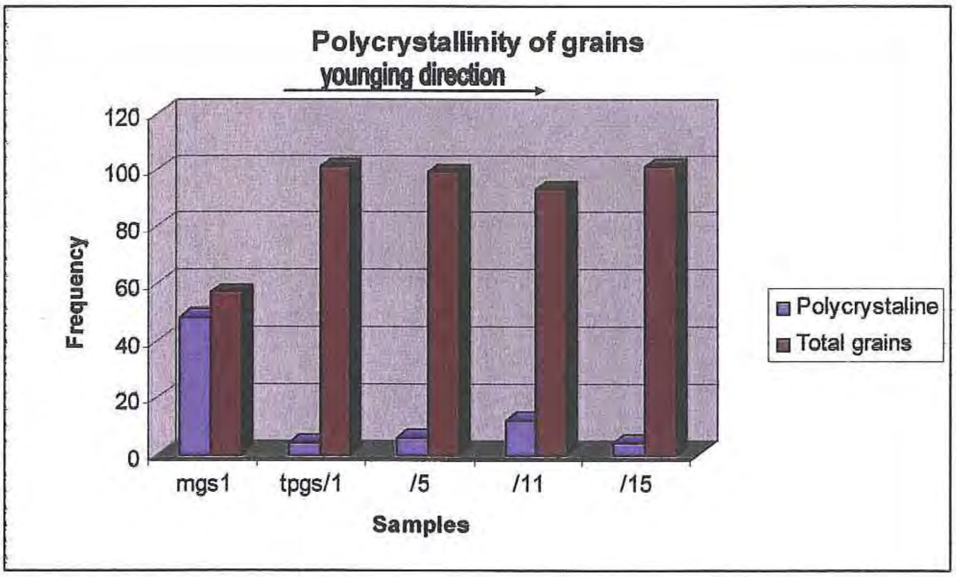

Figure 3.20: Proportion of polycrystalline grains compared with total amount of grains from the base of the Formation to the top.

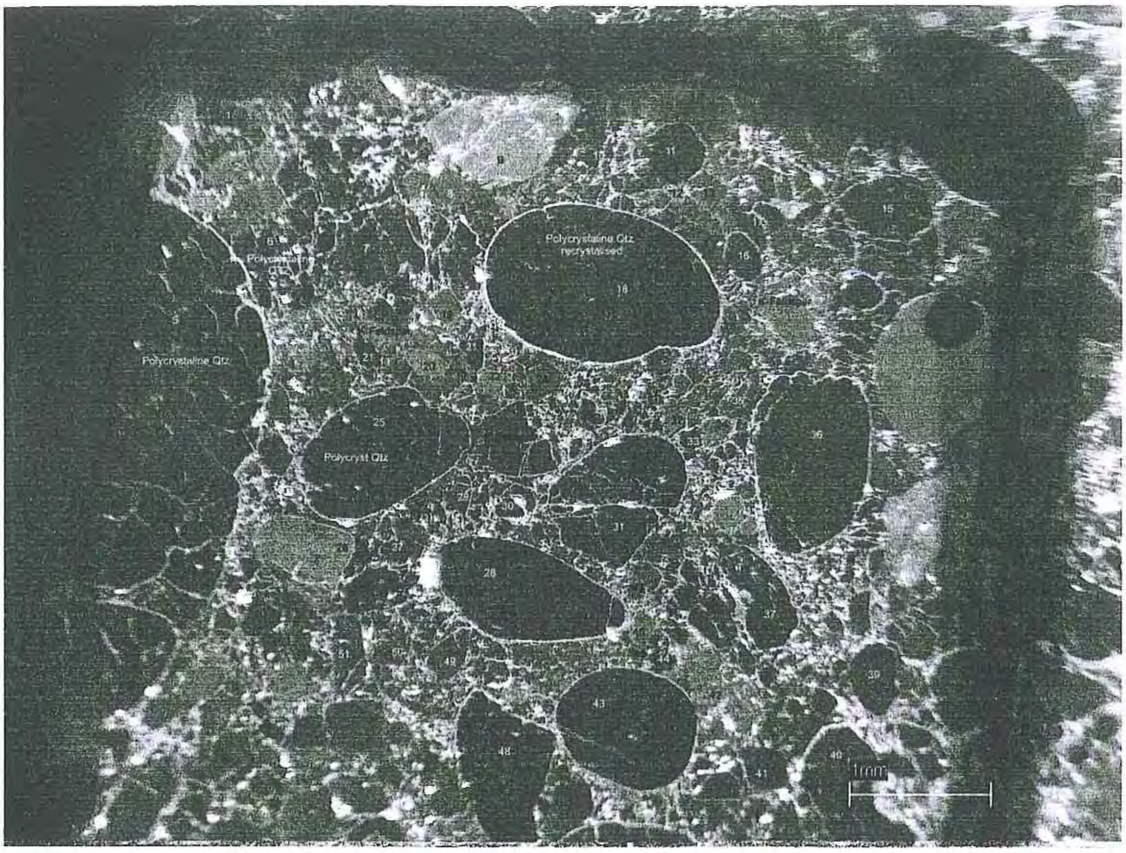

Figure 3.21: Sample cc4b, SEM-CL image of the Waipara Greensand at Coal Creek

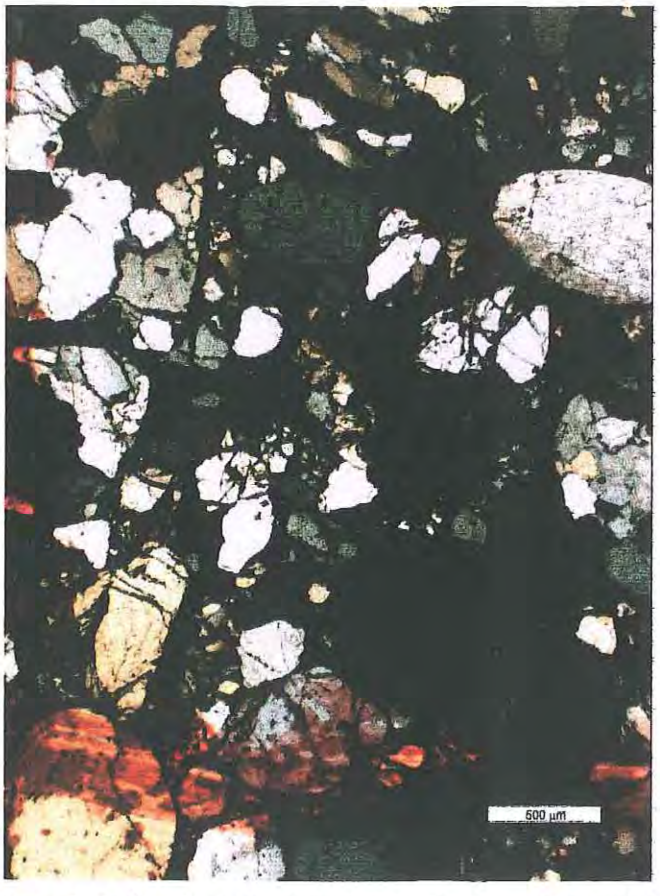

Figure 3.22: Sample cc4b, photomicrograph, cross polarized light

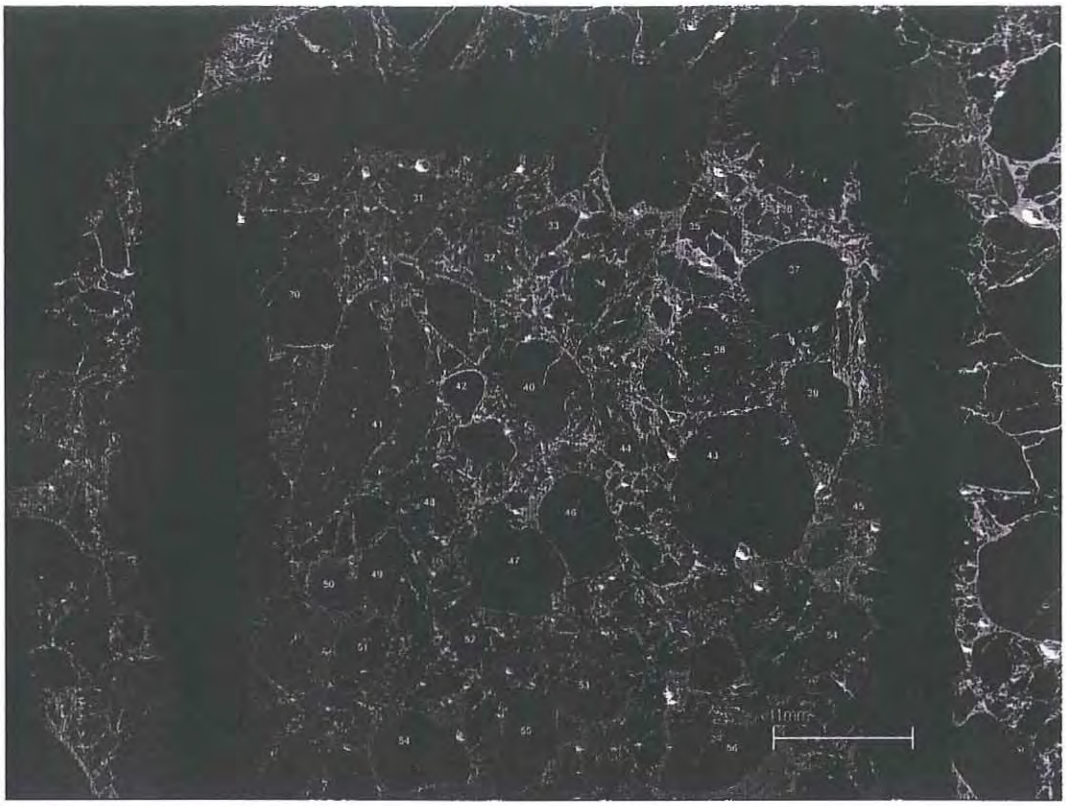

Figure 3.23: Sample MGS1, SEM-CL image of the Waipara Greensand at Mandamus River.

Figure 3.24: Sample MGS1, photomicrograph, cross polarized light.

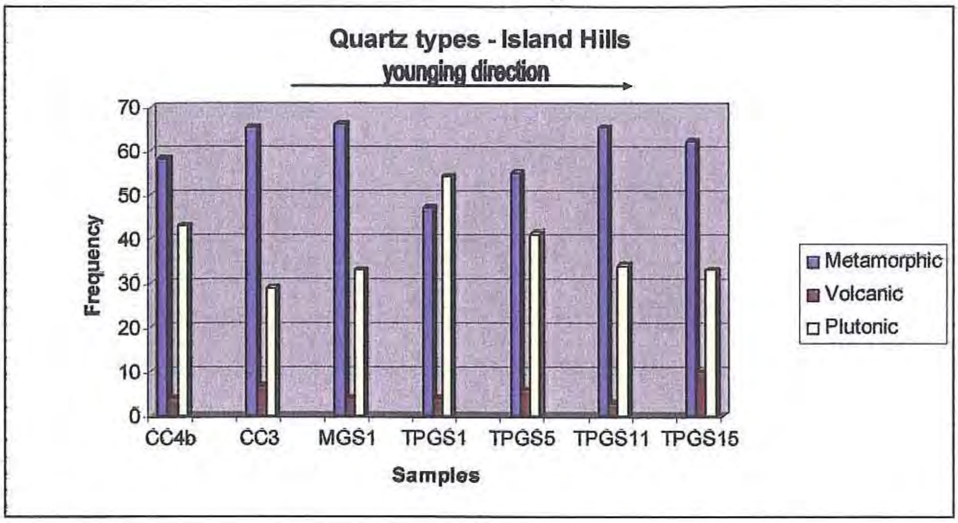

Figure 3.25: Frequency of grains displaying quartz types per sample from the basal Waipara Greensand to the upper beds. Metamorphic and Plutonic quartz types are dominant while the volcanic component is kept to a minimum.

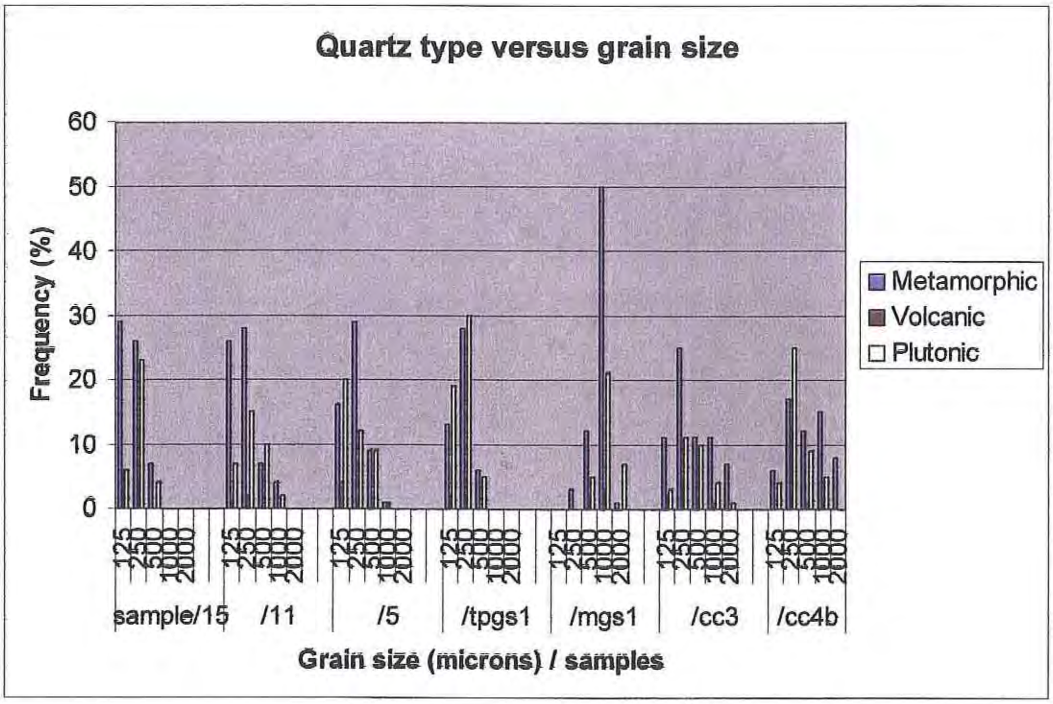

Figure 3.26: Frequency of quartz grains displaying quartz types per sample and per grain size.

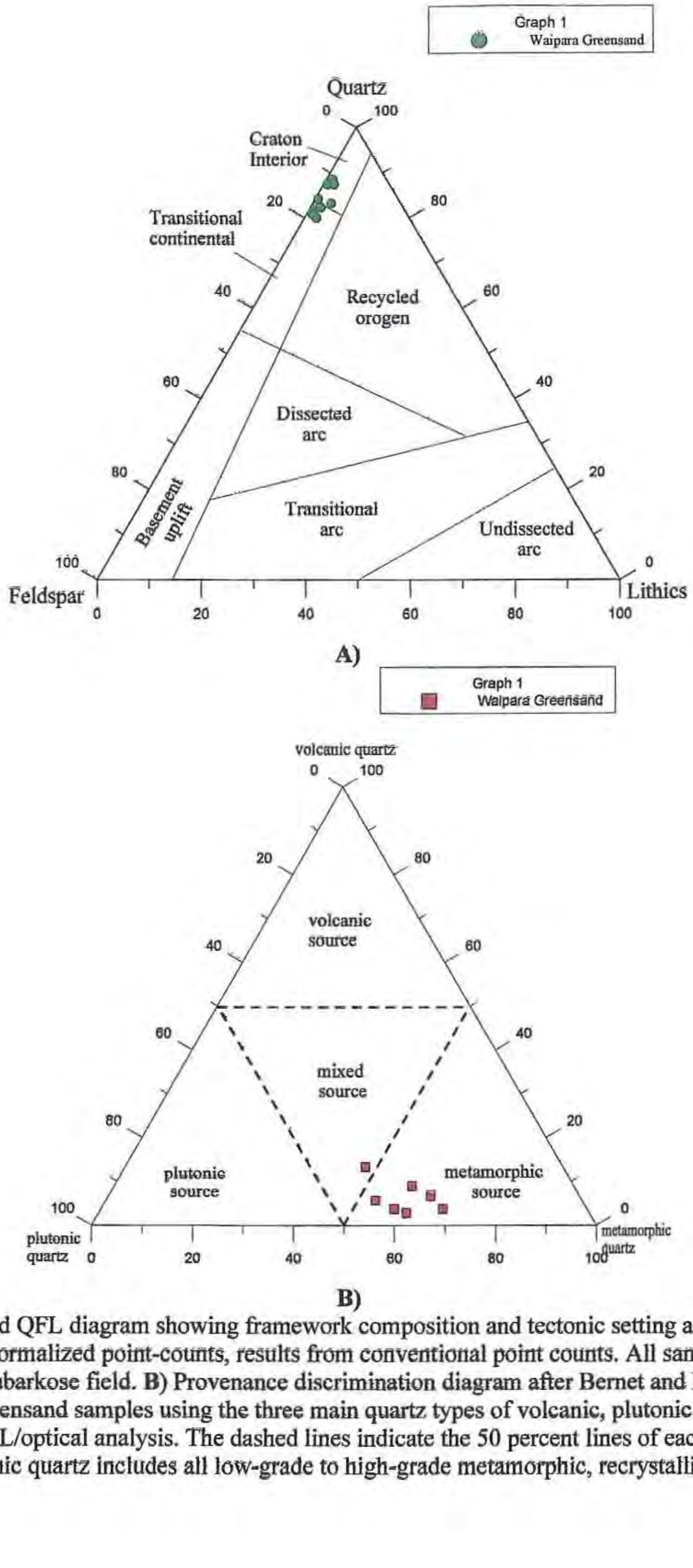

B)

Figure 3.27: **A)** Standard QFL diagram showing framework composition and tectonic setting after Dickinson et al (1983), on the basis of normalized point-counts, results from conventional point counts. All samples of the Waipara Greensand, plot in the subarkose field. **B)** Provenance discrimination diagram after Bernet and Bassett (2005), of Mandamus Waipara Greensand samples using the three main quartz types of volcanic, plutonic and metamorphic quartz, based on SEM-CL/optical analysis. The dashed lines indicate the 50 percent lines of each of the three main quartz types. Metamorphic quartz includes all low-grade to high-grade metamorphic, recrystallized, and vein quartz.

CHAPTER FOUR
WAIPARA RIVER

4.1 Regional Geologic Setting & Previous Work

The Waipara River section is accessed from State Highway 1 by turning into Georges Road ~ 1 km south of the Waipara River Bridge and then following Ram Paddock Road for 13 km. Turn northwards onto Laidmore Road and follow the road down into the river bed. A complete sedimentary succession is exposed for much of the length of the river, with sporadic un-exposed cliff and hillside sections. The sedimentary succession incorporates the length of the River from the entry into Doctors Gorge (Ohuriawa Gorge on topo/nz maps, 2474455E, 5794745N) to the top of the Amuri Group in the lower gorge (grid reference GPS: 2478895E, 5794405N).

For the purpose of this thesis the succession incorporates the area from Doctors Gorge (Ohuriawa Gorge, 2475494E, 5794550N) mid-upper Waipara downstream to the locality westwards before the Laidmore Road crosses through the Waipara River (2476375E, 5794010N) (fig. 4.1).

Structurally, the mid-Waipara River section lies on the south eastern limb of the Doctors Anticline (Wilson 1963, fig.4.1). The Tertiary stratigraphy spans the Early Cretaceous to mid Oligocene on Torlesse Supergroup basement rocks of Early Jurassic to Late Jurassic age. These form the hills towards the northwest to the Amuri Group limestones which form a prominent strike ridge to the southeast (fig. 4.1) (Morgans et al. 2005).

The oldest Tertiary stratigraphy is the Broken River Formation which overlies unconformably Torlesse Supergroup rocks close to the head of Doctors Gorge (Ohuriawa Gorge) (Morgan s et al. 2005).

The Waipara River area has a long history of geological observations and collections. Detailed mapping and collection of data occurred throughout the 19th and 20th centuries from an array of geologists, particularly from locations within the Waipara River and its various branches and tributaries (Morgans et al. 2005). The previous literature is too enormous to mention here and it is not the purpose of the thesis.

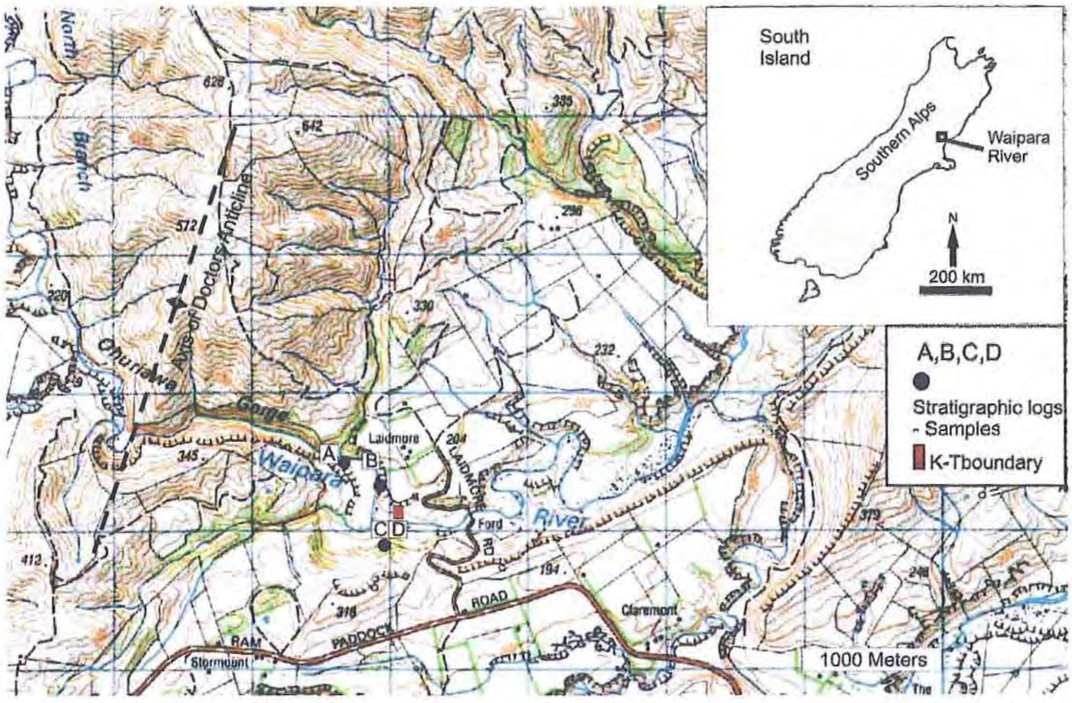

Figure 4.1: Topographic map of the mid-Waipara River outlining measured strtigraphic logs: A, B, C, D, and sample localities.

However, just to mention a few, Owen (1861) made the first discoveries of fossil marine reptiles followed by Hector (1869, 1874), Haast (1870), and Hutton (1894). Further discoveries of fossil fauna continued with Fordyce et al. (1986), Fordyce and Jones (1988), while a number of studies focused on palynology and stratigraphic successions (Morgans et al. 2005). Other researchers focused on the Cretaceous/Tertiary (K/T) boundary transition (Brooks et al., 1986a, b;Hollis and Strong 2003).

An array of authors focused on the stratigraphy and the structure of the mid-Waipara River section such as Jobberns (1937), Gregg (1959, 1978), Wilson (1963), Smale (1983), Browne and Field (1985), Andrews et al. (1987) and Field et al. (1989).

The oldest Tertiary stratigraphy consists of the Broken River Formation which unconformably overlies older Torlesse Supergroup terrane rocks. This sequence is then followed by the Late Cretaceous Conway Formation and subsequently followed by the Loburn Mudstone and the Waipara Greensand.

4.2 Stratigraphy

The mid Waipara River is characteristic of succession of Late Cretaceous sedimentary rocks (Haumurian) (Roncaglia and Schioler 1997), which rests on Torlesse Supergroup. The Broken River Formation that unconformably overlies the basement rocks consists of scarce basal conglomerates and sandstones. Subsequently the Broken River Formation is overlain by the Conway Formation which has a Late Haumurian age (Late Campanian/Early Maastrichtian-Late Maastrichtian (Roncaglia & Schioler 1997). It is a sandy siltstone with saurian bearing concretions (Morgans et al. 2005). The Loburn Mudstone lies conformably on the Conway Formation and its age is Teurian (Paleocene) (Roncaglia & Schioler 1997). The contact with the underlying Conway Formation is accepted as the K-T boundary.

The Loburn Formation is succeeded conformably by the Waipara Greensand having a Teurian to Waipawan (Paleocene to Early Eocene) age. The Waipara Greensand is succeeded stratigraphically by the Ashley Mudstone which is Early Waipawan (Early Eocene) at the base, to Kaiatan (Late Eocene) at the top (Brown & Field 1985). The succession is then followed by the Amuri Limestone, according to Morgans et al. (2005) it is Late Eocene (Kaiatan-Runangan) to Oligocene (Whaingaroan).

4.2.1 Basement Rocks – Torlesse Supergroup

The basement rocks consist of Torlesse terrane rocks which underlie the Late Cretaceous – Tertiary sequence. The basement is composed of complexly deformed interbedded greywacke and argillite (Nicol 1993).

4.2.3 Broken River Formation

The Broken River Formation at Doctors Gorge (Ohuriawa Gorge) is 40 metres thick and is a marginal marine unit composed of quartz sandstones. Hector (1887) did early work on an intraformational *Ostrea* bed and Wilson (1963) did work on the stratigraphy and mapped the mid-Waipara area while Browne and Field (1985) revised the stratigraphy of the region with emphasis on the Waipara River area.

At other localities in the Waipara such as Birch Hollow, a nonmarine basal conglomerate section has been studied. This is subsequently overlain by sandstones of the Broken River Formation. The base of the Broken River Formation consists of a 20-40 metre thick conglomerate (Morgans et al. 2005). Nicol (1993) reports a local source for the basal conglomerates with the deposit composed largely of Torlesse Group 10 cm argillite clasts with red chert, siliceous material and mudstone intraclasts. Brown and Field (1985) also made reference to the conglomerates as 'coarse clasts 1.5 m diameter that consist of angular to rounded greywacke sandstone with less abundant white quartz, red chert and weakly indurated "penecontemporaneous sandstone". Roncaglia and Schioler (1997) refer to the Broken River Formation as a non-marine unit with minor marine incursions.

The Birch Hollow locality with the preserved conglomerate section was not visited in the field for data collection for the Waipara area.

4.2.4 Conway Formation

The Conway Formation gradationally overlies the Broken River Formation. It is thick 185 metres thick. Earlier work done by Warren and Speden (1978) coined the name Conway Siltstone for a "dark grey massive jarositic siltstone with scattered spherical calcareous concretions". Browne and Field (1985) presented an overview of the Formation. Early nomenclature for the Conway Formation includes 'Saurian Beds' (Haast 1871), 'Saurian Sands' (Park 1988), 'Sulphur Sands' (Mason 1941) and Laidmore Formation (Webb 1971).

4.2.5 Loburn Mudstone

The Loburn Mudstone lies conformably on the Conway Formation. It is 12 metres thick in the mid-Waipara River. Browne and Field (1985) described the Formation as "black or dark grey, brown or purple, soft to moderately indurated, calcareous and non-calcareous, jarositic, micaceous, burrowed sandy mudstone". Andrews et al (1987) refer to the formation as being "slightly glauconitic".

4.2.6 Waipara Greensand

The Waipara Greensand erected by Hector (1884) for beds exposed in the Waipara River was described by Thompson (1920) who separated the Formation into lower alternating hard and soft green sandstone and an upper unit of softer dark greensands with argillaceous matter and shaly partings. Browne and Field (1985) subsequently subdivided the Formation into the lower Mt Ellen Member and the upper Stormont Member.

The Formations including the Broken River and Conway Formations as well as the Loburn Mudstone and Waipara Greensand were selected in this thesis for data collections and stratigraphic correlation as the regional correlatives to the Broken River Formation and Iron Creek Formation.

4.3. Sedimentary Descriptions

4.3.1 Broken River Formation

The exposure of Broken River Formation in mid-Waipara River is confined to the Doctors Gorge (Ohuriawa Gorge) locality (fig. 4.1; section A) where it is 40 metres thick (appendix 1 fig. 1.4); the exposure has a gentle 20 degree dip orientation towards the south-southeast. The Broken River Formation unconformably overlies Torlesse basement although the nature of the contact is covered by vegetation. Elsewhere in the Waipara River area, Nicol (1993) reports an unconformable contact. The exposure of Broken River Formation in mid-Waipara River was measured from 20cm to 1 metre intervals recording sedimentological detail such as structure, texture and composition. Also samples were obtained for petrographic analysis.

A continuous exposure occurs in the Doctors Gorge (Ohuriawa Gorge; appendix 1 fig. 1.4, section A). The sequence is characteristic of yellow-cream coloured sands, massive to bedded, moderately to poorly sorted sands at base alternating with well sorted beds upsection. The sandstones are friable, fine to medium, quartzose with occasional carbonaceous lamina and coal spar horizons, with alternating muddy laminations also occurring upsection (appendix 1 figs. 1.11). Occasional disarticulated *Ostrea* and bivalve shells occur in beds that display burrows while other layers are intensely bioturbated, with water escape structures (appendix 1 figs.1.8, 1.13). An intraformational *Ostrea* bed occurs near the lower base of the sequence (appendix 1 fig.1.10).

Minor cross beds and scours occur in some layers while others display sets of cross beds 10 -20 centimetres thick at a low angle (appendix 1 figs.1.9, 1.14). Other minor crossbeds are aligned with disarticulated shells, oysters and pectens, and upsection crossbed foresets are aligned with coal spars (appendix 1 fig. 1.12) and clay flasers at 20-30 centimetres thick.

At the top of the Broken River Formation alternating clay laminations and fine sand are present. Iron coated 2 cm concretions are present through out some layers while iron cemented horizons and jarosite staining are abundant upsection.

Cross beds occur within the Broken River Formation at certain beds and are not that common. Cross bed paleocurrents were measured in the field and restored to true azimuth direction using a stereographic projection. Only two paleocurrents were taken from this formation due to the scarcity of exposure. Paleocurrent directions were from the east to the north-east (fig. 4.2). Nicol (1993) obtained paleocurrents from another locality in the Waipara River area and inferred northeast and southeast paleocurrent directions. Cross bed foresets are at low angle10 degrees while others are at a 30 degree dip angle and occur within sets of 20-30 cm thick.

Section 4.5 includes petrographic data and provenance data from the Broken River Formation.

4.3.2 Conway Formation

The Conway Formation overlies the Broken River Formation gradationally with characteristic burrowed horizons (appendix 1 fig. 1.15). Although the nature of the contact has not been directly observed it is inferred, while Nicol (1993) records a gradational contact between Broken River Formation and Conway Formation at other localities. The Conway Formation is 180 metres thick in the mid- Waipara River (fig. 4.1, section B). Bedding is mostly indistinct while some obscure bedding planes exist with prominent flakiness developing parallel to weathering surfaces, although some weathering surfaces develop irrespective of bedding planes.

A complete sequence was measured at locality B (fig. 4.1) within the Waipara River (appendix 1 fig. 1.5). The sequence is characteristically composed of a friable, massive, moderately sorted, grey-green, silty fine to very fine, quartz sandstone. Low glauconite content is evident at the base of the sequence, however it is absent from the rest of the section. Occasional burrowing is evident in the section although the entire section is mottled and reworked by bioturbation that has resulted in the complete destruction of any sedimentary structures.

The sequence is overwhelmed by jarosite-sulphur staining and jarosite veins. The spectacular feature of the Conway Formation is the presence of large spherical calcareous concretions or "cannonball" concretions. Concretions range in size from 50 cm to 1 metre, with occasional 2.5 m diameter concretions. The concretions are calcareous but have similar composition with the surrounding non-calcareous silty sandstone (appendix 1 fig.1.16).

Up section the formation displays occasional micas while near the top of the sequence, fissile joint weathered planes (appendix 1 fig.1.17) and visible calcite grains occur. Soft sediment deformation structures are present at the top. The upper 13 metres at locality C (fig. 4.1; appendix 1 fig. 1.6) have a characteristic glauconite content of 10-20%, while the upper-most 4 metres are light grey fine sandstones with clay flasers and abundant jarosite grains/veins.

4.3.3 Loburn Mudstone

The Loburn Mudstone conformably overlies the Conway Formation with a sharp contact. This is the K-T boundary (Cretaceous-Tertiary) mentioned by Morgans et al. (2005). The contact is jarositic while the underlying beds are massive along fissile planes. The Loburn Mudstone is 12 metres thick at locality C (figs. 4.1, appendix 1 fig. 1.6) and it is a brown, highly weathered, soft to moderately indurated, jarositic, burrowed, bimodal siltstone-mudstone (appendix 1 fig. 1.18). The formation is slightly glauconitic at a content of 7-10%.

4.3.4 Waipara Greensand

The Waipara Greensand occurs in the mid-Waipara River at locality D (fig. 4.1) measured at 39 metres thick (appendix 1 fig.1.7). The formation conformably overlies the Loburn Mudstone (Morgans et al. 2005) although it was not possible to observe the contact in the field since it was covered by vegetation. The Waipara Greensand is a massive, friable-soft, moderately to well sorted, weathered, Fe+ stained, slightly jarositic, fine quartz glaucarenite with 60% glauconite. The glauconite is composed of two distinct populations; one of pale-olive green colour and the second of dark green colour. The glauconite grains range from fine to medium grain size. The Waipara Greensand contains vertebrate fossils/sharks teeth at the lower levels of the sequence, while its appearance is a characteristically "muddy" greensand (appendix 1 fig.1.19).

The formation contains 10-50 cm concretions forming resistant ledges/benches while the surrounding greensand has sparse 10cm concretions. Jarositic staining is present occasionally in some beds of the formation.

4.4 Interpretations of the Depositional Settings

4.4.1 Broken River Formation

The Broken River Formation fine-medium quartz sandstones are interpreted as a marginal marine depositional setting. The quartz sandstones containing beds with silt laminations, burrows and concretions indicating low energy conditions; they are interpreted as middle to low shoreface settings. Layers with disarticulated, shells and crossbed foresets are indicative of high-energy conditions and are interpreted as upper shoreface. The low angle cross beds may indicate a foreshore depositional setting.

The presence of an intraformational *Ostrea* bed is interpreted as a storm shell berm with high-energy conditions. Although no imbrication was present within this particular bed, Nicol (1993) refers to a location in the Waipara area where imbricated *Ostrea* shell beds are present with WNW transport direction. Alternating bioturbated layers with clay laminations indicates a shift to a lower shoreface environment within a fair weather base.

Paleocurrent directions (fig.4.2) suggest flow direction from the east and north-east. The directions are interpreted as currents produced most likely from waves. This reflects a marginal marine depositional environment during the onset of a marine transgression.

4.4.2 Conway Formation

The Conway Formation's silty fine sandstones are interpreted as a marine depositional environment. The silty-sandstones containing burrows indicate low energy conditions. The entire formation is mottled indicative of reworking by bioturbation. The presence of saurian bearing concretions and other fossil reptiles indicates a deep marine depositional setting. However, the jarosite-sulpur content indicates reducing anoxic conditions typical of a shallow marginal marine setting such as a transition between an estuary setting. Warren and Speden (1978) and Brown and Field (1985) suggested a depositional environment marked by gentle currents from suspension. The jarosite content was interpreted to have risen from authigenic bacterial reduction of sea water sulphates associated with an adequate supply of oxidisable organic carbon, in a low oxygen environment (Warren & Speden 1978; Brown & Field 1985). Warren and Speden interpreted the formation as a barred submarine depression, and it is adopted also in this study.

4.4.3 Loburn Mudstone

The Loburn Mudstone is interpreted as submarine setting beyond the tidal zone as indicated by burrows, calcareous muds, and minor glauconite content. The burrowed nature of the deposit indicates low energy conditions, while the jarosite staining indicates strong anoxic conditions. Warren and Speden (1978) and Brown and Field (1985) interpret the formation as a similar depositional environment to the Conway Formation, a barred submarine depression with deposition marked by gentle currents and suspension of fines. A similar depositional setting is adopted in this study.

4.4.4 Waipara Greensand

The presence of 40-50% glauconite with the content increasing upsection is clearly indicative of a marine depositional setting at low depositional rate since the detrital fines decline at the expense of glaucony grains. It is interpreted as a shallow marine deposit; further analysis of glauconite is given in the section 4.5.

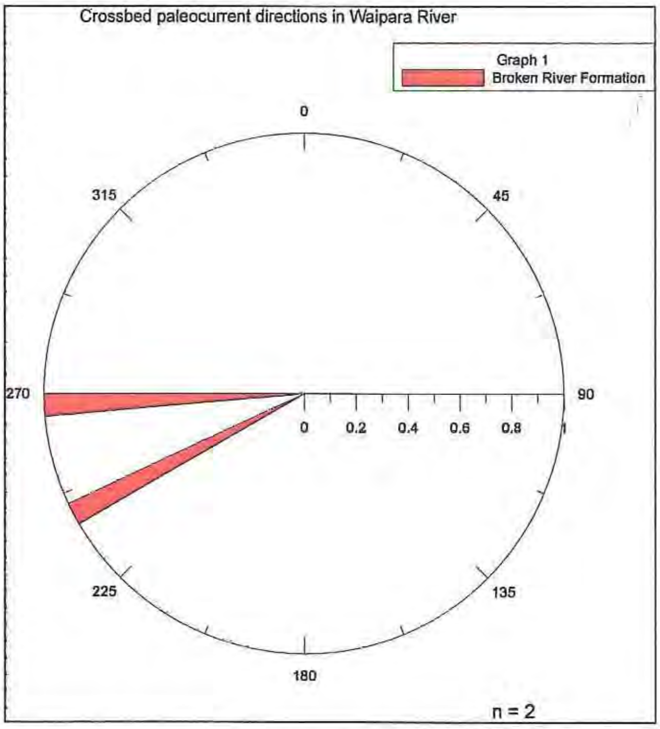

Figure 4.2: Restored azimuth cross bed foresets of the Broken River Formation at mid-Waipara River.

4.5 Glaucony as Sedimentation Indicator

4.5.1 Descriptions of glauconite

Glauconite grains are present in most formations ranging from the basal Broken River Formation, Conway Formation into the Loburn Mudstone and the upper Waipara Greensand. At the Waipara section, 3 varieties of glauconite have been observed, nascent, micaceous and evolved/mature varies. McConchie and Lewis (1978) described two major types of glauconite within the South Island of New Zealand from Cretaceous to Eocene glauconites: Type A and Type B, corresponding to the nascent and evolved varieties.

The Broken River Formation has a miniscule content of 1-7% (appendices 1, 2). Glauconite fecal pellets in granular form are the common form of the glauconite mineral. The glauconite type is nascent from the samples W03, W04, W06 (fig. 4.3) within the Broken River Formation, and it is present only in certain beds. The glauconite trend of nascent variety in the Broken River Formation is characteristic of pale green glaucony grains with irregular boundaries.

The Conway Formation upsection has 11% glauconite content; the nature of the glauconite is composed of nascent glaucony grains followed by a small increase in mature/evolved glaucony grains compared to the underlying Broken River Formation. A secondary population of micaceous glauconite grains occurs in the Conway

Formation which in turns marks an authigenic phase of dissolution-precipitation around a host mineral; this is evident in sample W07 in the Conway Formation (fig. 4.3). At the upper levels of the Conway Formation glauconite content rises to 15% relative to the entire composition (appendix 2). The glaucony composition contains a high frequency of evolved/mature, well rounded glaucony grains while nascent and micaceous glaucony varieties decrease dramatically (figs. 4.3, 4.4). Continuous increase in the overall glauconite content is evident in the upper 3 metres of the Conway Formation at 20% of the total composition of the sample. Here again sample W09 (fig. 4.3) displays a marked rise in mature/evolved glauconite at the expense of declining minor nascent and micaceous varieties. The Loburn Mudstone was not sampled due to its very fine – silt grain size, in addition the glauconite content was low.

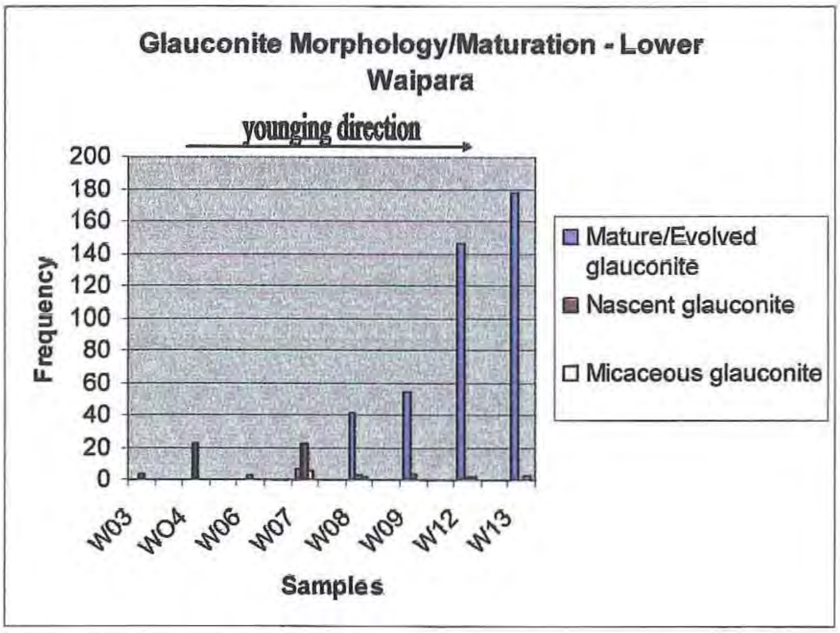

Figure 4.3: Frequency of glauconite grains displaying nascent stage, evolved/mature glauconite and micaceous glauconite. Evolved-mature glauconite increases up section at the expense of decreasing nascent glauconite up section. The small peak in micaceous glauconite represents a second growth episode.

The Waipara Greensand becomes entirely a glaucarenite with 50 to 61% glaucony grains. The majority of glaucony present in this formation is the evolved/mature glaucony variety seen in samples W12 and W13 (figs. 4.5, 4.6, 4.3) that form coalesced clusters of well rounded evolved/mature glaucony grains (fig. 4.7).

The general trend for the formations containing glauconite in the Waipara area is the abundance of nascent glauconite in the lower units of the sequence such as the Broken River Formation while up section this trend reverses and an increase of evolved mature glauconite grains occur at the expense of nascent and minor micaceous glauconite in the Conway Formation, while the Waipara Greensand has a entire evolved/mature glauconite population (fig. 4.3). The nascent glauconite resembles closely the Type A glauconite described by McConchie and Lewis (1978, 1980) and the evolved/mature glauconite resembles the Type B glauconite.

4.5.2 Glauconite Interpretation

The glauconites within the Broken River Formation are interpreted to have formed in marginal marine depositional settings. In detail the nascent variety depicts authigenic formation (McConchie & Lewis 1978) or autocthonous formation as adopted in this study. The possibility of recycled glauconite grains mentioned by McConchie and Lewis (1978) should be disregarded since glauconite grains are strongly subjected to fragmentation when transported, additionally it should be mentioned that the Broken River Formation is underlain by Mesozoic basement which does not contain glauconite minerals. Thus glauconite grains could not have been derived by erosion and reworking of older glaucony bearing horizons. The possibility however, that the glauconite grains are parautocthonous, that is transported locally, is strong, therefore an autochthonous -parautochthonous formation is likely. Amorosi (1997) discusses that the association of glaucony with high-energy and/or reworked deposits should not necessarily be regarded as diagnostic for an allochthonous origin of grains. In transgressive successions, glauconitization commonly post – dates coarse-grained sedimentation in nearshore areas (Amorosi 1997).

The Conway and Waipara Greensand glauconites are interpreted to have formed in marine depositional settings of moderate shallow to deeper marine setting.

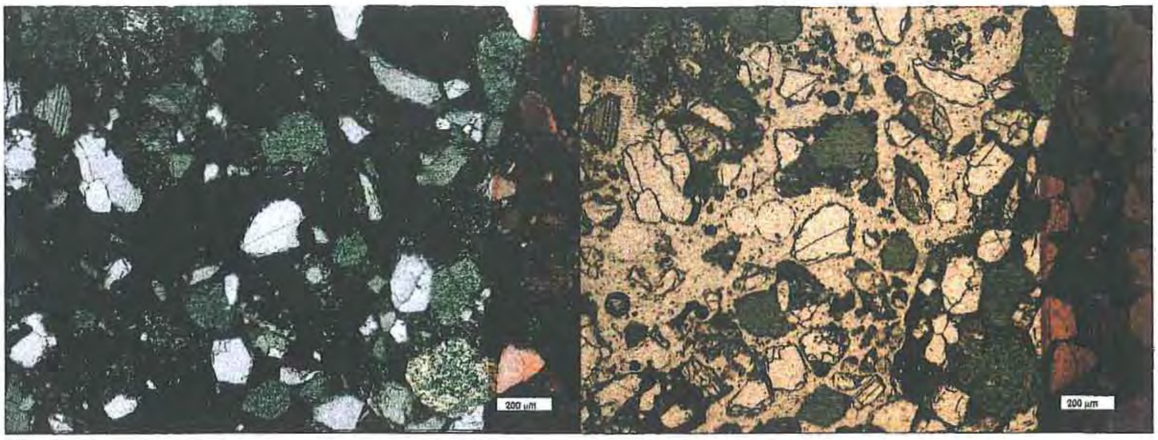

Figure 4.4: Cross polarized image and plane polarized petrographic image of sample W08 of the Conway Formation depicting well rounded dark green evolved/mature glaucony grains with very fine detrital quartz grains.

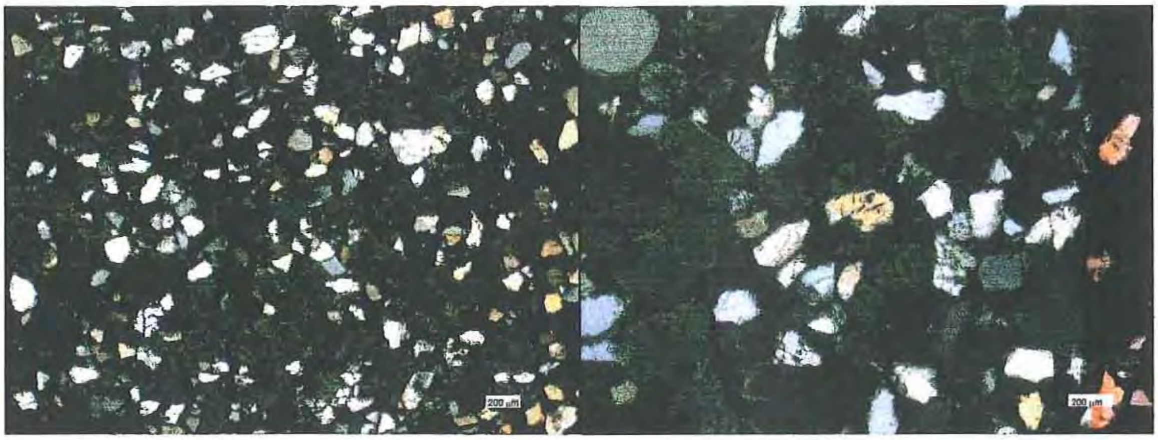

Figure 4.5: Cross polarized images of sample W12 of the Waipara Greensand depicting well rounded dark green – emerald evolved/mature glaucony grains with very fine detrital quartz grains.

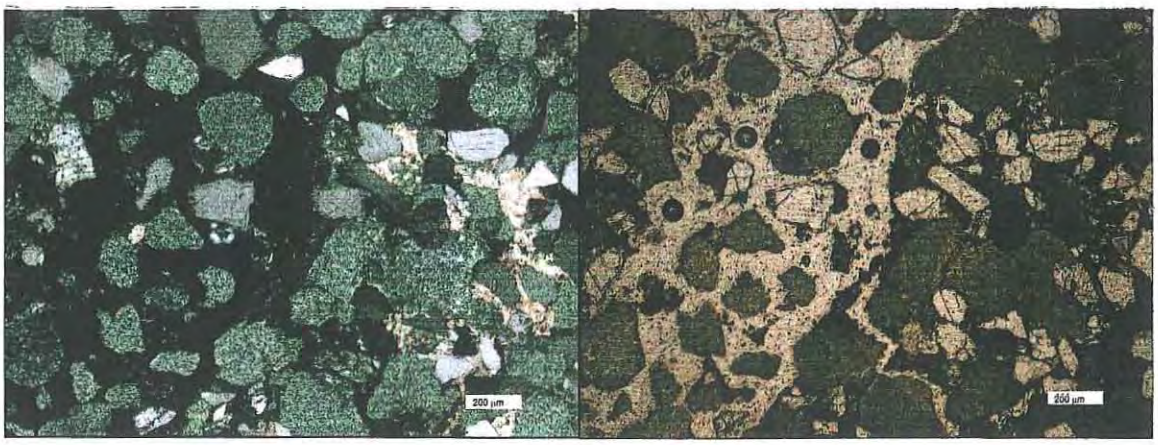

Figure 4.6: Cross polarized and plane polarized petrographic images of sample W13 of the upper levels of the Waipara Greensand depicting well rounded dark green evolved/mature glaucony grains with very fine detrital quartz grains.

Figure 4.7: SEM micrograph images of glaucony grains. In these images from sample W13 clusters of subrounded-rounded evolved/mature glaucony grains.

The glauconite grains are well rounded and evolved/mature grains while some are coalesced into clusters indicating in situ formation of glaucony. Therefore the petrographic data in conjuction with the sedimentary structures of the two formations indicate low energy deposition from suspension, therefore no significant disturbance. Amorosi (1997) interprets lithologically homogeneous successions with non selective spatial distribution of glaucony as likely to reflect an autochthonous origin of grains. In that case, a low sedimentation rate is interpreted and an autochthonous origin is interpreted glauconite grains in the Conway and Waipara Greensand Formations. While the presence of nascent glaucony grains in the fine detrital sands (lower shoreface-foreshore settings) of the lower Broken River Formation indicate at most a parautochthonous formation.

In the Waipara succession the glauconites are interpreted as parautochthonous at the lower formation and overwhelmingly autochthonous in the upper Conway and Waipara Greensand Formations indicative of a low sedimentation rate spanning the Late Haumurian to Waipawan time.

4.6 Provenance

4.6.1 Sandstone Composition

Compositionally the Broken River Formation is a subarkose – arkose arenite. The samples have minimum amount of lithics that range from 7-9%. The source type of the lithics for the basal Broken River Formation are predominantly volcanic, sedimentary and minor plutonic lithics, while upsection in the Broken River Formation plutonic lithics diminish and only volcanic and sedimentary lithics are present. The feldspars are dominated by plagioclase and alkali feldspars, higher percentages of plagioclase to alkali felspars occur in the lower levels of the Broken River Formation while upsection plagioclase decreases slightly and alkali feldspar increases. The Broken River Formation's composition is dominated by monocrystalline quartz, while polycrystalline quartz is between 2 and 7%. Muscovite is at a 1% of the total composition of the sandstones and glauconite is 1-7% of the entire composition (appendices 1, 2). The Broken River Formation's arenites have a mode of fine to medium grain size while they are moderately to well sorted.

The Conway Formation's composition is subarkose – arkose arenites with lithics at 5% composed of volcanic and sedimentary, while polycrystalline quartz is low at 2-3% (appendices 1, 2). Feldspars are dominated by alkali and minor plagioclase. Muscovite is the only accessory mica present and in certain samples rises to 16% of the entire composition, while the glauconite content steadily rises from 11 to 20%. The arenites are dominantly fine to very fine with silt grains around 32% and the sorting is moderate. The sandstones are calcareous in certain stratigraphic horizons with 30 – 7% calcite micrite matrix.

The succession is followed by the Waipara Greensand composed as subarkose – arkose arenites with low lithics at 4% confined to sedimentary and low quartz polycrystalline grains at 2-1%. Feldspars are dominated by plagioclase and secondary alkali feldspars. The composition of the Waipara Greensand is entirely glauconite greensand with 50 to 60% glauconite. While the grain size is very fine to fine and the arenites are well sorted. Calcite micrite matrix consists of 5 -2% upsection while silt also decreases upsection from 7 to 1%.

The Broken River Formation has a higher frequency of polycrystalline quartz grains compared with the detrital quartz grains compared with the upper Conway and Waipara Greensand which do have a polycrystalline component but at lesser extent than the middle Broken River Formation (fig. 4.8).

Alkali feldspars are essential constituents of several rocks such as felsic igneous rocks, pegmatites and many felsic and intermediate gneisses (Shelley 1985; Boggs 1992). They are especially abundant in syenites, granites, granodiorites and their volcanic equivalents (Shelley 1985). According to the presence of alkali feldspar felsic plutonic or volcanic and/or metamorphic rocks are likely to provide the source. Plagioclase also occurs commonly in volcanic and metamorphic rocks (Shelley 1985). The plagioclase feldspar components within the arenites are strong indicators of felsic/plutonic and/or metamorphic rocks. Therefore the combination of alkali feldspar and plagioclase suggests a western granitic suite and a metamorphic terrane such as the Haast or Alpine Schist are possible sources; alternatively the distant Mandamus Igneous Complex could have provided alkali feldspar components.

Lithoclasts also provide source type lithologies, in the Waipara area the dominant source types are a range from volcanic, plutonic and sedimentary. The most likely source for the minor plutonic lithics are a granitic suite, probably a western Karamea Batholith, or Separation Point batholith granite. The likely source for the volcanic lithics is the southern Mt Somers Volcanics and/or the Mandamus Igneous Complex, or the volcanic carapace from the Cretaceous volcanics. Sedimentary lithics are the common lithics in all formations and are most likely derived from the underlying fine grained, Torlesse greywacke-argillites.

Muscovite is common in regionally metamorphosed rocks, especially those derived from pelitic sediments, it is also a common detrital mineral (Shelley 1985). Muscovite also occurs in granites and pegmatites (Boggs 1992). The presence of abundant muscovite grains especially in the Conway Formation is most likely derived from a combined metamorphic terrane and granitic suite. The subarkose-arkose QFL composition indicates an interior craton, tectonic setting (fig. 4.10; A).

4.6.3 Quartz Provenance (SEM-CL)

The integrated SEM-CL/optical microscopy provenance technique of quartz was applied to the arenites of the Broken River and Conway Formations in the Waipara area. However SEM-CL/optical microscopy analysis was not done on the Loburn Mudstone and Waipara Greensand their grain size was too fine. 105 selected quartz grains were analyzed with integrated SEM-CL/optical analysis in each sample following the technique devised by Bernet and Bassett (2005). Detrital quartz was compared for its CL and optical properties (appendices 5, 6, 7) as described in chapter 2. Samples were collected from the Waipara River area (fig. 4.1; localities A, B and blue circles) for SEM-CL/optical analysis. The same samples used in petrographic point counts were also used in CL analysis, ignoring all the other minerals and establishing quartz types.

In the Broken River Formation 28 -34% of the quartz grains are plutonic while the frequency of plutonic grains in the Conway Formation remains between 22 and 35 % plutonic. The presence of deformed plutonic grains, displaying strong undulose extinction were minor compared to the total plutonic component, thus it was interpreted as arising from mild regional metamorphism or by deformation events.

Quartz grains displaying strong undulose extinction and black/dark CL and/or polycrystalline were interpreted as metamorphic. The samples displayed 46 – 60 % metamorphic quartz through out the Broken River and Conway Formations. In contrast the polycrystalline quartz grains are at a lesser degree than monocrystalline metamorphic quartz grains (fig. 4.8). The majority of total polycrystalline quartz grains display polygonized, to crenulated and polyhedral –recrystallized quartz mosaics, however total polycrystallinity is low compared to the monocrystalline quartz grains (fig.4.8). Overall the quartz grains are dominantly angular with some subrounded to rounded grains (appendix 7). The total polycrystalline grains ranging from polygonized to crenulated quartz leading to increased polyhedral quartz are interpreted as low to medium-high metamorphic grade based on Young's (1976) continuum of polycrystalline quartz deformation structures. However the abundance of total polycrystalline quartz grains is low compared to the entire population of monocrystalline quartz grains (fig. 4.8).

The volcanic quartz grains range from19 – 14% in the Broken River Formation and ranges from 16 to 17% in the Conway Formation without a significant change stratigraphically

The data obtained from the Broken River and Conway Formations arenites with the SEM-CL/optical microscopy technique reveal a strong bimodality of plutonic versus metamorphic grains with the metamorphic source type dominating over the plutonic counterpart (appendix 5 figs. 5.5–5.6, 5.7-5.8). The volcanic source type was moderate to low in the formations studied (appendix 5 fig. 5.5).

The trends of the quartz types depict overall a bimodality of metamorphic versus plutonic quartz signature with a lesser but moderate volcanic quartz signature through out the succession (fig. 4.9). The provenance is dominantly metamorphic and plutonic with a minor volcanic source, the source types indicate major metamorphic basement source while two samples plot in the mixed source field indicative of source from all three source types (fig. 4.10; B). The metamorphic source is more likely regional than local because the Torlesse basement is too fine grained to provide a major source for metamorphic grains. The volcanic quartz grains are most likely sourced from the southern Mt. Somers Volcanics Group. The plutonics are interpreted to have been derived from a distant plutonic suite, likely a western granitic suite (Karamea Batholith, Separation Point Batholith) while the metamorphic quartz grains were probably derived from a metamorphic terrane such as the Otago/Haast Schist and/or by alpine Schist, although a western quartzite source could have provided quartz detritus. The angularity of the quartz grains are interpreted to have been transported dominantly by fluvial conditions and then reworked locally in a marginal marine setting.

4.7 Summary of Results for Waipara River

The Waipara River area consists of Late Cretaceous – Tertiary sequence that unconformably overlies Mesozoic Torlesse Supergroup. The basal sequence consists in its regional sense of locally derived conglomerates (Nicol 1993) of the Broken River Formation (Haumurian) fluvial fresh water deposits succeeded by marginal marine lower shoreface – upper shoreface quartz sandstones, thus marking the onset of a marine transgression. Paleocurrents directions indicate sediment transport from the east and north-east reflecting minor waves. The presence of minor nascent type glauconite indicate autochthonous to parautochthonous formation of glauconite hence a medium to low sedimentation rate. The Broken River Formation is succeeded by the Teurian (Paleocene) Conway Formation, which is a mottled –bioturbated, jarositic, silty fine sandstone with large spherical concretions indicative of a submarine barred depression (Warren & Speden 1978) deposit formed by suspension and low sedimentation and modified by anoxic conditions. Up section the sequence is characterized by glauconite formation of the nascent and micaceous type followed by well rounded dark green evolved/mature glauconites typical of an autochthonous formation under low sedimentation rates.

The sequence is then followed by bioturbated, jarositic, sandy mudstone of the Loburn Mudstone that is Teurian in age (Paleocene). The succession is a submarine barred depression (Brown & Field 1985) formed by suspension deposition under low sedimentation conditions with minor glauconite. This sequence is followed by the Waipara Greensand, Teurian to Waipawan in age (Paleocene to Early Eocene), which is a glaucarenite with spherical concretions forming layers. The sequence is interpreted as a shallow marine depositional setting. The abundant mature/evolved glauconite content indicates autochthonous glaucony formation hence a low sedimentation rate for the sequence.

Provenance of QFL components indicates subarkose-arkose arenites for the sequence spanning the Broken River, Conway and Waipara Greensand Formations characteristic of a craton interior setting. The dominance of alkali feldspar with minor plagioclase indicated a felsic igneous source while an alternative metamorphic and/or plutonic regional source was possible. The presence of sedimentary lithics indicated a minor provenance contribution from the fined grained Torlesse, while volcanic lithics and plutonic lithics, indicate a Mt. Somers Volcanic source. A minor muscovite percentage suggests a granitic/pegmatitic or a metamorphic source.

The applications of the SEM-CL/optical microscopy technique on quartz provenance for the Waipara sequence reveal a strong bimodality of metamorphic and plutonic source with a minor volcanic input. A metamorphic terrane such as the Haast/Otago Schist and/or a western province quartzite is implied for the metamorphic quartz signature while a plutonic source such as the western Karamea or Separation Point Batholiths are implied for providing plutonic quartz grains. The minor volcanic quartz type is possibly from the Mount Somers Volcanic Group.

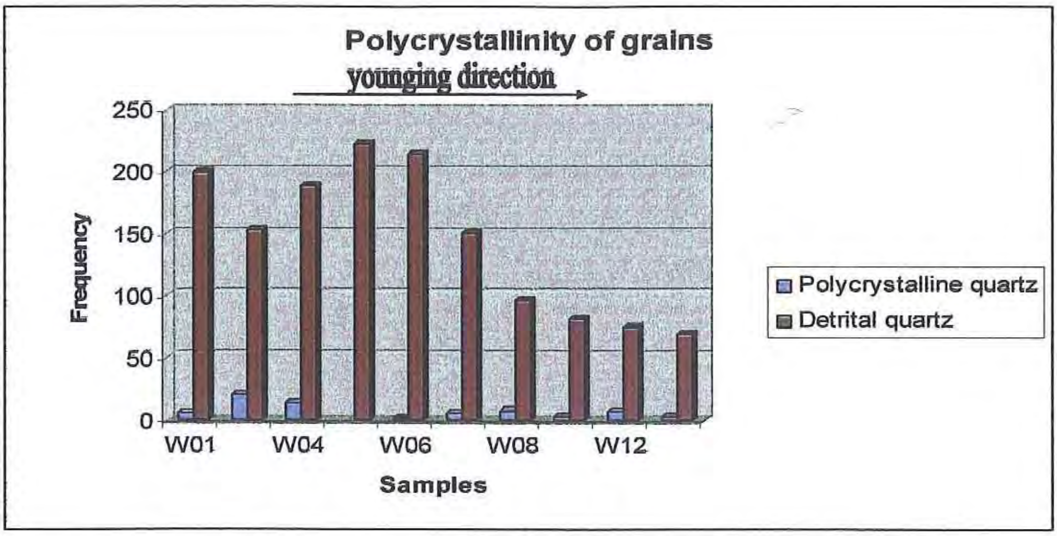

Figure 4.8: Proportion of polycrystalline grains compared with detrital quartz grains from the Broken River Formation to the top of the Waipara Greensand

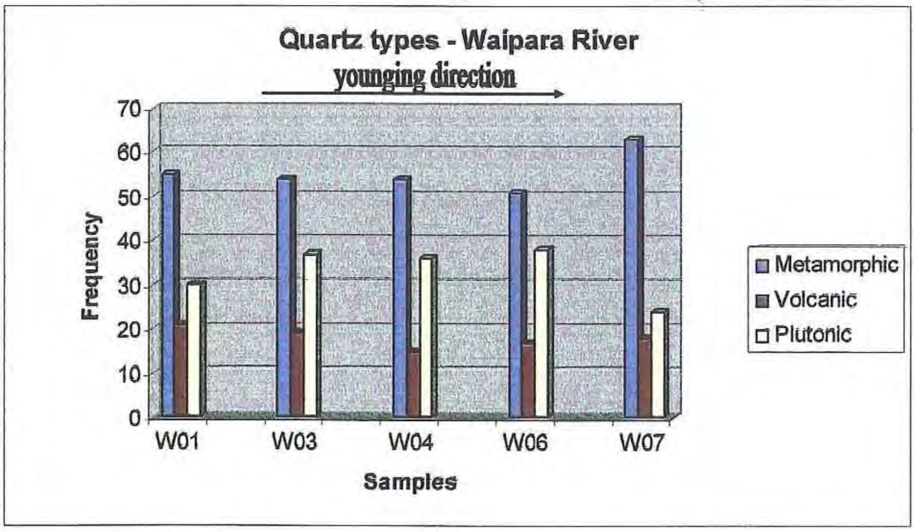

Figure 4.9: Frequency of grains displaying quartz per sample from the Broken River Formation to the lower beds of the Conway Formation. Metamorphic and plutonic quartz types are dominant while the volcanic component is low but moderate.

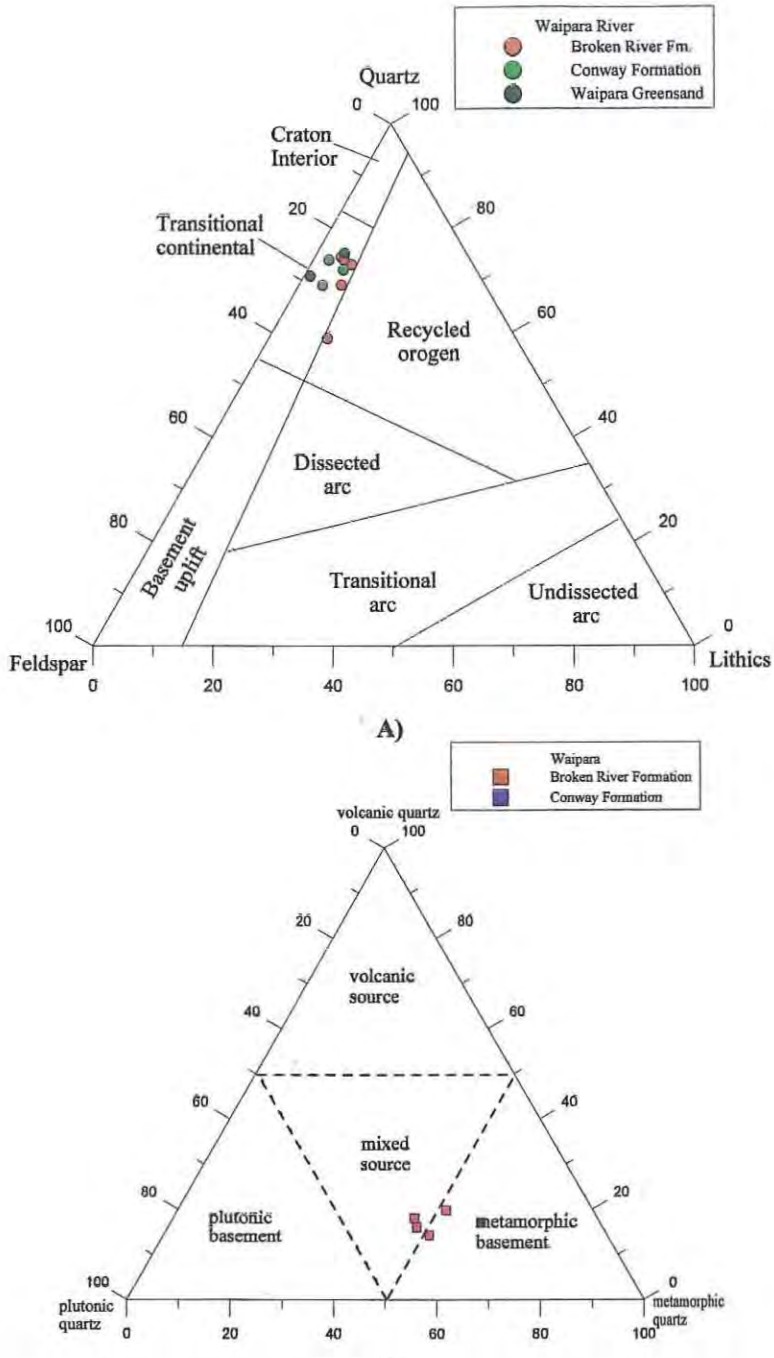

Figure 4.10: **A)** Standard QFL diagram after McBride (1963), on the basis of normalized point-counts, results from conventional point counts. Samples from the entire formations plot in the subarkose-arkose field. **B)** Provenance discrimination diagram after Bernet and Bassett (2005), of Waipara River's Broken River Formation and Conway Formation, samples using the three main quartz types of volcanic, plutonic and metamorphic quartz, based on SEM-CL/optical analysis. The dashed lines indicate the 50 percent lines of each of the three main types. Metamorphic quartz includes all low-grade to high-grade metamorphic, recrystallized and vein quartz.

CHAPTER FIVE
CASTLE HILL BASIN – CAVE STREAM

5.1 Regional Geologic Setting & Previous Work

The Castle Hill Basin is situated approximately 120 km west of Christchurch City accessed by state highway 73. The modern basin is a triangular tectonic depression bound by two major faults at the foot of the Craigieburn Range to the west, Broken Hill to the north and the Torlesse Range in the south. The headwaters of the Broken River and Porter River drain part of the basin (figs. 5.1, 5.2).

Torlesse Supergroup basement rocks are unconformably overlain by Late Cretaceous and Tertiary clastic and carbonate sedimentary rocks that occur as outliers to the Canterbury Basin. Pleistocene glacial deposits overlie the Cretaceous-Tertiary sequence and in parts obscure the underlying stratigraphy. In the Castle Hill basin area, the Cretaceous-Tertiary sequence is deformed by faults and folds with a north-east trend plunging to the southwest and west (fig. 5.2). The Late Cretaceous-Tertiary rocks record a transgressive sequence with fluvial to marginal marine, marine depositional settings, developing between the Rangitata-Kaikoura tectonic events, interrupted by uplift and tilting in the Eocene and by basaltic volcanism in the mid-Oligocene (Gage 1970). The most characteristic feature of the Castle Hill area is spectacular limestone bluffs and Pleistocene River terraces.

The Castle Hill basin has been studied numerous times in the past from the 1860's when J. D. Enys began collecting fossils (Gage 1970). The area was first named "Trellissick Basin" and was first mapped in 1872 by J. Hector (Gage 1970). A. McKay completed the first description of the area in 1881 with nine formations recognised and grouped into "Cretaceous-Tertiary", "Upper Eocene" and "Lower Miocene" (Gage 1970). In 1887, F. W. Hutton classified the Cretaceous and Tertiary strata into the "Waipara", "Oamaru" and "Pareora Systems" (Hutton 1887). R. Speight visited the area in 1917 and applied the "Pareora" stratigraphic name. Speight (1920) described the lower Broken River coal area in detail. Pleistocene moraines and glaciofluvial deposits were mapped by Maxwell Gage in 1958 and in Broken River by Breed (1960).

The most recent comprehensive description of the geology of the Castle Hill basin was by Gage (1970). Gage (1970) named the major faults and identified unconformities within the sedimentary sequence. The chemistry of glauconite within the Castle Hill basin was studied by McConhie and Lewis (1978), while Coates (1975) studied heavy minerals from the Coleridge and Wopereis (1975) studied the chemistry of basaltic dikes. Bradshaw (1975) studied the deformation and discussed the folds at Castle Hill in relation to the Kaikoura orogeny, while Congdon (2003) studied the Porter Group rocks of the Castle Hill Basin.

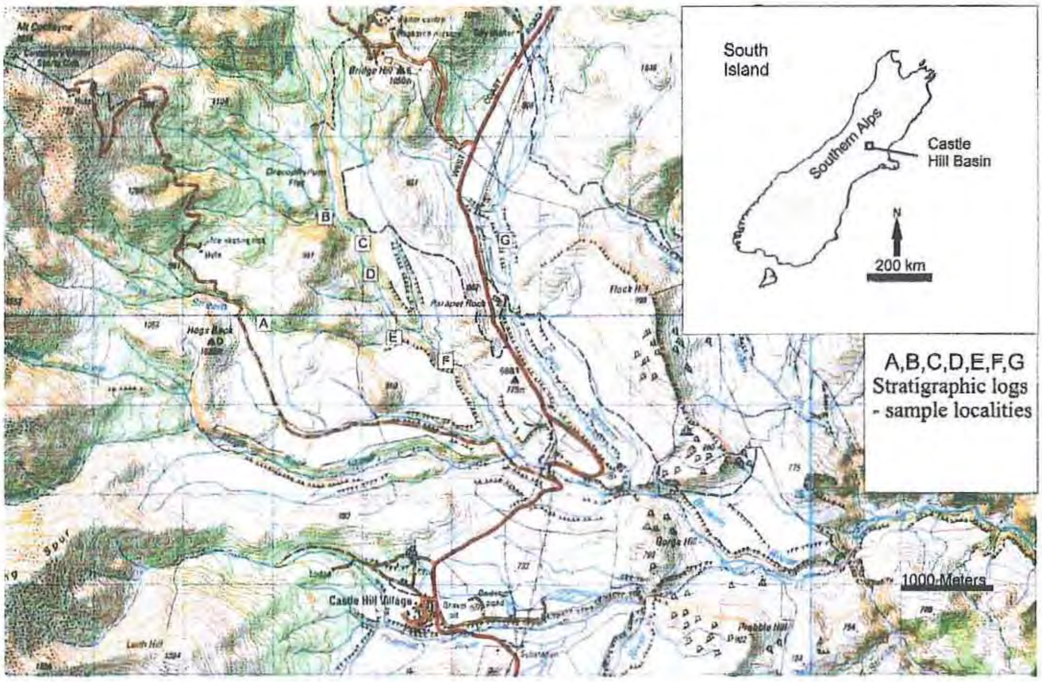

Figure 5.1: Topographic map of the Castle Hill Basin outlining sample localities and stratigraphic sections.

5.2 Stratigraphy

The Castle Hill basin is a succession of Late Cretaceous sedimentary rocks (Haumurian) (Gage 1970; Brown & Field 1985) which rest unconformably on Torlesse Supergroup (fig. 5.3). The Broken River Formation that overlies the basement rocks consists of basal conglomerates and sandstones; subsequently the Broken River Formation is succeeded gradationally by the Iron Creek Formation separated into lower glauconitic sandstone (Charteris Bay Sandstone) and an upper glaucarenite, the overlying Iron Creek Greensand respectively (Early Eocene – Late Eocene (Brown & Field 1985). Coleridge Formation massive quartz sandstones and micritic limestones (Early-Mid Oligocene) follow the succession, succeeded by the Thomas Formation composed of basaltic with minor tuffs and bryozoan limestones (Late Oligocene). An estimated age of mid-Miocene to Pliocene (Brown & Field) consisting primarily of quartz sandstones and glauconitic sandstones of the Enys Formation which unconformably overlies the Porter Group (fig. 5.3). The Broken

River and Iron Creek Formations will be the focus of this research and will be described in detail.

5.2.1 Basement Rocks – Torlesse Supergroup

Gage (1970) describes the basement rocks in Castle Hill as "strongly jointed greywacke and well indurated dark-grey siltstone and argillite, replaced locally by tuffaceous mudstone, chert, reddish or pure-coloured jaspillite and basic volcanic rock". The basement rocks were later named as The Torlesse Supergroup and Field and Brown (1989) described it as Rakaia Subterrane dominated by dark grey to green-grey sandstone, and dark grey to locally red siltstone beds, Late Triassic in age.

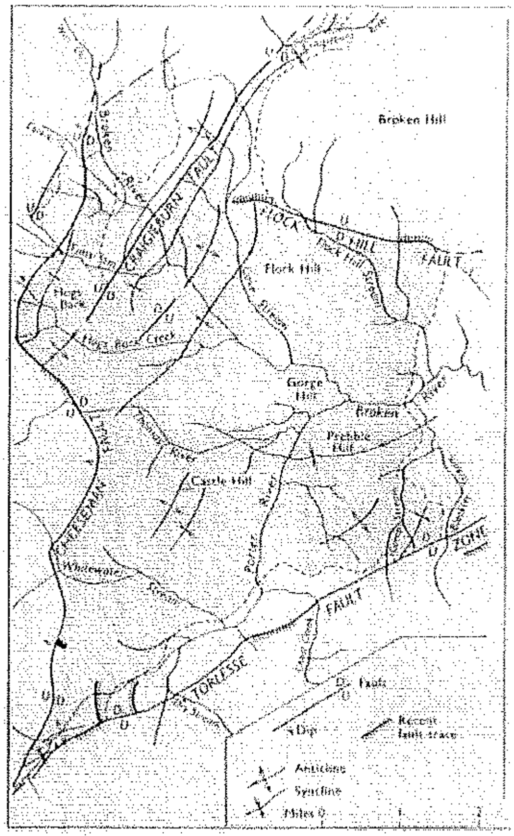

Figure 5.2: Structural map of Castle Hill Basin (From Gage 1970).

5.2.2 Broken River Formation

The Broken River Formation is separated from the underlying Torlesse Supergroup by a strong angular unconformity. The Torlesse rocks are commonly leached to depths of 2m (Gage 1970; Browne & Field; Young 1997) suggesting subaerial erosion in a low relief setting. In Broken River the succession is 150 metres thick according to Brown and Field (1985). However, exposure is not continuous due to grass covered cliff sections. The formation consists of basal conglomerates and breccias with greywacke and quartz pebbles up to 7cm in diameter (Gage 1970), while lensoid beds of sub-bituminous coal occur locally with sand (Gage 1970). Sandstones comprise the majority of the sequence with "unevenly stratified, current bedded, white quartz sandstone" (Gage 1970). Browne and Field (1985) further describe the formation as "light-grey to green, poorly indurated, non calcareous, massive, poorly to well sorted, fine to very fine quartzose sandstone with bioturbation, disrupted bedding, lenticular and crossbedding."

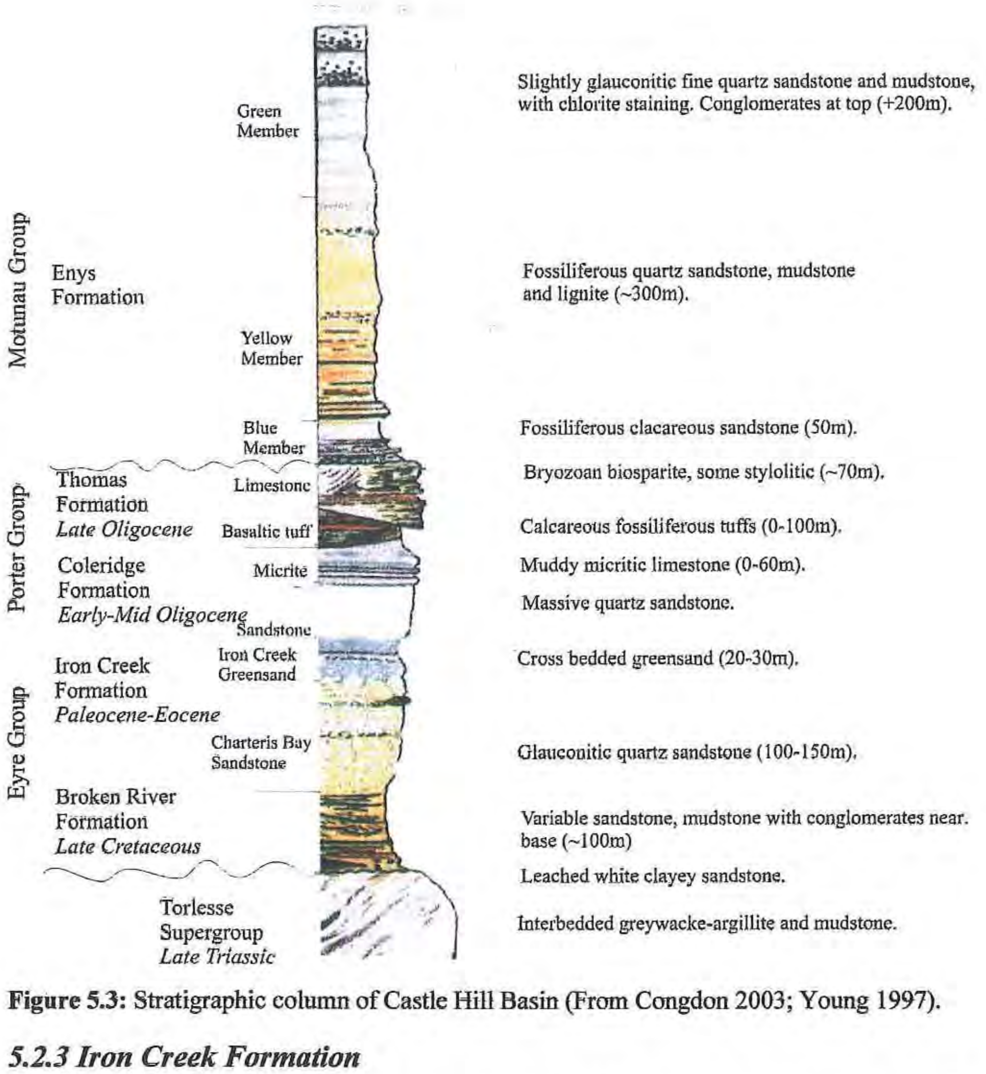

Figure 5.3: Stratigraphic column of Castle Hill Basin (From Congdon 2003; Young 1997).

5.2.3 Iron Creek Formation

The Iron Creek Formation rests conformably and with a sharp contact at Broken River, although at Avoca to the east, the contact is gradational (McLennan 1981). The formation is subdivided into the lower Charteris Bay Sandstone Member, previously named the Avoca Sand Member, and the upper Iron Creek Greensand Member (Brown & Field 1985; fig. 5.4).The Charteris Bay Sandstone at Broken River consists of pale greenish grey to white, poorly indurated bioturbated, glauconitic, moderately to well sorted, very fine to medium, quartzose sandstone (Brown & Field 1985).while Beds are massive, or centimetre bedded or cross stratified with some beds calcareous (Brown & Field 1985). Glauconite content is 5 to 20% (Brown & Field 1985). Bioturbation consists of millimetre diameter burrows and ophiomorpha.

The Charteris Bay Sandstone is overlain by the Iron Creek Greensand first studied by Gage (1970). The base of the Greensand Member was reported by Brown and Field (1985) as marked by strongly burrowed surface with burrows extending 30 cm into the underlying Charteris Bay Sandstone. It consists of dark green-grey to olive-grey, moderately to poorly indurated, bioturbated, muddy, very fine to fine greensand (Brown & Field 1985). The glauconite is dark, fine to medium sand sized grains, comprising over 50% of the lithology (Brown & Field 1985). "At Broken River, the basal 9 metres is very glauconitic (50-60% glauconite)" (Brown & Field 1985). McConchie and Lewis (1978) reported that the glauconite is crystallographically disordered with 15-25 expandable layers and occurs as pellets with spheroidal, ovoid morphology.

GAGE (1970)	McLENNAN (1981) AND McLENNAN & BRADSHAW (1984)		THIS PAPER
Coleridge and Puffer Formations	Puffer Formation		Amuri Limestone and Coleridge Sandstone
Iron Creek Greensand	Iron Creek Formation	Greensand Member	Iron Creek Greensand
		Avoca Sand Member	Charteris Bay Sandstone
Broken River Coal Measures	Broken River Coal Measures		Broken River Formation

Figure 5.4: Nomeclature of the Broken River and Iron Creek Formations (From Brown & Field 1985).

5.3 Sedimentary Descriptions

5.3.1 Broken River Formation

Exposures of Broken River Formation occur through out the length of the Broken River headwaters, exposed at intervals and not continuous due to successive folds and faults. It is not established here if the conglomerates are in their stratigraphic order underlying the Broken River Formation sandstones since there is no direct contact; however the conglomerates are in close proximity laterally to the underlying Torlesse - greywacke basement therefore an unconformable contact is likely. Two outcrops of conglomerates were observed in the field, and clast counts performed on both.

The first conglomerate is matrix supported and polymictic (appendix 1 fig. 1.24). It is massive, poorly sorted with clasts subrounded to rounded; matrix is fine sand to silt. The clasts are composed of greywacke clasts, smoky quartz, mud clasts, and sandstone clasts ranging on average from a mode of 1cm up to 4-6cm, while the deposit is iron and limonite stained. The second conglomerate deposit is composed of larger clasts; it is clast supported and monomictic (appendix 1 fig. 1.25). It is massive, poorly sorted with clasts subrounded to rounded, (the matrix is very well sorted fine to very fine sand). It is composed predominantly of greywacke clasts with very minor quartz pebbles ranging from 4 to 10cm.

At locality B (fig.5.1) an exposure of Broken River Formation sandstone occurs in close proximity to Torlesse greywacke. It consists of white-cream, grey coloured sands, friable, moderately well sorted, fine - medium quartzose sand with interbedded silt and carbonaceous mud layers. The deposit also has coal lenses grading into mud layers (appendix 1 fig. 1.23). Sedimentary structures within the sequence include cross beds with foresets of coarse sand and silt ripples (appendix 1 fig.1.22). At Tims Stream (locality A; fig. 5.1) exposures of interbedded coal seams and sand and coal fragments occur within the Broken River Formation

Cross beds occur within the formation at sets of 20 – 50 cm at a moderate dip angle of 25 to 32 degrees. Cross beds were measured in the field and restored to true azimuth direction. Only one cross bed paleocurrent was taken from the upper Broken River due to their scarcity. Paleocurrent direction flowed from the north-north-east (fig.5.5).

At a distant locality, Whitewater Stream further south from the Castle Hill basin a sequence is preserved recording an exposure of Broken River Formation unconformably overlying Torlesse Supergroup and overlain by the Iron Creek Formation (appendix 1 fig. 1.20). The Broken River Formation at this locality is characteristically interbedded fine sand with mudstones overlying iron leached and weathered Torlesse greywacke (appendix 1 fig.1.28). Up section the Broken River Formation is composed of poorly indurated-friable, moderately-well sorted quartz sandstone with coal stringers, coal spars and carbonaceous woody - peat material.

Glauconite is also present in the Broken River Formation at this locality with dark green glauconite grains increasing up section.

At Cave Stream in the north of the Castle Hill basin (fig. 5.1; locality G) a sequence of interbedded mudstones and sandstones of the Broken River Formation also occur.

5.3.2 Iron Creek Formation

The Iron Creek Formation overlies the Broken River Formation sharply although a direct contact was not established because of non-exposure; however it is inferred from the literature. In some localities the contact is gradational as in Avoca – Iron Creek while Brown and Field (1985) infer a sharp contact in the Castle Hill basin. In Broken River at locality D (fig. 5.1) glauconitic quartz sand of the Iron Creek Formation overlies white quartzose sand of the Broken River Formation (appendix 1 figs. 1.26, 1.27). The deposit consists of friable, moderately sorted, glauconitic, fine sand with limy concretions which in places have iron staining. It is therefore considered the lower Charteris Bay Sandstone Member of the Iron Creek Formation.

In locality E at the mouth of Tims Stream (fig. 5.1; appendix 1 fig. 1.21) a complete section is preserved as part of the Iron Creek Formation. The section consists of 35 metres of dark green, moderately indurated, moderately sorted, fine, quartz glaucarenite, iron stained, with abundant bioturbation and burrows 2cm in size (appendix 1 figs. 1.32, 1.33). Glauconite ranges in hand specimen from fine-very fine, 15-25% glauconite in the basal 5 metres to coarse, 40-50% glauconite content in the upper 30 metres of the sequence respectively. Very coarse, iron coated glauconite grains occur in the upper levels of the sequence. An intraformational oyster-shell bed is present in the basal lower 2 metres of the sequence. This sequence is characteristic of the Iron Creek Greensand Member of the Iron Creek Formation which overlies the Charteris Bay Sandstone.

At the Whitewater Stream (appendix 1 fig. 1.20) a section shows the transition from Broken River Formation into Iron Creek Formation. The section consists of friable, green coloured, well sorted, coarse sand to granule glaucarenite with a glauconite content of 30-40%. Up section the Iron Creek Formation is coarse sand with common granules, while coarse glauconite grains are abundant (appendix 1 figs. 1.28, 1.29).

5.4 Interpretations of Depositional Settings

5.4.1 Broken River Formation

The first conglomerates overlying Torlesse basement are interpreted to represent deposition by a river perhaps a braided river since there is a high percentage of matrix and the clasts are rounded to subrounded indicating fluvial to debris flow conditions. The clasts are clearly sourced from pre-unconformity local basement while mudstone and sandstone clasts are most likely penecontemporaneous. The second conglomerate is interpreted as a braided river deposit based on large rounded-subrounded boulders and clast supported nature was sourced from the pre-unconformity Torlesse rocks.

The successive interbedded sandstones carbonaceous muds and coal stringers of the Broken River Formation represent flood plain deposits of a fluviodeltaic setting. The sandstones were probably from crevasse splays. The cross beds are indicative of a foreshore depositional setting. Increased glauconite content implies a marine setting thus a transgression. The paleocurrent direction (fig. 5.5) flowed from the north, north-east indicative of north or north-east sources. The paleocurrents are interpreted as waves fluctuating during this time period reflecting marginal marine – near-shore nature of the deposit or possibly channelized fluvial currents.

5.4.2 Iron Creek Formation

The lower sequence of the Iron Creek Formation is represented by the glauconitic quartz Charteris Bay Sandstone. The Charteris Bay Sandstone (Brown & Field 1985) contains up to 16-21% glauconite and minor calcite micrite matrix (appendices 1, 2), so it is essentially marine. Moderate sorting with a few fines, occasional burrows and cross beds suggest a shallow marine environment influenced by waves. Rounded quartz granules suggest probable recycling from the lower Broken River Formation remobilised by longshore drift or waves.

The overlying glauconitic rich Iron Creek Greensand (appendix 1 fig. 1.33) Member contains almost 40-50 percent glauconite, 14-19% calcite matrix (appendices 1,2; section 5.5) with burrows present through out most of the sequence and an intraformational oyster-shell bed indicative of shallow marine to marine conditions. The glauconite is interpreted to form in normal shallow marine environment under low sedimentation conditions (further analysed in section 4.4) while the quartz granules are partially reworked from the underlying Broken River Formation due to the low detrital fines in the upper Iron Creek Greensand.

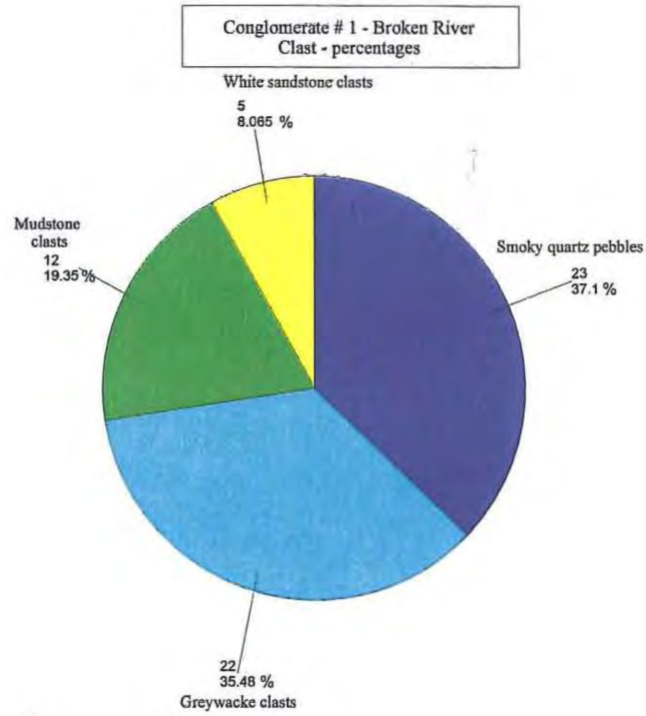

A)

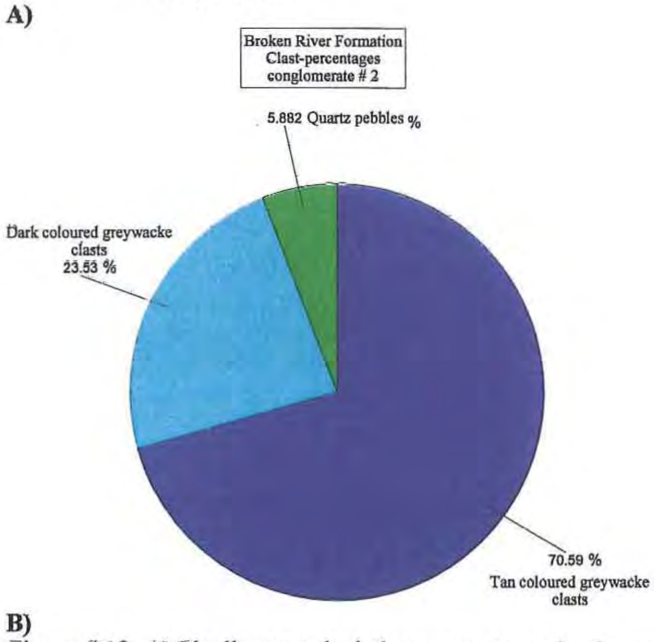

B)

Figure 5.12: A) Pie diagrams depicting source types for the conglomerates at Broken River. A) Polemic conglomerate,
Matrix supported, multiple source predominantly greywacke, smoky quartz pebbles, mudstone clasts and minor sandstone clasts. B) Clast supported monomictic conglomerate predominantly composed of greywacke clasts and minor quartz pebbles.

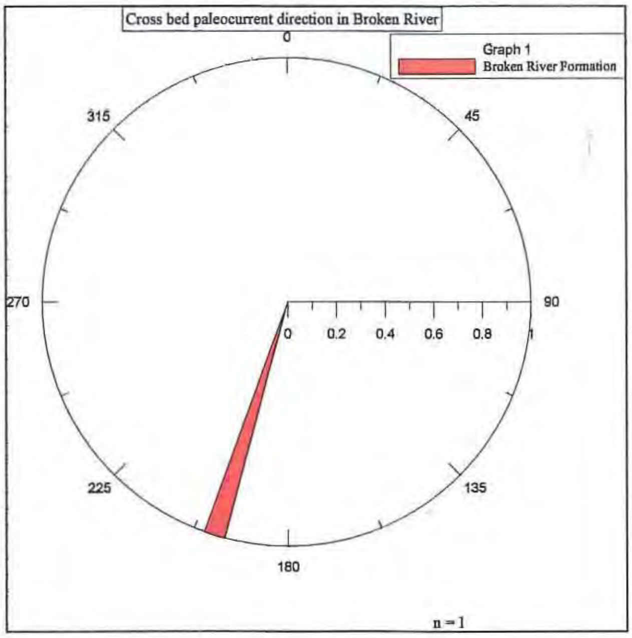

Figure 5.5: Single restored, azimuth cross bed paleocurrent from the Broken River Formation.

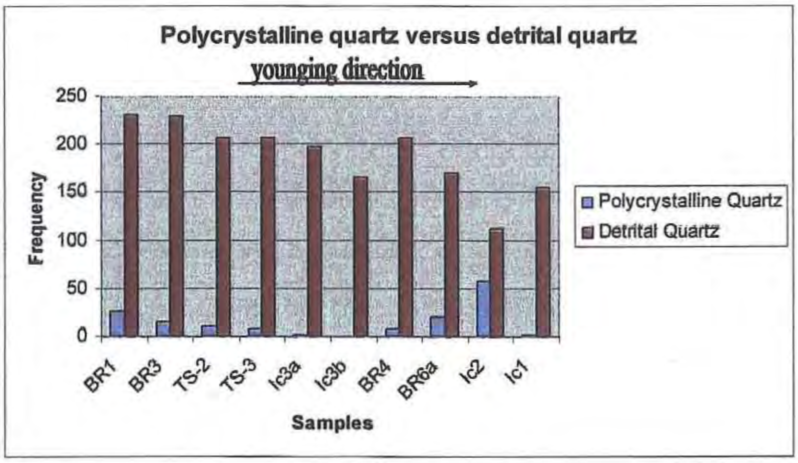

Figure 5.13: Histogram of polycrystalline quartz grains versus detrital quartz grains. Overall low polycrystalline content confined to the Broken River Formation (samples BR1-Ic3b, from various localities in the Castle Hill Basin) and a high polycrystalline peak in the upper Iron Creek Formation (Iron Creek Formation: samples BR4 – Ic1).

5.5 Glaucony as Sedimentation Indicator

5.5.1 Descriptions of Glauconite

Glauconite fecal pellets are the predominant form of the glauconitic minerals for the Castle Hill area. The Broken River Formation although not abundantly full of glauconite, some present, especially in Whitewater Stream, while it is absent elsewhere in the Broken River Formation. The subarkose arenites of the Broken River Formation in Whitewater Stream range in glauconite content from 12 to 33% (appendices 1, 2, 4). Samples from fine sandstones have fine glauconite grains. At the Whitewater Stream locality, 3 varieties of glauconite have been observed and recorded, the nascent, micaceous and the evolved/mature variety. In comparison to other localities the Broken River Formation at Whitewater Stream has a moderate to high population of evolved/mature grains. This can be seen from sample Ic3a from Whitewater Stream depicting almost equal proportions of evolved to nascent glaucony (fig. 5.6). Pale green nascent coexist with bright dark green mature glaucony grains. The evolved/mature glauconite usually appears further up section in the Iron Creek Formation; however at this locality the glauconite occurs almost equally in both forms (fig. 5.7). The micaceous variety is also present in the Broken River Formation.

The lower Iron Creek Formation, especially the glauconitic Charteris Bay Sandstone seen in sample BR4 (fig. 5.6) contains an average of 16% glauconite in total which corresponds in content to that described by McConchie and Lewis (1978) as the composition of the Charteris Bay Sandstone. The Charteris Bay Sandstone, although glauconitic in nature, has predominantly evolved/mature glaucony grains while the other counterparts are minor. In the Cave Stream locality G (fig. 5.1), sample BR6a (fig. 5.6) has a single high evolved/mature content while the total glauconite content reaches 21%, here again typical of the composition of the lower Charteris Bay Sandstone Member.

In Tims Stream, locality E, the Iron Creek Greensand Member has high glauconite content with sample TS11 reaching 60% total glauconite while the remaining detritals are composed of very fine quartz sand and silt grains. In detail the glaucony grains are all evolved/mature (fig 5.8) displaying well rounded and oblate shape (figs. 5.10, 5.11). Fibroradiated rims are evident in some glauconite grains in the Iron Creek Greensand (fig. 5.9). The presence of the rims clearly indicates a period where precipitation and maturation was facilitated by low sedimentation rate without significant sediment input. The well rounded oblate glaucony grains display minor surface abrasions and dissolution pits resulting from non reworking quiescent conditions.

The general trend for the formations in the Castle Hill area depict the presence of evolved/mature and nascent glaucony grains in the lower Broken River Formation while up section the Charteris Bay Sandstone Member and the Iron Creek Greensand Member of the Iron Creek Formation contains a marked increase in evolved/mature grains while nascent and micaceous glauconite grains decrease. These glaucony grains are similar to the Type A and B glauconites described by McConchie and Lewis (1978).

5.5.2 Glauconite Interpretation

The glauconites within the Broken River Formation at Whitewater Stream are interpreted to have formed in neritic conditions adjacent to an estuary or fluviodeltaic setting; this is in conjuction with the presence of carbonaceous muds and sandstones containing coal stringers and bioturbated sands. The possibility of post depositional formation of glaucony in water saturated sands is strong; in any case all the glaucony varieties point towards an autochthonous formation since transport and reworking from older formations is not feasible. Parautochthonous formation and transport is possible, however the sedimentary structures and the nature of the sequence indicate low energy conditions. Amorosi (1997) discusses that in transgressive successions, glauconitization commonly post –dates coarse grained sedimentation in nearshore areas. Overall the glaucony formation requires low sedimentation so a low sedimentation rate is interpreted along with autochtonous formation.

Higher in the section in the Iron Creek Formation the glauconite grains display well rounded and oblate evolved/mature variety with fibroradiated rims interpreted as clearly pre-dating clastic input all points towards in situ formation of glaucony. The petrography in conjuction with the sedimentary structures and the composition indicate low energy, deposition from suspension, reworking of fines and occasional transport of coarse detritus and shell material by longshore drift and storm events. Amorosi (1997) interprets lithologically homogeneous successions with non selective spatial distribution of glaucony as likely to reflect an autochthonous origin of grains. In this case a low sedimentation rate is interpreted and an autochthonous origin for the glauconite grains in the Iron Creek Formation in the Castle Hill basin area.

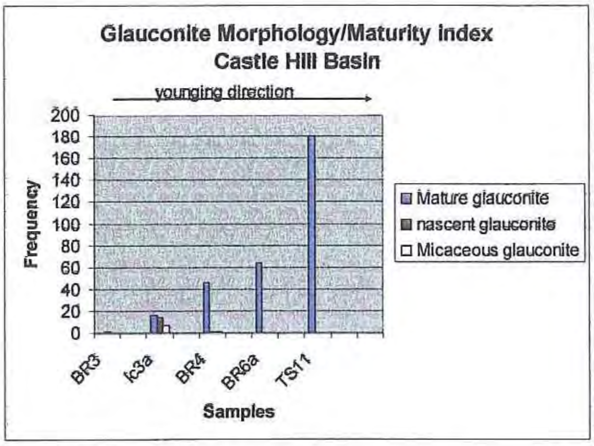

Figure 5.6: Frequency of glauconite grains displaying Nascent Stage; evolved/mature glauconite and micaceous glauconite. Evolved/Mature glauconite occurs from the upper beds of the Broken River Formation to the upper Iron Creek Formation. Nascent and micaceous glauconite dominates in the lower stratigraphy. Micaceous glauconite represents a secondary primitive growth episode. All samples represent stratigraphic order in the regional sense.

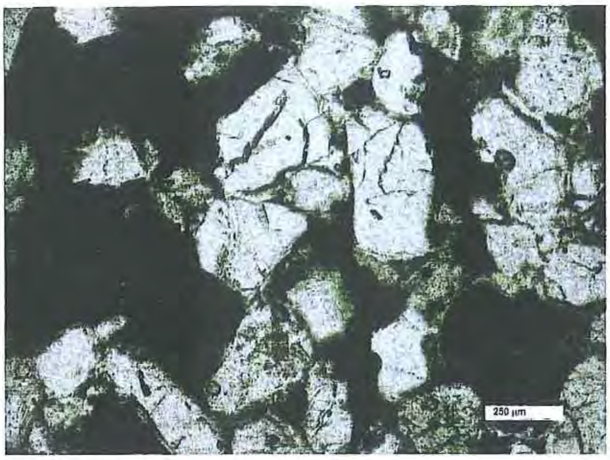

Figure 5.7: Well rounded glaucony grains of the Iron Creek Greensand at Whitewater Stream, occasional glaucony cement within the intergranular spaces.

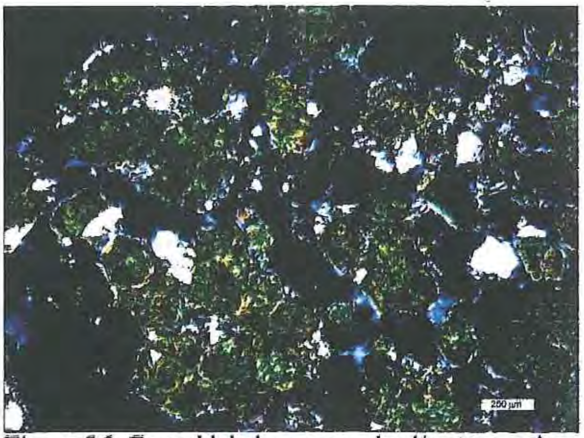

Figure 5.8: Emerald dark green evolved/mature grains of the Iron Creek Greensand in Tims Stream (sample TS11), cross polarized light – optical micrograph.

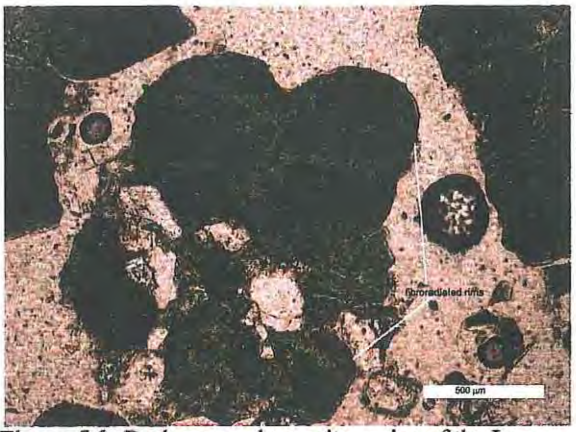

Figure 5.9: Dark green glauconite grains of the Iron Creek Greensand in Tims Stream (sample TS11), plane Polarized light – optical micrograph.

Figure 5.10: SEM micrograph of coalesced well rounded Evolved/mature glaucony grains (sample TS11 – Iron Creek Greensand).

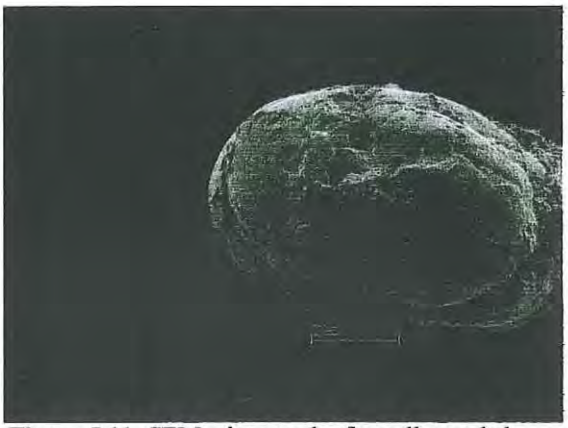

Figure 5.11: SEM micrograph of a well rounded evolved/mature glaucony grain with dissolution pit marks and cracks from compaction (sample TS11).

5.6 Provenance

5.6.1 Conglomerate Clast Counts

The clast counts reveal multiple sources for the matrix supported conglomerate at locality C (figs. 5.1; 5.12, A). The clast count revealed that 37% is quartz pebbles, 35% greywacke clasts, 19% mudstone clasts and 8% consists of white sandstone clasts. The greywacke clasts are interpreted as being source from the Torlesse basement while the quartz pebbles are either derived by a Haast Schist or Alpine Schist equivalent source. Alternatively the quartz pebbles could be sourced from older Torlesse conglomerates. The mudstone clasts are indicative of penecontemporaneous origin during faulting and half graben formation during the Late Cretaceous (Haumurian). The white sandstone clasts are more problematic since they may be recycled from older formations such as the Monro Conglomerate at Malvern; however a penecontemporaneous source is also feasible.

The clast count on the clast supported conglomerate (fig. 5.12; B) is clearly monomictic composed predominantly of greywacke clasts 93% and secondary minor quartz pebbles at 5%. Thus again a similar provenance is interpreted for this deposit, with the greywacke clasts sourced from the Torlesse basement and the quartz pebbles sourced either from a metamorphic terrane such as the Haast Schist or a granitic suite such as a western province granite.

5.6.2 Sandstone Composition

Compositionally the Broken River Formation is composed of subarkose arenites typical interior craton setting (fig. 5.15; A) with minor lithics and (appendices 1, 2) minor silt and sericite grains. The samples have a glauconite content of 12 up to 33% only in the Whitewater Stream sequence. Other minerals such as micas are minor and consist of the muscovite variety.

The overlying Iron Creek Formation is also composed of subarkose arenites with minor lithics. In the lower Charteris Bay Sandstone the glauconite content ranges from 16% and reaches 30% in the Iron Creek Greensand (appendices 1,2) while in certain areas, such as Tims Stream, glauconite reaches 60% of the total standard point counts. The Iron Creek Formation, especially the upper Iron Creek Greensand is composed of 14% calcite sparite and 5% calcite micrite; fossils include foraminifera and bryozoa constituting 10% of the total composition (appendices 1, 2).

The lithics are composed of 4% sedimentary lithics while 1% constitutes volcanic lithoclasts. The feldspars are almost entirely dominated by alkali feldspar (appendices 2, 3). The alkali feldspar is of the orthoclase variety while minor microcline occurs. Alkali feldspar constitutes about 8 to 14% of the total 300 point counts (appendix 2), while the total alkali feldspar content is about 10%.Plagioclase feldspar occurs in the upper Iron Creek Formation in Whitewater Stream where it displays about 8% while only 3% alkali feldspar exists.

The samples from the Castle Hill Basin and Whitewater Stream display low polycrystalline grains compared to the monocrystalline quartz grains (fig. 5.13). The presence of polycrystalline quartz grains is minor consisting of 3 to 8% for the Broken River Formation and a similar composition occurs for the Iron Creek Formation (appendices 1, 2), while in Whitewater Stream polycrystalline quartz grains reach 19% and well rounded granules but only in the Iron Creek Formation. The samples show initially a peak on the left of the histogram in the lower Broken River Formation at Broken River while it increases in the upper Iron Creek Formation at the Whitewater Stream in sample Ic2 (fig. 5.13).

Alkali feldspar is especially abundant in syenites, granites, granodiorites and their volcanic equivalents (Shelley 1985). Shelley (1985) describes that in felsic plutonic rocks and high grade metamorphic rocks, the alkali feldspars are usually orthoclase and microcline while in volcanic rocks sanidine and anorthoclase is common. It is interpreted that alkali feldspars are derived from plutonic, volcanic and/or metamorphic rocks. The probable source of the feldspar population is the Haast Schist to the south, or Karamea-Separation Point Batholith. Muscovite is common in regionally metamorphosed rocks, especially those derived from pelitic sediments, it is also a common detrital mineral (Shelley 1985). Muscovite occurs also in granites and pegmatites (Boggs 1992). Since the detrital muscovites are minor and confined to finer grain sizes a general interpretation of low grade metamorphic or granitic source is made.

A Torlesse greywacke source is interpreted for the presence of sedimentary lithics and occasional chert while volcanic lithics are attributed to the reworking and transport of the southern Mt. Somers Volcanics.

5.6.3 Quartz Provenance (SEM-CL)

The integrated SEM-CL/optical microscopy provenance technique of quartz was applied to the Broken River and Iron Creek Formations subarkose arenites. 105 selected quartz grains were analyzed with integrated SEM-CL/optical analysis in each sample following the technique devised by Bernet and Bassett (2005). Detrital quartz was compared for its CL and optical properties (appendices 6, 7) as described in chapter 2.

The Castle Hill Basin was sampled from the localities (B, C, D; fig. 5.1) and in the southern Whitewater Stream for SEM/CL-optical analysis. The same samples used in petrographic point counts were also used in CL analysis.

From the Broken River Formation, irrespective of location, plutonic quartz grains reach 36 to 39%, while the plutonic content slightly decreases in the upper Iron Creek Formation at 26 – 23%. About half of the plutonic grains are deformed while retaining their healed - microcracks and displaying strong undulose extinction (appendices 5, 7). The SEM-CL/optical technique reveals about half plutonic grains displaying deformation features thus interpreted as low deformational events in the course of a single plutonic quartz crystal.

Grains with strong undulose extinction and black-dark CL and/or polycrystalline were interpreted as metamorphic as mentioned in chapter 2. The samples from the Broken River Formation have on average 51 – 59% metamorphic quartz grains, while the Iron Creek Formation's metamorphic quartz population remains the same, however it increases significantly in the upper Iron Creek Formation at Whitewaters Stream. The metamorphic quartz grains are predominantly monocrystalline with the polycrystalline at low proportions.

The volcanic quartz component is minimal compared with the plutonic and metamorphic components. The volcanic component is about 11 to 18% of the total quartz types and remains stable through out all the formations; at Whitewater Stream it very slightly declines at 7%.

The data obtained from the Broken River and Iron Creek Formation's arenites with the SEM-CL/optical microscopy technique reveals a strong bimodality of metamorphic versus plutonic quartz grains with the metamorphic source type dominating over the plutonic counterpart while in some cases the proportions are almost equal (appendix 5 - figs. 5.9-5.10, 5.11-5.12) The volcanic source type was low in all the formations studied (fig.5.14).

The metamorphic quartz grains are monocrystalline angular to subangular and predominantly low grade since they do not display high grade deformation features as studied by Young (1976). Although the metamorphic quartz is determined by the combined SEM-CL/optical microscopy, the grade of metamorphism is established by the structures and textures of the grains in conventional microscopy. Lower grade rocks are characterized by a diversity of crystal sizes polygonized to recrystallized (50µm-500µm) while high grade rocks have slightly larger crystal sizes (Young 1976). Angularity is most common in all quartz types (appendix 7).

The provenance is dominantly metamorphic and plutonic with a minor volcanic source, the source types indicate major metamorphic basement source while one sample (sample BR4 of the Charteris Bay Sandstone), plots in the mixed source field indicative of a mixed provenance (fig.5.15; B). The metamorphic source is more likely regional than local because the Torlesse basement is too fine grained to provide a major source for metamorphic grains. The metamorphic quartz grains being derived from a metamorphic terrane such as the Otago/Haast Schist and/or by alpine Schist, alternatively a western quartzite source could have provided quartz detritus, since the Western Province Greenland Group contains quartzites. The volcanic quartz grains are most evident of being sourced from the southern Mt. Somers Volcanics Group. The plutonics are interpreted to have been derived from a distant plutonic suite provenance, likely a western granitic suite (Karamea Batholith, Separation Point Batholith) The angularity of the quartz grains are interpreted to have been transported dominantly by fluvial conditions and then reworked locally in a marginal marine setting.

5.7 Summary of Results for Castle Hill Basin

The Castle Hill Basin consists of Late Cretaceous – Tertiary sequence that unconformably overlies Triassic Torlesse Group rocks. The basal sequence consists of locally derived conglomerates of the Broken River Formation fluvial fresh water deposits succeeded by fluviodeltaic tidal estuarine deposits in the Broken River area and in Whitewater Stream. Paleocurrent direction indicates sediment transport from the north-east reflecting waves or river currents. The presence of evolved/mature and nascent glauconite in the Broken River carbonaceous mudstone and sandstones at Whitewater stream reflects in situ autochthonous formation hence a low sedimentation rate in a marine setting during the Late Cretaceous Early Paleocene. The Broken River Formation is then succeeded by the Iron Creek Formation comprising of low glauconitic and an upper glaucarenite member during the Paleocene-Eocene. The sequence is characteristic of tidal to shallow marine sequence with well rounded dark green evolved/mature glauconite grains characteristic of autochthonous formation and low sedimentation rate under quiescent conditions.

Provenance of QFL components indicates subarkose arenites for the sequence spanning the Broken River and Iron Creek Formations characteristic of a craton interior setting. The dominance of alkali feldspar indicated a felsic/plutonic source while an alternative metamorphic regional source was possible. The presence of sedimentary lithics indicated subsequently a minor provenance contribution from the fined grained Torlesse Supergroup, while volcanic lithics indicate a Mt. Somers Volcanic provenance.

The applications of the SEM-CL/optical microscopy technique on quartz provenance for the Castle Hill Basin sequence reveal a strong bimodality of metamorphic to plutonic source with a secondary minor volcanic source. A metamorphic terrane such as the Haast/Otago Schist and/or a western province Greenland Group quartzite source is implied for the metamorphic quartz signature while a plutonic source such as the western Karamea or Separation Point Batholiths are implied for providing plutonic quartz grains. The minor volcanic quartz type is indicative of a distant volcanic field more likely the Mount Somers Volcanic Group.

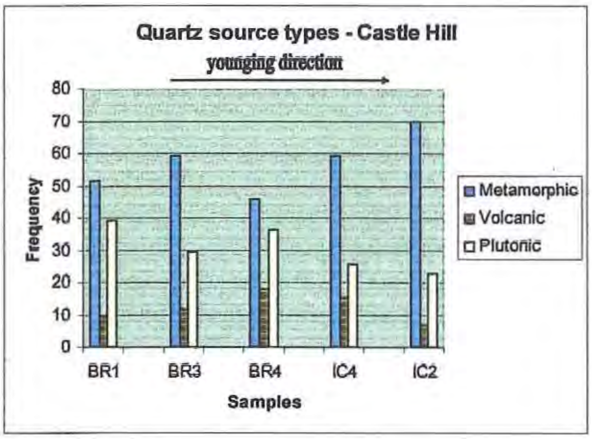

Figure 5.14: Frequency of grains displaying quartz per sample from the Broken River Formation to the upper beds of the Iron Creek Formation. Metamorphic and plutonic quartz types are dominant while the volcanic component is low but moderate. Sample BR1, BR3 are from the Broken River Formation (at Broken River), and sample Br4 is from the Iron Creek Formation in Broken River, while samples Ic4 and Ic2 are from the Iron Creek Formation at Whitewater Stream.

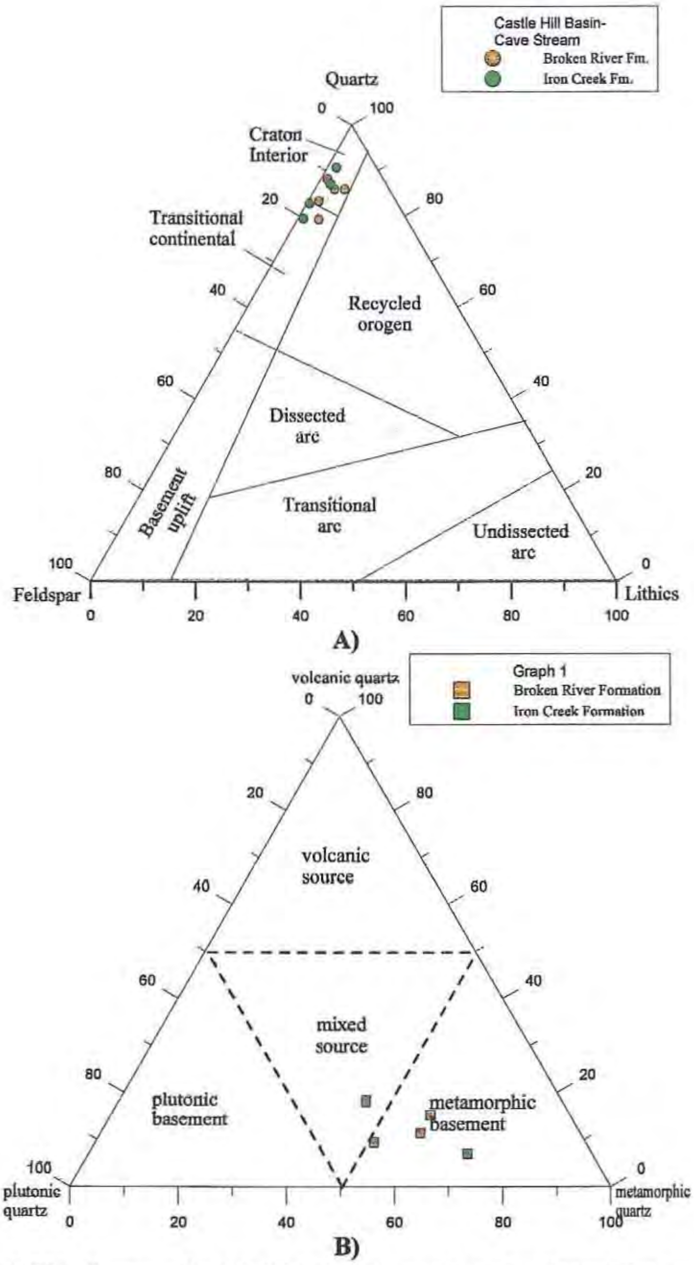

Figure 5.15: **A)** Standard QFL diagram after McBride (1963), on the basis of normalized point-counts, results from conventional point counts. Samples from the entire formations plot in the subarkose-arkose field. **B)** Provenance discrimination diagram after Bernet and Bassett (2005), of Castle Hill Basin's Broken River Formation and Iron Creek Formation, samples using the three main quartz types of volcanic, plutonic and metamorphic quartz, based on SEM-CL/optical analysis. The dashed lines indicate the 50 percent lines of each of the three main types. Metamorphic quartz includes all low-grade to high-grade metamorphic, recrystallized and vein quartz. (Not all samples used in QFL were used in SEM-CL point counts because of very fine grain size restriction in the technique).

CHAPTER SIX
AVOCA – IRON CREEK

6.1 Regional Geologic Setting & Previous Work

The Avoca Iron Creek area lies to the east of the Castle Hill Basin. The Broken River cuts through a rich succession of Late Triassic to Late Cretaceous Tertiary rocks. The sequence is preserved in Iron Creek a tributary of the lower Broken River and in the Avoca area further downstream to the east (fig. 6.1). In the Avoca area the sequence is exposed in the eastern parts of the Castle Hill Basin tectonic depression which is bound to the south-east by a fault with recent trace which can be seen on the northern flanks of the Torlesse Range (Bradshaw 1975; McLennan 1981) (fig. 6.2). Pleistocene glacial deposits form distinctive terraces overlie the Cretaceous-Tertiary succession at the Avoca and Iron Creek area.

The Late Cretaceous to Tertiary sequence encompasses the Broken River Formation (Late Cretaceous), Iron Creek Formation (Paleocene – Eocene), Coleridge Formation (Early Oligocene), Thomas Formation (Late Oligocene) and Enys Formation (Miocene) in which the four oldest formations represent a major transgression and the youngest records a regressive part of the cycle (McLennan 1981).

The earliest work in the Avoca – Iron Creek area was done by Speight (1915; 1920) although he merely made reference to the area; most of the research in this area was done by Gage (1970). Gage made the first detailed descriptions and revised the nomenclature. McLennan (1981) made some modifications to the stratigraphy and commented on the association of unconformities at the Avoca area attributed to local tectonic events.

6.2 Stratigraphy

The Avoca-Iron Creek area contains basal Torlesse Supergroup rocks (Late Triassic) which are succeeded unconformably by the Broken River Formation, a sequence of basal conglomerates, coal and carbonaceous sandstones indicative of non - marine to marginal marine settings. In turn the Broken River Formation is succeeded by the Iron Creek Formation by a disconformity at Avoca and Iron Creek (McLennan 1981). The Iron Creek Formation is composed of the lower glauconitic Avoca Sand Member and the upper glaucarenite Iron Creek Greensand Member (Gage 1970;

McLennan 1981). The Iron Creek is succeeded by the Colerdidge Formation of the Porter Group by a local unconformity. The Coleridge Formation is composed of quartz sandstones and marls according to McLennan (1981). Thomas Formation tuffs and limestones succeed, while Enys Formation coal measures, sandstones and siltstones overlie the sequence by an unconformable contact.

The Broken River and Iron Creek Formations will be the focus of this research and will be discussed in more detail.

6.2.1 Torlesse Supergroup Rocks

The Torlesse Supergroup at the Avoca – Iron Creek area consist of "strongly jointed greywacke and well indurated dark-grey siltstone and argillite, replaced locally by tuffaceous mudstone, chert, reddish or puce-coloured jaspillite and basic volcanic rocks"(Gage 1970). The Torlesse Supergroup in the Avoca- Iron Creek area consists of the Rakaia Terrane which is Triassic in age.

6.2.2 Broken River Formation

Gage (1970) named the formation as Broken River Coal Measures based on the abundance of coal and carbonaceous matter and it was later redefined by Browne and Field (1985) as Broken River Formation to encompass the carbonaceous quartzose sands overlying the basal conglomerates and coal measures. Gage (1970) described the Broken River Formation as "unevenly stratified, current-bedded, white, quartz sandstone, dark grey, carbonaceous silt and sand, and lensoid beds of sub-bituminous coal. Thin basal breccia including both greywacke and quartz pebbles up to 4in". McLennan (1981) described the composition of the formation as a carbonaceous feldsarenite to subfeldsarenite. McLennan (1981) further noted the presence of deformed coal beds with folds.

6.3.3 Iron Creek Formation

The formation was first defined by Gage (1970) as the Iron Creek Greensand. Gage (1970) described it as "massive to coarse greyish green glauconitic quartz sandstone predominates in the lower half of the formation. The upper part consists of medium to fine current bedded glauconitic sandstone with prominent bands of dark greensand". Gage (1970) describes concretionary bands, irregular spheroidal concretions, molluscan shells, burrows and iron stained yellow, red or brown sandstone in the lower part of the formation and darker greensand in the upper part of the formation. McLennan (1981) renamed the Iron Creek Formation and subdivided it into a lower glauconitic member, the Avoca Sand Member, and the upper Iron Creek

Greensand based on the higher glauconite content. Browne and Field (1985) renamed the Avoca Sand Member to the Charteris Bay Sandstone to include the regional stratigraphic similarity.

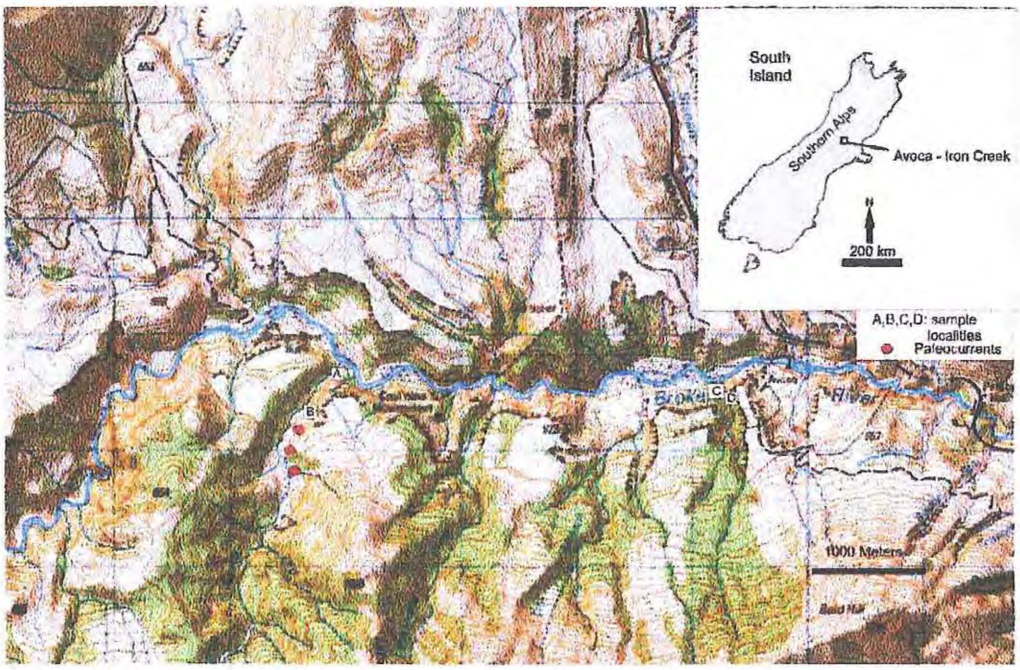

Figure 6.1: Topographic map of the Avoca – Iron Creek area outlining sample localities.

6.3 Sedimentary Descriptions

6.3.1 Broken River Formation

Exposures of the Broken River Formation occur at the confluence of the Iron Creek with the Broken River (fig. 6.1). A large exposure of Broken River Formation is preserved along strike paralleling the Broken River at locality A (fig. 6.1; appendix 1 figs. 1.35, 1.36). McLennan describes a thickness of ~60 metres for the Broken River Formation at Iron Creek. The Iron Creek parallels a north – south trending syncline where most of the Cretaceous - Tertiary sequence is preserved. Further to the east at localities C and D in Kowhai Canyon (fig. 6.1) a sequence of Broken River and Iron Creek Formations rests unconformably on Torlesse Supergroup rocks. The Broken River Formation at Avoca-Kowhai Canyon at locality C forms north south bands, (McLennan 1981) due to fault repetitions.

In detail the Broken River Formation at the Iron Creek location is characterized by basal conglomerates unconformably overlying Torlesse greywacke rocks. A large exposure of conglomerates was observed and one clast count performed on the deposit. The conglomerate is iron stained with bright red colour, is matrix supported and is monomictic (appendix 1 fig. 1.34).

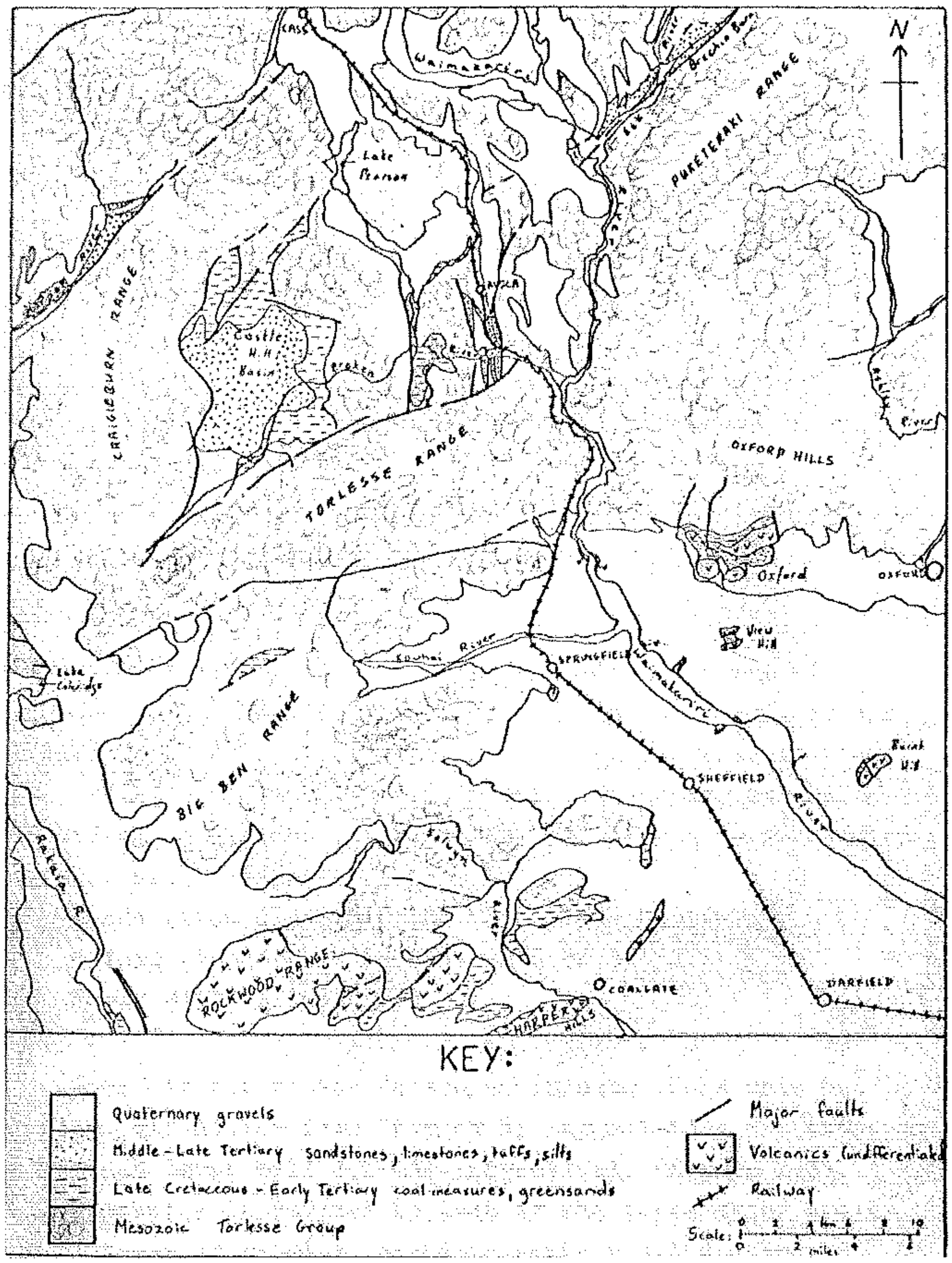

Figure 6.2: Simplified geological map of south-east North Canterbury showing the regional relationships. Areas examined to the east of the Castle Hill Basin (From Gregg 1964; McLennan 1981).

It is massive, poorly sorted with clasts and boulders of greywacke, and red chert; while the matrix is fine to medium quartz sand. The clasts are subangular to angular and have a maximum diameter of 15 cm while the median size of the clasts is 3 cm in diameter.

Overlying the conglomerates in close proximity is an exposure of sandstone (appendix 1 fig. 1.34). It consists of faintly cross bedded, white-cream coloured, moderately indurated, and well sorted, slightly glauconitic, fine quartzose sandstone with carbonaceous streaks and stringers and coal seams. Further to the east at Avoca-

Kowhai Canyon, locality C (fig. 6.1) an exposure of Broken River Formation unconformably overlies Torlesse rocks although a contact was not observable due to scrub covered sections. However, the deposit is composed of a massive, iron stained, white-grey coloured, moderately-well sorted, fine to medium sandstone with a glauconite content of 4% (appendix 1 fig. 1.41).

6.3.2 Iron Creek Formation

The Iron Creek Formation sharply overlies the Broken River Formation at Iron Creek. According to McLennan (1981), the contact is sharp, indicative of a possible disconformity. However, the contact was not observed in this research due to scrub-covered sections. The same occurs at Avoca although again the contact was not exposed. The Iron Creek Formation at locality B (fig. 6.1) is followed by the basal Charteris Bay Sandstone Member. This consists of iron stained, grey-cream coloured, moderately indurated, well sorted, medium quartzose sandstone with coalified wood fragments, burrows (appendix 1 fig. 1.42), calcareous-cemented sandstone lenses and faint cross bedding. Direct measurement of stratigraphic sections was not feasible due to the structure and the topography of the area; however representative samples and data were collected from the member.

Up stream in Iron Creek the Charteris Bay Sandstone increases in glauconite content from 6% in locality B to 30% and has a calcite micrite and sparite matrix reaching 27%. The Charteris Bay Sandstone is characterized by cross bed foresets (appendix 1 fig. 1.37), gravel lenses and calcareous cemented sandstone lenses towards the top. Glauconite is inhomogeneous distributed in the member in the lower section while in the upper parts of the Charteris Bay Sandstone it becomes concentrated within cross bed foresets (appendix 1 fig. 1.38). Up section the Iron Creek Greensand member becomes distinctively dark green with glauconite contents of 50% and trough cross beds (appendix 1 fig. 1.39).

Cross bed paleocurrents, measured and restored to true azimuth directions, gave paleoflow directions from the north and north-west (fig. 6.3). The crossbeds occur in sets of 1 to 60-30 cm thick.

The formation at Avoca at locality D (fig 6.1) is similar in composition to Iron Creek with massive, fine to medium, glauconitic, quartzose, bioturbated with calcareous cemented lenses; while the glauconite content is about 16%, characteristic of the Charteris Bay Sandstone. The upper Iron Creek Greensand was not observed.

6.4 Interpretations of Depositional Settings

6.4.1 Broken River Formation

The basal conglomerate overlying Torlesse Group rocks is interpreted as a fluvial deposit, most likely a meandering river deposit. The greywacke and chert clasts are interpreted to have been locally derived from the underlying Torlesse rocks. Coal seams are interpreted as forming in flood plain settings. McLennan (1981) interprets the slumped and disturbed coal seams to indicate penecontemporaneous deformation taking place in the Late Haumurian. The overlying Broken River Formation sandstones contain minor amounts of glauconite making them marginal marine.

6.4.2 Iron Creek Formation

The lower unit of the Iron Creek Formation, the Charteris Bay Sandstone is characteristic glauconitic burrowed sandstones with minor cross beds at the bottom to parallel cross bed foresets at the top, indicating a lower shoreface to foreshore depositional environment influenced by waves and tides. McLennan (1981) attributes a lack of beach deposits and the presence of gravel lenses a granule layers to indicate reworking from older deposits such as the Broken River Formation and high energy waves and currents would rip up underlying soft sediment, thus McLennan (1981) attributes a disconformity at the base of the Iron Creek Formation. However, the presence of glauconite in the Broken River Formation disregards any significant break in the sedimentation; the disconformity between the two formations is probably attributed to local erosion in a channel.

Paleocurrent directions (fig. 6.3) indicate flow from the north and north-west. The paleocurrent directions are interpreted as currents produced from longshore drift. This in conjuction with glauconite concentrated in cross bed foresets indicate a foreshore to shallow marine environment while the increase in glauconite upsection in the Iron Creek Greensand Member of the formation indicate a shallow marine environment still influenced by currents based on the presence of trough cross stratification.

6.5 Glaucony as Sedimentation Indicator

6.5.1 Descriptions of Glauconite

Glaucony occurs only in minor amounts 4% in the Broken River Formation at Avoca, while it is abundant in the overlying Iron Creek Formation. The arenites within the Charteris Bay Sandstone of the Iron Creek Formation at Iron Creek contain a minimal 0.6% glauconite while it reaches 30% in the Iron Creek Greensand Member. Further up section the Iron Creek Formation decreases in glauconite content to a consistent 21% of total composition. It is noted here that although samples were not taken up section, the Iron Creek Greensand increases dramatically in glauconite content to > 50%.

At Avoca the Broken River Formation is dominated by nascent glauconite (fig. 6.9) with minor amounts of micaceous glauconite. Up section in the Charteris Bay Sandstone the mature/evolved glaucony type increases at the expense of decreasing nascent glauconite (figs. 6.4, 6.10). Overall at the Avoca area the glauconite content in the Iron Creek Formation is low at 16%.

The Charteris Bay Sandstone has minor glauconite content and it is confined to the nascent variety in sample IC3 (fig. 6.4). Glauconite content increases dramatically in the Iron Creek Greensand Member and it is confined to the mature/evolved glaucony type within sample IC4. Glauconite declines in overall content in sample IC7 with both nascent and micaceous varieties present. Further up section in the Iron Creek Formation, glauconite decreases overall with both nascent and micaceous glauconite becoming abundant in sample IC8 (fig. 6.4).

The Iron Creek Greensand Member with sample IC7 displays mature/evolved glauconite (figs. 6.5, 6.6) with well rounded surfaces with cracks (fig. 6.7). Up section sample IC8 has grains that show compacted surfaces which may be mature/evolved glauconite cement or pre-existing evolved grains being compacted by detrital grains (fig 6.8).

6.5.2 Glauconite Interpretation

The glaucony grains in the Broken River and Iron Creek Formations are interpreted to have formed in marginal marine nearshore to shallow marine depositional settings.

The Broken River Formation displays nascent and secondary micaceous glauconite indicative of autochthonous formation and low sedimentation. In addition the lower Charteris Bay Sandstone Member displays nascent and micaceous glaucony indicative of autochthonous formation and low sedimentation. Therefore the lower succession of the Broken River Formation and Iron Creek formation represents an autochthonous formation of glaucony and a slow sedimentation rate while the upper sequence of the Iron Creek Formation represents parautochthonous formation of glaucony and a low to moderate sedimentation rate.

The morphology of well rounded dark green mature/evolved grains with cracks indicates in situ formation or autochthonous formation of glaucony, hence a low sedimentation rate. Also mature/evolved glauconite cement indicates autochthonous formation. However the glaucarenites of the Iron Creek Formation are cross stratified with parallel cross beds typical of foreshore setting with rapid sedimentation. This would argue against formation of glauconite under low sedimentation rates, however paraautochthonous formation and transport is likely, sine the grains showing cracks indicate possible breakage during transport. Chafetz and Reid (2000) make the case that glauconite grains cannot be transported very far without displaying evidence of abrasion. In detail glauconites abrade and fragment rapidly when agitated in water, therefore the result of such action would produce fragmented glauconite grains resembling recycled grains mentioned by McConchie and Lewis (1978).

It is interpreted that although the sedimentary structures indicate normal to rapid sedimentation the glauconite grains are probably autochthonous. Amorosi (1997) suggests that the association of glaucony with high-energy and/or reworked deposits should not necessarily be regarded as diagnostic for an allochthonous origin of grains. McConchie and Lewis (1978) studied glauconites from other locations in the wider Castle Hill Basin area and described authigenic, allogenic and perigenic types of glauconite. It is interpreted for the Iron Creek area that the glauconites had a parautochthonous origin, thus formed locally and transported from the source locally. Amorosi (1997) discusses how autochthonous evolved glauconite from a shallow marine setting can be transported to a near shore setting. Longshore drift and currents could transport evolved glauconite from shallow or moderate depths to the foreshore area, particularly during a transgression. Thus compared to the Castle Hill Basin the glaucony grains are most likely parautochthonous hence a moderate low sedimentation rate for the wider area.

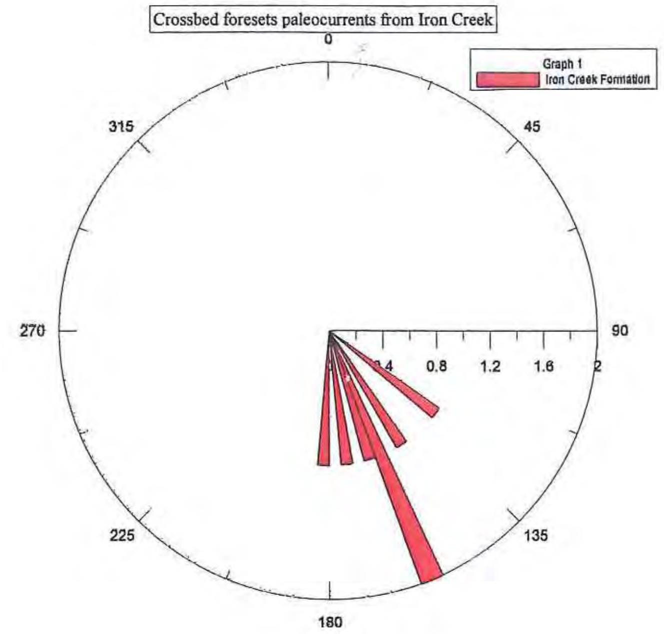

n = 7

Figure 6.3: Cross bed foresets from the Iron Creek Formation at Iron Creek.

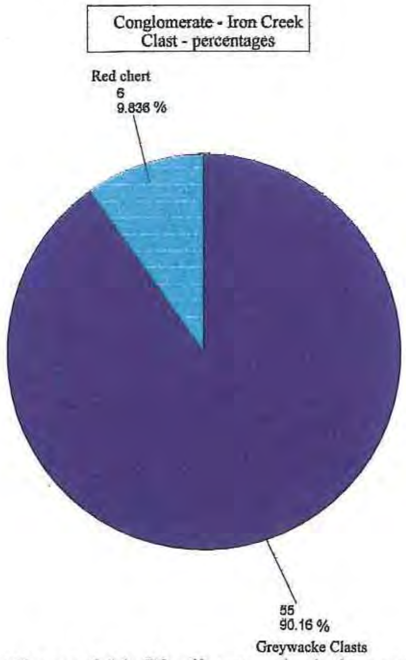

Figure 6.11: Pie diagram depicting composition for the conglomerate at Iron Creek.

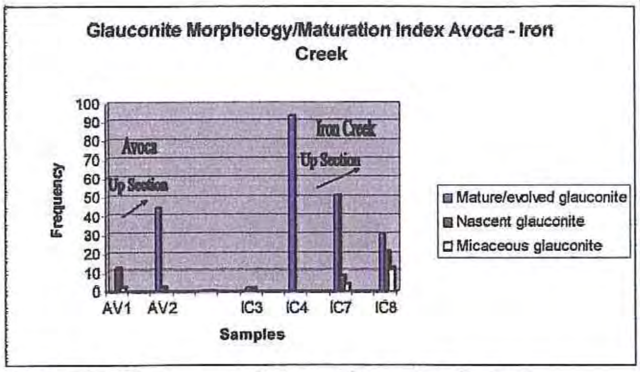

Figure 6.4: Frequency of glauconite grains displaying nascent stage, evolved/mature glauconite and micaceous glauconite. In the Broken River Formation at Avoca nascent and micaceous glaucony decreases while in the upper Iron Creek Fm. mature/evolved glauconite increases. The trend reverses at Iron Creek.

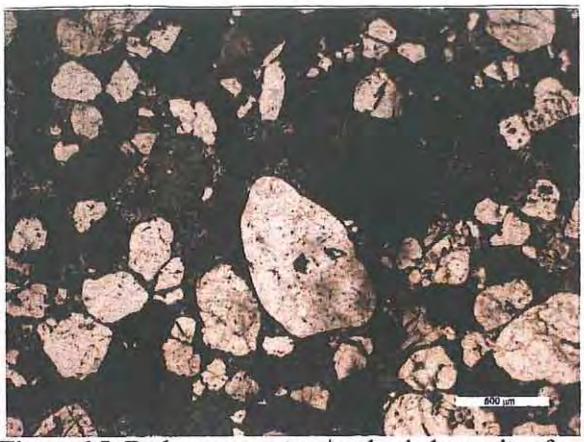

Figure 6.5: Dark green, mature/evolved glauconite of sample IC7 in Iron Creek (plane polarized light).

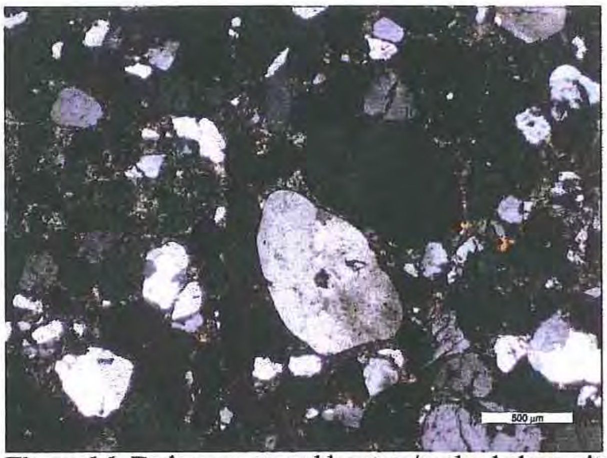

Figure 6.6: Dark green emerald mature/evolved glauconite of Sample IC7 in Iron Creek (cross polarized light).

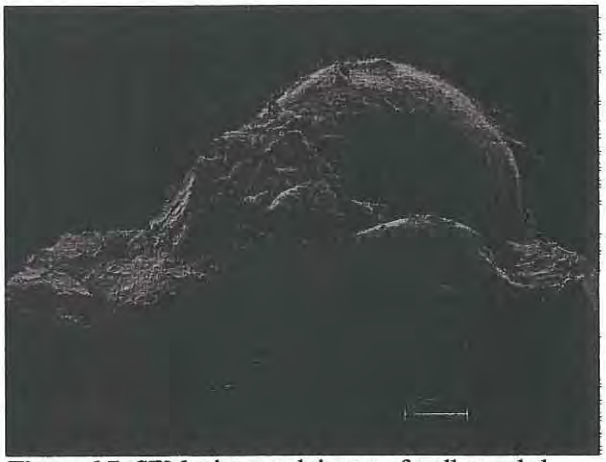

Figure 6.7: SEM micrograph image of well rounded Mature/ evolved glaucony grain with cracks.

Figure 6.8: autochthonous mature/evolved glauconite cement in sample IC8 (Iron Creek), SEM micrograph image.

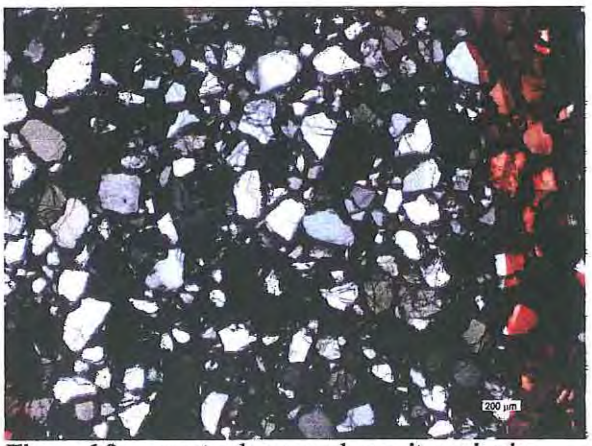

Figure 6.9: nascent pale green glauconite grains in Broken River Fm at Avoca (lower right of image cross polarized light). Sample AV1.

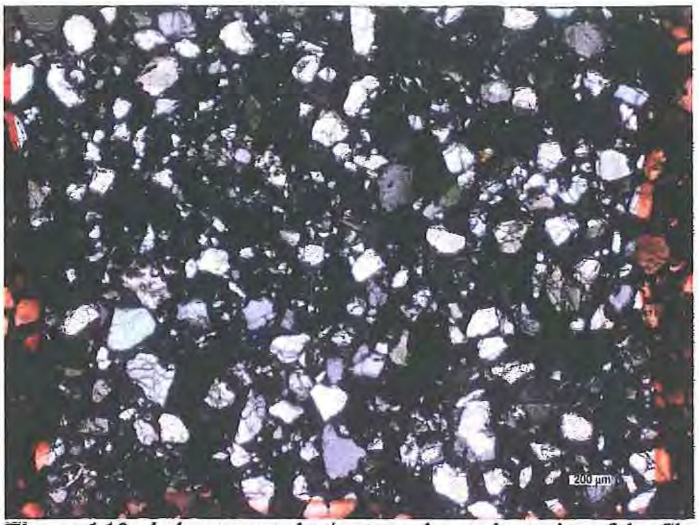

Figure 6.10: dark green evolve/mature glauconite grains of the Charteris Bay Sandstone at Avoca (cross polarized light), sample AV2.

6.6. Provenance

6.6.1 Conglomerate Clast Counts

Clast counts on the Broken River Formation conglomerate at Iron Creek suggest a single source for the deposit (fig. 6.11). The clast count shows 90% greywacke clasts, derived from the underlying Torlesse rocks, constitute almost the entire framework while 9% consists of minor chert source. The chert is most likely sourced from the Torlesse rocks. A single pre-unconformity Torlesse source is interpreted. The local Torlesse source is attributed to local uplift and down faulting causing erosion and deposition of Torlesse clasts in half grabens during the Early Haumurian (Browne & Field 1989). The chert is most likely derived also from the Torlesse Supergroup rocks.

6.6.2 Sandstone Composition

Samples were collected for petrographic analysis, point counts and subsequently CL analysis from the Broken River and Iron Creek Formations. It is noted here that only one sample of Broken River Formation was studied from the Avoca area, while the rest of the samples were from the Iron Creek Formation.

The composition of the Broken River Formation is a subarkosic arenite with minimal volcanic and sedimentary lithics (appendices 1, 2). Glauconite content is at 4% and the remaining accessory minerals comprise 1% muscovite. About 2% constitutes polycrystalline quartz while the majority of quartz grains are monocrystalline. Feldspars are dominated by 11% alkali feldspars while 5% are plagioclase feldspars, with the alkali feldspars predominantly orthoclase. The lithics are 1% sedimentary and a minor 0.6% volcanic lithics. The Broken River Formation arenites are predominantly fine to medium, moderately sorted. The sandstones plot in the transitional continental tectonic setting based on quartz, feldspar and lithic composition (fig. 6.13; A) (Dickinson 1983).

Since alkali feldspars are essential constituents of several felsic igneous rocks, pegmatites and many felsic and intermediate gneisses (Shelley 1985). Shelley (1985) describes how syenites, granites, granodiorites and their volcanic equivalents produce alkali feldspar. Based on the presence of alkali feldspar, it is interpreted that western province granites and/or the Haast Schist are possible sources for K- feldspar, alternatively the Mt. Somers Volcanics could provide a source. McLennan (1981) made the point that the presence of rare metamorphic and acid volcanic fragments in the Broken River Formation at Avoca is attributed to sources other than the Torlesse. The presence of plagioclase also indicates volcanic and metamorphic rocks (Shelley 1985). It is therefore interpreted that the plagioclase content may also be attributed to granites and/or metamorphic rocks. The Mt Somers Volcanics is the possible source for volcanic lithics. In turn the sedimentary lithics are more likely of a local Torlesse provenance, derived by erosion, uplift of lower rocks and subsequently reworked. The presence of muscovite is derived from either metamorphic terranes or granitic suite. Muscovite is common in granites and pegmatites (Shelley 1985).

The Iron Creek Formation is compositionally similar at Avoca as a subarkosic-arkose arenite typical of a transitional continental tectonic setting (Dickinson 1983). Lithics are minor 1% confined to sedimentary lithics (appendix 2) while accessory minerals are muscovite also 1%. Glauconite is common at 16%. Feldspars are dominantly alkali feldspar and minor plagioclase, and the same provenance is interpreted for much of the Iron Creek Formation as for the Broken River Formation.

At Iron Creek the arenites of the Charteris Bay Sandstone are slightly different in composition, which is a subarkose-subfeldsarenite that plots in the tectonic field of a recycled orogen (fig. 6.13; A). Sample IC3 is composed of 8% alkali feldspar while there is no plagioclase. The Charteris Bay Sandstone has a 9% sedimentary lithics and slightly higher polycrystalline quartz content at 7% than the 2% of the formations at Avoca. It is interpreted that the alkali feldspar has the same plutonic or metamorphic provenance with the Broken River Formation and Iron Creek Formation at Avoca. The high lithics content is possible due to the presence of a local disconformity between the top of the Broken River Formation and the base of the Charteris Bay

Sandstone, which would account for erosion and reworking of part of the underlying Broken River Formation.

Up section in the Charteris Bay Sandstone and in the Iron Creek Greeensand Member the arenites are subarkosic plotting in a craton interior tectonic setting. The composition is same while polycrystalline quartz increases to 9%. Overall quartz decreases in the Iron Creek Greensand Member of the Iron Creek Formation. The dominant feldspar type is alkali feldspar interpreted to have been sourced from either western province granite or the volcanic carapace of Cretaceous granites and/or sourced from the Haast Schist.

6.6.3 Quartz Provenance (SEM-CL)

The integrated SEM-CL/optical microscopy provenance technique of quartz was applied to four samples, 2 from the Avoca area and 2 from the Iron Creek localities. One sample was analysed from the Broken River Formation and 3 from the Iron Creek Formation. As the technique requires, 105 selected quartz grains were analysed from each sample and quartz was compared for its CL and optical properties (appendices 5, 6, 7). The same samples used for petrographic point counts were used in CL analysis.

In the Broken River Formation at Avoca 41% of the quartz grains are plutonic, while the frequency of deformed plutonic grains are minor compared to total number of plutonic grains (appendix 7). Thus deformed plutonic grains are interpreted as arising likely from deformation at source. Quartz grains displaying black/dark CL and strong undulose extinction and/or polycrystalline were interpreted as metamorphic. In the Broken River Formation the sample displayed 37% metamorphic quartz grains. The volcanic quartz content reaches about 21% for sample AV1 (appendix 5 figs.5.13, 5.14). The Iron Creek Formation at Avoca displays almost identical frequency of quartz types, with 41% plutonic quartz, 36% metamorphic quartz and 21% volcanic quartz (appendix 7) (appendix 5 figs 5.15, 5.16).

The Charteris Bay Sandstone at Iron Creek records 31% of plutonic quartz, 60% metamorphic quartz and 8% volcanic quartz. While in the upper Iron Creek Greensand the plutonic quartz reaches 40%, metamorphic 54% and volcanic quartz 6% for sample IC3 (appendix 5 fig. 5.17). The majority of the metamorphic quartz grains are monocrystalline while polycrystalline grains are minor. The total quartz grains from all the formations are fine grained and angular (appendix 7).

The data obtained with the SEM-CL/optical microscopy technique at Avoca reveal almost an equal proportion of all quartz types in both the Iron Creek and Broken River Formations with the metamorphic and plutonic quartz at a higher frequency (fig. 6.12). In contrast the two samples at Avoca from the Iron Creek Formation have a bimodality of metamorphic versus plutonic quartz, with the volcanic quartz type at a low frequency (fig. 6.12). Such a drastic change between two localities in quartz type percentages could be attributed perhaps to reworking due to local disconformity thus reworking of older metamorphic quartz crystals, however this is not a firm conclusion just a mere suggestion.

The trends of the quartz types overall reflect a mixed provenance with the metamorphics and plutonics dominating through out the succession therefore major metamorphic and plutonic sources are suggested (fig. 6.13; B). The metamorphic source is interpreted to be the same for all locations and it is most likely distal rather than local because the Torlesse basement is too fine grained to produce fine to medium quartz crystals plus the metamorphic grade of the Torlesse is not high enough. The metamorphic quartz grains were probably derived from a metamorphic terrane such as the Otago/Haast Schist and/or by alpine schist. The plutonics are interpreted to have been sourced from an exhumed plutonic suite, likely a southern or western granitic suite such as the Karamea Batholith or the Separation Point Batholith. The volcanic quartz grains are most evident of being sourced from the southern Mt Somers Volcanics Group. The angularity of the quartz grains are interpreted to have been transported by fluvial conditions and reworked locally.

6.7 Summary of Results for Avoca-Iron Creek

The Broken and Iron Creek Formations consist of Late Cretaceous – Tertiary sequence unconformably overlying Torlesse Group rocks reflecting non marine – fluvial to marginal marine to foreshore depositional settings. Paleocurrents reflect transport from the north, north-west reflecting longshore drift. The presence of nascent glauconite in homogeneous succession and evolved/mature well rounded glauconite in cross bed foresets indicate autochthonous and parautochthonous formation of glauconite respectively. Overall there is a trend of increasing evolved/mature glauconite upsection with periodic decreases in total glauconite content, while in the Iron Creek Greensand Member evolved/mature glauconite overwhelms the succession. Therefore a low to moderate sedimentation rate is interpreted. The presence of glauconite in the Broken River Formation increasing upsection in the Iron Creek Formation, most likely negates previous interpretations of a disconformity present between the two formations.

Provenance of conglomerates suggest local provenance from pre-unconformity Torlesse Group rocks. Provenance of sandstone components suggests largely an interior craton tectonic setting to a transitional tectonic setting; although a minor recycled orogen tectonic setting is implied. Alkali feldspar content reflects a felsic igneous source while an alternative metamorphic and/or plutonic regional source is also possible. The presence of sedimentary lithics reflect reworking from the Torlesse Supergroup for the Broken River Formation and likely reworking of a portion of the Broken River Formation for the presence of sedimentary lithics in the Iron Creek Formation. Minor volcanic lithics indicate the distant Mt Somers Volcanic Group as a source.

Provenance of quartz reflects overall a bimodality of metamorphic to plutonic source type at the Iron Creek area with minor volcanic source. A metamorphic terrane such as the Haast/Otago Schist is implied for the metamorphic quartz source while a western Karamea or Separation Point Batholiths are implied for plutonic quartz sources. The minor volcanic quartz type is probably from the Mount Somers Volcanics.

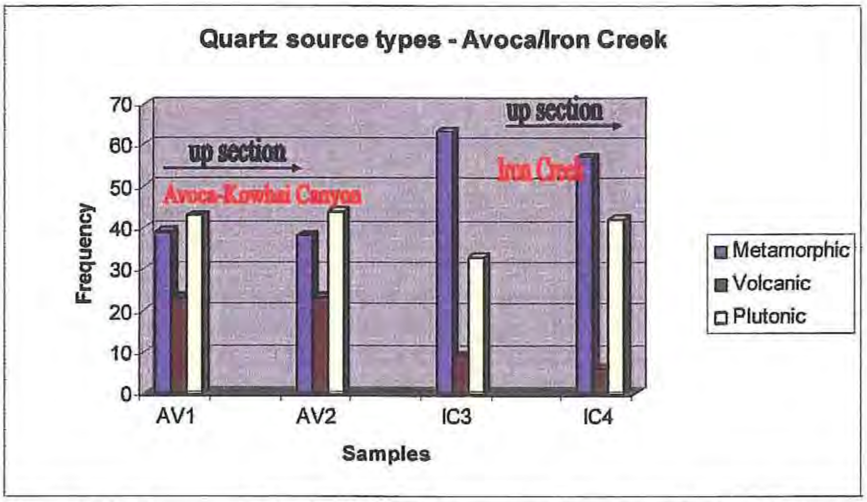

Figure 6.12: Frequency of grains displaying quartz grain per sample from the Avoca and Iron Creek Localities (AV1: Broken River Formation, AV2, IC3, IC4: Iron Creek Formation). Quartz show mixed types at Avoca while at Iron Creek samples are predominantly bimodal, metamorphic to plutonic.

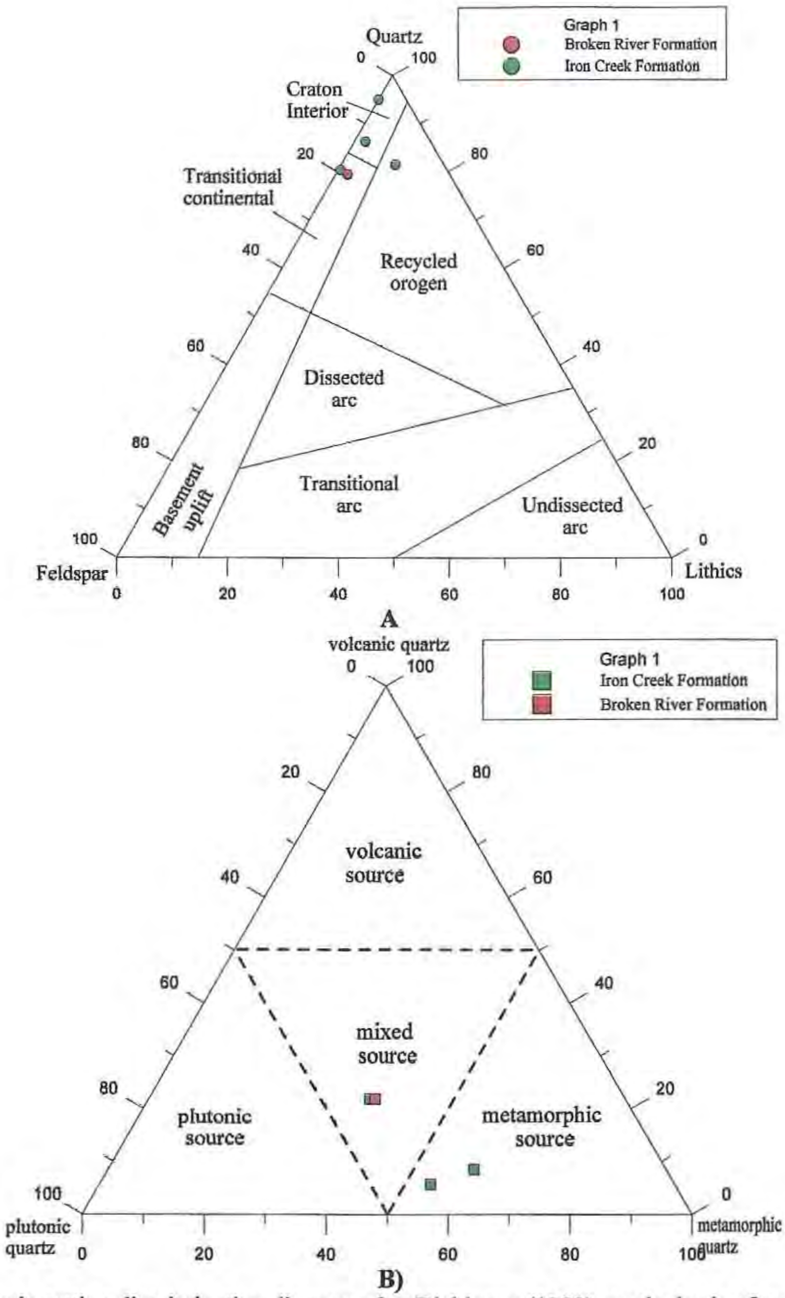

Figure 6.13: A) Tectonic setting discrimination diagram after Dickinson (1983), on the basis of normalized point-counts, results from conventional point counts. Sample from BRF plot in the transitional continental field, IRF plots in Craton Interior-Recycled orogen. **B)** Provenance discrimination diagram after Bernet and Bassett (2005), of Iron Creek Fm and Broken River Fm, samples using the three main quartz types of volcanic, plutonic and metamorphic quartz, based on SEM-CL/optical analysis. The dashed lines indicate the 50 percent lines of each of the three main types. Metamorphic quartz includes all low-grade to high-grade metamorphic, recrystallized and vein quartz.

CHAPTER SEVEN
MOUNT SOMERS

7.1 Regional Geologic Setting & Previous Work

The Mt Somers area is located near the foothills of the Southern Alps at the western margin of the Canterbury Plains in inland mid Canterbury. The south branch of the Ashburton River drains the area in study. The Mt Somers area is known for its extensive thick coalfields and its rhyolite domes. The Mt. Somers Coalfield is approximately one and a half hours drive from Christchurch to Mt. Somers Township, then northwest up Ashburton Gorge Rd for approximately 10km (fig. 7.1). The stratigraphic succession exposed in the Mt Somers area consists of Late Cretaceous to Early Tertiary sediments (Broken River Formation), overlying a basement of Mesozoic Torlesse Supergroup greywacke and argillites, and mid-Cretaceous calc-alkaline volcanics of the Mt Somers Volcanics Group (van deer Lingen 1988) (fig. 7.2). Mathews (1989) recognised lower conglomerates, sands and coal and upper fine sands clay and coal in the Broken River Formation. Coal measures are overlain by transgressive sediments also part of the Broken River Formation (Mathews 1988). The sequence is followed by Oligocene Limestone. The Cretaceous – Tertiary sequence is preserved in small outliers as consequence of differential uplift, tilting and erosion during the Late Tertiary Kaikoura orogeny (Oliver 1977). Glacial outwash occurs as minor terraces in the area.

Speight (1938) did the earliest work in Mt Somers region with first detailed mapping and descriptions while Oliver (1977, 1979) investigated the structure and tectonic history of Mesozoic rocks in the Mt. Somers area. Detailed sedimentology and interpretation of paleoenvironments for transgressive sediments of the Broken River Formation was done by van der Lingen (1988) and Oliver and Keene (1989) published a detailed geological map of the Mt. Somers district. Tappenden (2003) did a detailed geochemical research on the Mt Somers Volcanics, while Bernet and Bassett (2003) did a preliminary provenance study of quartz with the SEM-CL/optical technique.

7.2 Stratigraphy

The oldest known rocks of the area are greywacke-type sandstone with interbedded siltstones belonging to the Torlesse Supergroup (Oliver & Keene 1989).

In the area Torlesse Supergroup rocks are subdivided into the Mount Taylor Group (Triassic) and the Clent Hills Group (Jurassic). The stratigraphy is succeeded by the Cretaceous volcanics in the Mt Somers area as part of a larger volcanic suite of calc-alkaline rocks that extend from the Malvern Hills. The Mount Somers Volcanics are subdivided into several formations; these are Somers Rhyolite, Barrosa Andesite, Grahams Creek Dolerite, Alford Rhyolite, Hinds River Dacite (Oliver & Keene 1989). The volcanics are succeded by the Broken River Formation which incorporates the basal Late Cretaceous – Paleocene Stour Coal Measures (Haumurian-Teurian), the succeeding Mid Eocene Blondin Sand Member (Bortonian) and the overlying Homebush Sandstone Formation Late Eocene – Early Oligocene (Bortonian – Whaingaroan) (van der Lingen 1988; Oliver & Keene 1989). The sequence is followed by the Mid Oligocene Kokoamu Greensand Formation (Duntroonian) and the overlying Otekaike Limestone of Mid Oligocene-Late Oligocene age (Duntroonian – Waitakian) which both form the Otaike Group (Gage 1957). The stratigraphy is succeeded unconformably by Quaternary glacial deposits of the Windwhistle Formation (Oliver & Keene 1989).

The Broken River Formation which includes the Stour Coal Measures, the Blondin Sand Member and the Homebush Sandstone Formation are the subject of this research at the Mt Somers area and are discussed in more detail.

7.2.1 Torlesse Supergroup Rocks

In detail the Torlesse Supergroup comprises of greywacke sandstone and siltstone of the Mount Taylor Group. The Balmaccan Formation (Latest Middle Triassic) consist of medium to fine grained, dark grey to greenish grey quartzofeldspathic sandstone interbedded with dark grey siltstone and occasional conglomerate beds. The Fingers Formation (Middle- Late Triassic) of the Mount Taylor Group consists of coarse to medium sandstone, characteristically of white micaceous, well sorted feldsarenite and interbedded siltstones and sandstones with white large muscovite flakes and common lithics (Oliver & Keene 1989). The Torlesse Supergroup also consists of the Pudding Hill Formation a thin bedded quartzo-feldspathic flysch with alternating medium to fine grained sandstone and dark grey siltstone (Late Triassic). The Clent Hills Group is also composed of interbedded sandstone and siltstone with conspicuous conglomerates. The sandstone are composed of poorly to moderately sorted, medium grained feldsarenite and lithic feldsarenite, with subangular to subrounded quartz and alkali feldspar and occasional plagioclase, while muscovite is also present (Oliver & Keene 1989). According to Oliver and Keene (1989) metamorphism is low grade zeolite facies and induration is moderate for the Glent Hill Group, while the age is Middle to Late Jurassic.

7.2.2 Mount Somers Volcanics

The basement is overlain by Cretaceous calc-alkaline volcanic rocks of the Mount Somers Group which range in composition from high-alumina basalt to rhyolite continuum (Tappenden 2003). The Mount Somers Volcanics consist of large suite of volcanic and extrusive rocks. The extrusive and intrusive phases of volcanism were contemporaneous over a period of several million years and included cyclic acid and basic eruptions (Oliver & Keene 1989). The Mount Somers Volcanics is dominated by rhyolites which cover a large area. The Barrosa Andesite is a calc-alkaline basaltic-dacite andesite which consists of black flows and some tuffaceous and scoriaceous layers. In addition the Surrey Hills Tuff formation consists of the earliest rhyolitic phase of the Mount Somers Volcanics with ignimbrites and silicified tuff which occurs in isolated outcrops along the basal contact of the volcanics. The Alford Rhyolite is a black basal pitchstone with bypyramidal quartz and sanidine phenocrysts in a devitrified glass groundmass (Oliver & Keene 1989). Another formation includes the Grahams Creek Dolerite, a porphyritic intrusive with plagioclase, hypersthene and interstitial pigeonite (Oliver & Keene 1989). Chemically it is tholeitic basalt (Oliver 1977). The Mount Somers Rhyolite forms a sequence of coalesced domes and is composed of quartz bypyramids and subhedral sanidine phenocrysts (Oliver & Keene 1989), and it covers a large proportion of the area. Finally the Hinds River Dacite occurs as non vesicular black glassy flows with plagioclase and hypersthene phases, while minor magnetite and pigeonite occurs (Oliver & Keene 1989).

7.2.3 Mount Somers Kaolinized Rhyolite-Ignimbrite

The Mount Somers Volcanics Group is overlain by kaolinized volcanics. Although not observed in this study they were studied analyzed in detail by van der Lingen (1988) in the Pottery Clay quarry. The clays are structureless and homogeneneous, and they contain evenly distributed volcanic quartz crystal fragments and sporadic gravel-sized kaolinized volcanic rock fragments with and without subhedral-euhedral quartz crystals (van der Lingen 1988). In addition the Kaolinite consists of pyrite concretions coal horizons with roots extending into underlying clays and subsequent brown clays predominantly kaolinites with subordinate quartz silt and plant material overlie the succession (Van der Lingen 1988). Van der Lingen (1988) notes the presence of quartz grains which include volcanic monocrystalline and non volcanic polycrystalline grains. Strong kaolinization of rhyolite and deposition of coal measures are an indication of humid and warm climatic conditions in the Mount Somers area during the Late Cretaceous Eocene (Bernet & Bassett 2003). According to Van der Lingen (1988) the origin of clays were possibly reworked from previously kaolinized Mt Somers Volcanics or they were arkosic sands, derived from eroding Mt Somers Volcanics and kaolinized after deposition; or they were rhyolitic pyroclastic flows and ignimbrites kaolinized. The third possibility is in favour as it accounts for the distribution of the quartz phenocryst fragments (van der Linen 1988).

7.2.4 Broken River Formation

The overlying Late Cretaceous – Tertiary succession consists of the basal Broken River Formation, a terrestrial non marine to marine estuary – tidal deposit, which encompasses the Stour Coal Measures followed by the Blondin Sand Member. The contact with the underlying volcanics is sharp while in places the Broken River Formation rests on Torlesse Supergroup rocks (Van der Lingen 1988).

Oliver and Keen (1989) defined the basal Stour Coal Measures as "kaolin clay and coal measures of low grade lignite to sub-bituminous rank". Coal measures exposed in the Mt Somers Mine are inferred to represent a minor marine influenced coastal embayment or lagoon (van der Linen 1988), with both allochthonous and autochthonous deposition of peat evidenced by coal petrology (Mathews 1989). Mathews (1989) recognized 3 coal types based on plant types and detrital minerals in the Mount Somers area.

According to Mathews (1989) the Mount Somers coals consist of type-5 high vitrinite (72-75%) with high percentage of well preserved coal submacerals tellinite, collinite and tellocolinite which indicates coal formation in swamps with fluctuating water table or a high amount of woody vegetation in the swamp. Woody vitrinites indicate forest moor type of settings; also an autochthonous to paratochthonous origin is inferred for low inertodetrinite, formed by oxygenation of the peat in relatively dry periods (Mathews 1989). In addition type-6 coal has variable vitrinite (56-70%), high inertinite (18-35%) and high ash indicates a relatively wet swamp environment subjected to seasonal drying and a high water table in a forest moor (Mathews 1989). The following coal type-7 is markedly different from the other coal types characterized by high volatile matter, high ash (detrital minerals) and framboidal pyrite interpteted to result from a brackish or marine influence in the peat swamp with a moderate percentage of woody vegetation indicating a wet swamp (Mathews 1989).

Van der Lingen (1988), Oliver and Keen (1989) described the coal grading up into silica sand with thin carbonaceous clay beds. Van der Lingen (1988) describes the composition as "lenticular bedded, flaser bedded, dark to light brown clay and quartz sand". The overlying Blondin Sand Member is separated by an erosional contact (Van der Lingen 1988) and consists largely of friable sand of nearly pure quartz with local minor iron stained horizons. The sand is typically cross bedded on a decimetre to metre scale (Oliver & Keene 1989). The Blondin Sand Member is largely quartzose, while at an isolated exposure glauconite was found in minor amounts in this study.

7.2.5 Homebush Sandstone

Following the Blondin Sand Member of the Broken River Formation is the Homebush Sandstone Formation according to Oliver and Keene (1989). It overlies the Blondin Sand Member by an erosional contact (Oliver & Keene 1989). However, in this research a gradational contact was observed between the underlying Blondin Sand Member of the Broken River Formation and the overlying Homebush Sandstone Formation. Van der Lingen (1988) refers to the unit as "glauconitic gravelly muddy sand with a polymodal grain size distribution and a 20% mud fraction".

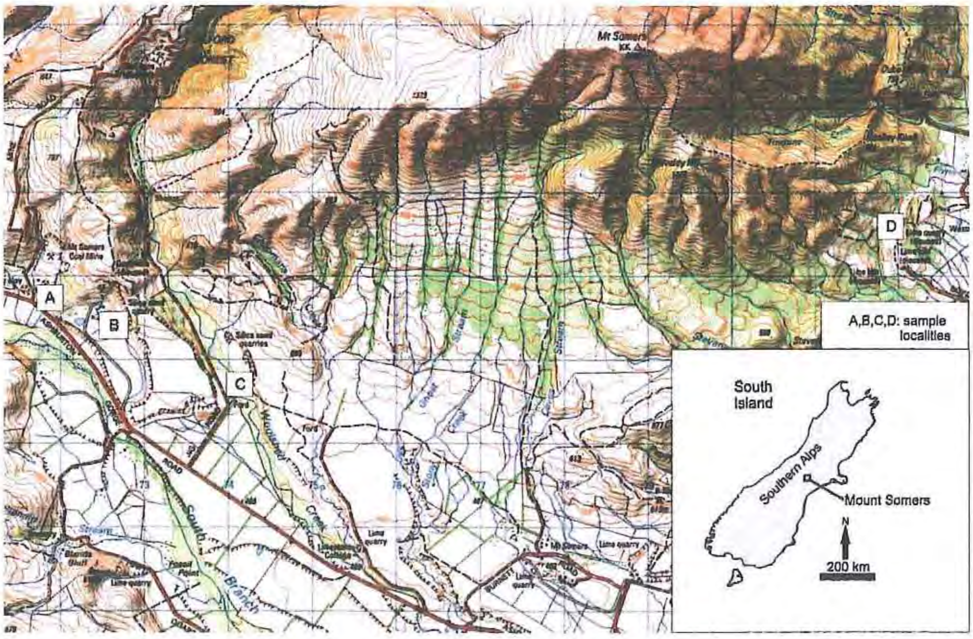

Figure 7.1: Topographic map of the Mount Somers area outlining sample localities and stratigraphic columns.

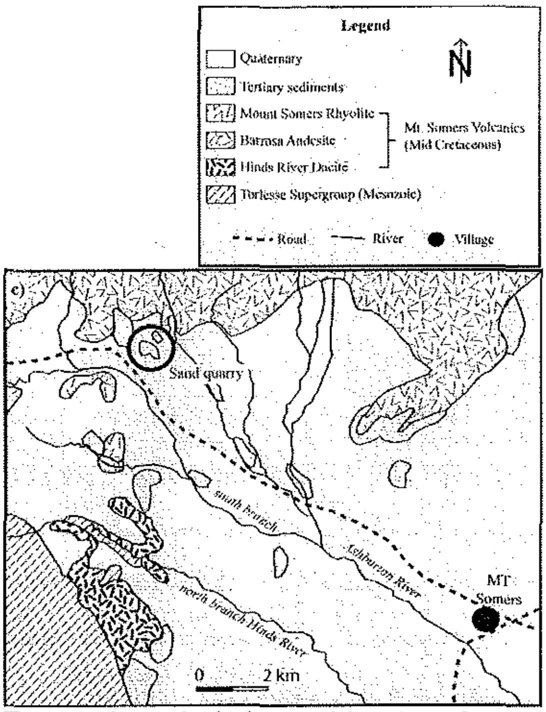

Figure 7.2: Geological map of the Mount Somers (from Bernet & Bassett 2003).

7.3 Sedimentary Descriptions

7.3.1 Broken River Formation

Exposures of the Broken River Formation's Stour Coal Measures Member occur in the Mount Somers coal mine (locality A fig. 7.1). A sequence of non marine to marine sedimentary rocks was measured and samples collected thus supplementing prelimary research in the area by Bernet and Bassett (2003). The direct contacts with underlying Mt Somers Volcanics and kaolinized rhyolite and clay are not present at the coal mine (fig. 7.1); however they outcrop at other areas not visited in this research. In detail the Stour Coal Measures consist of 28.5 metres (appendix 1 fig. 1.43) of basal coal interbedded with poorly sorted, quartz sandstone lenses, which are overlain sharply by moderately sorted, quartzose sandstones, interbedded with carbonaceous silt flasers and lenticular bedding (appendix 1 fig. 1.44) with occasional cross stratification (appendix 1 fig. 1.45). Up section the Stour Coal Measures contain major single set cross beds while at the top inclined silt and sandstone laminar also occur (appendix 1 figs. 1.46, 1.43). Cross bed directions collected from Van der Lingen (1988) show major west and south-west paleoflow directions, from east to west.

The next overlying Blondin Sand Member occurs at the Silica Sand Quarry (locality B fig. 7.1). The sequence was measured and described by (Van der Lingen 1988), and consists of 44 metres (fig. 7.3) of white, very well sorted, quartzose sand with trough cross bedding, mud drapes, wave ripples and *Ophomorpha nodosa* trace fossils (appendix 1 figs. 1.47, 1.48). Further up section lenticular bedded and cross bedded coarse sands and gravels occur (appendix 1 fig. 1.49). A clast count on the conglomerate was done and recorded a poorly sorted, polymictic conglomerate with clasts composed of quartz, smoky quartz pebbles, red chert and sandstone clasts (appendix 1 fig. 1.50). Further to the east in Woolshed Creek (locality C, fig. 7.1), a small exposure of 3 metres was measured containing the Blondin Sand Member (appendix 1 fig. 1.54). It consists of white-cream, iron stained, poorly indurated, poorly sorted, medium, quartzose sandstone with occasional quartz pebbles and mud drapes (appendix 1 fig. 1.51). Up section the Blondin Sand Member contains a poorly sorted, matrix supported, polymictic conglomerate with dominant quartz pebbles and subordinate basaltic and red chert clasts (appendix 1 fig. 1.52), while it grades into the Homebush Sandstone.

7.3.2 Homebush Sandstone

The next unit in the study is the Homebush Sandstone Formation. At the Silica Sand quarry, locality B, only a thin 30 cm layer is exposed. It is glauconitic, muddy sandstone, poorly sorted, and fine grained, with quartz pebbles and glauconite content reaching 18% with a sharp underlying contact (appendix 1 fig. 1.53). A similar deposit occurs at Woolshed Creek with a thickness of 1.5 metres, and contains poorly sorted, poorly indurated, muddy - fine grained, 20% glauconitic sandstone with quartz pebbles and *Ophiomorpha nodosa* trace fossils, while the underlying contact is gradational.

7.4 Interpretations of Depositional Settings

7.4.1 Broken River Formation

The basal Stour Coal Measures Member is interpreted as a terrestrial peat body possibly coastal, but not influnced by saline waters. Up section the deposits of the Stour Coal Measures indicate a tidal – flat depositional environment influenced by currents. Overlying the Stour Coal Measures is the Blondin Sand Member interpreted as an intertidal – subtidal setting as indicated by mud drapes, *Ophiomorpha nodosa,* and also by the trough cross stratification. The cross bedded sandstones with grit and conglomerates indicate fluviodeltaic – beach face deposits.

7.4.2 Homebush Sandstone

The glauconitic pebbly sandstones of the Homebush Sandstone Formation are interpreted as a moderate energy setting with trace fossils although Van der Lingen (1988) interprets *Ophiomorpha nodosa* trace fossils as opportunistic organisms that thrive under moderate energy conditions. Therefore, a marine depositional setting is interpreted, probably a shallow shelf.

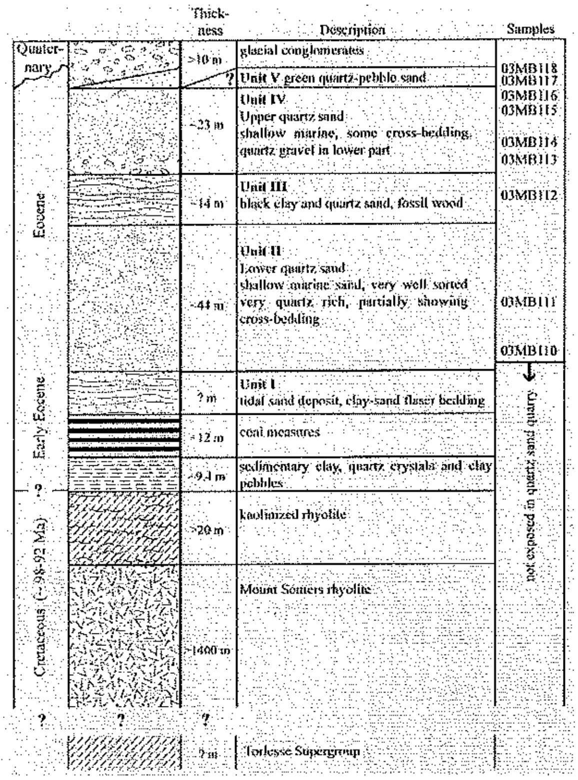

Figure 7.3: Stratigraphic log of the Stour Coal Measures, the Blondin Sand Member and the Homebush Sandstone at Mount Somers (from Van der Lingen 1988, modified by Bernet and Bassett 2003).

7.5 Glaucony as Sedimentation Indicator

7.5.1 Descriptions of glauconite

Glauconite bearing units are at a minimum thickness and extent and confined to one locality in Blondin Sand Member of the Broken River Formation, and at two localities glauconite occurs in the overlying Homebush Sandstone. The arenites of the Blondin Sand Member do not contain glauconite at the localities B and C of the silica sand quarry and Woolshed Creek respectively; however glauconite occurs as a minimal amount of 4% in the Blondin Sand Member at locality D (fig. 7.1). The deposit is largely covered by scrub and trees. The glauconite content is confined to the nascent and micaceous variety with the micaceous glaucony the dominant type (fig. 7.4). Glauconite increases dramatically up section in the Homebush Sandstone at the silica sand quarry (locality B). It consists of 18% glauconite with a dominant nascent variety; the evolved/mature well rounded grains are kept to a minimum content (sample SQ3, fig. 7.4). The glauconite grains are very fine grained. The Homebush Sandstone at the silica sand quarry with sample SQ3 displays nascent irregular pale green glauconite grains (figs. 7.5, 7.6). At Woolshed Creek (locality C, fig. 7.1) the

Homebush Sandstone unit is the lateral equivelant of the unit at the silica sand quarry. The glauconitic arenite has a content of 20% with a dominant nascent glaucony type and minor evolved/mature and micaceous grains (sample WC6, fig. 7.4). Sample WC6 from Woolshed Creek also displays irregular pale green nascent glauconite types (figs. 7.7, 7.8).

7.5.2 Glauconite Interpretation

The glaucony grains in the Blondin Sand Member and the Homebush Sandstone indicate in situ formation and in turn a marine depositional setting. However, stratigraphically, the glauconite rich units, especially the Homebush Sandstone, form thin relicts within the Mount Somers area, thus establishing a stratigraphic trend is not possible with so few data points. It is possible that the original substrate for glauconite formation was kept at a minimum and was largely part of the edge of the marine depositional setting where glauconite formation is facilitated. Further more the underlying units are non glauconitic confined only to one distal locality, therefore recycling of glauconite is not possible unless it is allochthonous. The glauconitic arenites are distinctively muddy and, combined with the absence of sedimentary structures, indicate relative quiescence with little reworking taking place. However, the presence of quartz pebbles and the poorly sorted nature of the deposit point towards an allochthonous formation of glauconite.

The trace fossils in the lower Homebush Sandstone at Woolshed Creek are *Ophiomorpha nodosa,* opportunistic organisms that survive on substrates subject to strong currents and high energy according to van der Lingen (1988). The glauconitic rich unit is described by van der Lingen (1988) to rest unconformably on top of the Blondin Sand Member at the silica sand quarry. It is interpreted that glauconite formed in a marine setting, likely a shallow shelf with an autochthonous mode of formation while the quartz pebbles indicate an exogenous source contributing detritus perhaps by storm events, or transport along a paleoslope. In turn Amorosi (1997) described how high energy and/or reworked deposits do not always indicate an allochthonous origin of grains. The absence of paleocurrents in the Homebush Sandstone indicates autochthonous formation. The thicknesses of the underlying units indicate a relative high sedimentation and aggradation. Field and Browne (1989) show a subsidence pattern for the wider Mt Somers area which corresponds to the transgression taking place. The glauconite is part of a small unit, therefore a low sedimentation rate would by confined to the Late Eocene Early Oligocene period, while the underlying sequence reflects a relatively high sedimentation rate for the Mount Somers area. Except coal is also a very low sedimentation rate indicator. The real change is from terrestrial to marginal marine. Most of the sequence has low sedimentation rate.

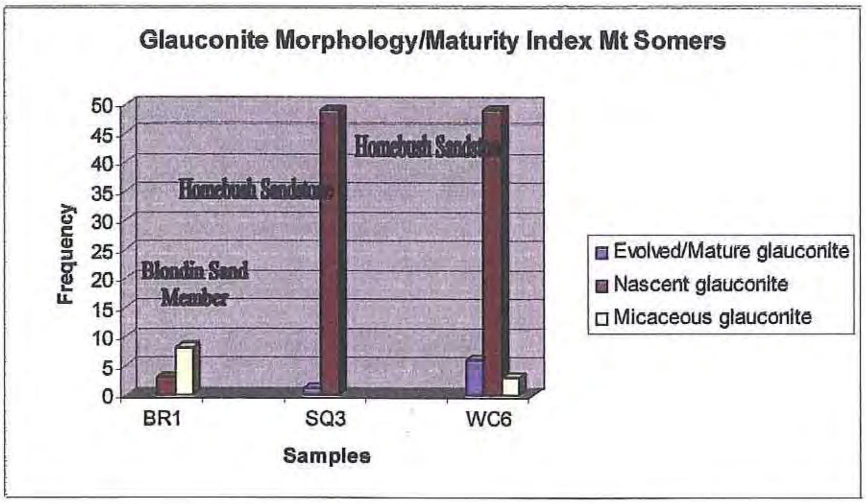

Figure 7.4: Frequency of glauconite grains displaying nascent stage, evolve/mature and micaceous glauconite. Nascent variety is dominant in the Blondin Sand Member of the Broken River Formation and in the Homebush Sandstone Formation (BR1: locality D, SQ3: locality B – silica sand quarry, WC6: locality C – Woolshed Creek).

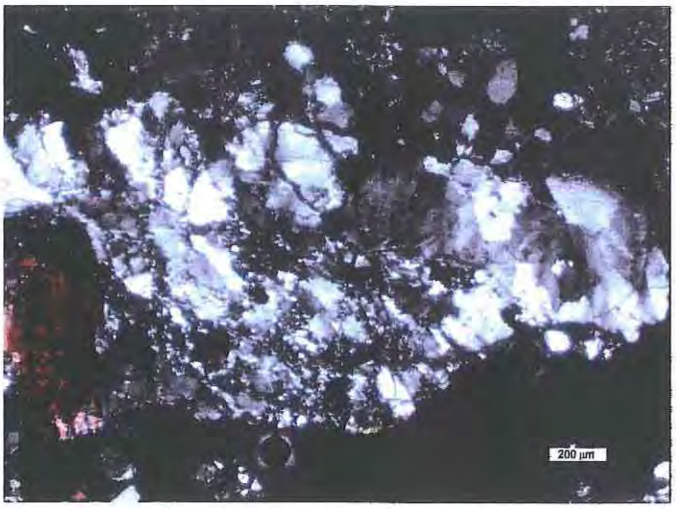

Figure 7.10: large schistose polyhedral quartz granule from sample SQ3 in the Blondin Sand Member (silica sand quarry).

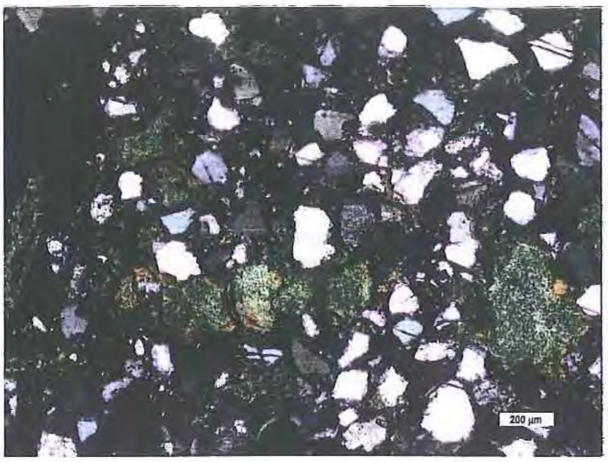

Figure 7.5: Irregular shape nascent glauconite of sample SQ3 (cross polarized light, optical micrograph).

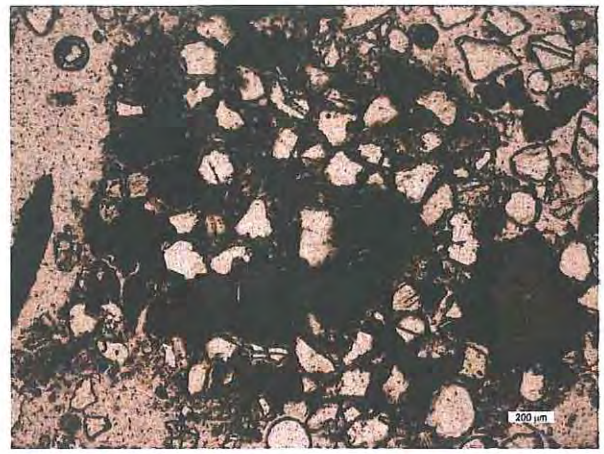

Figure 7.6: Irregular shape nascent glauconite, slight pale green of sample WC6 (plane polarized light).

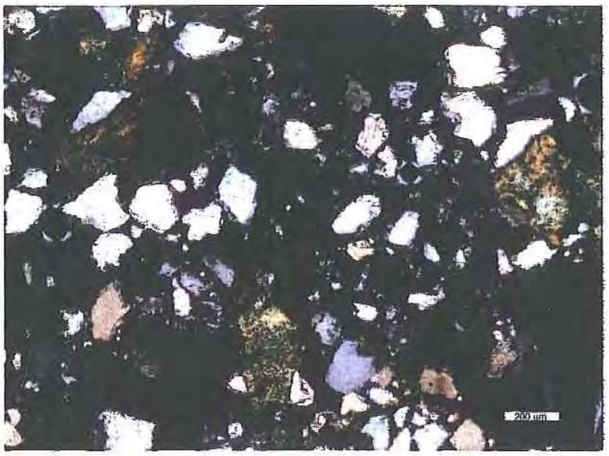

Figure 7.7: Irregular shape nascent glauconite of sample WC6 (cross polarized light, optical micrograph).

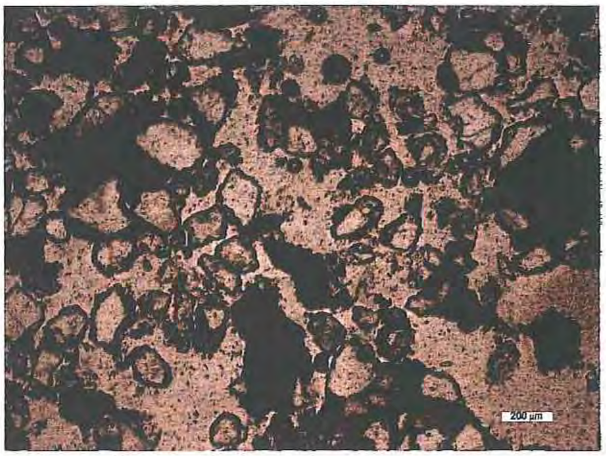

Figure 7.8: Irregular shape nascent glauconite of sample WC6 (cross polarized light, optical micrograph).

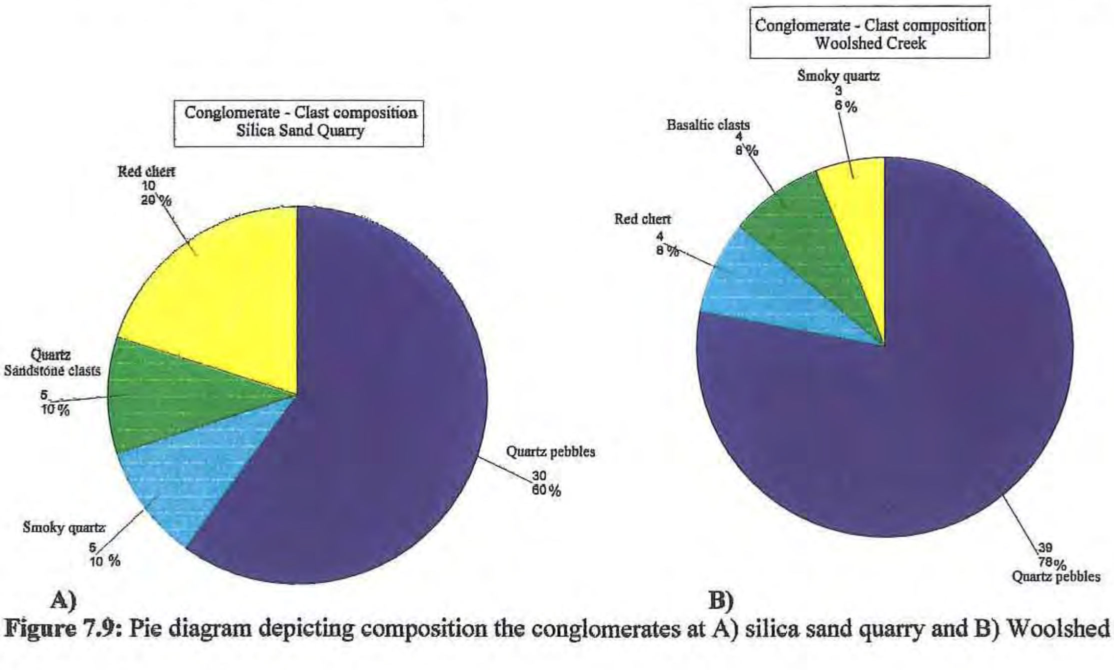

A) B)

Figure 7.9: Pie diagram depicting composition the conglomerates at A) silica sand quarry and B) Woolshed Creek.

7.6 Provenance

7.6.1 Conglomerate Clast Counts

Clast counts on the Blondin Sand Member were done on two conglomerates, one at the silica sand quarry (locality B) and one at the Woolshed Creek (locality C) (fig. 7.1). The clast count for the silica sand quarry shows an overwhelming 60% of quartz pebbles, 10% composed of smoky quartz pebbles, 10% sandstone clasts and 20% red chert (fig. 7.9, A). The quartz pebbles according to Van der Lingen (1988) have a schistose source. A Haast Schist and Torlesse Supergroup source is interpreted for the majority of the quartz pebbles and the red chert clasts. However a granitic source is also possible especially for the smoky quartz pebbles derived from possible reactivation of old faults during the Late Paleocene- Early Eocene (Bradshaw pers. comm. 2005). In contrast the sandstone clasts are most likely sourced from older Broken River Formation such as the Stour Coal Measures. The provenance of the conglomerate deposit at Woolshed Creek is very similar, with 78% of the clasts quartz pebbles, 6% smoky quartz, 8% red chert and finally 8% basaltic clasts (fig. 7.9, B). Similar Haast Schist - Torlesse sources are interpreted for the quartz pebbles, while basaltic clasts are clearly sourced from the extrusive phase of the Mount Somers Volcanics perhaps the Barrosa Andesite. Red chert pebbles are possibly sourced also from the Mount Somers Volcanics, while a Torlesse provenance is also likely.

7.6.2 Sandstone Composition

Samples were collected for petrographic analysis, point counts and CL analysis from the Broken River Formation's Stour Coal Measures, Blondin Sand Member and Homebush Sandstone Formation. One sample was analysed from the basal Stour Coal Measures while most of the samples were derived from the Blondin Sand Member and a few from the Homebush Sandstone.

The composition of the Stour Coal Measures is subarkosic arenite with minor volcanic and sedimentary lithics (appendices 1, 2, 3). Accessory minerals such as sericite are present but at a very minor 3%. Polycrystalline quartz is minor at 3.6% while the majority of quartz crystals are monocrystalline. Feldspars are dominantly alkaline at 10% while plagioclase is minor less than 1%. Lithics are composed of minor volcanics less than 1% and sedimentary lithics less than 1%. In terms of provenance, the Stour Coal Measures plot in a craton interior tectonic setting based on quartz, feldspar and lithic composition (fig. 7.13, A).

Provenance of alkali feldspars suggests a possible Mount Somers Volcanics source. Alkali feldspars are essential constituents of several felsic igneous rocks, pegmatites and many felsic and intermediate gneisses (Shelley 1985). Shelley (1985) also notes how syenites, granites, granodiorites and their volcanic equivalents produce alkali feldspar. Based on the presence of alkali feldspar, it is interpreted that a local volcanic source is the major source; however the Haast Schist is also possible as a provenance. Alternatively the granites of the Karamea – Separation Point Batholiths are strong candidates for alkali feldspar grains. The same sources could also provide the minor plagioclase crystals. The volcanic lithics are likely eroded from the Mount Somers Volcanics.

The Blondin Sand Member at the silica sand quarry, Woolshed Creek and locality D, is subarkosic to arkose arenites typical of a craton interior – transitional continental setting based on Dickinson (1983). Lithics are minor volcanic and sedimentary (appendix 2). Feldspars are dominantly alkali feldspar with minor plagioclase and are interpreted to have the same provenance as the Stour Coal Measures. The polycrystalline quartz grains have a higher content between 10 and 20% relative to the underlying Stour Coal Measures at 3% (appendix 2). Most of the polycrystalline quartz grains are schistose and recrystalized indicative of high grade metamorphism and therefore interpreted as sourced from the Haast/Otago Schist (fig. 7.10).

The overlying Homebush Sandstone is compositionally different as a subarkosic- sublitharenite that plots in the tectonic field of a recycled orogen (fig. 7.13, A). It is largely fine to very fine sandstone and poorly sorted. Samples SQ3 and WC6 range in polycrystalline quartz content from 6 to 11% (appendix 2). The Homebush Sandstone Member arenites have low feldspar content primarily alkali feldspar ranging from 5% to 6% interpreted to have the same provenance as the Stour Coal Measures and the Blondin Sand Member. The lithics range from 24% to 8% and are primarily sedimentary ones with 2-1% volcanic lithics. Large volcanic lithics exhibit feldspar laths in a dark oxidized groundmass indicative of volcanic source rocks. It is interpreted that the high lithic content is due to a local unconformity or erosional contact between the Blondin Sand Member and the Homebush Sandstone which indicates erosion and reworking from the lower Stour Coal Measures and Blondin Sand Members. Therefore in detail the sedimentary lithics are most likely sourced from the underlying arenites and/or sourced from Torlesse while the volcanic lithics are sourced from extrusive Mount Somers Volcanics.

7.6.3 Quartz Provenance (SEM-CL)

The integrated SEM-CL/optical microscopy technique of quartz was applied to five samples, 1 from the Stour Coal Measures (locality A, fig. 7.1), 2 samples from the upper Blondin Sand Member (silica sand quarry) supplementing research by Bernet and Bassett (2003); and 2 samples from the upper Blondin Sand Member at Woolshed Creek. The SEM-CL analysis of the Mount Somers Broken River Formation builds on the research done by Bernet and Bassett, (2003). Preliminary research from Bernet and Bassett (2003) showed that half of the grains of the Mount Somers quartz arenites are of local volcanic origin derived from weathering and reworking of rhyolitic source rocks, metamorphic/recrystallized quartz grains make up 20% of total quartz composition derived from Otago Schist and Torlesse Supergroup, while 30% of the grains are of plutonic origin and have been derived from distant sources, which include Carboniferous, Devonian and Cretaceous granitic rocks of the Western Province (fig.7.12, A)

In the Stour Coal Measures at the Mount Somers coal mine (sample CM1), 21% of the quartz grains have plutonic characteristic of healed microcracks and straight/low undulose extinction, with a low content of deformed plutonic grains (appendix 7). Quartz grains displaying black/dark CL and strong undulose extinction and/or polycrystalline were interpreted as metamorphic. Sample CM1 displayed 33% metamorphic quartz grains. The volcanic quartz content reaches 44% for sample CM1 (appendix 5 figs. 5.18, 5.19).

Polycrystalline quartz grains are dominant in the Blondin Sand Member than the basal Stour Coal Measures. Sample SQ1 from the upper Blondin Sand Member below the conglomerate unit (fig. 7.3), records 20% plutonic quartz, 51% metamorphic quartz and 27% volcanic quartz. Sample SQ2 from above the conglomeratic unit has 39% plutonic quartz grains, 35% metamorphic quartz grains and 25% volcanic grains approximately (appendix 5 figs. 5.20, 5.21). At Woolshed Creek sample WC1 displays 14% plutonic grains, 36% metamorphic quartz and 49% volcanic quartz. Sample WC3 is also again very similar in composition with 28% plutonic, 36% metamorphic and 35% volcanic quartz (appendix 5 figs. 5.22, 5.23).

The data obtained from the SEM-CL technique at Mt Somers reveal an overall mixed proportion of all quartz types in both members of the Broken River Formation (fig. 7.11), however, the samples CM1, SQ1and WC1 in the Stour Coal Measures and Blondin Sand Members respectively reveals a metamorphic and volcanic quartz at a slightly higher frequency than in the samples SQ3 and WC3 which occur in the Blondin Sand Member above the conglomeratic units. This slight trend suggests that there could have been a change in sources up section to produce a more mixed provenance than in the lower sedimentary section (fig. 7.11).

The trends of the of the quartz types at Mt Somers overall reflects a mixed provenance with the lower section characterized by slight dominant bimodal metamorphic and volcanic source types, while up section a mixed source of all quartz types is prominent (fig. 7. 13 B). van deer Lingen (1988) estimated that a change from non-marine to marine sedimentation is highlighted by the change from a single to multiple sediment sources, while he also attributed quartz to be derived from the volcanics and much of the non volcanic quartz in the marine deposits to be derived from a metamorphic terrane such as the Otago Schist to the South. It is interpreted here that multiple sources contributed quartz to the Broken River Formation. The metamorphic source is interpreted to be the Otago-Haast Schist to the South and/or the Alpine Schist rather than the fine grained Torlesse Supergroup while a local volcanic provenance such as the Mount Somers Volcanics is interpreted for the strong volcanic signature. The plutonic quartz signature is interpreted as being sourced from an exhumed plutonic suite, most likely the western Karamea-Separation Point Batholiths.

7.7 Summary of Results for Mount Somers

The Broken River Formation unconformably overlies the Mount Somers Volcanics Group. It consists of the Stour Coal Measures Member followed by the Blondin Sand Member and the Homebush Sandstone Formation. These were deposited in non marine coastal swamps to tidal-intertidal estuary and finally marine shelf depositional settings. The presence of nascent glauconite in the uppermost Blondin Sand Member and Homebush Sandstone Formation units indicates autochthonous formation and low sedimentation rate during the Bortonian – Whaingaroan (Late Eocene- Early Oligocene) during the marine transgression, while the underlying Stour Coal Measures also indicate a low sedimentation rate. Provenance of conglomerates suggests local derivation from underlying Torlesse

Supergroup rocks, the southern Haast Schist and minor sources from the Mount Somers Volcanics. Provenance of sandstones suggests largely an interior craton tectonic to transitional continental setting for the Stour Coal Measures and the Blondin Sand Member, while the Homebush Sandstone indicates a recycled orogen tectonic setting. Alkali feldspar content reflects a felsic igneous source while an alternative metamorphic and/or plutonic source is also likely. The presence of sedimentary lithics in the Blondin Sand Member reflects reworking from lower stratigraphic members, while volcanic lithics indicate a local Mount Somers Volcanics source.

Provenance of quartz in the Mt Somers region records an overall mixed source of all 3 quartz types for the Stour Coal Measures and the Blondin Sand Member. A metamorphic terrane such as the Haast/Otago Schist is implied for the high grade metamorphic quartz; a local volcanic source such as the Mount Somers Volcanics for the volcanic quartz, while a western-south Karamea or Separation Point Batholith source are implied for the plutonic quartz types. A minor fluctuation in source types occur in the lower Stour Coal Measures with dominantly metamorphic and volcanic quartz source types, while the plutonic quartz type increases in the upper units.

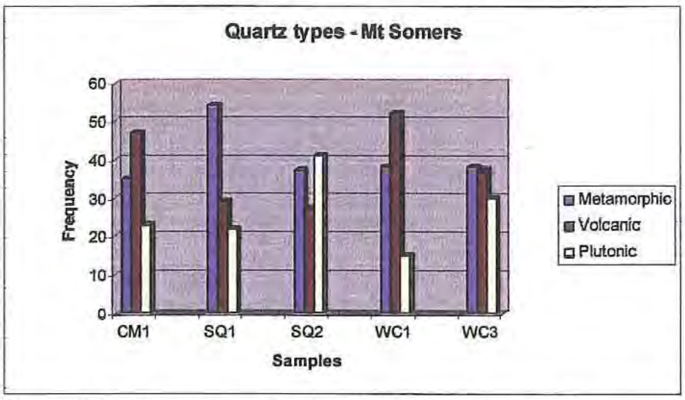

Figure 7.11: Frequency of grains displaying quartz grain per sample from the Mount Somers area (CM1: Stour Coal Measures – locality A, SQ1: Blondin Sand Member – silica sand quarry, SQ2: Blondin Sand Member-silica sand quarry, WC1/WC3: Blondin Sand Member – Woolshed Creek.

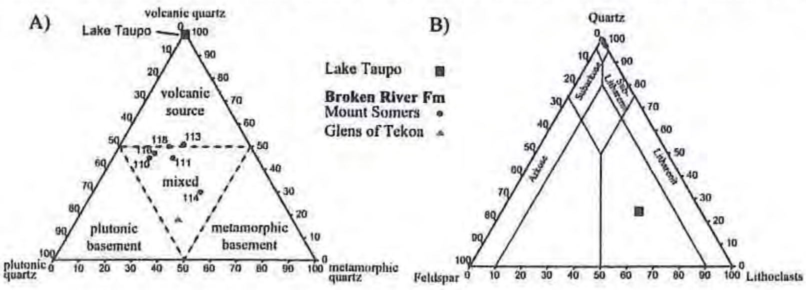

Figure 7.12: A) SEM-CL results and provenance discrimination diagram of the Mount Somers quartz arenites (from Bernet and Bassett, 2003).

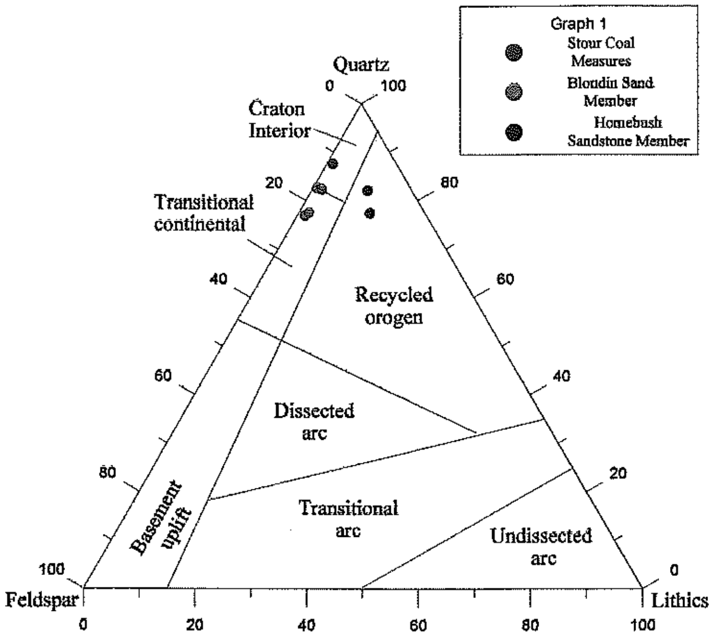

A)

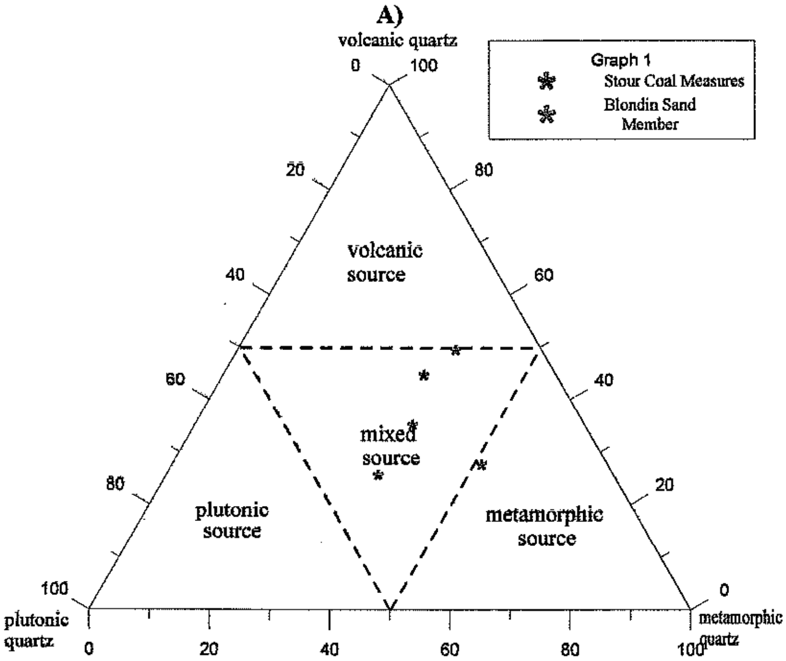

B)

Figure 7.13: A) Tectonic setting discrimination diagram after Dickinson (1983), on the basis of normalized point counts, results from conventional point counts. Sample from Stour Coal Measures plot in the Craton Interior, Blondin Sand Member plot in the transitional continental field, Homebush Sandstone plot in the recycled orogen. **B)** Provenance discrimination diagram after Bernet and Bassett (2005), of Broken River Formation's Stour Coal Measures Member and Blondin Sand Member, samples using the three main quartz types of volcanic, plutonic and metamorphic quartz, based on SEM-CL/optical analysis. The dashed lines indicate the 50 percent lines of each of the three main types. Metamorphic quartz includes all low-grade to high-grade metamorphic recrystallized and vein quartz.

CHAPTER EIGHT
MALVERN HILLS

8.1 Regional Geologic Setting & Previous Work

The Malvern Hills area is a large coalfield area (Mathews 1989), that crops out in the southwest-northeast trending foothills along the western margin of the central Canterbury plains. The Malvern area is drained by the Selwyn River flowing in a southeast direction through Whitecliffs toward Glentunnel (fig. 8.1). The highest peak is Mt Misery at 666 metres. The geology of the area is dominated by Triassic -Jurassic basement rocks intruded by Mid Late Cretaceous Mt Misery Volcanics of the Mount Somers Group (Mathews 1989). It is followed unconformably by Late Cretaceous – Tertiary sedimentary rocks which record a transgression (Late Cretaceous – Early Oligocene) followed by uplift to the north and west recording regression during the Miocene – Holocene (Mathews 1989).

Earlier work in the area was done by Haast (1872) recording the stratigraphy of the sedimentary and volcanic rocks and the nature of the coal seams. Speight (1928) carried out the most extensive geological work to date, although numerous other authors revised the stratigraphy. For example Andrews et al. (1987) divided the basal Monro Conglomerate from the overlying Broken River Formation as a separate Formation. Mathews (1989) produced a geological map and studied the coal geology of the area thus interpreting the paleoenvironment for the Monro Conglomerate and the Broken River Formation. Most of the mapping was done prior to the extensive reforestation of the area by the Selwyn Plantation Board in 1985. Therefore exposures are limited with only small patches and outliers exposed, and some formations not exposed at all.

8.2 Stratigraphy

In the Malvern Hills area, basal Torlesse Supergroup rocks (Late Triassic – Jurassic) are succeeded by garnet bearing rhyolite, pitchstone and agglomerate of the Mount Misery Volcanics (Late Cretaceous) dated at 97.5 Ma (Tappenden 2003). The volcanics in turn are succeeded unconformably by the Monro Conglomerate of the Piripauan stage (Late Cretaceous), followed upsection gradationally by the Broken River Formation dated at Haumurian (Late Cretaceous) (Mathews 1989). The Broken River Formation at Malvern is succeeded gradationally by the Conway Formation with an age of Haumurian to Teurian (Mathews 1989). The sequence is cut by an unconformity and overlain by the Eocene View Hill Volcanics and the Homebush Sandstone with Mangaorapan – Bortonian ages respectively (Early to Mid Eocene). This is unconformably overlain by the Burnt Hill Group a series of volcaniclastic and extrusive Formations ranging from Late Eocene to Late Miocene.

Due to lack of exposure one conglomerate clast count was done on a Monro Conglomerate exposure, a small stratigraphic section measured for the Broken River Formation and one sample was collected from the Conway Formation at Malvern Hills and analysed for petrographic and SEM-CL/optical analysis as a representative sample from this location.

8.2.1 Torlesse Supergroup Rocks

In detail the pre-volcanic stratigraphy is dominated by Torlesse fresh water conglomerates and Wakaepa Plant Beds (Gregg 1964). The Wakepa Plant Beds, according to Mathews (1989), consist of "well – indurated, light brown to brownish grey, massive, clast supported conglomerate interbedded with lenticular brown mudstones and sandstone up to 50 cm thick. Conglomerate clasts are Torlesse Supergroup sandstones and mudstones". The Wakepa Plant Beds also consist of interbedded fine laminated sandstone and siltstone (Mathews 1989). The Wakepa Plant Beds make up most of the Torlesse basement rocks in the area and are Late Triassic to Early Jurassic (Mathews 1989).

8.2.2 Mt Misery Volcanics

The volcanics of the Malvern Hills comprise andesite, pitchstone, rhyolite and ignimbrite with a notable absence of dacite (Tappenden 2003). According to Tappenden (2003) the Mt Misery Volcanics (97.5 Ma) are part of the Mount Somers Volcanic Group, although the extent of the Mt Misery Volcanics is confined to the Malvern area. The succession of volcanics is different from that of the Mount Somers Volcanics because the uppermost unit at Malvern Hills is andesite rich rather than rhyolite rich (Tappenden 2003). In detail the composition of the Malvern rhyolites is "porphyritic in a cryptocrystalline, felsitic, devitified groundmass. The phenocryst phases are quartz, plagioclase, alkali feldspar, garnet, biotites and ilmenite" (Tappenden 2003).

8.2.3 Monro Conglomerate

The Monro Conglomerate is a brown to light grey, conglomerate interbedded with pebbly sandstones and rests unconformably on the Mt. Misery Volcanics of the

Mt. Somers Volcanics Group and Torlesse Supergroup sediments. The conglomerate contains rhyolite clasts derived from the underlying Mt Somers Volcanics Group, mudstones, carbonaceous sandstones and thin lenses of dirty coal (Mathews 1989). The sequence is Piripauan (Mid-Late Cretaceous) and it grades into the overlying Broken River Formation. The Monro Conglomerate according to Andrews et al. (1987) is over 1000 metres in the Malvern Hills area; however its exposure is limited in the Malvern area while it is more exposed in the Rakaia Gorge further south. Mathews (1989) studied the Monro Conglomerate associated rocks and concluded that the sequence represents a proximal to gradually more distal braided river paleoenvironment as part of an alluvial fan complex. Conglomerates represent longitudinal, diagonal and transverse bars, while finer sediments represent bar-top deposition during low flow regime and sediment discharge (Mathews 1989).

8.2.4 Broken River Formation

The Broken River Formation at Malvern is composed of quartzose sandstones, mudstones, carbonaceous mudstones and thick coal seams (Mathews 1989). The formation is 200 metres thick in the Malvern area but the exposure is often interrupted by vegetation (Andrews et al. 1987). The Broken River Formation is Haumurian (Late Cretaceous) Mathews (1989). The Broken River Formation is inferred by Mathews (1989) to be a transgressive back-barrier lagoon setting with swamps developing in interdistributary bays and margins of the lagoon with coal seam splitting as a function of that environment. The coals at Malvern are sub-bituminous with high inertinite coal maceral and low ash content (detrital input) which represents well preserved peat swamps with poor drainage (Mathews 1989). According to Mathews (1989) the Malvern coal fields are correlative to the Mount Somers Broken River Formation coals.

8.2.5 Conway Formation

The Conway Formation comprises "light grey, brown to greenish grey, friable to well indurated, micaceous, quartz rich, fossiliferous, glauconitic, jarositic, burrowed, fine sandstones and siltstones"(Mathews 1989). The Conway Formation's estimated thickness is 100-120m thick (Andrews 1987). The age of this formation is Late Haumurian (Late Cretaceous), while the contact with the underlying Broken River Formation is gradational (Mathews 1989). The Conway Formation which occurs in the east of the Canterbury region interfingers into the Charteris Bay Sandstone (Brown & Field 1985).

The Monro Conglomerate, the Broken River Formation and the Conway Formations are the subject of study and limited amount of data were collected since stratigraphic exposure was limited.

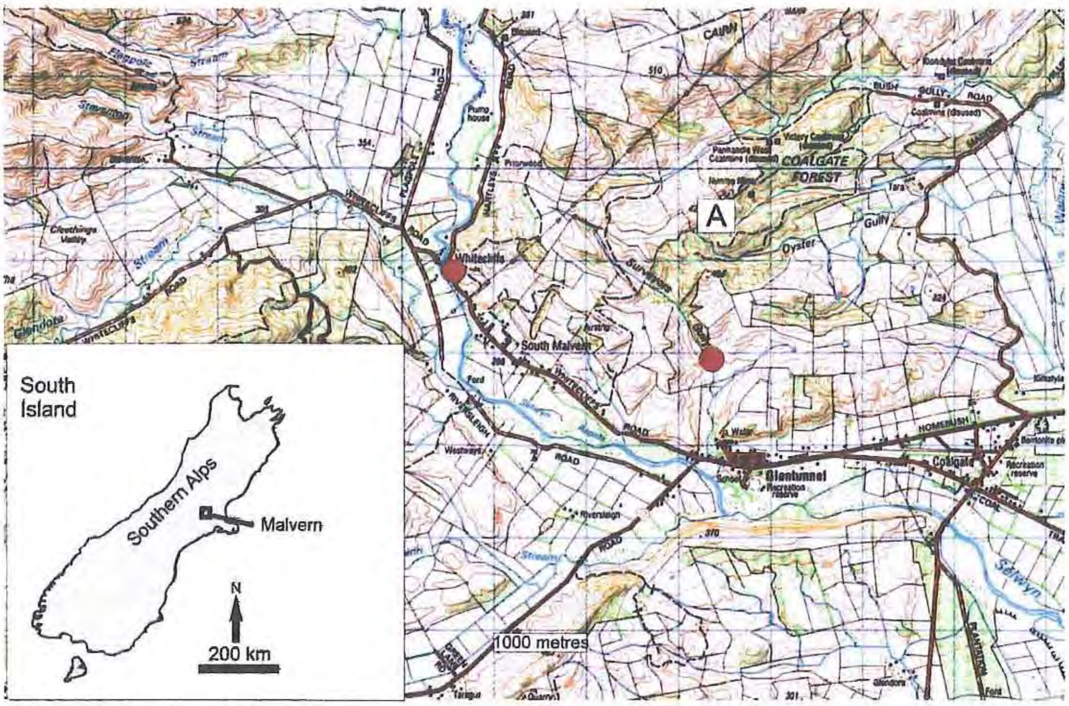

Figure 8.1: Topographic map of Malvern with sample localities, Whitecliffs – Monro Conglomerate clast count (red circle), Surveyors gully -sample locality from Conway Formation (red circle), locality A measured section of Broken River Formation.

8.3 Sedimentary Environments

8.3.1 Monro Conglomerate

Exposure of the Monro Conglomerate occurs along Whitecliffs (locality- red circle, fig. 8.1). A description and clast count was done on a conglomerate deposit. The Monro Conglomerate consists dominantly of massive, poorly sorted, matrix supported (poorly sorted fine sand matrix) polymictic conglomerate composed of well rounded pebbles and clasts ranging from a 3-4cm average diameter while the maximum size of the clasts range from 13 to 15 cm in diameter. The conglomerate clasts are composed dominantly of greywacke fine sandstone and rhyolite clasts with minor quartz pebbles, siltstone and mudstone clasts. The conglomerates are interbedded with poorly sorted carbonaceous mudstones, siltstones and sandstone beds.

8.3.2 Broken River Formation

The only exposure of Broken River Formation was observed and measured in the Nimmo Mine (locality A, fig. 8.1; appendix 1 fig. 1.55). The sequence consists of moderately sorted interbedded mudstones, siltstones with sandy horizons and sub-bituminous coal seams. The dominant structures in the succession are mud flasers with occasional fossil leafs. The succession's grain size was not sufficient for obtaining petrographic samples used in optical/SEM-CL analysis.

8.3.3 Conway Formation

The Conway Formation was limited in exposure so only a representative description and sample was collected from Surveyors Gully (locality – red circle, fig. 8.1). The deposit consists of moderately sorted, fine to very fine, grey-cream colour, quartzose sandstone, slightly glauconitic, jarositic and iron stained with spherical 5cm diameter concretions, burrows and micas. The deposit resembles the eastern Conway Formation at Waipara River.

8.4 Interpretations of Depositional Settings

8.4.1 Monro Conglomerate

The basal Monro Conglomerate is interpreted largely as a braided river deposit with splay and channel deposits. Mathews (1989) studied in detail the various fluvial facies of the Monro Conglomerate and interpreted a continuum of environments ranging from alluvial fan to conglomeratic longitudinal and transverse bars while the finer sediments represent bar-top deposition during low flow regime and sediment discharge.

8.4.2 Broken River Formation

The succession studied here represents a quiescent setting characteristic of an estuary or laggonal back-barrier setting according to Mathews (1989). Mathews (1989) interprets the coal forming as peat swamps in interdistributary bays and margins of the lagoon, while seam splitting results from frequent flooding from landward sources. Although in contrast most modern interpretations of coal require fresh water and no marine influence. The presence of coal is interpreted as a low deposition rate taking place.

8.4.3 Conway Formation

The Conway Formation is interpreted as a nearshore submarine depression based on Warren and Speden's (1978) interpretation with deposition resulting from slow suspension of fines. Mathews (1989) adds that minor cross beds within the formation indicate bottom currents during deposition.

8.5 Provenance

8.5.1 Conglomerate Clast Counts

Clast counts on the Monro Conglomerate (fig. 8.2) reveal that 35% of clasts consist of rhyolite, 26% greywacke –argillite sandstone clasts, 11% quartz pebbles, 11% siltstone, 8% mud clasts, 3% chert and 3% concretions. The underlying Mount Misery Volcanics of the Mount Somers Volcanics Group is interpreted as the major source, while the greywacke clasts are most likely derived from Wakepa Plant Beds of the Torlesse Supergroup. Well rounded quartz pebbles are most likely derived from the distant Haast-Otago Schist or Alpine Schist, while siltstone and mudstone clasts are probably intraformational. Minor chert is source from the underlying Torlesse Supergroup. It is noted therefore that the provenance of the Monro Conglomerate although of scarce exposure is similar in local provenance with the conglomerates at other locations.

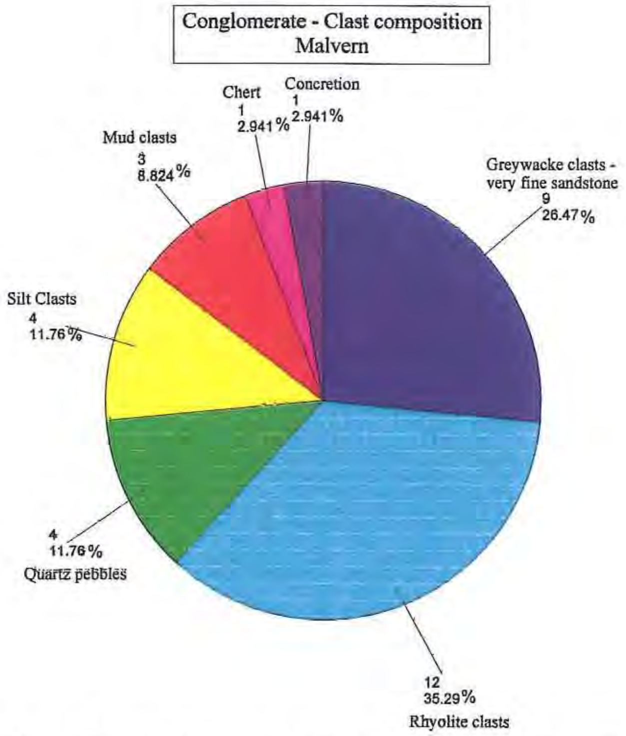

Figure 8.2: Pie diagram depicting composition of Monro Conglomerate (percentages of clasts).

8.5.2 Sandstone Composition

One sample was collected from the Conway Formation at the Surveyors Gully at Malvern (fig. 8.1). The composition of the Conway Formation is a subarkosic arenite with minor sedimentary lithics (3%) and volcanic lithics (1%) (appendices 1, 2, 3). The majority of the detrital grains are monocrystalline quartz grains. Glauconite content is only 4% therefore no study was done on glauconite morphology. 4% of the grains are muscovite and 5% of the quartz grains are polycrystalline. Feldspars are alkali at 6%. The Conway Formation is fine to very fine, moderately to well sorted. In terms of sandstone provenance the sample (SGM1) plots in the craton interior setting based on Dickinson's (1983) classification (fig. 8.4, A).

Based on the presence of the alkali feldspars, it is interpreted that possible sources are the underlying Mt Misery Volcanics or the more distant parts of the Mt Somers Volcanic Group. Alternatively the western province granites (Karamea – Separation Point Batholiths) and/or the Haast Schist could also provide alkali feldspar crystals. Syenites, granites, granodiorites and their volcanic equivalents produce alkali feldspar (Shelley 1985). The presence of volcanic lithics is most likely derived from the distal Mount Somers Volcanics Group than the underlying Mt Misery volcanics, counterpart since the Mt Misery Volcanics are andesitic and minor source rocks for quartz. The very proximity of the Mount Somers Volcanics Group suggest a likely source. The sedimentary lithics indicate reworking from underlying formations. Muscovite as a common detrital mineral could have been sourced from either the source areas mentioned above or recycled from the underlying Monro Conglomerate or Broken River Formation, although no major unconformity with the underlying formations has been described from the previous research.

8.5.3 Quartz Provenance (SEM-CL)

The same sample analysed for sandstone provenance was used for SEM-CL/optical microscopy analysis of quartz (appendix 7). This revealed that 46% of the quartz grains are plutonic with healed microcracks and non undulose to weak undulose extinction, 36% are metamorphic quartz grains with dark/black CL and strong undulose extinction, while 17% of the grains are volcanic quartz with homogeneous CL with straight extinction and/or CL zoning (appendix 5 figs. 5.24, 5.25). The data obtained indicates a bimodality of plutonic versus metamorphic quartz crystals with minor volcanic quartz (fig. 8.3). It is interpreted that the trends of quartz indicates a dominant plutonic source, most likely a granite source area, such as the Karamea – Separation Point Batholiths while the metamorphic quartz could have been derived from either Alpine Schist or Haast/Otago Schist. The volcanic source signature is surprisingly low, considering the local Mt Misery Volcanics as a potential source area. Tappenden (2003) refers to the extent of the Mt Misery Volcanics and describes that the volume of rhyolites is low compared to the southern Mount Somers Volcanics and instead the Mt Misery volcanics are more andesitic. In any case the volcanic signature is low which indicates that the local source rock composition didn't have any quartz and the major volcanic source was further south at Mount Somers. The sample on a quartz provenance discrimination diagram plots in the mixed source area with dominant plutonic and metamorphic sources, while volcanic source areas are low (fig. 8.4, B). The basal Torlesse Supergroup is unlikely as a source area since its composition is not composed of coarse quartz crystals.

8.6 Summary

The Monro Conglomerate indicates a fluvial depositional environment typical of braided river deposit with overbank crevasse splay deposits. In turn the source rocks reflect local derivation predominantly from the Mount Somers Volcanics Group but its local counterpart, the Mt Misery Volcanics, hence characteristic rhyolite clasts. The other source rocks are the Torlesse Supergroup with very fine poorly sorted greywacke rocks. Quartz pebbles indicate a Haast-Otago/Alpine Schist source while mudstone and siltstone clasts indicate a penecontemporaneous provenance.

The Broken River Formation is characteristic of peat swamps forming near the proximity of a lagoonal-estuarine setting with interbedded carbonaceous mudstones and siltstones indicating flooding events. The overlying Conway Formation is interpreted as a barred submarine depression with low deposition by suspension of fines. Provenance of the Conway Formation sandstone indicates an interior craton tectonic setting. Alkali feldspar indicates a felsic igneous source either the Mount Somers Volcanics Group or the Western Province granites while a metamorphic source is also likely such as the Haast-Otago/Alpine Schist. The sedimentary lithics indicate possibly reworking from underlying formations or sourced from the Torlesse Supergroup while the volcanic lithics strongly suggest a Mount Somers Volcanics Group provenance.

Provenance of quartz in the Malvern area shows a mixed provenance with dominant bimodal metamorphic and plutonic source areas. A metamorphic terrane such as the Haast-Alpine Schist is implied for the metamorphic quartz. Since the metamorphic grade of the grains is low the low grade metamorphic Alpine Schist is the most likely source. The plutonic quartz grains in turn are most likely attributed to a granitic source rock area; most likely the Western Province Karamea-Separation Point Batholiths. The Mount Somers Volcanics is the predominant source rock area for the volcanic quartz grains.

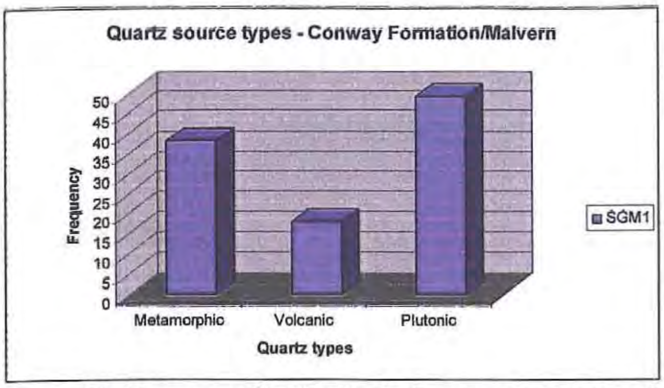

Figure 8.3: Frequency of grains displaying quartz source type for sample SGM1 (Conway Formation).

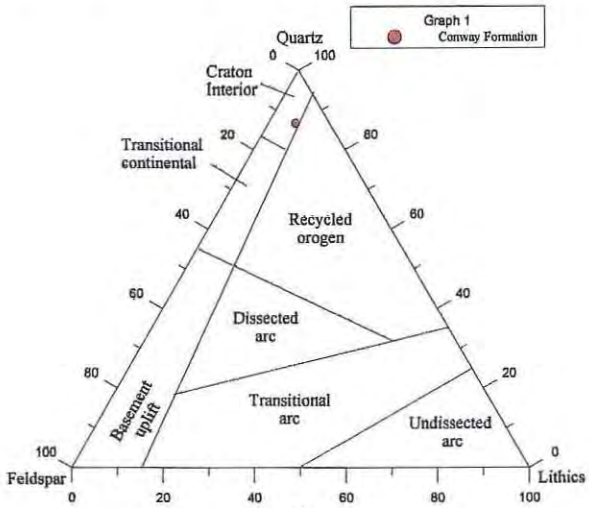

A)

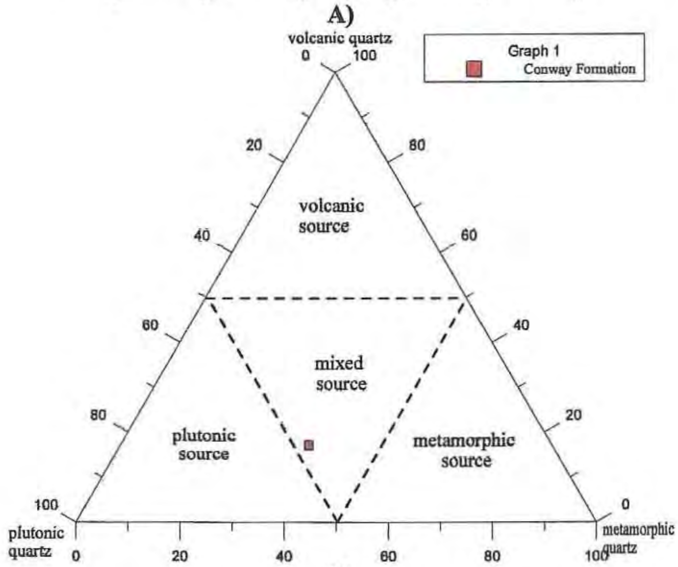

B)

Figure 8.4: A) Tectonic setting discrimination diagram after Dickinson (1983), on the basis of normalized point counts, results from conventional point counts. Sample from Conway Formation plot in the Craton Interior tectonic field. **B)** Provenance discrimination diagram after Bernet and Bassett (2005), of Conway Formation, sample using the three main quartz types of volcanic, plutonic and metamorphic quartz, based on SEM-CL/analysis. The dashed lines indicate the 50 percent lines of each of the three main types. Metamorphic quartz includes all low-grade to high metamorphic, recrystallized and vein quartz

CHAPTER NINE
SYNTHESIS – DISCUSSION

9.1 Introduction

The analysis of the Broken River Formation, the Iron Creek Formation and their regional correlatives indicate that similar trends occur at each location in depositional environments, sedimentation rates and provenance with minor local variations. In this chapter, data and interpretations from all previous chapters are synthesized starting with a correlation of formations with equivalent lateral formations. The regional depositional setting is interpreted in terms of paleoenvironment and sedimentation rates. The provenance is assessed based on the reconstructed paleogeographic distribution of source rocks and the regional scale tectonic setting during the Late Cretaceous – Late Eocene.

9.2 Regional Correlations

Despite a relatively simple transgressive stratigraphy of basal conglomerates, quartzose coal measures and glauconitic quartz arenites, there are multiple formation names reflecting subtle differences between localities. The plethora of formation names given by different authors to mark the local characteristics thus masks the correlation of regional geology. Brown and Field (1985) and Andrews et al (1987) correlated the different formations. However, in this research it is important to correlate the different localities studied with respect to their sedimentary structures and composition. The various formations are the basal Monro Conglomerate, the Broken River Formation and the Stour Coal Measures corresponding to the quartzose coal measure sequence and the Charteris Bay Sandstone- Iron Creek Greensand Members of the Iron Creek Formation and the Waipara Greensand for the glauconitic and glaucarenite sandstones. Overall water deepens to the east and north with more proximal subaerial deposits to the west and south.

The rocks of the Monro Conglomerate and Broken River Formation consist largely of basal conglomerates, coal and carbonaceous sandstones – siltstones and are easily correlated over the Canterbury region. Clast composition consists of Torlesse Supergroup derived clasts and locally derived volcanics resting unconformably on underlying Torlesse Supergroup basement rocks common to most of the region. The exception is the Stour Coal Measures at Mount Somers which rests on kaolinized rhyolite of the Mount Somers Volcanics Group. The Mandamus conglomerates and coal rest on the Mandamus Igneous Complex trachyte/Syenite. The Broken River Formation's basal conglomerates in North Canterbury in the Mandamus area correlate well with the conglomerates of the western Castle Hill Basin and Avoca – Iron Creek areas, which are also locally derived from pre-unconformity rocks (fig. 9.1). In addition the basal conglomerates of the Broken River Formation in the eastern Waipara River area described by Nicol (1993) as locally sourced from the Torlesse Supergroup rocks are correlative with the conglomerates in the north and west. The coal measures and the overlying sandstones between all locations are correlative as well. Biostratigraphic markers such as shell beds are not that easily correlated over the region as they tend to be local occurrences. For example the Broken River Formation at Waipara River contains an *Ostrea* shell bed interbedded with carbonaceous sands that is intraformational shell bed.

The overlying contact of the Broken River Formation and the glauconitic Charteris Bay Sandstone Member of the Iron Creek Formation is interpreted as a disconformity at Avoca (McLennan & Bradshaw 1984). That conclusion is untrue since the presence of minor glauconite in the underlying Broken River Formation found in this research negates the possible presence of disconformity. Therefore a gradational contact is instead most likely. It is also gradational in the Castle Hill Basin (fig. 9.1). The Charteris Bay Sandstone at Castle Hill Basin and Avoca-Iron Creek contains about 16-21% glauconite which correlates possibly with the Waipara Greensand Formation at Mandamus with a 13-20% glauconite content. The Charteris Bay Sandstone at Castle Hill and Avoca – Iron Creek correlates with the upper Conway Formation sandstone at Waipara River which contains 11-20% glauconite (fig. 9.1). In more detail, Brown and Field (1985) show the Charteris Bay Sandstone interfingering with the Conway Formation in the east (fig. 9.2) which thickens to its thickest at Haumuri Bluff to the north-east (Warren & Speden 1977). The Loburn Mudstone at Waipara is considered by Brown and Field (1985) as the underlying member of the Waipara Greensand and it interfingers with the Charteris Bay Sandstone (figs.9.1, 9.2).

In the south at Mount Somers the Blondin Sand Member of the Broken River Formation contains minor glauconite and is most likely the correlative to the Charteris Bay Sandstone Member of the Iron Creek Formation in the north since it is dated at Waipawan to Bortonian (Early Eocene – Late Eocene) (Oliver & Keene 1989). In addition, the unit is cross stratified with mud drapes and *Ophiomorpha nodosa* trace fossils similar to the cross stratified Charteris Bay Sandstone Member of the Iron Creek Formation at Castle Hill. The age of the Blondin Sand Member is Bortonian (Mid-

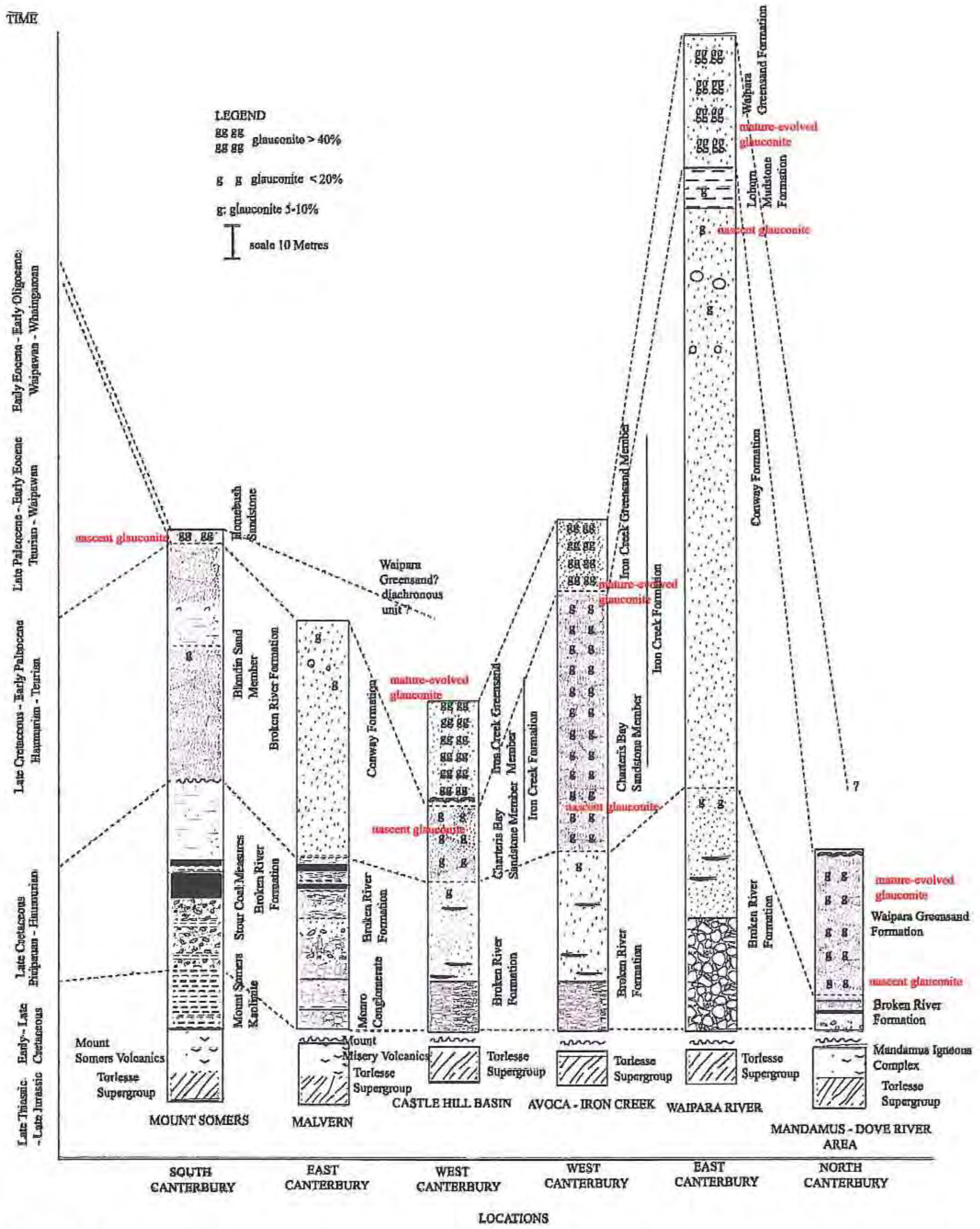

Figure 9.1: Correlation transect between formations and members of the Monro Conglomerate, Broken River Formation – Stour Coal Measures, Iron Creek Formation – Conway Formation – Blondin Sand Member, Loburn Mudstone, Waipara Greensand and Homebush Sandstone at localities studied in this research. Dashed lines are correlation markers between localities and coeval formations and members. Nascent glauconite dominates while it increases in the upper Charteris Bay Sandstone Member of the Iron Creek Formation and its correlative formations-members. Evolved-mature glauconite dominates in the Iron Creek Greensand – Waipara Greensand.

Eocene) while the Charteris Bay Sandstone is Teurian (Early – Late Paleocene). It is probable the two members are diachronous of the same lithology.

The Iron Creek Greensand Member of the Iron Creek Formation at Castle Hill Basin is marked by 40-50% glauconite content and characteristic oyster shell beds near the contact with the underlying Charteris Bay Sandstone. It is correlated with the glauconitic rich Iron Creek Greensand Member at Iron Creek, Avoca (fig. 9.1). Furthermore, the oyster shell bed at the top of the Charteris Bay Sandstone Member resembles the oyster shell bed in the upper Waipara Greensand in Mandamus River, North Canterbury. This reinforces the probability that the lower glauconitic sands at Mandamus are the correlative with the Charteris Bay Sandstone and not the Waipara Greensand. The Iron Creek Greensand of Castle Hill Basin – Avoca/Iron Creek is correlative, based on the glauconite content, with the Waipara Greensand at Waipara River. Gage (1970) noted that the Iron Creek Greensand is the inland equivalent of the Waipara Greensand.

However, the Waipara Greensand in the east is Teurian (Early-Mid Paleocene) significantly older than the Early Eocene-Late Eocene Iron Creek Greensand in the west. Brown and Field (1985) show, in a correlation transect, the Iron Creek Greensand separated by a large period of non deposition/erosion from the underlying Charteris Bay Sandstone and the Waipara Greensand in the east (fig. 9.2). Instead the issue of diachronous units also applies here.

The two distant members are probably correlative since the inland Iron Creek Greensand marks the inland progression of the marine transgression, hence a much younger member. The eastern Waipara Greensand and the younger western Iron Creek Greensand is more likely correlative since the latter marks the height of the inland marine transgression. In detail Brown and Field (1985) show in figure 9.2 a large period of non deposition/erosion between the Charteris Bay Sandstone and the Iron Creek Greensand. This can not be correct since the members grade into one another at Castle Hill Basin, and the disconformity at Iron Creek has been reinterpreted as continuous deposition. Even if there is a wider regional disconformity, the large period of non deposition can be better explained by low sedimentation rate based on the presence of autochthonous glauconite indicating in situ formation, which is analysed later into further detail.

The glauconitic Homebush Sandstone in the upper stratigraphy of the Mount Somers area is younger at Bortonian to Whaingaroan (Late Eocene – Early

Oligocene) than the Iron Creek Formation and the Waipara Greensand in North Canterbury. Brown and Field (1985) describe the Homebush Sandstone as the underlying layer of the Ashley Mudstone elsewhere in the Canterbury region. Furthermore Field and Brown (1989) describe interfingering relationships between the Homebush Sandstone and the top of the Charteris Bay Sandstone southwest of the Castle Hill Basin area which means the former formation and the latter member of the Iron Creek Formation are correlative.

The glaucarenites of the Charteris Bay Sandstone/Conway Formation and Iron Creek Greensand/Waipara Greensand respectively were distinguished in this research based on the percentage of glauconite. This was based on data from the literature and from this research. In more detail, the Charteris Bay Sandstone/Conway Formation has a 15-20% glauconite content thus distinguished from the Iron Creek Greensand Member/Waipara Greensand which contains 40-50% glauconite. The percentage of glauconite and the stratigraphy was used in correlating localities and formations with different names. The glauconite types were also considered in the correlation although they transgressed the correlation boundaries (fig. 9.1).

The Charteris Bay Sandstone Member/Conway Formation contains predominantly nascent glauconite which increases upsection in the formation to evolved-mature glauconite. In contrast, the overlying glaucarenites of the Iron Creek Greensand/Waipara Greensand consist predominantly of evolved/mature glauconite (fig. 9.1). Based on the nascent glauconite in the Homebush Sandstone at Mount Somers it could be possible that the formation is diachronous and lateral correlative to the Charteris Bay Sandstone/Conway Formation, however its very young age Bortonian- Whaingaroan (Late Eocene – Early Oligocene) relative to the other nascent glauconite greensand makes that unlikely. In addition Andrews et al (1987) describes the age of the Homebush Sandstone as based entirely on stratigraphic relationships since it is largely unfossiliferous.

9.3 Depositional Environments

9.3.1 Broken River Formation

The research done on the Mandamus –Dove River, Waipara River area, Iron Creek-Avoca, Castle Hill Basin, Malvern and Mount Somers locations shows that the basal conglomerates of the Broken River Formation are largely braided river deposits based on large clasts, minor cross beds, debris flows and meandering river deposits based on fine sands, and muds-crevasse splays interbedded with coal and carbonaceous mudstones. Coals formed in interdistributary floodplain - alluvial settings or abandoned channels as peat swamps and other larger terrestrial peat bogs. These form thick coal seams near fluviodeltaic – estuarine settings but were not influenced by saline waters.

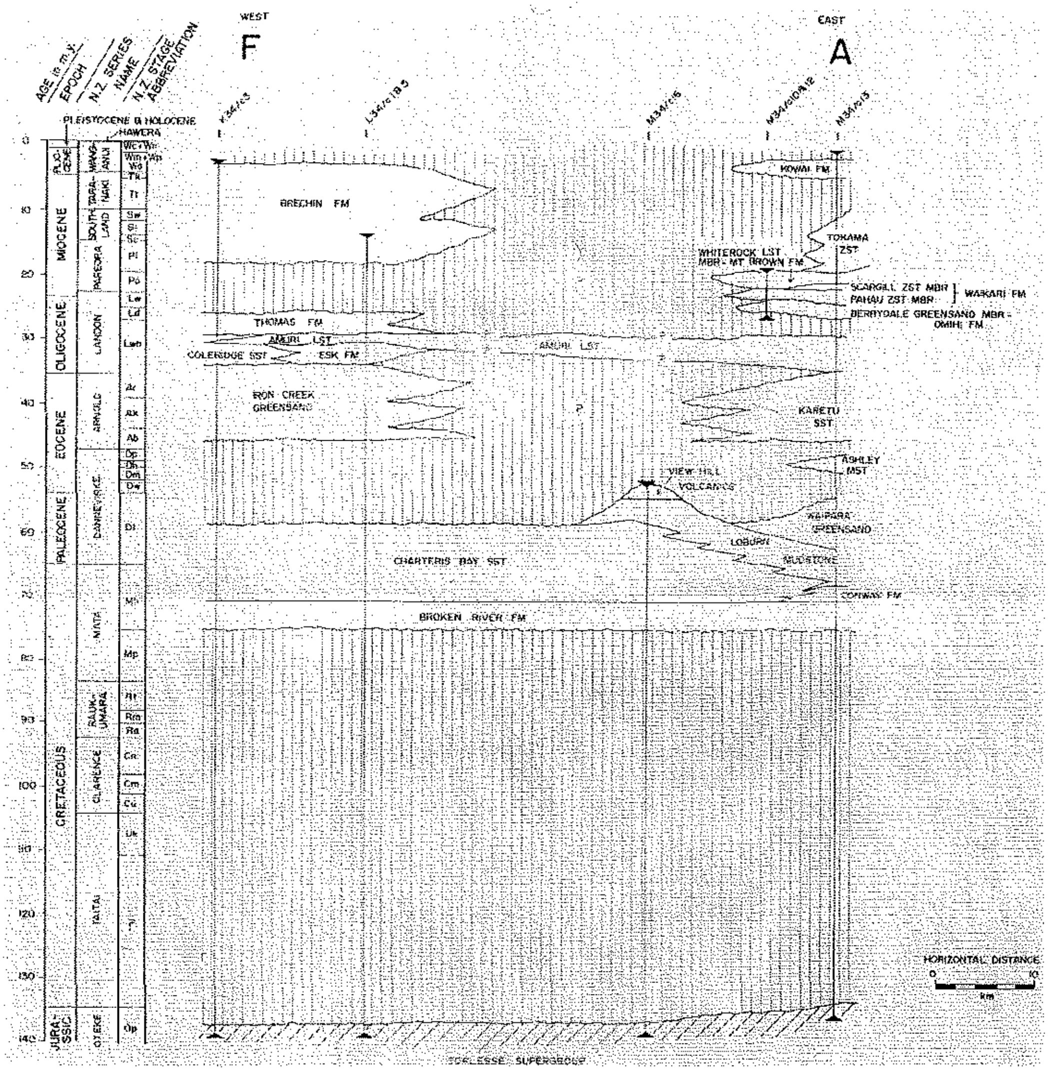

Figure 9.2: Correlation transect diagram for west-east trending transect through northern Canterbury: from F (Broken River) to A (Grey River). Vertical line pattern indicates periods of non deposition or erosion. Vertical bars indicate the stratigraphic interval at which rocks are exposed in each section (from Brown & Field 1985).

Upsection the Broken River Formation becomes marginal marine with faintly cross bedded carbonaceous sandstones, interbedded siltstones and coal stringers, bioturbated layers, and shell beds indicative of fluviodeltaic to lower shoreface - upper shoreface depositional settings. The latter two settings were dominated by waves and storm events as indicated by the abundance of cross stratification and high degree of sorting. In some areas, the quartz arenites of the upper Broken River

Formation contain nascent glauconite indicating a transition into estuarine settings. Most of the quartz rich sandstones of the Broken River Formation are dominated by fine – medium grain sizes that are angular which indicates primarily fluvial transport deposited in marginal marine settings.

The dominant depositional environment interpreted for the Broken River Formation is an alluvial – fluvial setting grading into marginal marine estuary-lower shoreface depositional setting.

9.3.2 Iron Creek Formation – Waipara Greensand

The characteristic cross bedded glauconitic sandstones of the Charteris Bay Sandstone Member (Haumurian –Teurian) in the west (Castle Hill Basin, Avoca –Iron Creek) indicates a marginal marine to shallow marine depositional setting that is largely foreshore subtidal. The cross stratification indicates major currents produced by longshore drift and/or by waves in dominantly north- north-east and south-south-west or south-east directions. In addition thin conglomerates in the Blondin Sand Member at Mount Somers are largely foreshore to marginal marine.

Laterally, the Charteris Bay Sandstone interfingers with the Conway Formation to the north-east. The Conway Formation, exposed in the Waipara River area and at Malvern, is largely a shallow marine depression composed of siltstones with slightly glauconitic fine sandstones. It is typically jarositic with increasing concretions and glauconite content up section. The glauconite within the Conway Formation is nascent becoming mature/evolved in the upper part of the formation. The petrographic data in conjunction with sedimentary structures indicate low energy deposition from suspension, therefore no significant disturbance. Lithologically homogeneous successions with non selective spatial distribution of glaucony are likely to reflect an autochthonous origin of grains (Amorosi 1997). The autochthonous origin of the glaucony grains of the Conway Formation indicates a shallow submarine depression combined with bioturbation and absence of moderate energy. In addition the jarosite content was interpreted by Warren and Speden (1978) as indicative of authigenic bacterial reduction of sea water sulphates in a low oxygen environment, a good chemical setting to form glauconite.

The glauconite content of the Conway Formation which overlies the Broken River Formation in the east (fig.9.1) is similar to the Charteris Bay Sandstone in the west, therefore supporting the interpretation that the two formations are laterally correlative. The Loburn Mudstone is also correlative to the Charteris Bay Sandstone, a slightly glauconitic sandy siltstone at the Waipara River to the east, which is a submarine- shallow marine depositional setting beyond the tidal zone. This interpretation is based on the minor glauconite content.

Components which characterize a lower shoreface – foreshore depositional environment are the presence of micrite, marine fossils (bryozoa – foraminifera) as well as well - rounded polycrystalline quartz grains indicating transport by longshore drift and/or by waves. It is therefore interpreted that the Charteris Bay Sandstone reflects a depositional environment influenced by the encroaching marine transgression, characteristic of a foreshore-lower shoreface marine setting; while the Conway and Loburn Mudstone formations reflect local variations in depositional settings.

The Charteris Bay Sandstone at Castle Hill Basin and Avoca –Iron Creek shows a marked increase in glauconite content to an average of 15 – 20% indicating the progression of the marine transgression up section. The glauconitic sandstones of the Waipara Greensand at Mandamus, correlated with the Charteris Bay Sandstone, have the same glauconite percentage. In detail the Charteris Bay Sandstone is dominated by the nascent, pale green, irregular glaucony grains which change up section to evolved/mature, well rounded glaucony grains associated with an overall increase in glauconite percentage.

The nascent grains are randomly distributed in the Charteris Bay Sandstone in lithologically homogeneous units or beds whereas in upper units or beds, the rounded glaucony grains are concentrated in crossbed foresets. These are compacted and damaged during transport; however they retained their rounded appearance. According to Amorosi (1997), lithologically homogeneous successions with non selective spatial distribution of glaucony are likely to reflect autochthonous origin of grains. In this case the nascent glaucony grains reflect autochthonous mode of formation. In contrast, the alternation of glaucony – rich and glaucony free layers in the crossbed foresets is interpreted to indicate allochthonous origin of glaucony (Amorosi 1997). The fact that well rounded glaucony grains are degraded easily in water indicates a parautochthonous origin of glauconite in the crossbeds. Its relatively undamaged morphology indicates it was transported from the source to the site of deposition locally before it became degraded or recycled.

The overlying Iron Creek Greensand Member of the Iron Creek Formation in the east (Castle Hill Basin – Iron Creek/Avoca) is a glaucarenite with well rounded mature/evolved glauconite grains, and has characteristics of a foreshore to shallow marine – shelf depositional setting. Laterally it correlates with the Waipara Greensand in the East at Waipara River (fig. 9.1). The existence of beds with very fine detrital grains indicates low energy conditions and deposition from suspension, while beds with coarse, well rounded quartz grains and granules indicate occasional transport by storms and waves.

The succession is glauconite rich with 40-50% glauconite, all of it composed of well rounded, mature/evolved, dark green glaucony grains. Glaucony is commonly concentrated in parallel crossbeds and in trough cross stratified layers, as in Iron Creek, or in lithologically homogeneous successions with an even spatial distribution. This combination points towards a gradation between parautochthonous and autochthonous origin of glaucony grains in the Iron Creek Greensand – Waipara Greensand.

In terms of assessing the paleoenvironment of the Iron Creek Formation - Waipara Greensand the presence and mode of glaucony formation, occasional micrite, well rounded detritus alternating with fine detritus, and cross bed foresets indicates a marginal marine to lower shoreface-foreshore setting leading to a shelf-shallow marine depositional environment. Glauconite was formed wherever there were low energy conditions, both in estuary and shallow marine shelf settings.

9.3.3 Regional Paleogeography

Depositional and regional paleogeographic setting responded to the encroaching marine transgression which was dominating the Late Cretaceous-Early Paleocene to Eocene. For most of the time the region was comparatively quiescent (Field & Brown 1989). McLennan (1981) interpreted the coal measures as accumulating in swamp fluviatile and estuarine settings over the region during the early Haumurian at least as far west as Castle Hill Basin. On a larger scale quartzose coal measure deposition in the west of the region passed eastwards into shallow marine shelf sands, greensands and silts which passed rapidly further east to bathyal silts and, in the far north to micritic carbonates (Field & Browne 1989; fig. 9.3). Field and Brown (1989) describe that the Canterbury region continued to have low relief through out the Eocene and the region was divided from the deeper water to the north by the Chatham Rise which was a submarine high or a very low lying peneplain (fig. 9.4). Coal measure deposition in eastern South Canterbury was drawing to a close in the Eocene (Field & Brown 1989).

In relation to the regional paleogeographic setting the Broken River Formation during the Late Cretaceous – Paleocene was characteristic of an alluvial to fluvial-fluviodeltaic setting adjacent to basement highs (fig. 9.5). In contrast the setting of the Iron Creek Formation during the Late Paleocene – Eocene showed extremely low relief in marginal marine to marine depositional settings, in detail lower shoreface – foreshore to shelf and shallow marine depositional settings with glauconite formation (fig. 9.6).

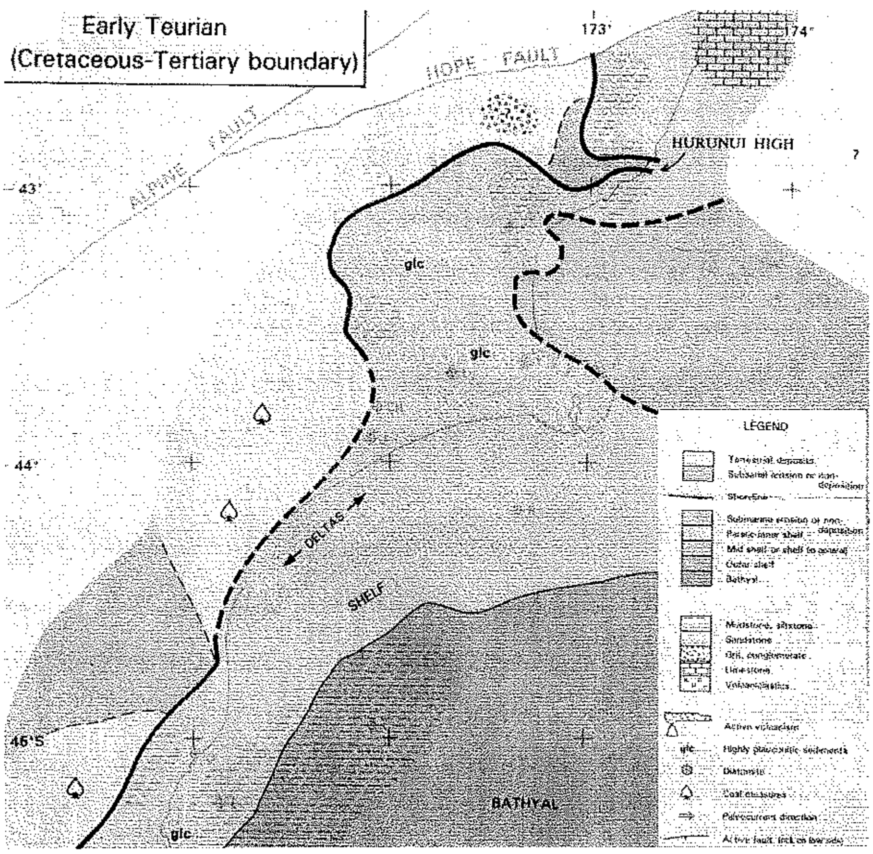

Figure 9.3: Paleoenvironment of the Canterbury region during the Early Teurian (from Field & Brown 1989).

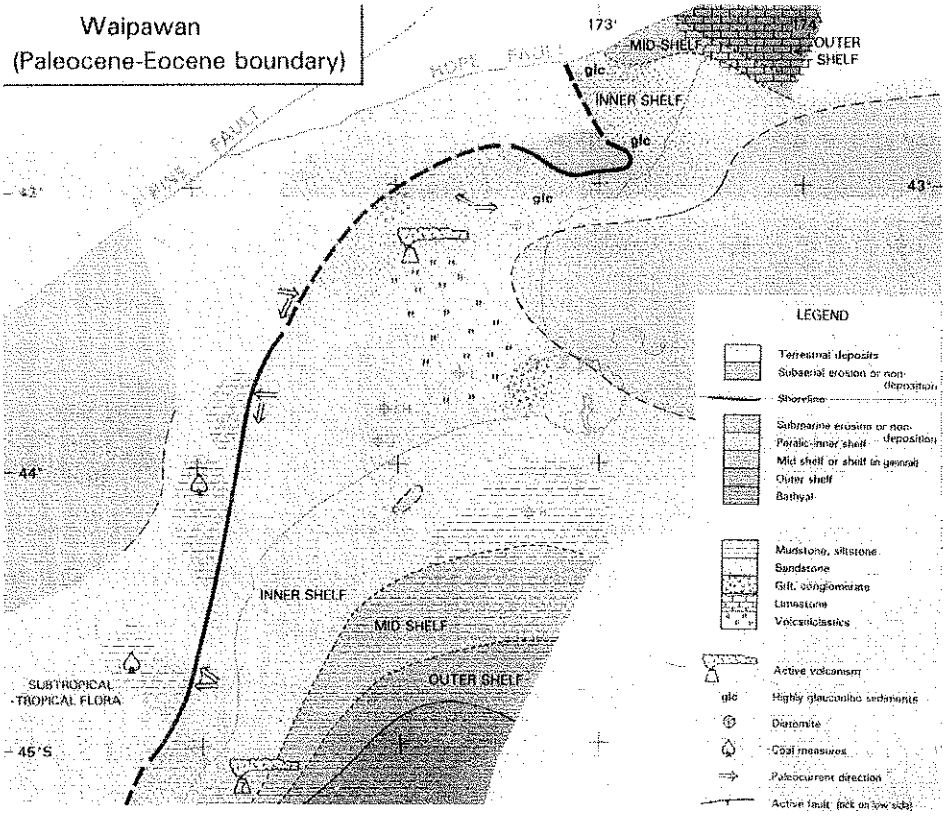

Figure 9.4: Paleoenvironment of the Canterbury region during the Paleocene – Eocene (from Field and Brown 1989).

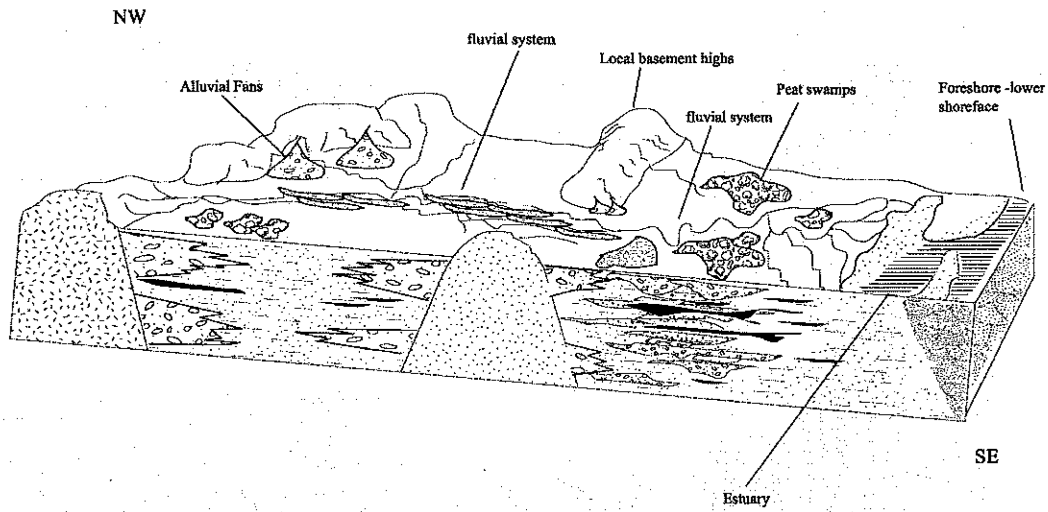

Figure 9.5: Paleoenvironment model of the Broken River Formation with alluvial fans to braided river and meandering fluvial systems draining into fluviodeltaic systems. Formation of peat swamps and coalfields dominantly in interdistributary and fluviodeltaic settings and minor peat swamps forming in alluvial fan-plains. Relative peneplanation indicated with localised Torlesse basement highs.

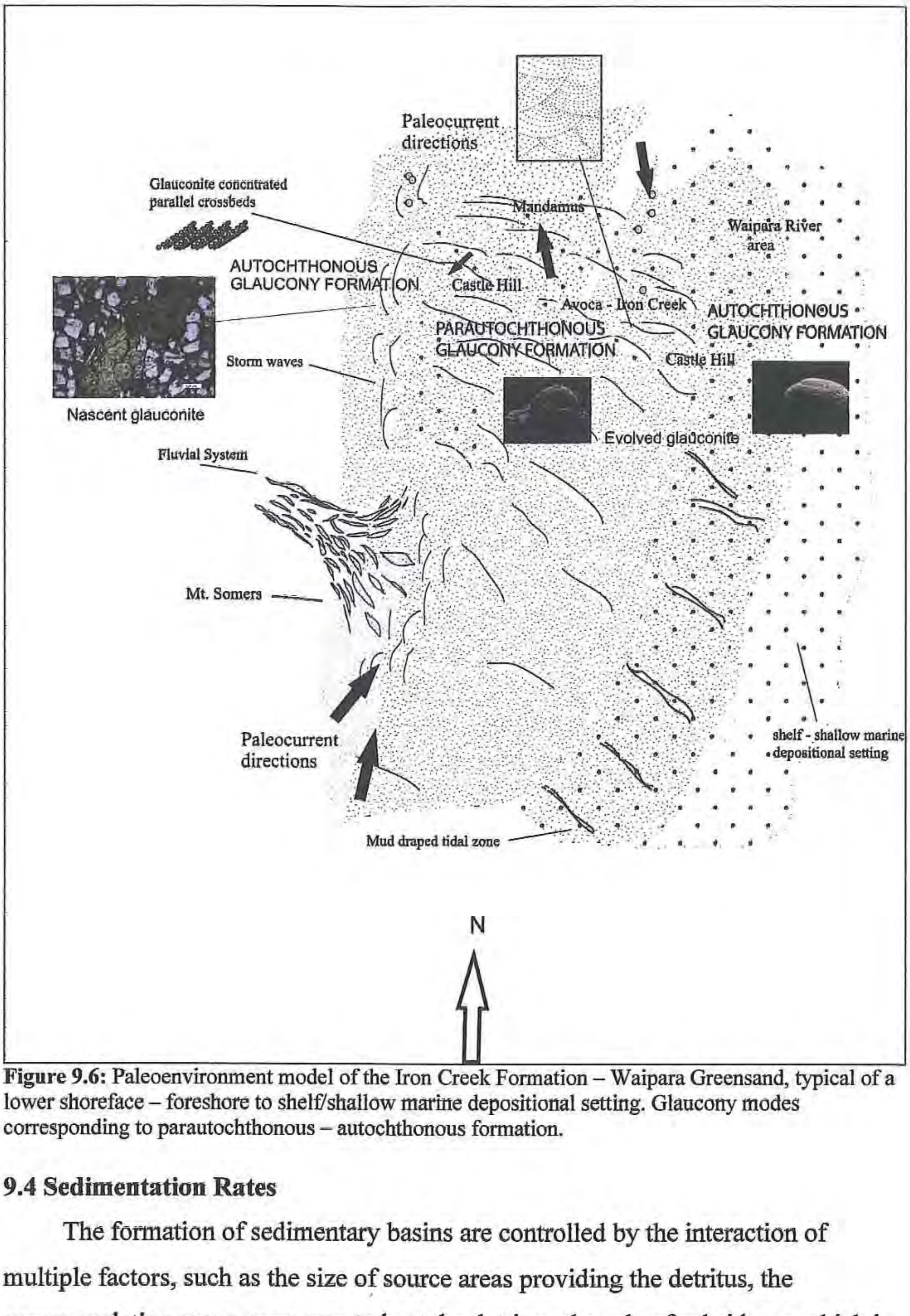

Figure 9.6: Paleoenvironment model of the Iron Creek Formation – Waipara Greensand, typical of a lower shoreface – foreshore to shelf/shallow marine depositional setting. Glaucony modes corresponding to parautochthonous – autochthonous formation.

9.4 Sedimentation Rates

The formation of sedimentary basins are controlled by the interaction of multiple factors, such as the size of source areas providing the detritus, the accommodation space necessary to host the detritus, the role of subsidence which in turn is related to tectonic influences, sea level rises, tectonic or eustatic and the process of uplift and exhumation in relation to erosion and transport of sediments. Einsele (2000) describes that in the beginning of basin formation, tectonic subsidence must predate sedimentation, whereas later, subsidence may also be actively driven by an increasing sediment load.

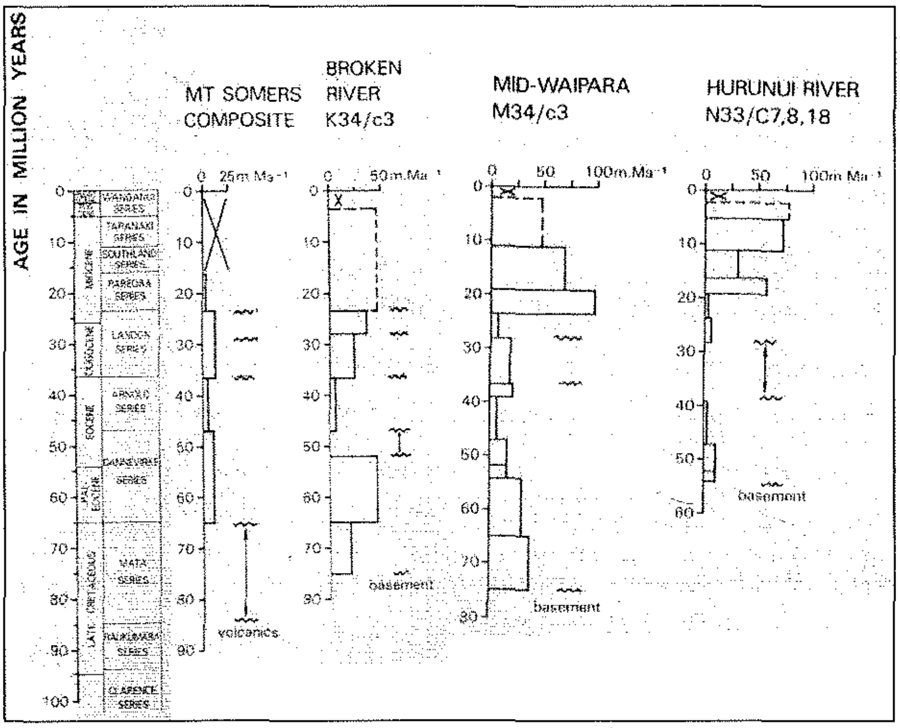

Figure 9.7: Histograms of sedimentation rates from various from various Canterbury localities, note low sedimentation rate for the Paleocene – Eocene for most localities (From Field and Brown 1989).

9.4.1 Coal as Sedimentation Rate Indicator

Coal is an important indicator of low sedimentation rate and the Broken River Formation's coal measures reflect that low sedimentation rate. Important prerequisites for coal formation are: 1) the evolution of plant life on the continents; 2) a relatively high plant productivity under favourable climatic conditions with sufficient nutrient supply; 3) Very low input of detrital material into the peat accumulating basin; 4) a depositional environment where plant remains can be preserved (Einsele 2000).

Subsidence, accommodation space and sedimentation are all interrelated in the formation of coal. A balance must be reached aided by tectonic subsidence between optimal peat growth and necessary accommodation space (Einsele 2000). The accommodation space must keep up with peat growth; if it exceeds peat growth the peats become drowned and finally buried under clastic sediments (Einsele 2000). With accommodation too low, the growing peat is exposed to the air and cannot be preserved, or it is reworked. Sedimentation rates of peat horizons are distinctively lower than the rates for the associated clay horizons, each of which can be interpreted as a period of flooding at the beginning of the depositional cycle (Diessel et al 2000).

Peat accumulation could begin only after the relative sea-level rise had decelerated to a rate that was in tune with the growth rate of peat producing plants (Diessel et al 2000). In addition Diessel et al (2000) refer to the beginning of peat formation as the terrestrialisation process that leads to regressive coals. Thus the peat growth according to Einsele (2000) depends on the frequency and amplitude of sea level changes. Mires in which the rates of accommodation and peat accumulation remain well balanced for a long period of time lead to the formation of thick coal seams with minimum ash content and maximum tissue preservation, the latter in the form of structured vitrinite (Diessel et al 2000). If the accommodation/peat accumulation ratio is low, the inherent ash content of the peat increases because of oxidation of the organic matter. Conversely, an accelerated rise in the accommodation rate causes frequent flooding of the peat which raises the adventitious mineral content (Diessel et al 2000)

Therefore a delicate balance must be reached for preservation of peat and formation of coal. The Broken River Formation's coal facies is transgressive formed in fluvial flood plains and backbarrier lagoonal settings while some coals have a brackish water influence interpreted from the presence of sulphur and pyrite (Mathews 1989). In coastal areas, peat formation is therefore favoured by relative sea-level rise, but this rise must not be too slow or too rapid (Einsele 2000).

Peat accumulation and coal formation requires minor or intermittent sediment supply thus reflecting a low sedimentation rate followed by moderate sedimentation rate. The Broken River Formation coal measures reflect overall a low sedimentation rate.

9.4.2 Glauconite as Sedimentation Rate Indicator

Glauconitic minerals are common authigenic constituents of marine sediments and are good indicators of sedimentation rates (Pasquini et al. 2004). The evidence for the rate of deposition is obvious from the presence and the morphology of glauconite in the sedimentary successions. Glaucony formation requires low sedimentation rate, because major detrital input during formation would inhibit growth. The presence of sparse nascent irregular and minor mature/evolved well rounded, dark green glauconite marks the onset of the marine transgression in the upper Broken River Formation and lower Iron Creek/ Conway-Waipara Formations. The random distribution of nascent – evolved/mature glaucony in lithologically homogeneous successions reflects autochthonous glaucony formation. A low to moderate sedimentation rate is proposed for certain successions of the Broken River Formation where sparse nascent glauconite is present. The Iron Creek Formation's Charteris Bay Sandstone concentration of nascent irregular glauconite grains with fibroradiated rims indicates in situ formation which pre - dates the arrival of coarse detritus. The presence of early stage micaceous glauconite also suggests autochthonous formation. In detail the evidence on microscale (petrography) and in mesoscale (sedimentary structures – stratigraphy) suggests again random distribution of glaucony in lithologically homogeneous successions indicative of low sedimentation rate with the glauconite forming in protected estuarine/lagoonal settings.

Up section, the Charteris Bay Sandstone contains well rounded dark/green evolved/mature glauconite grains which exhibit cracks or indentation features by detrital grains but retain an overall well rounded surface. These grains occur lining foresets in parallel cross beds, suggesting local reworking or parautochthonous formation of glauconite. Well rounded, dark green evolved/mature glauconite grains disaggregate with transport, reducing the size and the shape of those grains to recycled glauconite, a variety described by McConchie and Lewis (1980). Chafetz and Reid (2000) and Amorosi (1997) indicate the presence of mature/evolved glauconite in high energy successions represents parautochthonous glauconite, formed and transported locally from the site of formation to the nearby locus of deposition.

Thus in turn a parautochthonous formation and origin of glauconite is interpreted of well rounded evolved/mature grains concentrated in cross stratified layers. A locally moderate sedimentation rate is interpreted for those settings representing fair weather to storm conditions. However, overall the lithologically homogeneous successions with evolved/mature glaucony grains and the alternating inhomogeneous successions with glauconite rich and glauconite free layers represent autochthonous to parautochthonous formation, hence alternation of low to moderate-sedimentation rates in the Charteris Bay Sandstone.

Higher in the section, glauconite within the Iron Creek Greensand Member – Waipara Greensand show a progressive increase of well rounded, dark green, mature/evolved glauconite grains upsection at the expense of nascent and micaceous glauconite lower in the successions. Well rounded, dark green, mature evolved glauconite is dominant in the Iron Creek Greensand, in the upper Conway Formation and in the Waipara Greensand. The presence of evolved glauconite in shallow marine and submarine depressions together with evenly spaced distribution of glaucony in lithologically homogeneous successions suggests autochthonous glauconite formation in mid to outer shelf. The autochthonous formation of glauconite in the glaucarenites and the dominantly fine to very fine-silt grain size is indicative of low clastic input, hence low sedimentation rates for the upper Iron Creek Greensand – Waipara Greensand and upper Conway Formation.

An overall low sedimentation rate based on mesoscale and microscale (stratigraphic – petrographic) evidence supports the low sedimentation rates proposed from calculated stratigraphic thicknesses from Field and Brown's (1989) work. Variations between autochthonous and parautochthonous glaucony formation and low to moderate sedimentation rates also coincide with variations in sedimentation rates through out areas observed from calculated thicknesses. These variations are possibly attributed to the local paleo - topographical features of the Paleocene - Late Eocene period, where certain uplifted basement highs such as the Hurunui High provided shelter in certain areas for autochthonous formation of glauconite while in other areas paleocurrents transported glauconite grains from nearby locations. In addition, sedimentation rate would have varied from shallow marine – outer shelf locations to foreshore depositional settings. The evidence from Schioler et al. (2002) suggesting a non uniform transgression interrupted by unconformities and minor regressive phases points towards a possibility of erosion or non deposition between formations, thus a variable sedimentation rate. Although the Iron Creek Formation, Conway Formation and Waipara Greensand indicate low sedimentation rates overall.

9.4.3 Regional Setting

In the South Island there was considerable variation in the rate of subsidence (Field & Brown 1989). The greatest subsidence occurred in the Clipper Basin which lies offshore from present day Canterbury towards the east. Subsidence rates were higher for the coarse conglomerate filled half grabens in western Canterbury (such as the Monro Conglomerate of the Malvern Hills) and possibly also for the Broken River – Waipara River areas (Field & Brown 1989). Field and Brown (1989) suggested that subsidence was widespread over the region but decreased from the Late Cretaceous to the Paleocene Eocene; this is supported by this research.

Field and Brown (1989) calculated variable sedimentation rates in the Late Cretaceous with anomalous high sedimentation rates (70m.Ma-1) in the Malvern Hills area where the Monro Conglomerate was accumulating. In the north the Hurunui High separated the Waipara Basin in the south from the Mandamus area in the north (rates up to 40m.Ma-1) (fig. 9.7). Sedimentation rates declined substantially in the early Paleogene in keeping with the reduced rates of subsidence (Field & Brown 1989). In general, sedimentation rates less than 25 m Ma-1 were common for the Canterbury area while little or no deposition occurred in the north of the region, particularly in Paleocene time (Field & Brown 1989). This evidence coincides with the Hurunui River area (fig. 9.7) in close proximity to the Mandamus area, where Broken River Formation interbedded conglomerates and coal are succeeded by glauconitic sandstones of the Waipara Greensand lateral equivalent to the Iron Creek Formation's Charteris Bay Sandstone, thus missing out the sedimentation of the Broken River Formation's carbonaceous sands. Sedimentation rates slightly increased in the Waipara River to the south (fig. 9.7) (Field & Brown 1989). The low but variable sedimentation rates may also be influenced by the sheltering of certain areas such as the Mandamus – Dove River area by paleogeographic highs such as the elongate east west trending Hurunui High separating the Mandamus area to the North from the Waipara River area to the south - east (figs. 9.3, 9.4).

Low sedimentation rates in the southwest at Mount Somers (fig. 9.7) are also responsible for the formation of extensive peat swamps and the subsequent maturation and formation of coal fields, where detrital input should not surpass accumulation of organic materials. Topographic highs of the volcanic domes could also have kept the rivers away from the area.

Large scale marine transgression was the hallmark of the New Zealand continent during the Late Cretaceous – Eocene periods. The transgression is inferred to have resulted from increased subsidence induced by the beginning of sea floor spreading between New Zealand and Australia and Antarctica (Raine et al. 1981). Schioler et al. (2002) interpreted that the transgression did not take place smoothly but came in pulses separated by minor regressions, each regression culminating in the development of an unconformity sequence boundary based on lithological and/or palynological evidence. Schioler et al. (2002) suggested that regional tectonics rather than eustasy controlled the East Coast Basin.

9.5 Provenance

Source rock composition, climate, relief, slope, vegetation and characteristics of the depositional environment all play important roles in controlling the composition of fluvial sands (Blatt 1967). The crystal size especially for quartz is significant as it marks source areas with significant amounts of quartz and large grain sizes. Plutonic, metamorphic and volcanic source areas would have provided grains of significant size.

9.5.2 Provenance of the Broken River Formation

Provenance of the Monro Conglomerate and Broken River Formations indicate local sources for the larger grain sizes such as the basal conglomerates and a mixture of local and more distal sources for the fine-medium and coarse sandstones.

The clasts in the Monro Conglomerate of Malvern and the Broken River Formation's basal conglomerates are completely derived from local sources. The former is composed predominantly of rhyolite clasts and the latter composed of very fine grained metasedimentary greywacke clasts and volcanic, trachytic and syeno-microsyenite clasts which are limited in extent and occur in certain localities such as Castle Hill, Avoca and the Mandamus area. Furthermore, the clast composition includes sandstone clasts and minor quartz pebbles, chert - clasts and altered basic/intermediate volcanic clasts. The composition reflects relatively local or proximal sources. These deposits are debris flow and predominantly fluvial with their transport distance often limited in extent when compared with transport of fine grained sediments such as sands and silts.

The most likely sources for the Monro Conglomerate and Broken River Formation conglomerates are local source rocks such as the Mount Somers Volcanics Group – Mandamus Igneous Complex for the volcanic and hypabyssal clasts. The source area for the Torlesse fine grained, greywacke clasts and for minor sedimentary lithics in arenites are most likely the Rakaia Terrane for the locations where Broken River Formation directly overlies Rakaia Terrane basement from North Otago to North Canterbury, while the source area for the greywacke clasts of the Broken River Formation at Mandamus may be the underlying Pahau sub-terrane. A distal metamorphic schistose source area such as the Haast-Otago Schist-Alpine Schist can account for the more durable quartz pebbles. In addition the mudstone and sandstone clasts are most likely penecontemporaneous.

The Broken River Formation marks a transition from relatively local sources for the basal conglomerates to predominantly distal sources for the upper Broken River and Iron Creek Formations. The sandstones of the Broken River Formation are dominantly subarkose and minor arkose arenites indicating a craton interior setting to a transitional continental tectonic setting (fig. 9.8).

The Broken River Formation is the second oldest sedimentary unit after the Monro Conglomerate overlying Rakaia and Pahau Terranes of the Torlesse Superterrane. Field and Brown (1989) argued that recycling from Torlesse appeared to be likely since heavy mineral assemblages of the Cretaceous – Tertiary rocks indicate Torlesse or Haast Schist sources in most areas. However if these terranes were potential source areas, the resulting sands eroded or weathered would have been smaller in grain size relative to the dominant population of the Broken River Formation. According to Smale (1990), most Cretaceous and Cenozoic sediments reflect derivation from local basement rocks, chiefly granitoids of the Karamea and Golden Bay terranes and older Maitai terranes. Post – mid Cretaceous volcanics have also contributed new material to the basins in Canterbury and east Otago.

Van der Lingen (1988) first presented the possibility of more distal sources for the Broken River Formation at the Mount Somers area based on the abundance of volcanic quartz in the non marine sediments changing to nonvolcanic quartz grains in the marine sediments derived from the Otago Schist to the south via longshore drift. In exploring further that argument Bernet and Bassett (2003) presented evidence of a mixed provenance of quartz based on SEM-CL/optical microscopy; whereas the Mount Somers Volcanics accounted for half of the volcanic quartz while 20 and 30% where attributed to the metamorphic and plutonic sources respectively.

Based on SEM-CL/optical data presented in this research, it is interpreted that from mid to north Canterbury for the Broken River Formation the quartz reflects a bimodal quartz composition of metamorphic versus plutonic quartz with the metamorphic quartz being the dominant source. Most samples plot in the metamorphic source terrane such as the Mandamus, Waipara, Castle Hill and Avoca while other areas that occur closer to local volcanic sources such as Malvern and Mount Somers plot in the mixed provenance areas (figs. 9.9, 9.10).

The dominant plutonic quartz types and minor coarse plutonic lithics of holocrystalline alkali feldspar and quartz through out the succession of the Broken River Formation are most likely attributed to sources large in volume which would produce enough plutonic quartz for the deposits. The feldspar components dominated by alkali feldspar and minor plagioclase also suggest plutonic and/or felsic igneous sources. Therefore a provenance area such as the Western Province plutonic suites is likely for the alkali feldspar and quartz content. The plutonic quartz grains with healed microcracks have dominantly weak to non undulose extinction with occasional strong undulose extinction are interpreted as derived from the large granitic and granodioritic batholiths of the Western Province and/or Fiorldland (Karamea Batholith – Separation Point Batholith).

The most likely source terrane for the metamorphic quartz population in the Broken River Formation is the Haast – Alpine Schist terranes, while the presence of alkali-plagioclase feldspars is also possibly derived from those terranes. The monocrystalline metamorphic quartz grains with dark CL and weak-strong undulose extinction are interpreted as sourced from the low metamorphic grade Alpine Schist. The minor polycrystalline metamorphic quartz grains displaying crenulated, polyhedral and recrystallized quartz coupled with dark CL and strong undulose extinction are interpreted as sourced from a high grade metamorphic source such as the southern Haast Schist terrane. Other terranes are not possible to provide the source for the high grade metamorphic quartz, since they are fine grained. The minor very fine sedimentary lithics are interpreted as derived from the Torlesse Supergroup hence the only local influence for the Broken River Formation's subarkosic arenites.

Volcanic quartz component remains low except at Mount Somers for the Broken River Formation where the abundant rhyolite supplied quartz to the basin (figs 9.9, 9.10). The presence of minimal volcanic quartz in north and north-mid Canterbury suggests a minor volcanic provenance resulting from reworking of local to distal volcanic source areas. In most of mid to north Canterbury the grain size of volcanic quartz grains with zoning and/or homogeneous CL with straight extinction is fine. In contrast the Mount Somers area depicts a strong volcanic provenance indicative of derivation from the underlying Mount Somers Volcanic Group with fine- medium to coarse quartz crystals. The fine aphanitic volcanic lithics are minor and derived mainly from the local Mount Somers Volcanic Group and secondarily from the Mandamus Igneous Complex.

9.5.3 Provenance of the Iron Creek/Conway-Waipara Greensand Formations

The overlying Iron Creek/Conway-Waipara Greensand Formations display overall the same provenance of distal sources for the sandstones while minor conglomerates display a local source confined to Mount Somers area. Minor conglomeratic units in the Blondin Sand Member – Charteris Bay Sandstone at Mount Somers reflect local to distal sources with dominantly quartz pebbles and secondary basaltic-chert clasts indicative of a Haast-Schist/Otago Schist source and a Mount

Somers Volcanics Group source respectively or a Rakaia Terrane for the chert clasts. The sandstones are subarkosic- arkosic arenites (fig. 9.8).

The SEM-CL/optical petrography data presented in this research shows that from mid to north Canterbury for the Iron Creek Formations the quartz reflects a bimodal composition of metamorphic versus plutonic quartz with the metamorphic quartz being the dominant source. Most samples plot in the metamorphic source terrane such as at Mandamus, Waipara, Castle Hill and Avoca while other areas such as Malvern and Mount Somers plot in the mixed provenance areas (figs. 9.9, 9.10).

The plutonic quartz types combined with plutonic lithics and alkali feldspars indicate a large granitic source such as the large granitic and granodioritic batholiths of the Karamea – Separation Point Batholiths (Western Province and/or Fiordland).

The presence of low grade metamorphic quartz, monocrystalline with dark CL and weak-strong undulose extinction, is interpreted as sourced from the low metamorphic grade Alpine Schist. Metamorphic quartz with strong polygonization increases up section to dominantly polycrystalline metamorphic quartz grains displaying crenulated, polyhedral and recrystallized quartz coupled with dark CL and strong undulose extinction. These are interpreted as sourced from a high grade metamorphic source such as the southern Haast Schist Terrane, while alkali feldspars also indicate a similar provenance. However departures from this interpretation are possible if the monocrystalline low grade metamorphic quartz grains represent originally polycrystalline high grade metamorphic Haast Schist derived grains that have been broken due to transport. In detail the high grade metamorphic grains with polycrystallinity, are confined to the Charteris Bay Sandstone of the Iron Creek Formation and they are coarse to very coarse and well rounded.

Volcanic quartz remains low except at Mount Somers for the Blondin Sand Member – Charteris Bay Sandstone Member where the rhyolites were the main source (fig 9.9). The presence of minimal volcanic quartz in north and north-mid Canterbury suggests only a minor volcanic provenance influencing the formations in the study resulting from reworking of local to distal volcanic source areas. This is supported by the fine grain size of quartz with zoning and/or homogeneous CL and straight extinction. In contrast, the Mount Somers area depicts a strong volcanic provenance indicative of the underlying Mount Somers Volcanic Group with fine- medium to coarse quartz crystals. The fine aphanitic volcanic lithics are derived mainly from the local Mount Somers Volcanic Group and secondarily from the Mandamus Igneous Complex in the Mandamus Waipara Greensand.

Finally, the distribution of certain quartz types to grain size and angularity is not entirely consistent through out the formations. The Broken River Formation quartz types are predominantly angular reflecting transportation via rivers, while the Iron Creek and correlative Formations contain abundant well rounded, coarse, metamorphic quartz crystals indicative of transport via longshore drift and waves mixed with a finer angular grain size fraction. The grain size does not correlate with quartz type despite preliminary indications that it might do so from the sandstones of the Mandamus area.

9.5.4 Summary

All source types in turn point towards local provenance for conglomerates and distal provenance for sandstones.

Paleocurrents reflected minor fluvial influence with a transport direction for the Broken River Formation from a north - north/west source to the south-south east while paleocurrents for the Iron Creek associated formations reflected a bimodal pattern of paleoflow toward the north-north west and south-south east indicating longshore drift and wave action transporting sands. Paleocurrent directions coincide largely with the locations of source type areas during the Late Cretaceous – Paleocene/Late Paleocene –Eocene period (figs. 9.11, 9.12) for paleocurrents from the south, while paleocurrents from the north possibly reflect reactivation of surfaces by bidirectional longshore drift. In fact the tectonic setting and the plate reconstruction reflected largely juxtaposed terranes which, prior to the development of the present day Alpine fault during the Mid Cenozoic, formed north to northwest trending curvilinear belts (Bradshaw 1989).

The Western Province terranes were adjacent and were docked to the Eastern Province terranes further south at Fiordland which preceded separation from the Gondwana margin (Kimbrough et al. 1993, Bradshaw 1989, Muir et al. 1997).

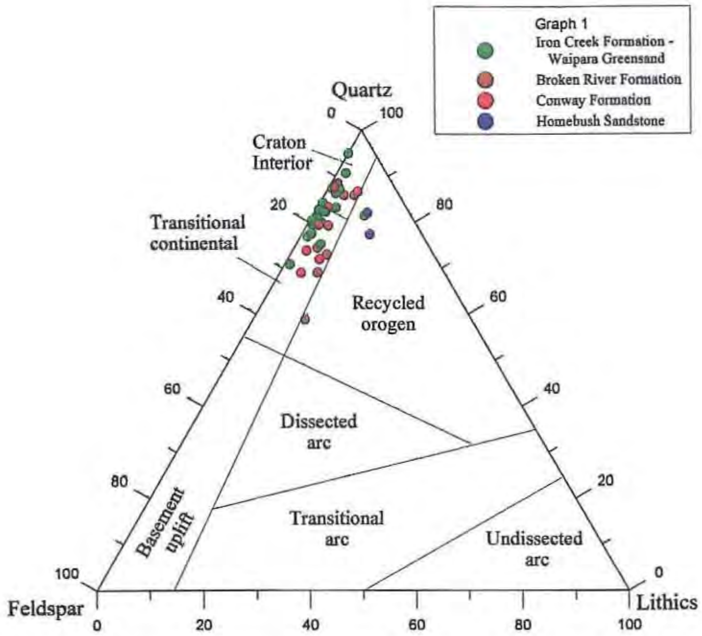

Figure 9.8: Tectonic setting discrimination diagram after Dickinson (1983), on the basis of normalized point counts, results from conventional point counts. Sample overview of all the formations studied, samples plot in the Craton Interior – Transitional continental field, except Homebush Sandstone which plots in the recycled orogen.

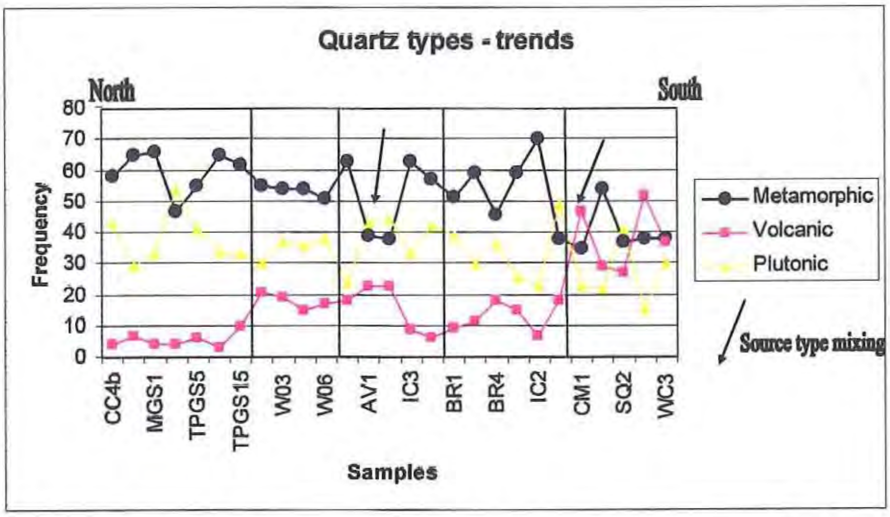

Figure 9.9: Composite frequency diagram displaying quartz grain per sample from the Mandamus area in the North to the Mount Somers in the South (from left to right). Dominant Metamorphic – Plutonic/ quartz type, bimodality through out most of Canterbury. Arrows depicting partial mixed provenance (first arrow on the left) at Avoca – Iron Creek and dominant mixed provenance at Mount Somers (arrow on the right). Samples of Broken River and Iron Creek Formations combined.

9.6 Quartz Enrichment, Chemical Weathering & Paleoclimate

The presence of quartz rich arenites in the Broken River and Iron Creek Formations combined with weathered rhyolites and kaolinites low in the succession at Mount Somers implies amplified chemical weathering; possibly due to a warmer/wetter climate and low relief.

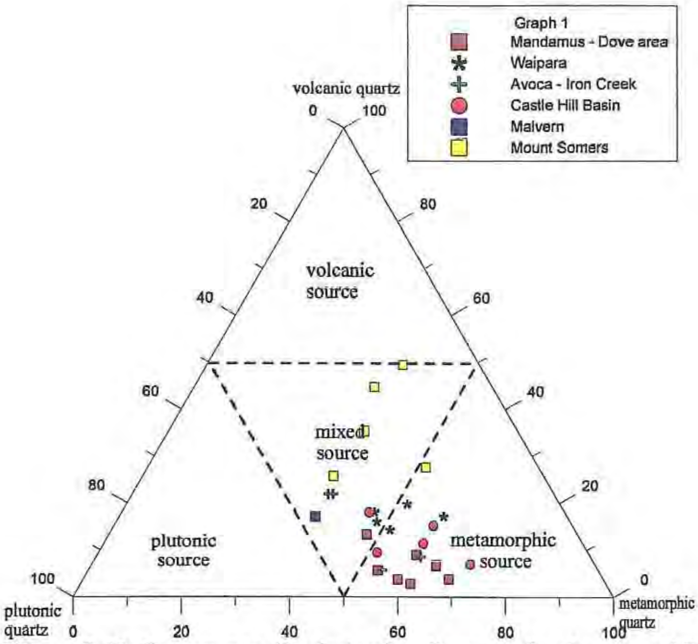

Figure 9.10: Provenance discrimination diagram after Bernet and Bassett (2005) of combined Broken River, Iron Creek Formations – Waipara Greensand, Conway Formation's samples. Samples using the three main quartz types of volcanic, plutonic and metamorphic quartz, based on SEM-CL/optical analysis. The dashed lines indicate the 50 percent lines of each off the three main types. Metamorphic quartz includes all low-grade to high-grade metamorphic recrystallized and vein quartz.

Chemical weathering may overprint the source rock signal substantially (Johnsson & Stallard 1989). In the case of chemical weathering as the cause of production of the subarkosic arenites, it is sufficient to remove significant amounts of lithics and breakdown feldspars on transport. The quartz-rich nature of the Broken River – Iron Creek/Waipara Formations reflects local to regional Cretaceous – Paleogene topographic maturity, with peneplanation and leaching (Field & Brown 1989).

Chemical breakdown of unstable lithic fragments and feldspars, plagioclase in particular, is the main factor for relative quartz enrichment, while mechanical destruction of non quartz components plays only a secondary role under tropical climatic conditions (Johnsson et al 1988). The dominance of chemical weathering is obvious in the Late Cretaceous succession, especially at Mount Somers with the kaolinized rhyolite and the overlying clays. Leaching-chemical weathering in combination with erosion from mechanical breakdown of source rocks could lead to the production of the Broken River Formation subarkosic arenites.

Johnsson (1990) who studied modern fluvial sands derived from volcanic arcs and plutons in the Andes proposed that sands exposed to chemical weathering for extended periods during alluvial storage are progressively enriched in stable mineral phases (quartz). With increased weathering, sands from continental terrains converge toward a supermature quartz arenite end member and the imprint left by source rock composition and tectonic setting is obscured (Johnsson 1990). The arenites of the Broken River Formation are relatively poor in sedimentary, volcanic and plutonic lithics. The presence of minor lithics does not reinforce or dismiss quartz enrichment from a previous lithic rich source. In fact most source areas proposed in this research are quartz rich. The subarkosic arenites of the Broken River Formation are largely texturally immature (angular) and compositionally mature (quartz rich) while the Iron Creek/Conway-Waipara Greensand Formations are texturally mature (well rounded) and compositionally mature (quartz rich). Enhanced Chemical weathering can create texturally immature but compositionally mature arenites.

Johnsson et al. (1988) describes that arenites of first cycle origin are texturally immature, and angular which form under intense chemical weathering and extended time provided by temporary storage of orogenically derived sediments on extensive alluvial plains. According to Johnsson et al. (1988) these sandstones become more texturally mature (rounded) as they reach low lying alluvial plains. In addition Johnsson (1990) discussed how the ratio of unstable monomineralic components such as magnetite, amphibole, and pyroxene decreased to more stable monomineralic components (quartz, feldspar) as rivers cross the alluvial plains.

The subarkosic – arkosic arenites of the all the formations reflect largely distal source areas, while there are no indications such as the presence of quartz overgrowths that sediment recycling has taken place.

In recent studies Yang et al (2004) indicated that loess that been subjected to chemical weathering left its imprint on elemental compositions reflecting paleoclimate control. Chemical weathering indices produced thicker paleosol layers during summer monsoons than winter monsoons in China during the Quaternary, thus reflecting a strong link between warm climate and chemical weathering (Yang et al. 2004). Furthermore, temperature is not the only mechanism that controls chemical weathering (Dupre et al. 2003). Other parameters, like nature and age of the soils, mineralogy and chemistry of source rock and runoff play an important role (Dupre et al. 2003).

The dominant composition of the Broken River Formation/Iron Creek-Conway-Waipara Greensand Formations as subarkosic retains a significant amount of feldspar which was not all reduced by chemical weathering. Thus the arenites do partially reflect their source rock areas but are highly quartz enriched.

The effect of climate as well as the low relief with low sedimentation rate could have amplified chemical weathering and quartz enrichment in the formations studied. Hornibrook (1971) interprets cool temperate conditions of the Cretaceous giving way to warm temperate – subtropical conditions in the Paleocene based on faunal data. Crouch and Brinkhuis (2005) presented data in which fluctuations in dinocyst-dinoflagellates assemblages coincided with intense warmth and excess carbon of the Initial Eocene Thermal Maximum (IETM) in sea water temperatures while terrestrial vegetation such as mangroves possibly showed a response to the IETM after the Paleocene. Coastal mangroves during the Eocene reflected mean annual temperatures of 20 – 24 C (Pocknall 1990).

Therefore a combination of low relief and low sedimentation rate plus the importance of a warm climate during the Late Paleocene –Eocene were likely major contributors to chemical weathering of source rock areas in the South Island creating quartz rich deposits.

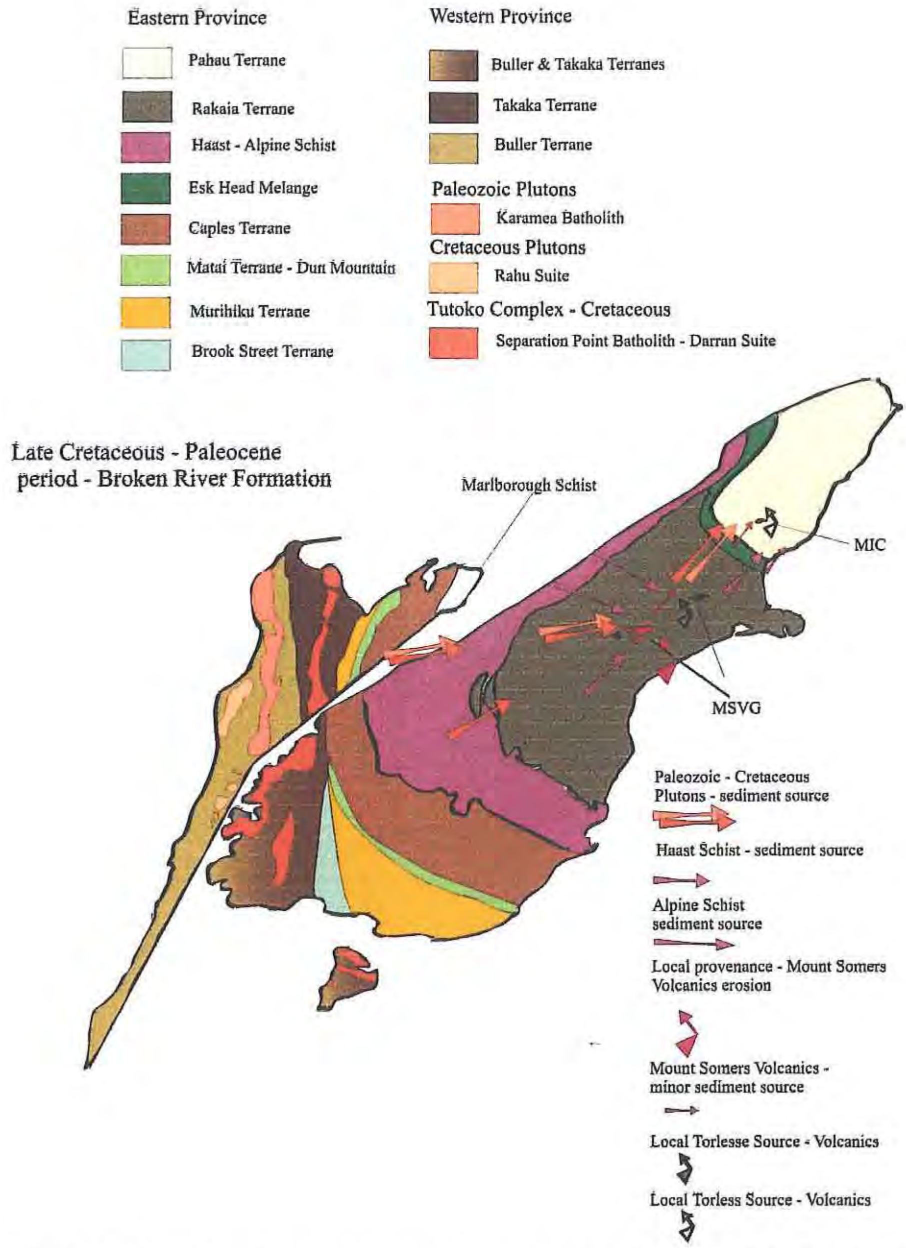

Figure 9.11: Configuration – Paleotectonic reconstruction of the South Island during the Late Cretaceous – Paleocene before inception of the Alpine Fault (reproduced from Landis & Coombs 1967, Bradshaw et al. 1980, Muir et al. 1995, Bradshaw pers. Comm.. 2005). Sediment sources modified from Bernet and Bassett (2003), interpretations from this research. MSVG: Mount Somers Volcanics Group, MIC: Mandamus Igneous Complex. Metamorphic quartz was predominantly low grade and sourced from the Alpine Schist during this period.

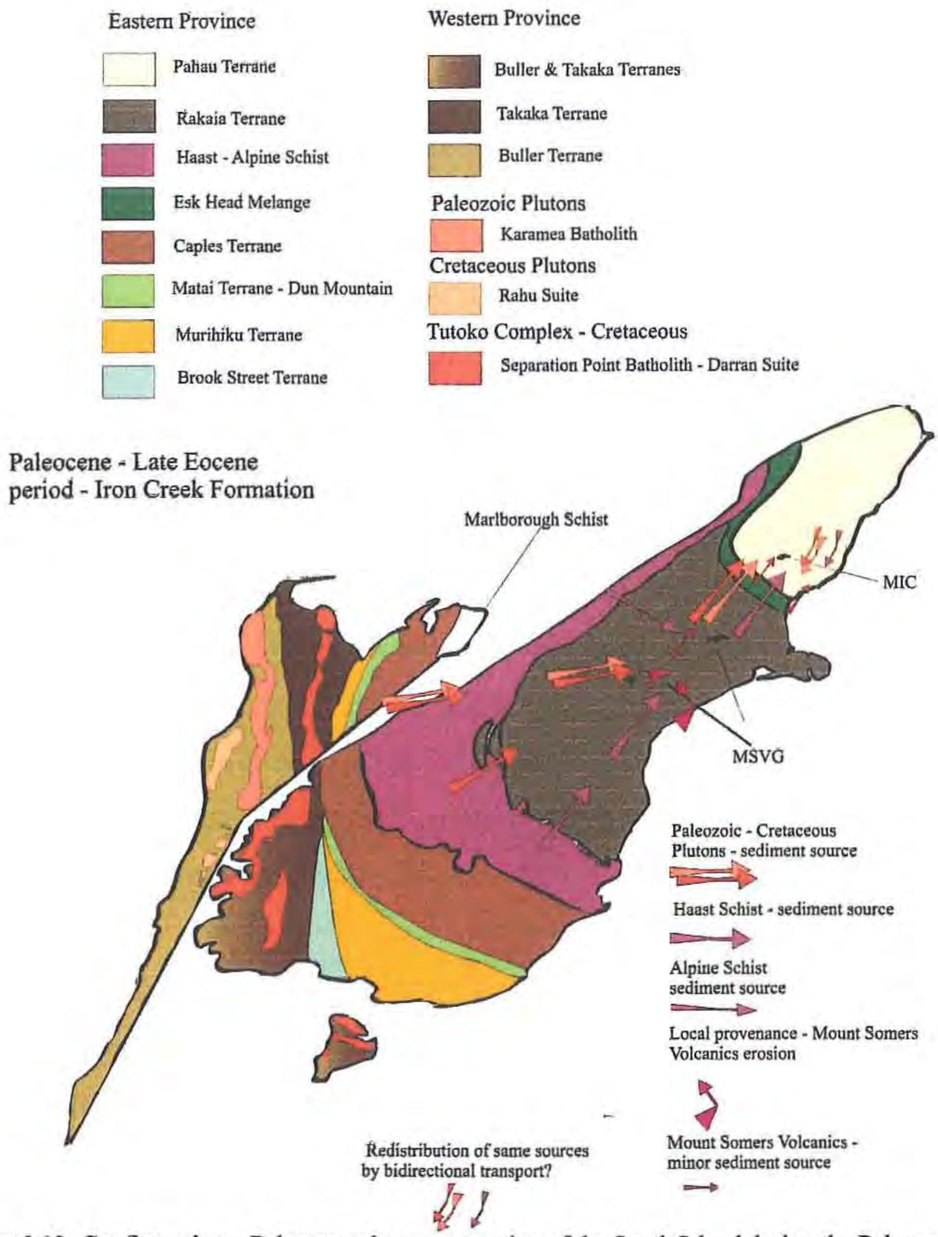

Figure 9.12: Configuration – Paleotectonic reconstruction of the South Island during the Paleocene – Late Eocene before inception of the Alpine Fault (reproduced from Landis & Coombs 1967, Bradshaw et al. 1980, Muir et al. 1995, Bradshaw pers. Comm. 2005). Sediment sources modified from Bernet and Bassett (in review), interpretations from this research. MSVG: Mount Somers Volcanics Group, MIC: Mandamus Igneous Complex. Increased high grade metamorphic quartz was dominantly sourced from the Haast Schist during this period.

9.7 Summary

The correlative coal measures – carbonaceous, quartz rich sandstones of the Broken River Formation and the glauconitic quartz rich – greensands of the Iron Creek/Conway-Waipara Greensand Formations reflect a fluvio-deltaic marginal marine to marine lower shoreface-foreshore to shelf depositional environment. It is characterized by the onset of the marine transgression during the Late Cretaceous – Eocene while relief was being reduced during peneplanation and transgression reflecting relative low basement highs separating areas within the Canterbury Basin. Deposition within the basement was characterized by low sedimentation rate based on coal measure formation and glauconite content and morphology/type (irregular/nascent, fibroradiated rims – well rounded mature/evolved) indicating autochthonous-parautochthonous glauconite formation and low to medium sedimentation rate.

Intense chemical weathering responded to a warm-tropical climate during the Paleocene-Eocene thus eroding and producing quartz rich successions. The production of coarse conglomeratic deposits reflected localized derivation while the sandstones reflected predominant distal derivation. In addition the sandstones did not display any evidence suggesting recycling such as abundant quartz overgrowths, therefore the successions are most likely first cycle.

The sandstones of the Broken River Formation and Iron Creek Formation/correlative formations show a bimodal metamorphic to plutonic quartz type for all the formations with minor volcanic quartz, while abundant predominant volcanic quartz and mixing of all sources occurred at Mount Somers. The distribution of certain quartz types to grain size and angularity is not entirely consistent through out the formations. The Broken River Formation quartz types are predominantly angular reflecting transportation via rivers, while the Iron Creek and correlative Formations contain abundant well rounded, coarse, metamorphic quartz crystals indicative of transport via longshore drift and waves mixed with a finer angular grain size fraction. The grain size does not correlate with quartz type despite preliminary indications that it might do so from the sandstones of the Mandamus area.

The tectonic setting and the juxtaposition of those source areas provided the detritus from local and distal terranes for the Broken River Formation during the Late Cretaceous and for the Iron Creek Formation during the Paleocene - Eocene from Western Province and the south – Eastern Province with local reworking from the Late Cretaceous Mount Somers Volcanic Group (figs. 9.11, 9.12). The dominant sources for the basal Broken River Formation conglomerates were the Pahau and Rakaia Terranes and the Mandamus Igneous Complex. For the upper sandstones of the Broken River – Iron Creek Formations the Haast-Alpine Schist, Karamea Batholith – Separation Point Batholith and the Mount Somers Volcanics Group were the main sources.

Acknowledgements

A great deal of appreciation and gratitude goes to my supervisor Dr Kari Bassett for constantly probing me to deliver consistent science and always having answers to my questions. Thank you for the hours spent on helping with this research.

Thank you to my associate supervisor, Professor John Bradshaw for answering questions concerning New Zealand geology and plate tectonic reconstructions. I wish to thank Dr. Anekant Wandres for assistance in occasional petrographic thin sections.

Thank you to all technicians for the time and endless patience. Thanks Rob Spiers, for producing excellent petrographic thin sections to work with. I am thankful to Neil Andrews from the department of Plant and Microbial Studies, University of Canterbury for his help and kind nature with using the scanning electron microscope.

Thanks to Dr. Kerry Swanson for repairing microscopes and for assisting with photomicrographs.

Thanks to the Mason Trust for providing financial assistance with some aspects of this research.

Thanks to Garry Webb at Mount Somers for permission to enter the Silica Sand Quarry and Woolshed Creek. Thanks also to the unknown tour bus driver for towing the van out of Slovens Stream.

Very big thanks to my parents, Kiriakos and Jenny for providing support during my studies.

Thanks to Carl, Ronel, Alexis, Sav for entertaining me. A great deal of appreciation goes to fieldman Pirvine for assisting in fieldwork and engaging in useless but entertaining discussions. A great deal of respect to Tom Green, you know who you are!

REFERENCES

Adams, C. J., and Graham, I.J., 1997, Age of metamorphism of Otago Schist in eastern Otago and determination of protoliths from initial strontium isotope characteristics: New Zealand Journ. Geol. and Geophysics, v. 40, p. 275-286.

Amorosi, A., 1997, Detecting compositional, spatial, and temporal attributes of glaucony: a tool for provenance research: Sedimentary Geology, v. 109, p. 135-153.

Andrews, P. B., Field, B.D., Browne, G.H., McLennan, J.M., 1987, Lithostratigraphic nomeclature for the Upper Cretaceous and Tertiary sequence of central Canterbury, New Zealand: New Zealand Geological Survey record, v. 24, p. 518.

Basu, A., Young, S.W., Suttner, L.J., James, W.C., Mack, G.H., 1975, Re-evaluation of the use of undulatory extinction and polycrystallinity in detrital quartz for provenance interpretation: Journal of Sedimentary Petrology, v. 45, p. 873-882.

Bernet, M., and Bassett, K., 2003, Provenance of Mount Somers quartz arenites; combined SEM-CL and optical microscopy analysis: Geological Society of America-Abstracts with programs, v. 35, p. 391.

Bernet, M., and Bassett, K., 2005, Provenance analysis by single-quartz grain SEM-CL/Optical microscopy: Journal of Sedimentary Research, v. 75, p. 492-500.

Bishop, D. G., Bradshaw, J.D., Haudis, C.A., 1985, Provisional terrane map of South Island, New Zealand, *in* Howel, D. G., ed., Tectonostratigraphic terranes of the circum Pacific region. Earth Science Series: Houston, Circum Pacific council for minerals and energy, Houston Texas, p. 515-521.

Blatt, H., 1967, Provenance determinations and recycling of sediments: Journal of Sedimentary Petrology, v. 37, p. 1031-1044.

Blatt, H., and Christie, J.M., 1963, Undulatory extinction in quartz of igneous and metamorphic rocks and its significance in provenance studies of sedimentary rocks: Journal of Sedimentary Petrology, v. 33, p. 559-579.

Boggs, S. J., 1992, Petrology of sedimentary rocks: New York, Macmillan, 707 p.

Boggs, S. J., 2001, Principles of sedimentology and stratigraphy: New York, Prentice Hall, 726 p.

Boggs, S. J., Kwon, Y.I., Goles, G.G., Rusk, B.G., Krinsley, D., Seyedolali, A., 2002, Is quartz cathodoluminescence color a reliable provenance tool? A quantitative examination: Journal of Sedimentary Research, v. 72, p. 408-415.

Bradshaw, J. D., 1975, The folds at Castle Hill (Canterbury) and their bearing on Kaikouran deformation style in the Canterbury Basin: Jour. Royal Soc. N.Z, v. 5, p. 209-217.

Bradshaw, J. D., 1989, Cretaceous Geotectonics of the New Zealand Region: Tectonics, v. 8, p. 803-820.

Breed, W. J., 1960, Pleistocene terraces of Castle Hill Basin.: Unpub. M.Sc. thesis, University of Arizona.

Brooks, R. R., Hoek, P.L., Reeves, R.D., Strong, C.P., 1986, Geochemical delineation of the Cretaceous/Tertiary boundary in some New Zealand rock sequences: New Zealand Journ. Geol. and Geophysics, v. 29, p. 1-8.

Brown, G. H., and Field, D.D., 1985, The lithostratigraphy of Late Cretaceous to Early Pleistocene rocks of northern Cantrebury, New Zealand: New Zealand Geological Survey record, v. 6, p. 63.

Chafetz, H. S., and Reid, A., 2000, Syndepositional shallow-water precipitaion of glauconitic minerals: Sedimentary Geology, v. 136, p. 29 - 42.

Coates, J. W., 1975, Textural and heavy mineral analysis of the white quartz sands of the Coleridge Formation, Broken River, University of Canterbury.

Congdon, L. M., 2003, Basin analysis of the Porter Group, Castle Hill Basin, Canterbury, University of Canterbury, 197 p.

Coombs, D. S., Landis, C.A., Norris, R.J., Sinton, J.M., Borns, D.J., Craw, D., 1976, The Dun Mountain ophiolite belt, New Zealand, its tectonic setting, constitution, and origin, with special reference to the southern portion: American Journal of Science, v. 276, p. 561-603.

Crouch, E. M., and Brinkhuis, H., 2005, Environmental change across the Paleocene-Eocene transition from eastern New Zealand: A marine palynological approach: Marine Micropaleontology, v. 56, p. 138-160.

Dickinson, W. R., Beard, L.S., Brakenridge, G.R., Erlavec, J.L., Ferguson, R.C., Inman, K.F., Knepp, R.A., Lindberg, F.A., Ryberg, P.T., 1983, Provenance of North American Phanerozoic sandstones in relation to tectonic setting: Geological Society of America Bulletin, v. 94, p. 222-235.

Diessel, C., Boyd, R., Wadsworth, J., Leckie, D., Chalmers, G., 2000, On balanced and unbalanced accommodation/peat accumulation ratios in the Cretaceous coals from Gates Formation, Western Canada, and their sequence-stratigraphic significance: International Journal of Coal Geology, v. 43, p. 143-186.

D'Lemos, R. S., Kearsley, A.T., Pembrooke, J.W., Watt, G.R., Wright, P., 1997, Complex quartz growth histories in granite revealed by scanning cathodoluminescence techniques: Geological Magazine, v. 134, p. 549-552.

Dupre, B., Dessert, C., Oliva, P., Godderis, Y., Viers, J., Francois, L., Millot, R., Gaillardet, J.,, 2003, River, chemical weathering and Earth's climate: Comptes Rendus Geosciences, v. 335, p. 1141-1160.

Einsele, G., 2000, Sedimentary basins: Evolution, facies and sediment budget: Berlin, Springer, 354 p.

Ettmuller, F., 2003, The integrated CL method and the Paparoa Trough: A new approach to provenance analysis, University of Canterbury, 61 p.

Field, B. D., 1989a, Cathodoluminescence of quartz in paleozoic to mesozoic basement rocks and cretaceous-cenozoic sedimentary rocks, Canterbury and North Otago, New Zealand, New Zealand Geological Survey report SL; 21, New Zealand Geological Survey, p. 11.

Field, B. D., and Browne, G.H., 1989b, Cretaceous and Cenozoic sedimentary basins and geological evolution of the Canterbury Region, South Island, New Zealand, New Zealand Geological Survey Basin Studies 2: Lower Hutt, New Zealand Geological Survey.

Folk, R. L., Andrews, P.B., Lewis, D.W., 1970, Detrital sedimentary rock classification and nomeclature for use in New Zealand: New Zealand Journ. Geol. and Geophysics, v. 13, p. 937-968.

Fordyce, R. E., Jones, C.M., Field, B.D., 1986, The world's oldest penguin?: Geological Society of New Zealand newsletter, v. 74, p. 56-57.

Forster, M. A., and Lister, G.S., 2003, Cretaceous metamorphic core complexes in the Otago Schist, New Zealand: Australian Journal of Earth Sciences, v. 50, p. 181-198.

Gage, M., 1957, The geology of Waitaki subdivision: New Zealand Geological Survey bulletin, v. 55, p. 135.

Gage, M., 1970(a), Late Cretaceous and Tertiary rocks of Broken River, Canterbury: New Zealand Journ. Geol. and Geophysics, v. 13, p. 507-559.

Garlick, G. F. I., 1966, Cathodo- and radioluminescence, *in* Goldberg, P. G., ed., Luminescence of inorganic solids: New York, USA, Academic Press, p. 685-731.

Gotze, J., Plotze, M., Haberman, D., 2001, Origin, spectral characteristics and practical applications of the cathodoluminescence (CL) of quartz-a review: Mineralogy and Petrology, v. 71, p. 225-250.

Gregg, D. R., 1964, Sheet 18 Hurunui; Geological Map of New Zealand 1:250,000, N.Z. Dept. Scientific and Industrial Research, New Zealand.

Gregg, D. R., 1978, Stratigraphy of the lower Waipara Gorge, North Canterbury. New Zealand: New Zealand Journ. Geol. and Geophysics, v. 2, p. 501 - 527.

Grindley, G. W., 1963, Structure of the Alpine Schists of south Westland, Southern Alps, New Zealand: New Zealand Journ. Geol. and Geophysics, v. 6, p. 872-930.

Haast, J., 1870, Notes on a collection of Saurian remains from the Waipara River, Canterbury in the possession of J.H Cockburn Hood, Esq: Transactions of the New Zealand Institute, v. 2, p. 186-189.

Haast, J., 1871, On the Geology of the Waipara District, Canterbury; with Geological Map and Sections: New Zealand Geological Survey report Geological Exploration 1870-71, v. 6, p. 5-19.

Haast, J., 1872, Report on the geology of the Malvern Hills: New Zealand Geological Survey report Geological Exploration 1871-72, p. 1-85.

Hollis, C. J., and Strong, C.P., 2003, Biostratigraphic review of the Cretaceous/Tertiary boundary transition, mid-Waipara River section, North Canterbury, New Zealand: New Zealand Journ. Geol. and Geophysics, v. 46, p. 243 - 253.

Hornibrook, N. d. B., 1971, New Zealand Tertiary climate, New Zealand Geological Survey report 47, New Zealand Geological Survey, p. 19.

Hutton, F. W., 1887, Geology of the Trelissick or Broken River Basin, Selwyn County: Transactions of the New Zealand Institute, v. 19, p. 392-412.

Hutton, F. W., 1894, On a new Plesiosaur from the Waipara River: Transactions of the New Zealand Institute, v. 6, p. 333-358.

Jobberns, G., 1937, The Lower Waipara Gorge: Transactions of the Royal Society of New Zealand, v. 67, p. 125 - 132.

Johnsson, M. J., 1990, Tectonic versus chemical-weathering controls on the composition of fluvial sands in tropical environments: Sedimentology, v. 37, p. 713-726.

Johnsson, M. J., and Stallard, R.F., 1989, Physiographic controls on the composition of sediments derived from volcanic and sedimentary terrains on Barro Colorado Island, Panama: Journal of Sedimentary Petrology, v. 59, p. 768-781.

Johnsson, M. J., Stallard, R.F., Meade, R.H., 1988, First cycle quartz arenites in the Orinoco River Basin, Venezuela and Colombia: Journal of Geology, v. 96, p. 263-277.

Kimbrough, D. L., Tulloch, A.J., Geary, E., Coombs, D.S., Landis, C.A., 1993, Isotopic ages from the Nelson region of South Island, New Zealand; crustal structure and definition of the Median Tectonic Zone: Tectonophysics, v. 225, p. 433-448.

Kwon, Y. I., and Boggs, S., 2002, Provenance interpretation of Tertiary sandstones from the Cheju Basin (NE East China Sea): a comparison of conventional petrographic and scanning cathodoluminescence techniques: Sedimentary Geology, v. 152, p. 29-43.

Leverenz, J. W., 1968, An introduction to luminescence of solids: New York, Dover.

Lewis, D. W., and McConchie, D.M., 1994, Analytical Sedimentology: New York, Chapman & Hall.

Marshall, D. J., 1988, Cathodoluminescence of geological materials: London, Unwin Hyman Ltd.

Mason, B., 1949, The geology of the Mandamus-Pahau District, North Canterbury: Transactions of the Royal Society of New Zealand, v. 77, p. 403-428.

Mathews, S. J., 1989, Geology of the Monro Conglomerate and Broken River Coal Measures at Malvern Hills, University of Canterbury, 174 p.

McBride, E. F., 1963, A classification of common sandstones: Journal of Sedimentary Petrology, v. 33, p. 664-669.

McConchie, D. M., and Lewis, D.W., 1978, Authigenic, perigenic, and allogenic glauconites from the Castle Hill Basin, North Canterbury, New Zealand: New Zealand Journ. Geol. and Geophysics, v. 21, p. 199 - 214.

McConchie, D. M., and Lewis, D.W., 1980, Varieties of glauconite in Late Cretaceous and Early Tertiary rocks of the South Island of New Zealand, and new proposals for classification: New Zealand Journ. Geol. and Geophysics, v. 23, p. 413 - 437.

MCLennan, J. M., 1981, The Cretaceous - Tertiary rocks of Avoca, Oxford and Burnt Hill, Central Canterbury, University of Canterbury, 234 p.

McLennan, J. M., and Bradshaw, J.D., 1984, Angular unconformity between Oligocene and older Cenozoic rocks at Avoca, Canterbury, New Zealand: New Zealand Journ. Geol. and Geophysics, v. 27, p. 299-303.

Milliken, K. L., 1994, Cathodoluminescent textures and the origin of quartz silt in Oligocence mudrocks, South Texas: Journal of Sedimentary Research, v. A64, p. 567-571.

Morgans, H. E. G., Jones, C.M., Crouch, E.M., Field, B.D., Hollis, C.J., Raine, J.I., Strong, C.P., Wilson, G.J., 2005, Upper Cretaceous to Eocene stratigraphy and sample collections, mid-Waipara River section, North Canterbury, Institute of Geological and Nuclear Sciences science report 2003/08: Lower Hutt, Institute of Geological & Nuclear Sciences, p. 101.

Moss, A. J., 1972, Initial fluviatile fragmentation of granitic quartz: Journal of Sedimentary Petrology, v. 42, p. 725 - 728.

Muir, R. J., Ireland, T.R., Weaver, S.D., Bradshaw, J.D., Evans, J.A. Eby, G.N., Shelley, D., 1998, Geochronology and geochemistry of a Mesozoic magmatic arc system, Fiordland, New Zealand: Journal of the Geological Society, London, v. 155, p. 1037-1053.

Muir, R. J., Weaver, S.D., Bradshaw, J.D., Eby, G.N., Evans, J.A., 1995, The Cretaceous Separation Point Batholith, New Zealand: granitoid magmas formed by melting of mafic lithosphere: Journal of the Geological Society, London, v. 152, p. 689-701.

Muir, R. J., Weaver, S.D., Bradshaw, J.D., Eby, G.N., Evans, J.A., Ireland, T.R., 1996, Geochemistry of the Karamea Batholith, New Zealand and comparisons with the Lachlan Fold Belt granites of SE Australia: Lithos, v. 39, p. 1-20.

Nicol, A., 1993, Haumurian (c66-80 Ma) half-graben development and deformation, mid-Waipara, North Canterbury, New Zealand: New Zealand Journ. Geol. and Geophysics, v. 36, p. 127 - 130.

Odin, G. S., and Fullagar, P.D., 1988, Geological significance of the glaucony facies, *in* Odin, G. S., ed., Green Marine Clays: Oolitic ironstone facies, verdine facies, glaucony facies and celadonite -bearing facies - a comparative study. Developments in sedimentology 45: New York, Elsevier.

Odin, G. S., and Matter, A., 1981, De glauconiarum origine: Sedimentlogy, v. 28, p. 611-641.

Oliver, P. J., 1977, Mesozoic geology of the Mt. Somers area, Canterbury, University of Canterbury.

Oliver, P. J., 1979, Structure and tectonic history of the Mesozoic rocks of the foothills of the southern Alps in mid Canterbury: Royal Society New Zealand Bulletin, v. 18, p. 105 - 111.

Oliver, P. J., and Keene, H.W., 1989, Sheet K36AC and part Sheet K35, Mt Somers, Geological map of New Zealand 1:50,000 (1 sheet) and notes: New Zealand Geological Survey.

Pagel, M., Barbin, V., Blanc, P., Ohnenstetter, D., 2000, Cathodoluminescence in Geosciences: An introduction, *in* Pagel, M., Barbin, V., Blanc, P., Ohnenstetter, D., ed., Cathodoluminescence in Geosciences: Berlin, Springer, Verlag.

Park, J., 1888, On the Geology of Waipara and Weka Pass Districts.: New Zealand Geological Survey report Geological Exploration 1887-88, v. 19, p. 25-35.

Pasquini, C., Lualdi, A., Vercesi, P., 2004, Depositional dynamics of glaucony-rich deposits in the Lower Cretaceous of the Nice arc, southeast France: Cretaceous Research, v. 25, p. 179 -189.

Passchier, C. W., and Trouw, R.A.J., 1996, Microtectonics: Berlin, Springer - Verlag, 289 p.

Pocknall, D. T., 1990, Palynological evidence for the early to middle Eocene vegetation and climate history of New Zealand: Review of Paleobotany and Palynology, v. 65, p. 57-69.

Prothero, D. R., and Schwab, F., 1999, Sedimentary Geology: An introduction to sedimentary rocks and stratigraphy: New York, W.H. Freeman and Company.

Raine, J. I., Speden, I.G., Strong, C.P., 1981, Aspects of Mid-Cretaceous regional geology, New Zealand: London, Academic Press, London, United Kingdom, p. 221-267.

Reed, R. M., and Milliken, K.L, 2003a, How to overcome imaging problems associated with carbonate minerals on SEM-based Cathodoluminescence systems: Journal of Sedimentary Research, v. 73, p. 328-332.

Reed, R. M., and Milliken, K.L, 2003b, SEM-based cathodoluminescence imaging in sandstone provenance analysis, quartz and feldspar grains, zircons, and siliceous rock fragments: Geological Society of America-Abstracts with programs, v. 35, p. 391.

Roncaglia, L., and Schioler, P., 1997, Dinoflagellate biostratigraphy of Piripauan-Haumurian sections in southern Marlborough and northern Canterbury, New Zealand, Institute of Geological and Nuclear Sciences science report 97/9: Lower Hutt, Institute of Geological and Nuclear Sciences, p. 48.

Schioler, P., Crampton, J.S., Laird, M.G., 2002, Palynofacies and sea-level changes in the middle Coniacan-late Campanian (Late Cretaceous) of the East Coast Basin, New Zealand: Palaeogeography, Palaeoclimatology, Palaeoecology, v. 188, p. 101-125.

Sevon, W. D., 1969, Stratigraphy and sedimentology of the Tertiary rocks of the Mandamus-Dove River area, North Canterbury, New Zealand: New Zealand Journ. Geol. and Geophysics, v. 12, p. 429.

Seyedolali, A., Krinsley, D.H., Boggs Jr. S., O'Hara, P.F., Dypvik, H., Goles, G.G.,, 1997, Provenance interpretation of quartz by scanning electron microscope-cathodoluminescence fabric analysis:: Geology, v. 25, p. 787-790.

Shelley, D., 1975, Metamoprhic belt and volcanic arc migration in New Zealand: Nature, v. 258, p. 668-672.

Shelley, D., 1985, Optical Mineralogy: New York, Elsevier, 321 p.

Shelley, D., 1993, Igneous and Metamorphic rocks under the microscope: Classification, textures, microstructures and mineral preferred-orientations: London, Chapman & Hall.

Silberling, N. J., Nichols, K.M., Bradshaw, J.C., Blome, C.D., 1988, Limestone and chert in tectonic blocks from the Esk Head subterrane, South Island, New Zealand: Geological Society of America Bulletin, v. 100, p. 1213-1223.

Sippel, R. F., 1968, Sandstone petrology, evidence from luminescence petrography: Journal of Sedimentary Petrology, v. 38, p. 530-554.

Smale, D., 1990, Distribution and provenance of heavy minerals in the South Island; a review: New Zealand Journ. Geol. and Geophysics, v. 33, p. 557-571.

Speight, R., 1920, The geologic features of the Broken River coal area: New Zealand journ. Sci. Tech., v. 3, p. 93-104.

Speight, R., 1938, The geology of the Mt. Somers district: New Zealand Geological Survey Memoir, v. 3, p. 116.

Sprunt, E. S., and Nur, A., 1979, Microcracking and healing in granites: New evidence from cathodoluminescence: Science, v. 205, p. 495-497.

Tappenden, V. E., 2003, Magmatic response to the evolving New Zealand margin of Gondwana during the mid-late Cretaceous: Unpub. Phd thesis, University of Canterbury, 261 p.

Thompson, J. A., 1920, The Notocene Geology of the Middle Waipara and Weka Pass District, North Canterbury, New Zealand: Transactions of the New Zealand Institute, v. 52, p. 322-415.

Triplehorn, D. M., 1966, Morphology, internal structure, and origin of glauconite pellets: Sedimentology, v. 6, p. 247-266.

van der Lingen, G. J., 1988, Lower Tertiary transgressive sediments of the Broken River Formation, Mt Somers area, Canterbury, New Zealand: New Zealand Journ. Geol. and Geophysics, v. 31, p. 287 - 304.

Wandres, A. M., and Bradshaw, J.D., 2005, New Zealand tectonostratigraphy and implications from conglomeratic rocks for the configuration of the SW Pacific margin of Gondwana, *in* Vaugham, A. P. M., Leat, P.T., Pankhurst, R.J., ed., Terrane Processes at the margins of Gondwana., 246. Geological Society, London, Special Publications, p. 179-216.

Wandres, A. M., Bradshaw, J.D., Weaver, S., Maas, R., Ireland, T., Eby, N.,, 2004(a), Provenance analysis using conglomerate clast lithologies; a case study from the Pahau Terrane of New Zealand: Sedimentary Geology, v. 167, p. 57-89.

Wandres, A. M., Bradshaw, J.D., Weaver, S., Maas, R., Ireland, T., Eby, N.,, 2004(b), Provenance of the sedimentary Rakaia sub-terrane, Torlesse Terrane, South Island, New Zealand; the use of igneous clast compositions to define the source: Sedimentary Geology, v. 168, p. 193-226.

Warren, G., and Speden, I., 1978, The Piripuan and Haumurian Stratotypes (Mata Series, Upper Cretaceous) and correlative sequences in the Haumuri Bluff District, South Marlborough: New Zealand Geological Survey bulletin, v. 92, p. 60.

Weaver, S. D., Pankhurst, R.J., 1991, A precise Rb-Sr age for the Mandamus Igneous Complex, North Canterbury, and regional tectonic implications: New Zealand Journ. Geol. and Geophysics, v. 34, p. 341-345.

Webb, P. N., 1971, New Zealand Late Cretaceous (Haumurian) foraminifera and stratigraphy: a summary: New Zealand Journ. Geol. and Geophysics, v. 14, p. 795-828.

Wilson, D. D., 1963, Geology of the Waipara subdivision (Amberley and Motunau Sheets, S68 and S69): New Zealand Geological Survey bulletin, v. 64, p. 124.

Winkler, H. G., 1974, Petrogenesis of Metamorphic rocks: New York, Springer - Verlag, 320 p.

Wopereis, P., 1975, The basic dikes of Castle Hill Basin and the Avoca area, University of Canterbury, 46 p.

Yang, S. Y., Li, C.X., Yang, D.Y., Li, X.S., 2003, Chemical weathering of the loess deposits in the lower Changjiang Valley, China, and paleoclimatic implications: Quaternary International, v. 117, p. 27-34.

Young, S. T., 1976, Petrographic textures of detrital polycrystalline quartz as an aid to interpreting crystalline source rocks: Journal of Sedimentary Petrology, v. 46, p. 595-603.

Zinkernagel, U., 1978, Cathodoluminescence of quartz and its application to sandstone petrology, *in* Fuechtbauer, H., Lisitzyn, A.P., Milliman, J.D., Seibold, K., ed., Contributions to sedimentology: Stuttgart, E. Schweizerbart'sche Verlagsbuchhandlung, p. 1-67.

APPENDIX 1
HAND SPECIMEN DESCRIPTION

Sample	Location	Hand Specimen Description
tpgs-1 Island Hills	Mandamus	Tan, grey, massive, moderately indurated, fine sand, subangular to subrounded, moderately sorted, glauconite 10-15%, calcite matrix, calcareous glauconitic sandstone. Subarkose arenite.
-5	Mandamus	White-grey, massive, friable sand, grain size: Max. coarse, Min. medium, mode(s) medium sand. Subangular to subrounded, poorly sorted, disarticulated shells, scaphopods-tusk shells, calcite matrix. Calcareous glauconitic sandstone. Subarkose arenite
-8	Mandamus	Green-cream, very well indurated, massive, Grain size: Max. v. coarse sand, Min. coarse, Mode(s) coarse, subrounded, poorly sorted, 25- 30% glauconite, calcareous glauconiticsandstone. Subarkose arenite
-9	Mandamus	Cream-white-green, moderate indurated, massive, grain size: max. coarse min. fine, mode(s) medium, subrounded-rounded, moderately sorted, 10-15% glauconite. Subarkose arenite
-11	Mandamus	Cream-grey, well indurated, grain size: max. coarse, min. fine, mode(s) medium sand, rounded – well rounded, poorly sorted, shellmaterial, glauconite 5%, Greensandstone. Subarkose arenite
-15	Mandamus	Cream-grey, grain size: max. medium, Min. very fine, mode(s) fine sand, Subangular to subrounded. Greensandstone. Subarkose arenite
-17	Mandamus	Cream-grey, well indurated, massive, grain size: max. fine, min. fine, mode(s) fine sand, well sorted, 30% glauconite. Glauconitic sandstone. Subarkose arenite.
MGS-1	Mandamus	Grey-green, friable sand, massive, grain size: max. very coarse, min. coarse, mode(s) coarse, moderately sorted, glauconite 20-25%, well rounded. Glauconitic sandstone. Subarkose arenite.
cc3	Mandamus	Poorly indurated, poorly sorted, grain size: max. granule, min.medium, mode(s) coarse, glauconite15-20%. Glauconitic sandstone. Subarkose arenite.
cc1a	Mandamus	Grey-cream, friable sand, poorly sorted , grain size: max: fine, min. coarse silt, mode(s) very fine sand. 20% glauconite. Glauconitic sandstone. Subarkose arenite
cc1b	Mandamus	Grey-cream, poorly sorted, grain size: max. very fine, min. silt, mode(s) very fine. 20-25%glauconite. Glauconitic sandstone. Subarkose arenite.
cc4a	Mandamus	Grey-cream, moderately sorted, grain size: max. coarse, min. medium mode(s) coarse, cross bedded, rounded-well rounded, glauconite. Glauconitic sandstone. Subarkose arenite.

cc4b	Iron Creek	Grey-cream, moderately sorted, grain size: max. coarse, min. medium mode(s) coarse, cross bedded, rounded-well rounded, glauconite 5-7%. Glauconitic sandstone. Subarkose arenite
Sb2	Iron Creek	Poorly indurated, poorly sorted, cream-white, grain size: max. granule to coarse, min. very fine-silt,mode(s) very fine, calcite, 2-3% glauconite, Calcareous sandstone. Subarkose arenite
Sb3	Iron Creek	Poorly indurated, poorly sorted, cream-white, grain size: max. granule to coarse, min. very fine-silt, mode(s) very fine, glauconite 3%, calcite, calcareous sandstone. Subarkose arenite
W01	Waipara River	Poorly indurated, fine sandstone, moderately sorted, soft sediment deformation, Fe+ stained. Subarkose arenite.
W03	Waipara River	Cream coloured, poorly indurated, moderately sorted, medium grains size, dispersed shell fragments, well bedded, Fe+ stained, cross bedded, coarse grained lenses. Arkose arenite.
W04	Waipara River	Cream coloured, poorly indurated, jarositic, moderately sorted, Medium sandstone, quartz rich, minor glauconite. Subarkose arenite.
W05	Waipara River	White coloured, friable, moderately – well sorted, medium – fine grained Sandstone. Subarkose arenite.
W06	Waipara River	Moderately indurated, moderately sorted, glauconitic sandstone, Fe+stained, Fine – very fine sand. Subarkose arenite.
W07	Waipara River	Grey colour, jarositic - mottled, friable, massive, moderately-well sorted, Traces of calcite and glauconite. Subarkose arenite.
W08	Waipara River	Grey – yellow coloured, jarositic, 5-10% glauconite, glauconite grains well rounded, moderately sorted, fine grained. Arkose arenite.
W09	Waipara River	Massive, friable, moderately – well sorted, highly jarositic – mottled, 20% Glauconite – 2 populations dark green and olive green, occasional Very coarse glauconite, mica traces, fine sand. Glauconitic sandstone. Subarkose arenite.
W12	Waipara River	Massive, poorly indurated, poorly sorted, glauconite 30%, fine – medium grain size. Glaucarenite. Subarkose arenite.
W13	Waipara River	Massive, well sorted, fine grained, glauconite 30%-40%- 2 populations of dark green and olive green glauconite, fine sandstone.Glaucarenite. Subarkose arenite.
BR1	Castle Hill Basin – Cave Stream	Friable sand, white-cream colour, well sorted, coarse-medium grain size. Subarkose arenite.
BR3	Castle Hill Basin – Cave Stream	Poorly indurated, very well sorted, cream coloured, fine – medium Sandstone. Subarkose arenite.

BR4	Castle Hill Basin – Cave Stream	Pale green coloured Massive, poorly indurated, fine grained, moderately sorted, glauconitic sandstone. Subarkose arenite.
BR6	Castle Hill Basin – Cave Stream	Poorly indurated, moderately sorted, fine grained, glauconite 30%. Glauconitic sandstone. Subarkose arenite.
TS-2	Castle Hill Basin – Cave Stream	Carbonaceous sand, poorly sorted, fine grained, coal spars. Subarkose arenite.
TS-3	Castle Hill Basin – Cave Stream	White colour, Carbonaceous sand, poorly sorted, medium – fine sand, coal spars. Subarkose arenite.
Ic1	Castle Hill Basin – Cave Stream	Friable, green colour, very well sorted, fine sand, glauconitic, calcareous. Glauconitic sandstone. Subarkose arenite.
Ic2	Castle Hill Basin – Cave Stream	Friable, moderately sorted, fine sand, coal spars, well rounded quartz granules. 30% glauconit, glauconitic sandstone. Subarkose arenite.
Ic3a	Castle Hill Basin – Cave Stream	Friable, moderately – well sorted, coal spars, fine grained, 10% glauconite, Glauconitic sandstone. Subarkose sandstone.
Ic3b	Castle Hill Basin – Cave Stream	Moderately- well sorted, very - fine sand, 30% glauconite, glauconitic sandstone, subarkose arenite.
Ic4	Castle Hill Basin – Cave Stream	Moderately sorted, fine sand, 30% glauconite, glauconitic sandstone. Subarkose arenite.
AV1	Avoca	Massive, Fe+ stained, white cream coloured, moderately sorted, fine-medium grained, glauconite content 4%. Subarkose arenite.
AV2	Avoca	Friable sand, green colour, massive, fine – medium, glauconite 10%, Glauconitic sandstone. Subarkose arenite.
3	Iron Creek	Cream colour, massive, moderately indurated, well sorted, medium sand, Subarkose arenite.
4	Iron Creek	Green colour, cross bedded, moderately sorted, 30% glauconite, fine sand, Glauconitic sandstone. Subarkose arenite.
7	Iron Creek	Green colour, cross bedded, glauconite rich, fine – medium sand, well sorted, 20% glauconite. Glauconitic sandstone. Subarkose arenite.
8	Iron Creek	Green colour, cross bedded, glauconite rich, fine – medium sand, well sorted, 20% glauconite. Glauconitic sandstone. Subarkose arenite.
SGM1	Malvern	Cream-grey colour, massive, moderately – well sorted, Fe+stained,, 5% micas, fine-very fine sand, 5% glauconite. Subarkose arenite.

CM1	Mount Somers	Carbonaceous sand, grey-white, clay lamina, moderately sorted, fine sand, Subarkose arenite.
SQ1	Mount Somers	Moderately sorted, fine grained, grit, occasional coarse and granule size detritus, subarkose arenite.
SQ2	Mount Somers	Poorly sorted, medium grained, grit, occasional coarse and granule size detritus, subarkose arenite.
SQ3	Mount Somers	Pale olive green, poorly sorted, occasional smoky quartz pebbles, fine sand, 20% glauconite, fine-medium glauconite grains. Glaucarenite. Subarkose-Sublitharenite.
WC1	Mount Somers	Poorly sorted, pebbly, fe+stained, medium sand, quartz rich, Subarkose arenite.
WC3	Mount Somers	Poorly sorted, occasional quartz grit, medium sand, quartz rich, Subarkose arenite.
WC6	Mount Somers	Poorly indurated, poorly sorted, quartz granules – pebbles, glauconite rich, 20-30%, Glaucarenite. Subarkose-Sublitharenite.
BR1	Mount Somers	Tan-orange, massive, moderately – well sorted, fine sand, quartz rich, minor mica, minor glauconite. Subarkose arenite.

APPENDIX 1
STRATIGRAPHIC COLUMNS & ROCK EXPOSURE IMAGES FROM FIELD LOCATIONS

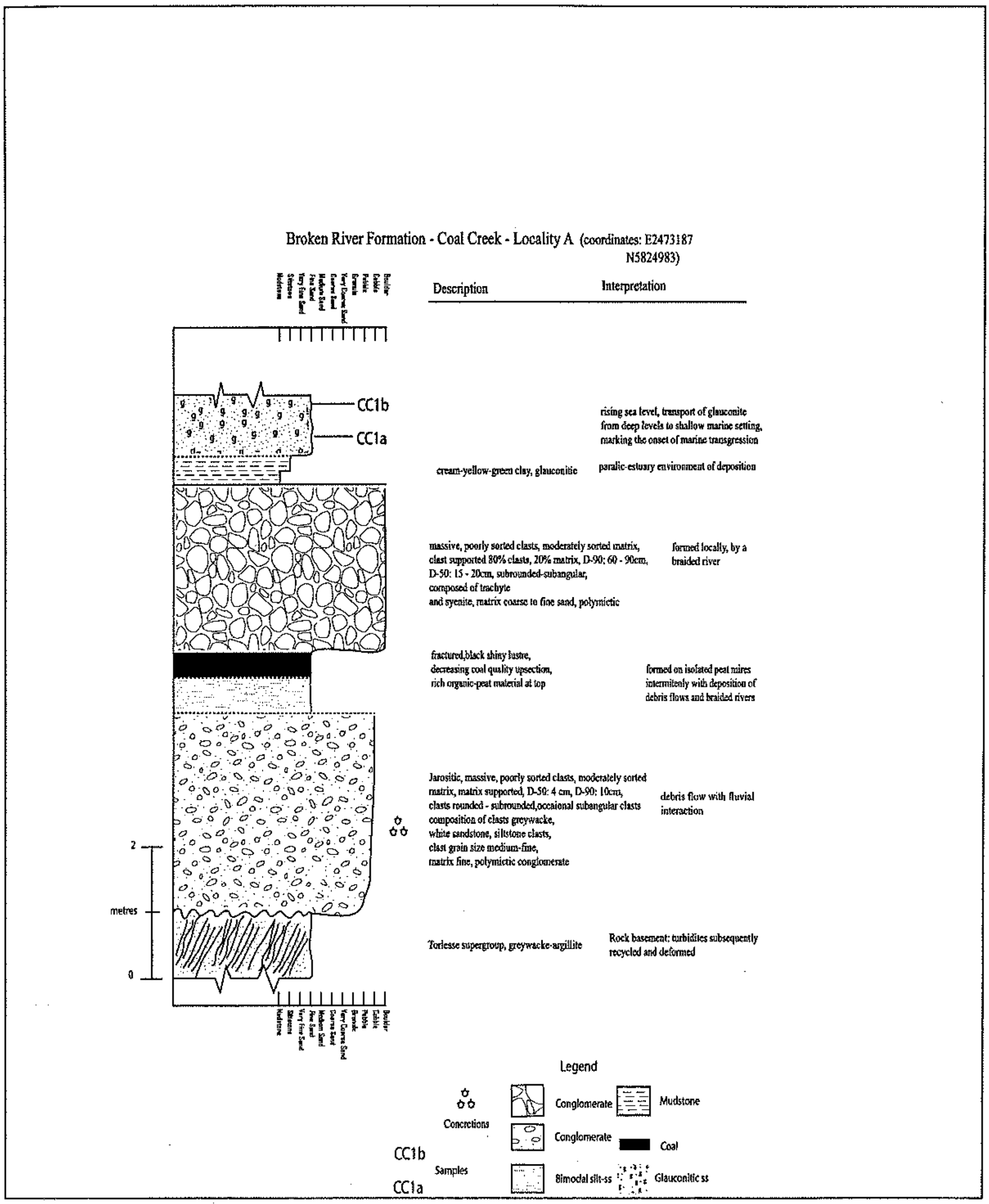

Figure 1.1: Measured Stratigraphic log of the Broken River Formation at Coal Creek (locality A).

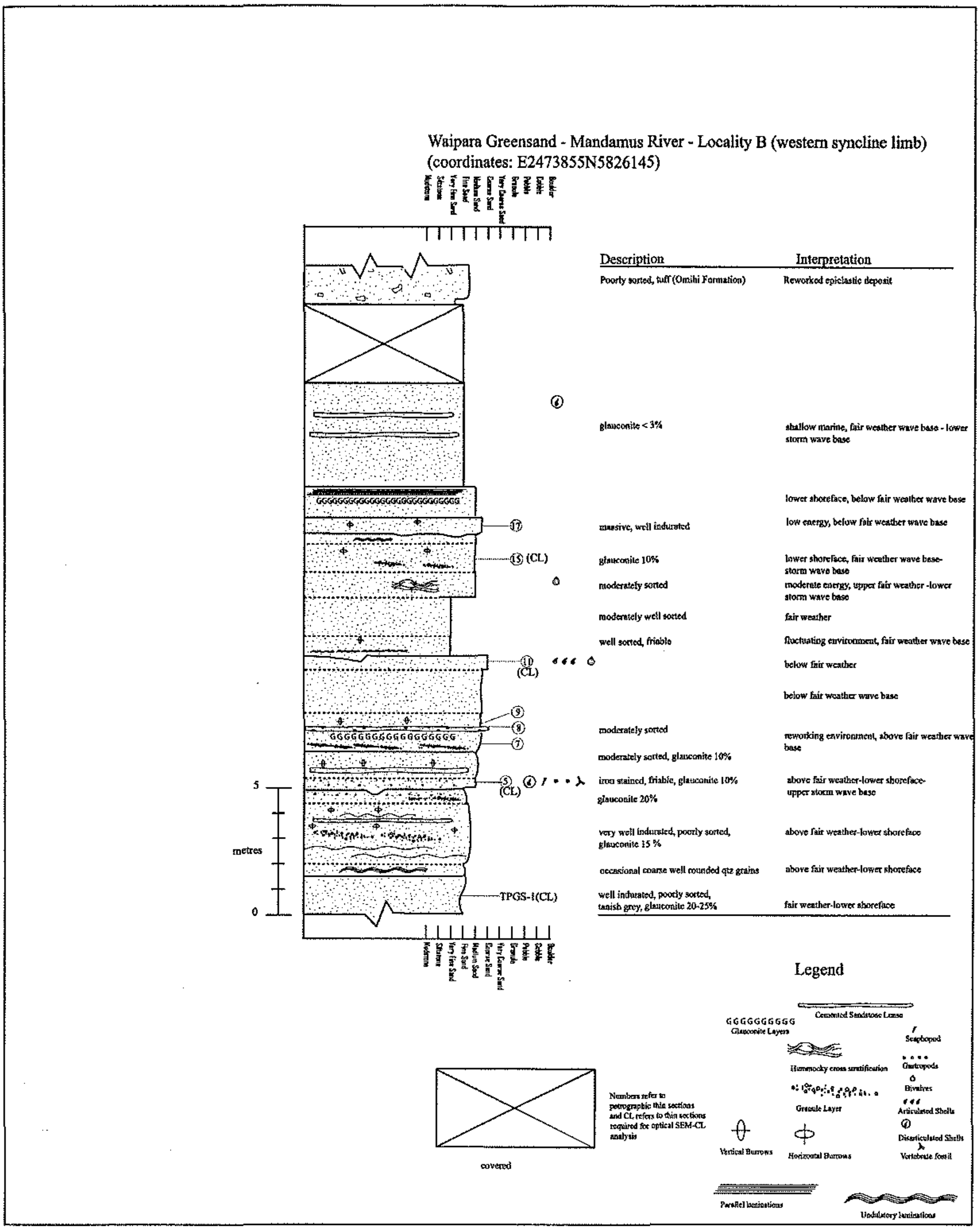

Figure 1.2: Measured stratigraphic column of the Waipara Greensand at the Mandamus River (locality B).

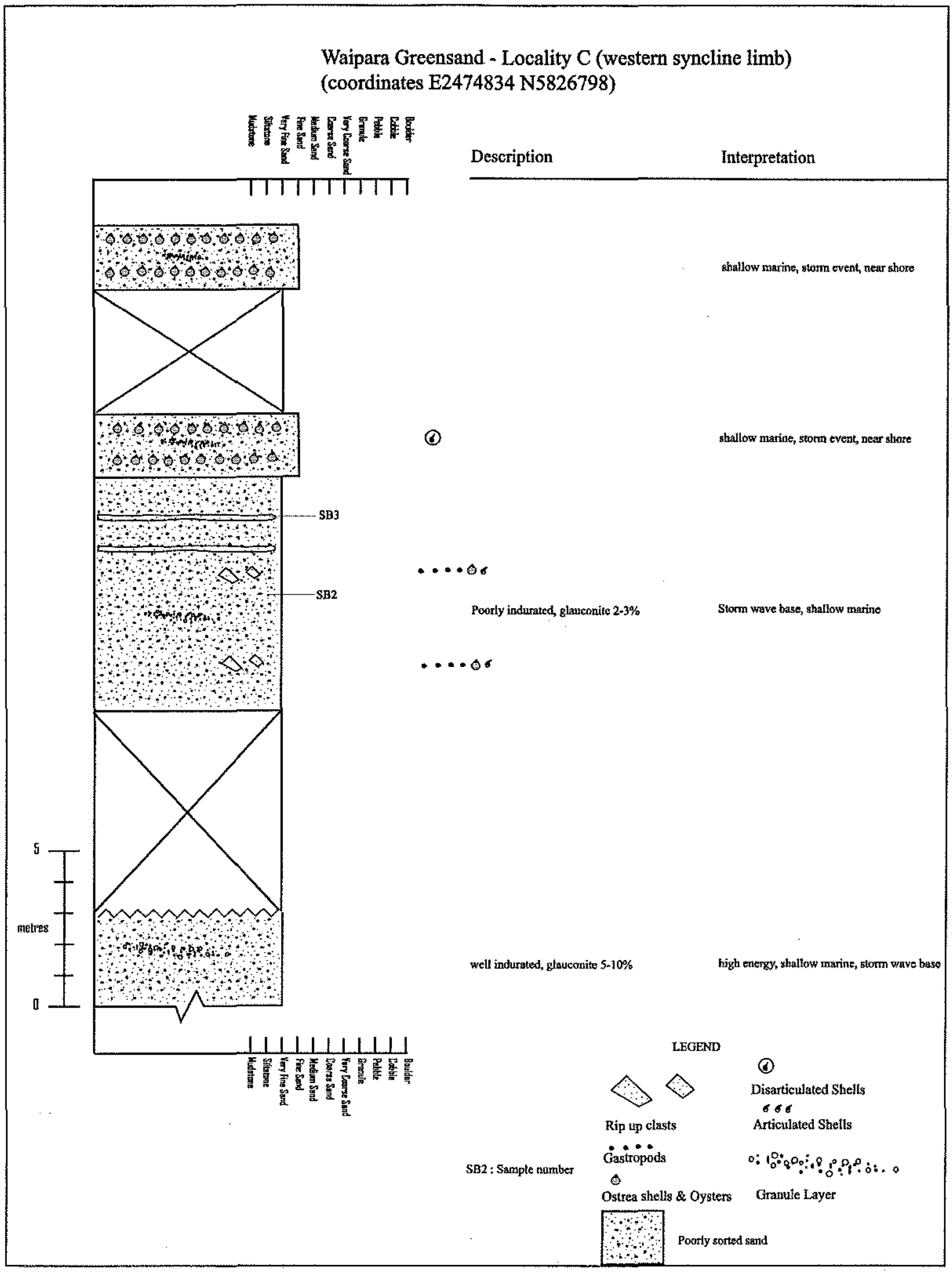

Figure 1.3: Stratigraphic section of the Waipara Greensand at Mandamus at locality C (western syncline limb).

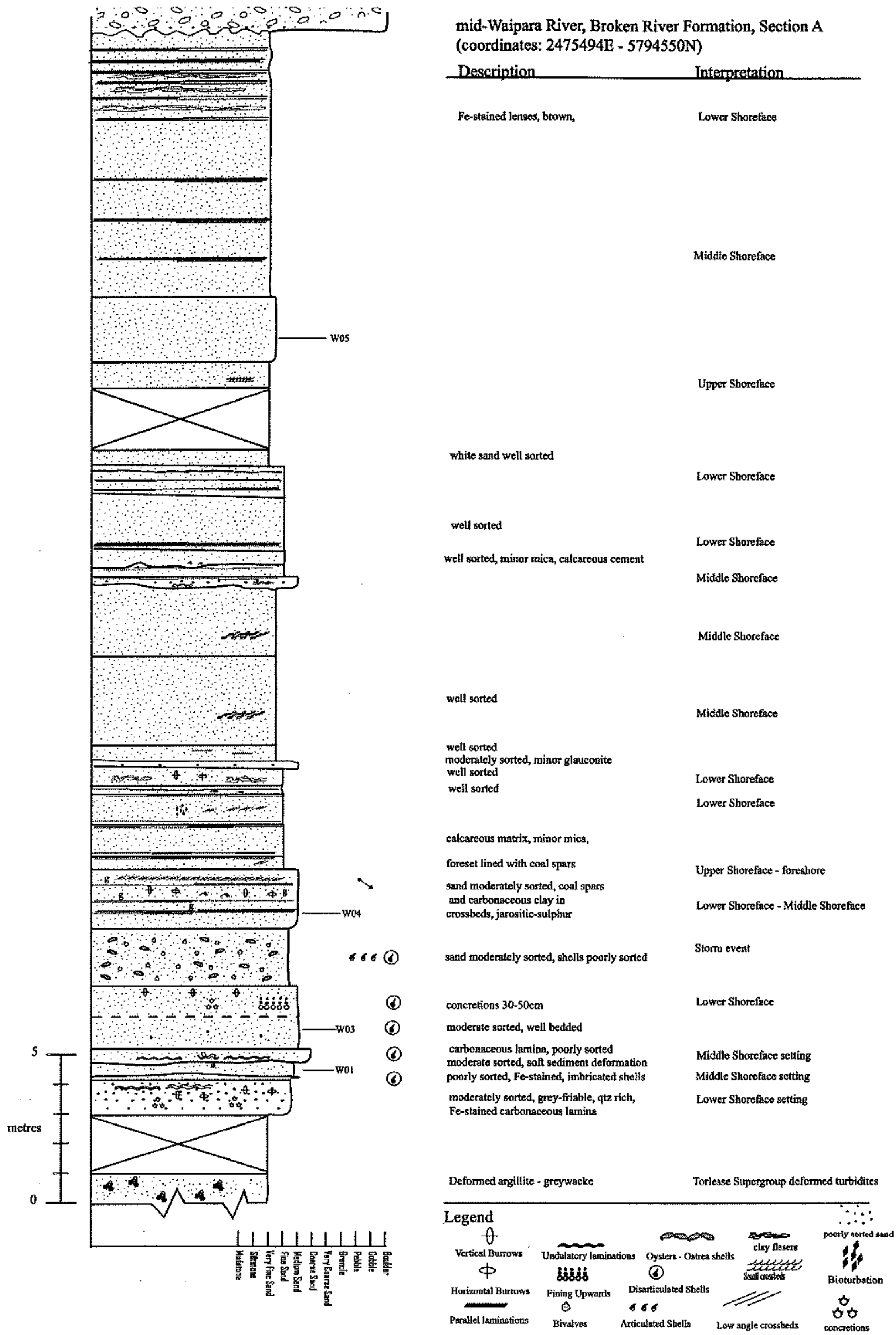

Figure 1.4: Measured stratigraphic section of the Broken River Formation in mid-Waipara River, Doctors Gorge (Ohuriawa Gorge) locality A.

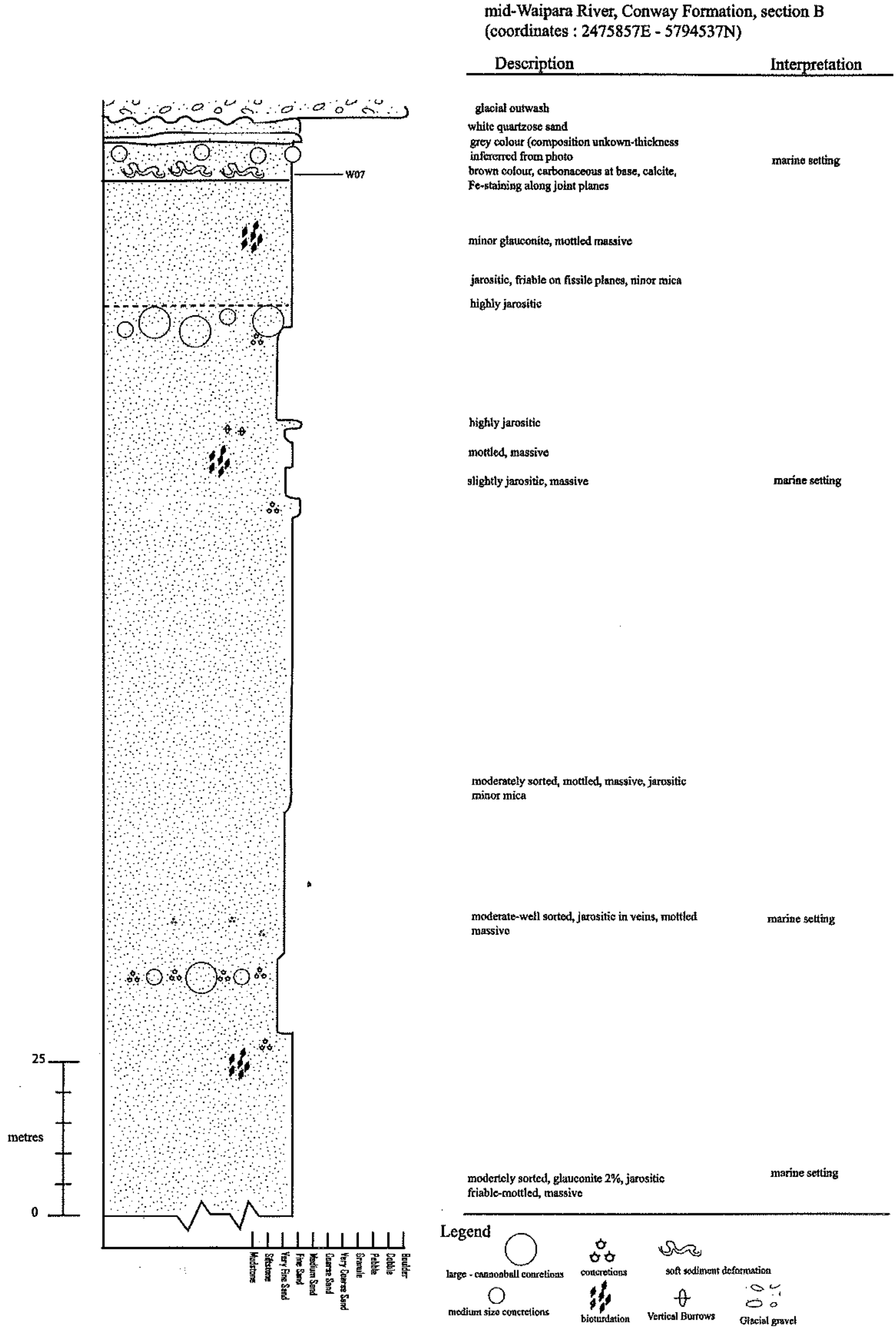

Figure 1.5: Measured stratigraphic section of the Conway Formation in mid-Waipara River at locality B.

mid-Waipara River, Conway Formation - Loburn Mudstone, section C
(coordinates : 2475917E - 5794284N)

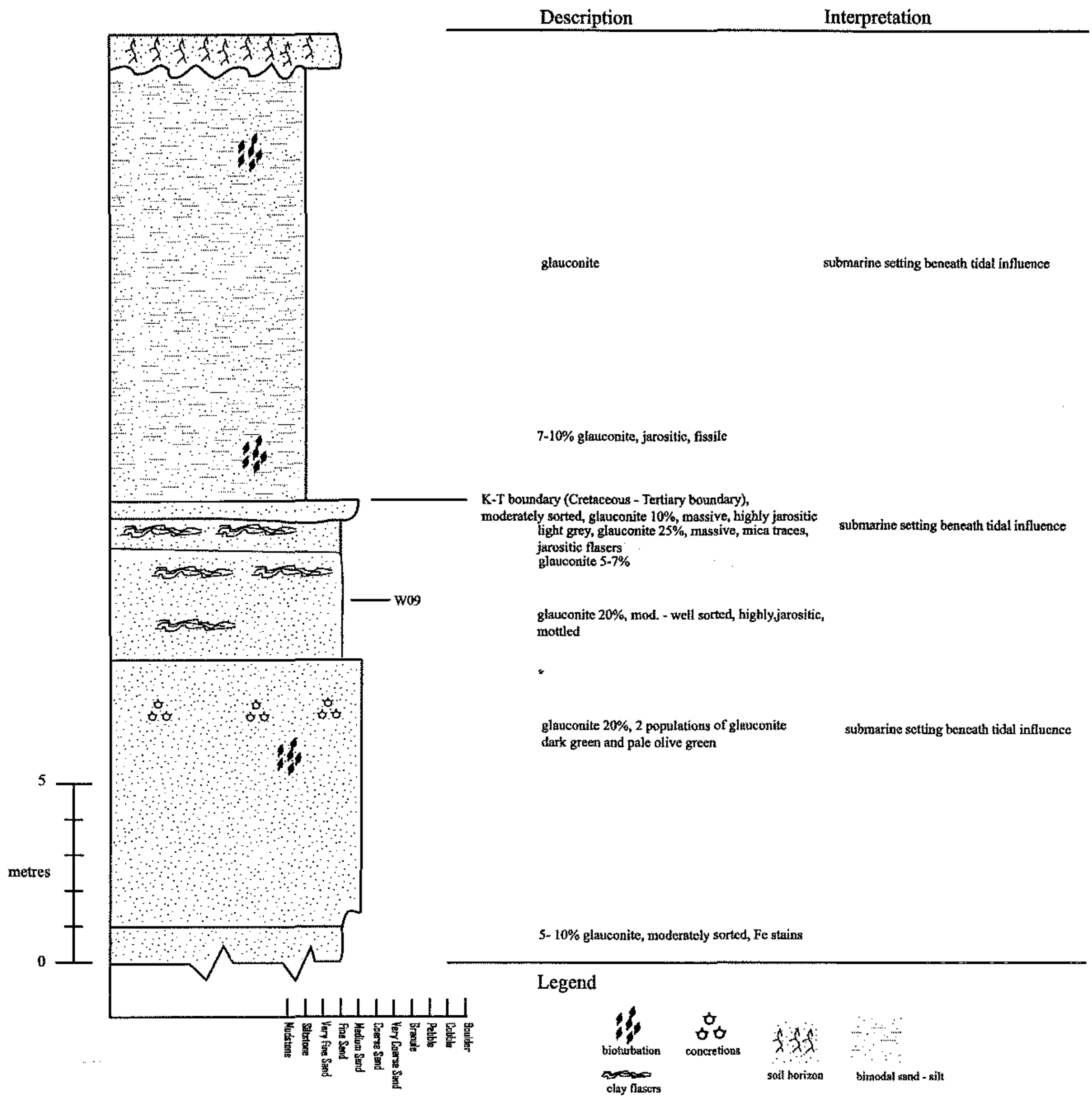

Figure 1.6: Measured stratifraphic section of the Loburn Mudstone overlaying the Conway Formation in the mid-Waipara River at locality C.

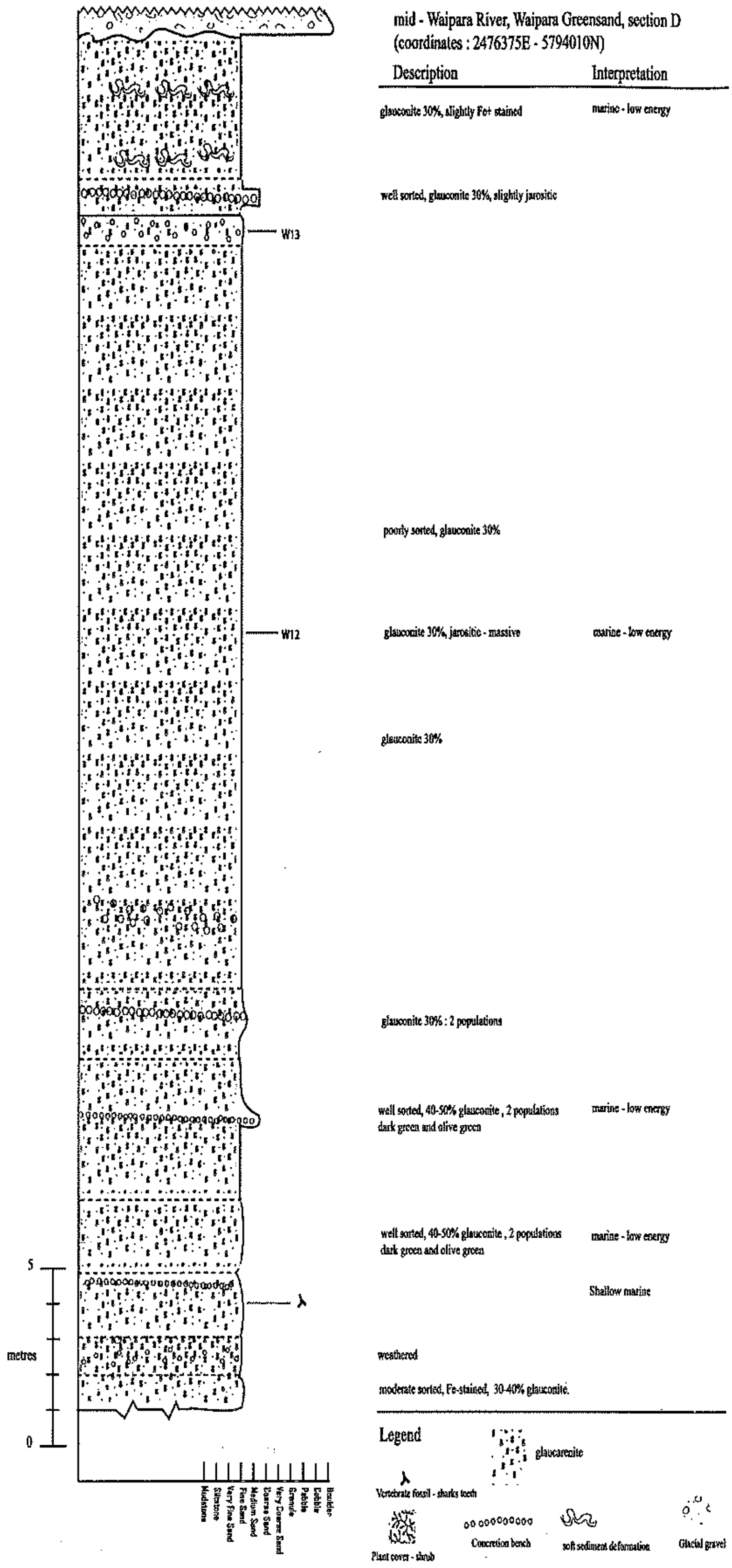

Figure 1.7: Measured stratigraphic section of the Waipara Greensand in the mid-Waipara River at locality D.

Figure 1.8: Burrowed surface within the Broken River Formation.

Figure 1.9: Alligned disarticulated shells within a crossbed and scoured surfaces in the Broken River Formation.

Figure 1.10: *Ostrea* shell bed with oysters, pectens and bivalves of the Broken River Formation.

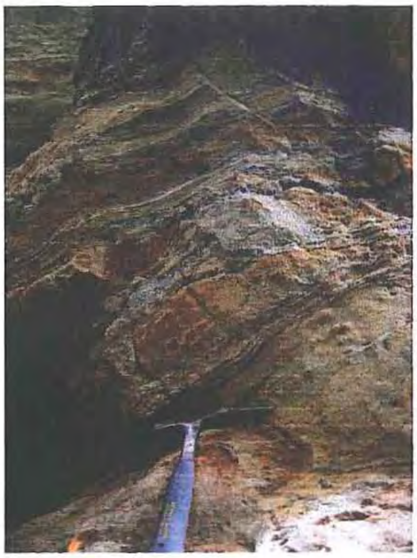

Figure 1.11: Carbonaceous and clay laminations interbedded with sandstone and iron cemented concretions of the Broken River Formation.

Figure 1.12: Coal spars aligned in crossbed foresets of the Broken River Formation.

Figure 1.14: Water escape structures of the Broken River Formation.

Figure 1.14: Crossbed foresets overlain by water-escape structures of the Broken River Formation.

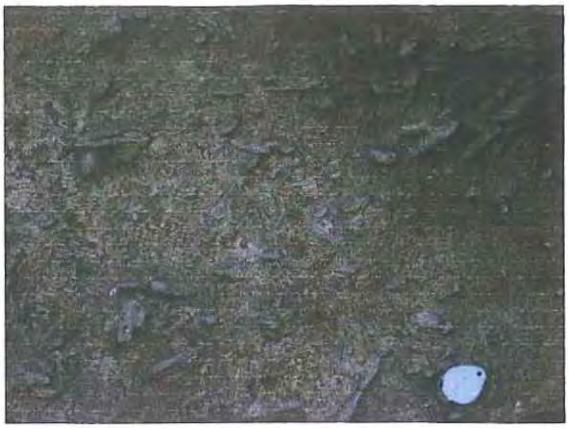

Figure 1.15: Large burrows upsection close to the start of the Conway Formation.

Figure 1.16: Exposure of the Conway Formation with large spherical concretions and soft sediment Deformation at the top of the sequence (white pole 1.8m at the middle bottom for scale).

Figure 1.17: Fissile planes and flaky joint planes at the top of the Conway Formation

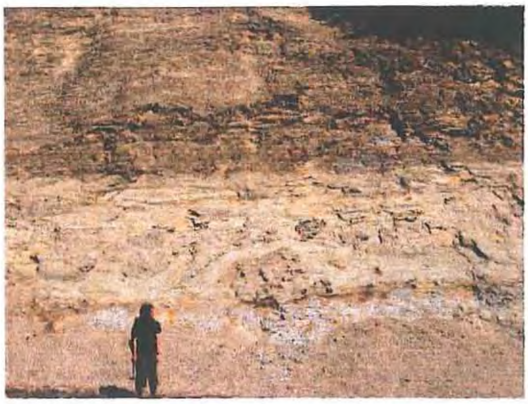

Figure 1.18: brown Loburn Mudstone overlying the creamy grey Conway Formation (contact at the middle top).

Figure 1.19: Exposure of the Waipara Greensand with characteristic spherical concretions Forming resistant layers/benches.

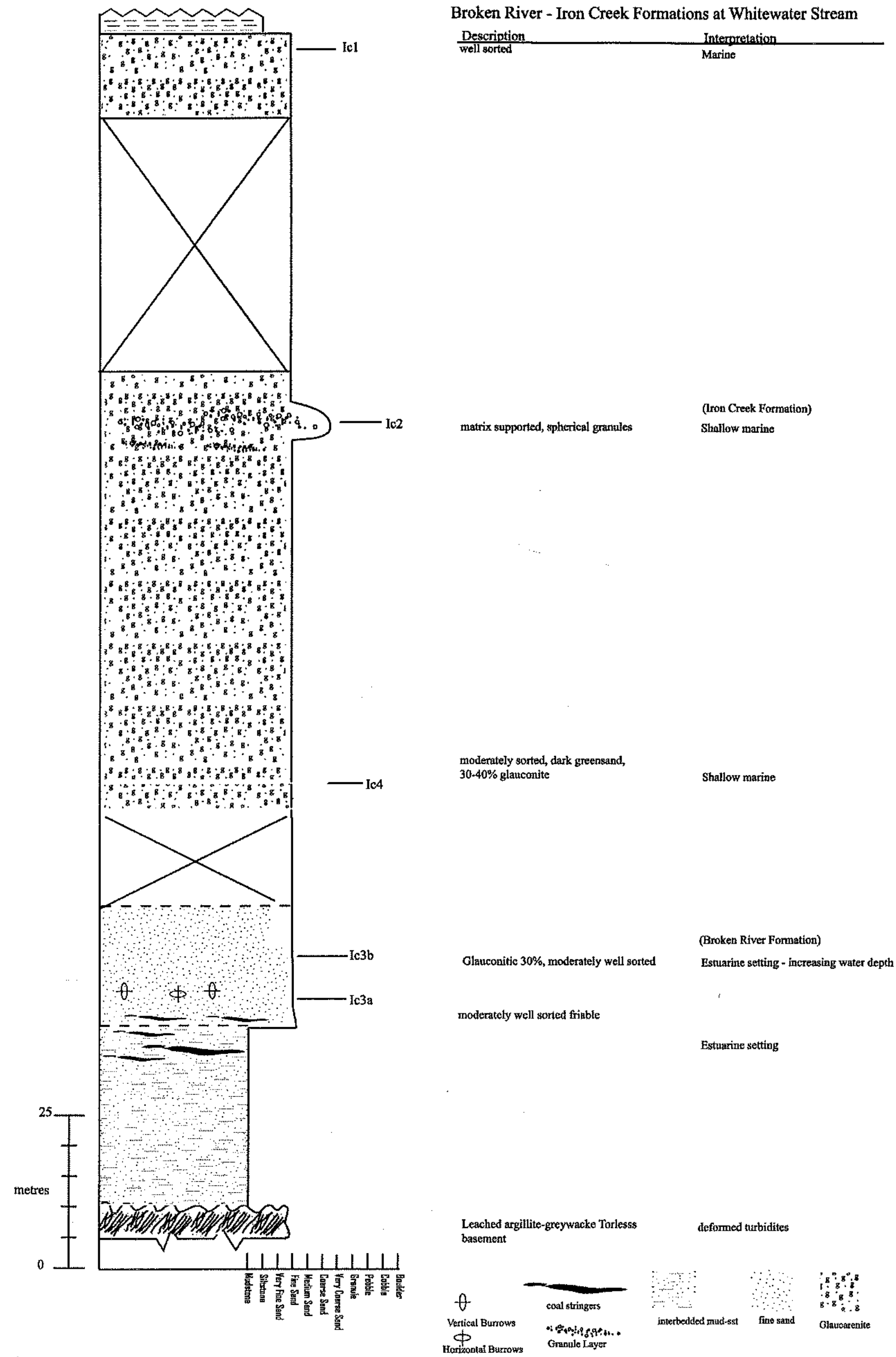

Figure 1..20: Stratigraphic column of the Broken River and Iron Creek Formations measured by calculating from true and apparent thickness in Whitewater Stream.

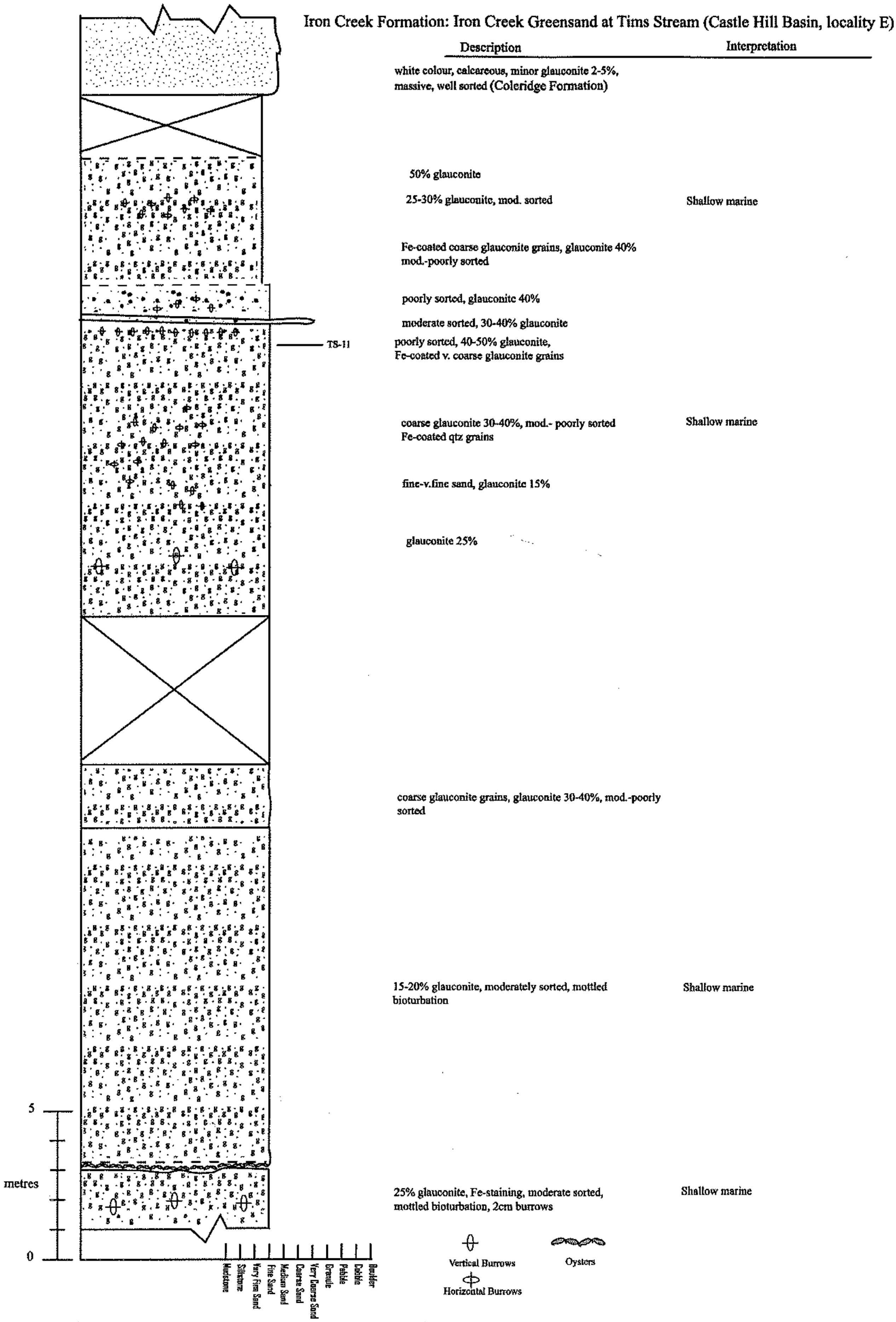

Figure 1.21: Measured stratigraphic column of the Iron Creek Formation's Greensand Member in Tims Stream.

Figure 1.22: Cross beds and coal stringers in the Broken Formation in Broken River (Cuckoo Creek; locality B).

Figure 1.23: Coal interbedded with intraformational mud of Broken River Formation (Cuckoo Creek).

Figure 1.24: Matrix supported greywacke-qtz pebble Polymictic conglomerate of the Broken River Formation (locality C).

Figure 1.25: Clast supported, monomictic greywacke conglomerate of the Broken River Formation (locality C ;Broken River).

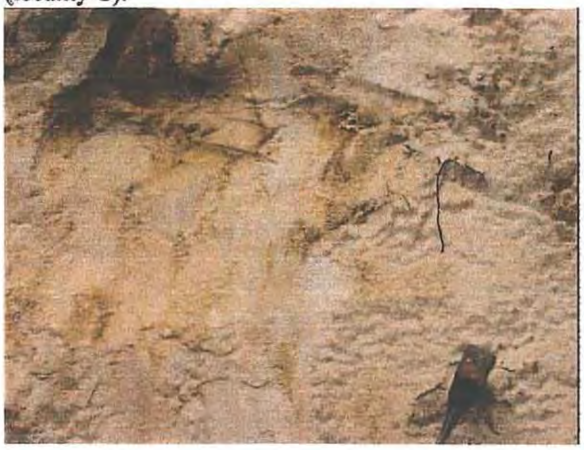

Figure 1.26: Broken River Formation quartzose sand (locality D; Broken River).

Figure 1.27: Glauconitic sand with limy concretions of Iron Creek Formation's Charteris Bay Sandstone Member (locality D; Broken River).

Figure 1.28: Broken River Formation, interbedded Glauconitic sand with carbonaceous muds and coal Stringers (Whitewater Stream).

Figure 1.29: Glauconitic sands of the Broken River Formation (upper Whitewater Stream).

Figure 1.30: Glaucarenite of the Iron Creek Formation with quartz granules (Whitewater Stream).

Figure 1.31: Interbedded carbonaceous muds and quartz Sandstones of the Broken River Formation (locality G; Cave Stream).

Figure 1.32: White burrows in the Iron Creek Greensand (Iron Creek Formation; locality E Tims Stream).

Figure 1.33: Exposure of dark green glaucarenite in Tims Stream (locality E).

Figure 1.34: Exposure of Broken River Formation basal greywacke conglomerates characterized by red coloured iron staining in the foreground, overlain by quartzose glauconitic sandstone in the background (above racksack).

Figure 1.35: Exposure of Broken River Formation with coal stringers, along strike in Broken River.

Figure 1.36: The mouth of Iron Creek with an Exposure of Broken River Formation.

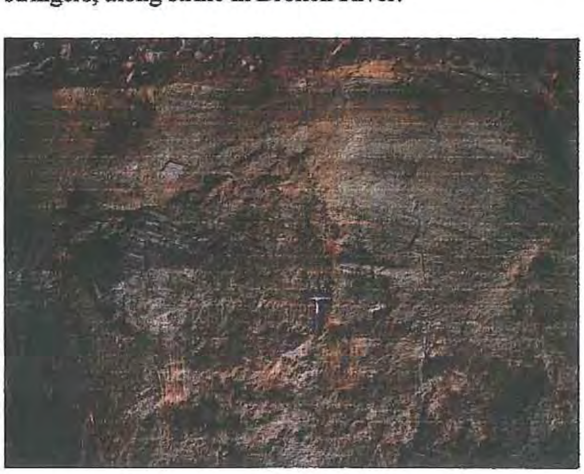

Figure 1.37: Charteris Bay Sandstone Member of the Iron Creek Formation showing parallel cross beds in Iron Creek.

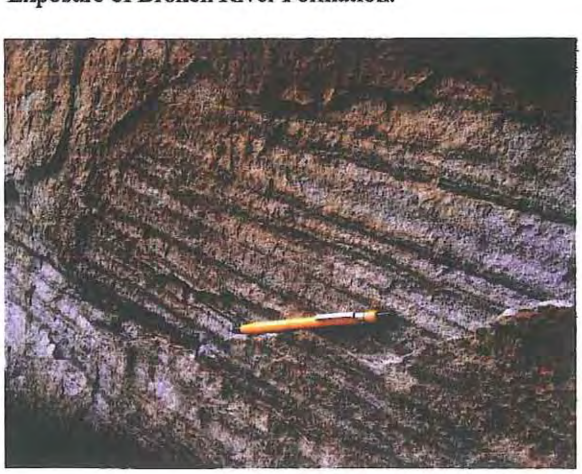

Figure 1.38: Glauconite grains aligned along parallel cross beds in the Iron Creek Formation.

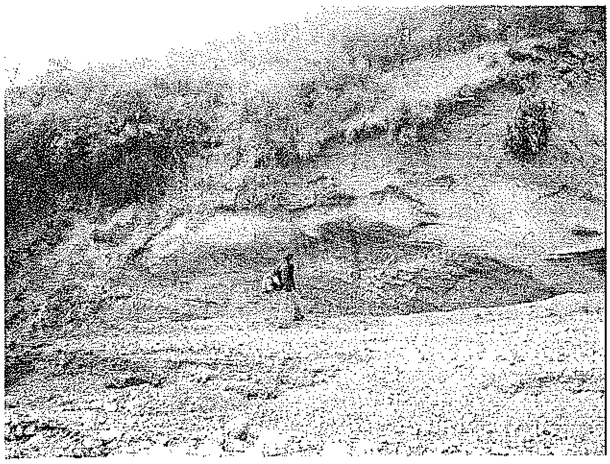

Figure 1.39: Hummocky cross stratification from the Iron Creek Greensand Member.

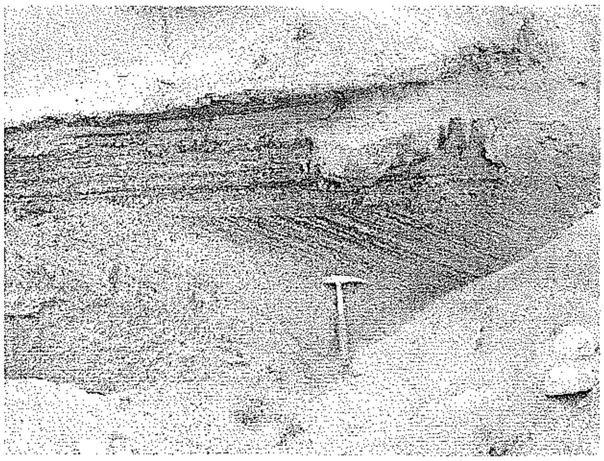

Figure 1.40: Concretionary lens in cross bedded Iron Creek Greensand Member.

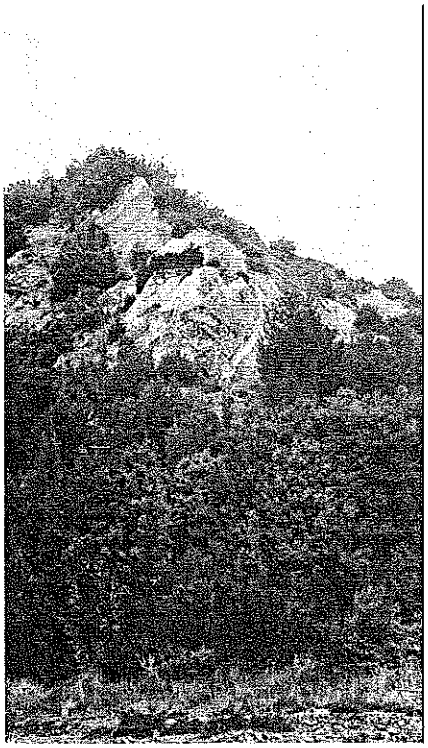

Figure 1.41: Exposure of Broken River Formation at Avoca area.

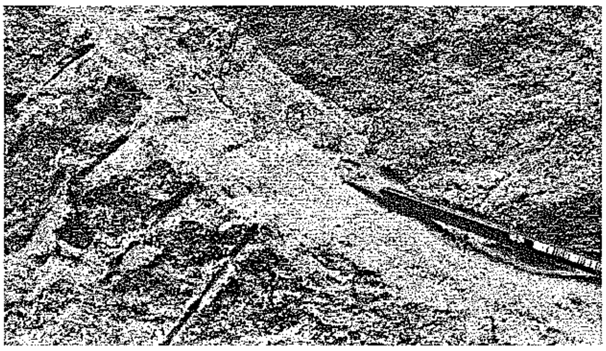

Figure 1.42: Burrows in the Charteris Bay Sandstone at Avoca-Kowhai Canyon.

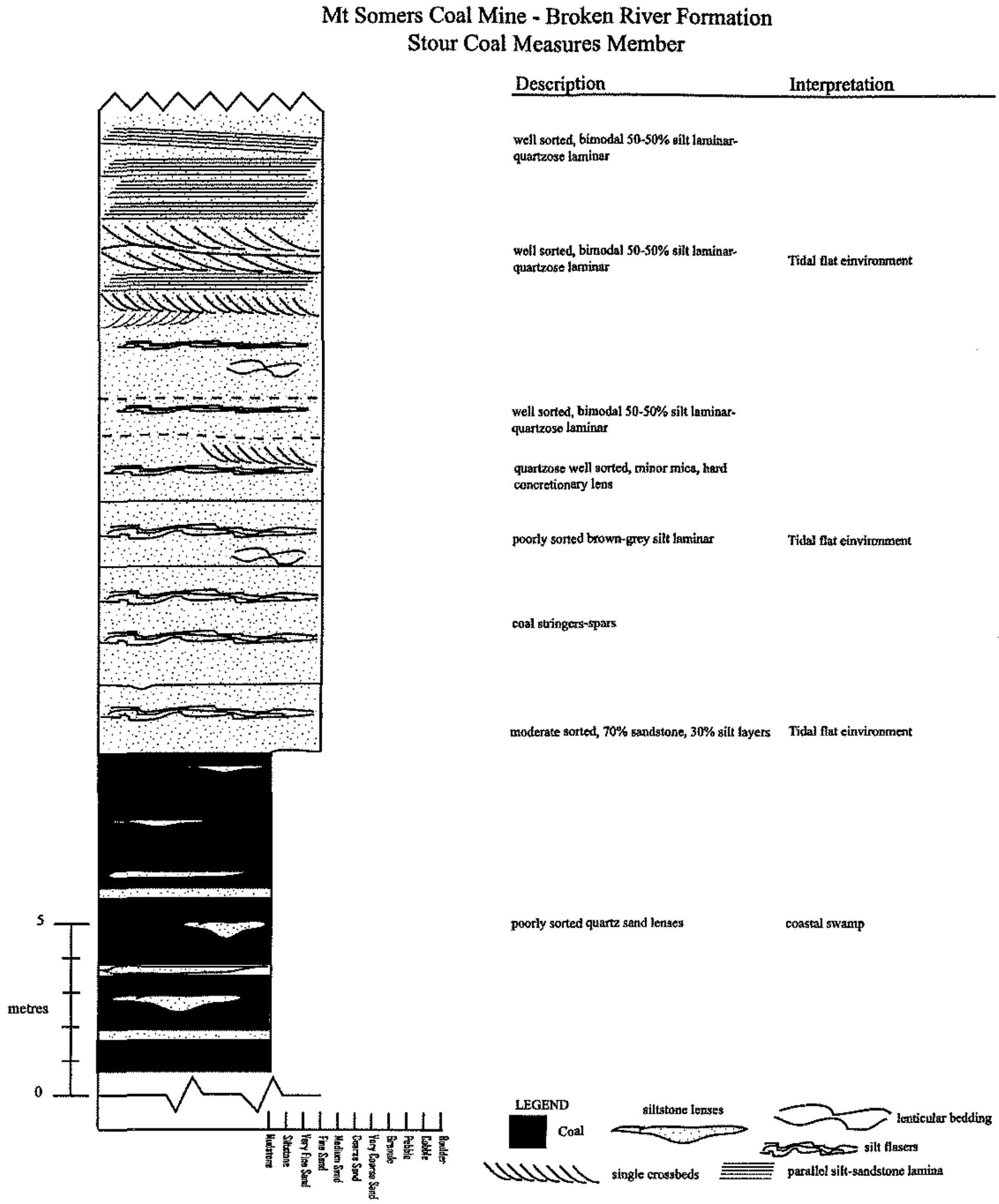

Figure 1.43: Stratigraphic column of the Stour Coal Measures of the Broken River Formation at locality A (Mount Somers coal mine).

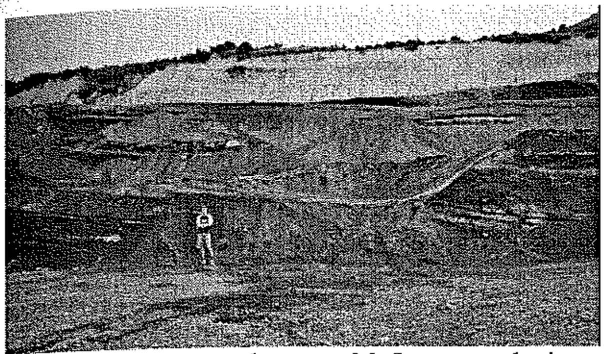

Figure 1.44: Large coal seam at Mt Somers coal mine, with occasional siltstone lenses of the Stour Coal Measures.

Figure 1.45: Interbedded sandstones with carbonaceous silt flasers and lenticular bedding of the Stour Coal Measures.

Figure 1.46: Single cross bed sets of the Stour Coal Measures at Mt Somers coal Mine.

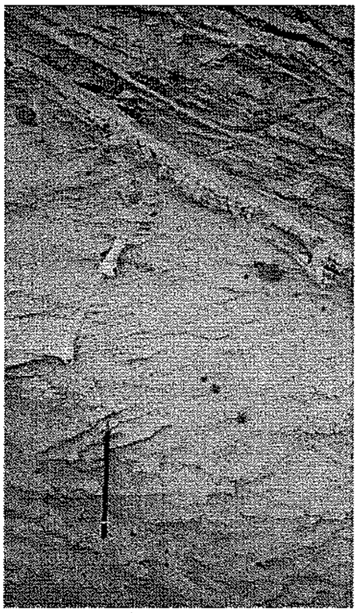

Figure 1.47: *Ophiomorpha nodosa* trace fossils perpendicular to cross bedding in the Blondin Sand Member at the Silica sand

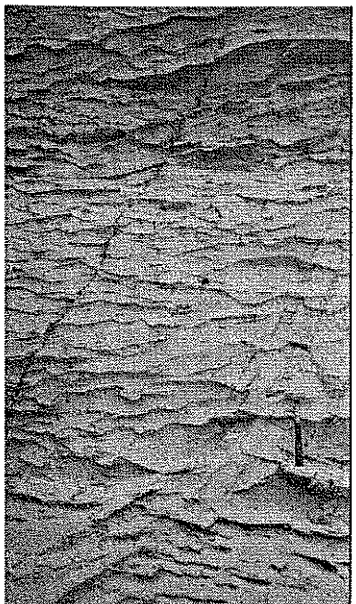

Figure1.48: Ripples in the Blondin Sand Member (silica sand quarry).

Figure 1.49: Herringbone cross stratification with coarse quartz grit of the Blondin Sand Member (silica sand quarry), very low angle indicates beach face.

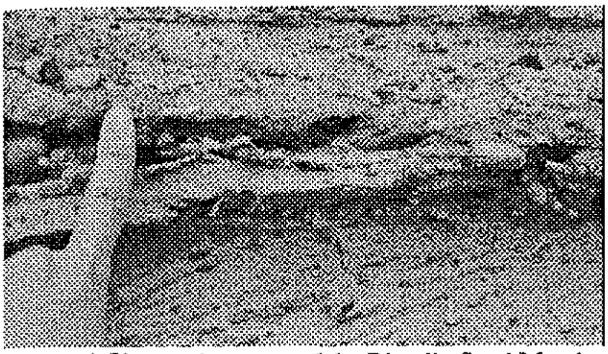

Figure 1.50: conglomerate of the Blondin Sand Member Within cross beds (Silica Sand quarry).

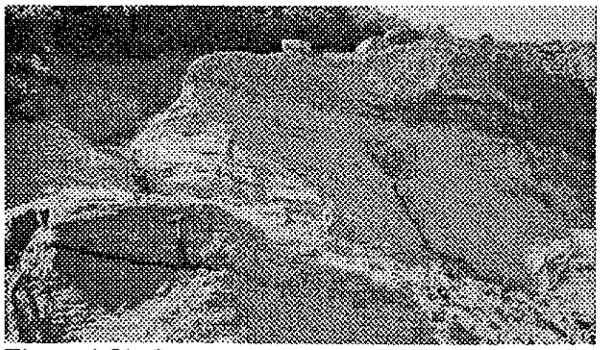

Figure 1.51: Quartzose sandstone with mud drapes of the Blondin Sand Member overlain with an iron Stained conglomerate band (Woolshed Creek).

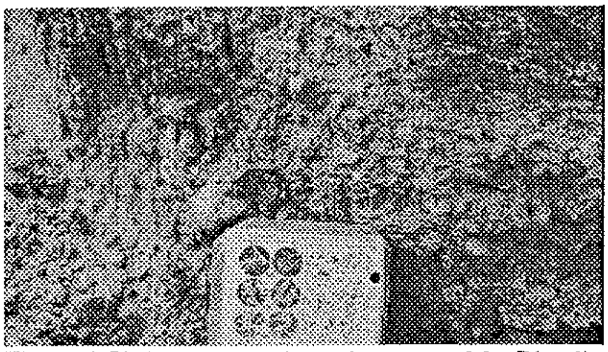

Figure 1.52: Poorly sorted conglomerate of the Blondin Sand Member (Woolshed Creek).

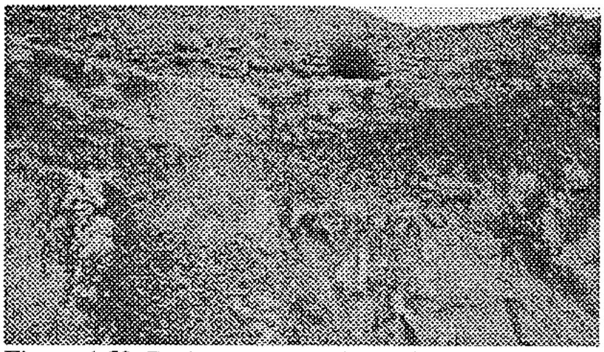

Figure 1.53: Dark grey-green glauconite layer of the Homebush Sandstone overlain unconformably by Windwhistle Formation – glacial gravel at the silica sand quarry.

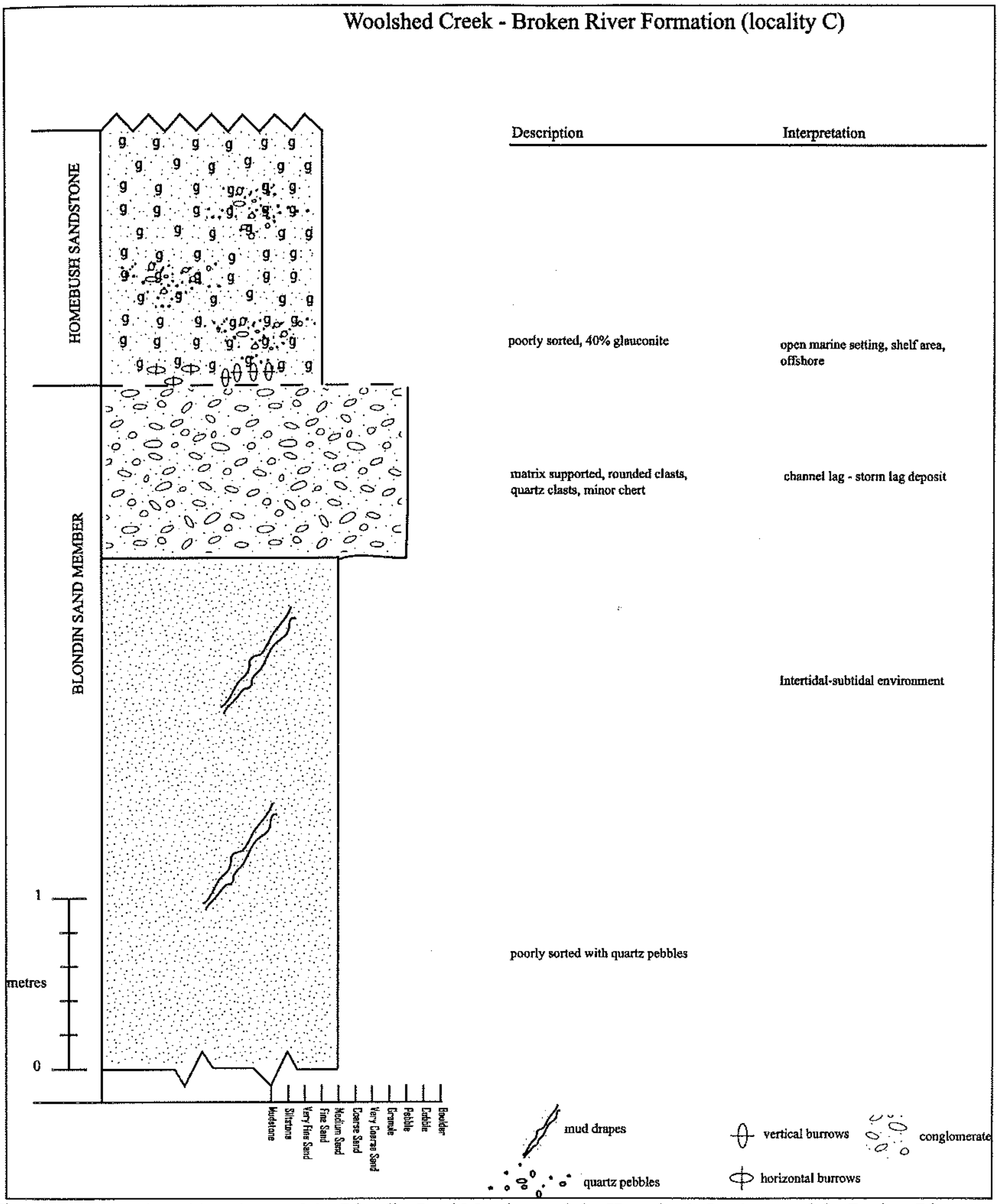

Figure 1.54: Stratigraphic column of the Blondin Sand Member and the Homebush Sandstone of the Broken River Formation atLocality C (Woolshed Creek).

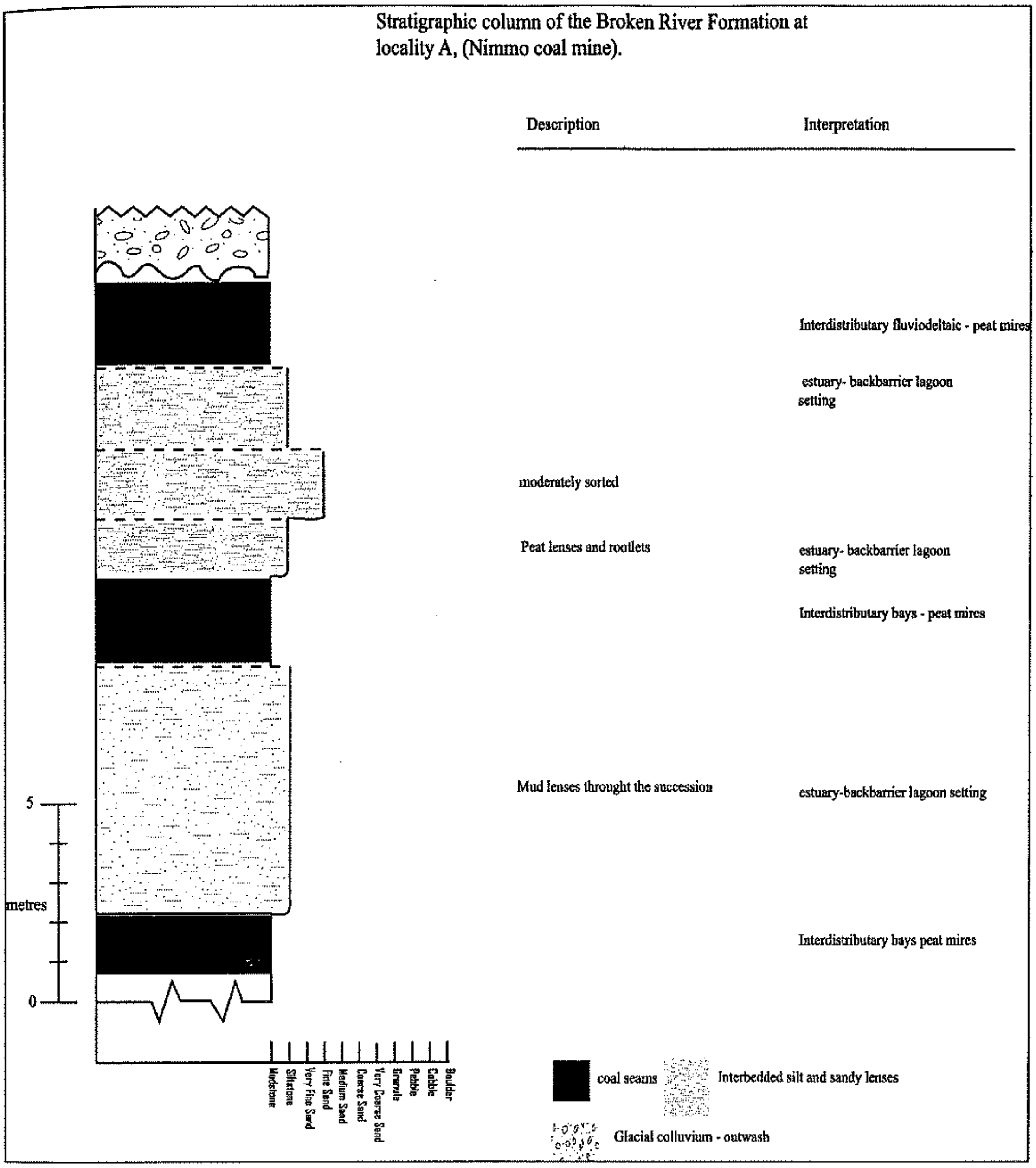

Figure 1.55: Measured stratigraphic column of the Broken River Formation at Nimmo Mine, locality A – Malvern.

Location Island Hills	**Sample**	Quartz	Polycrystalline Quartz	K-Feldspar	Plag-Feldspar	Glauconite	Muscovite	Sed. Lithics	Chert	Matrix	Cement	others	Calcite	**Total**
Section B - Mandamus River	**TPGC-1**	99	5	22	1	26		3	1	93(calcite)	47(calcite)	3(sericite)		300
Section B - Mandamus River	**5**	165	19	40	1	51		2	2	8(calcite)		12(calcite)		300
Section B - Mandamus River	**8**	145	15	28	1	68		1		20(calcite)		22(fossils)		300
Section B - Mandamus River	**11**	88	6	14	1	23		4		12(calcite)	149(calcite)	3(fossils)		300
Section B - Mandamus River	**15**	178	6	37	4	45	5	3	7			11(sericite)	4	300
Section B - Mandamus River	**17**	167		28	4	47		4			50(calcite)			300
Mandamus River - Glens of Tekoa	**MGS1**	164	59	25	1	43	1		3	2		2		300
Section A - Coal Creek	**CC1a**	92		19		73	11	1		102(sericite)		2		300
Section A - Coal Creek	**CC1b**	85		18	3	58	12			121(sericite)			3	
Coal Creek	**CC3**	184	17	22	1	27	2		21	26				300
Coal Creek	**CC4a**	180	25	39		31	1	5	9	9		1		300
Coal Creek	**CC4b**	134	89	29	1	9			4		34(Calcite)			300
Section C - Western Syncline limb	**SB2**	117	15	14	2	11	1	3	8	118(calcite)	8(Calcite)	3		300
Section C - Western Syncline limb	**SB3**	101	24	13	4	5	1	1	1	139(calcite)	11(calcite)			300

APPENDIX 2
SANDSTONE POINT COUNT DATA

Location Mid Waipara	Sample	Quartz	Polycrystalline Quartz	K-Feldspar	Plag-Feldspar	Glauconite	Muscovite	Volcanic Lithic	Sedim. Lithic	Plutonic lithic	Chert	others	Calcite	Sericite	**Total**
Lower Doctors Gorge	**W01**	200	6	21	50		1	12	5	4	1				300
Lower Doctors Gorge	**W03**	154	21	31	62	3		8	16	5					300
Lower Doctors Gorge	**W04**	189	14	33	23	22		6	13						300
Lower Doctors Gorge	**W05**	222		38	25		2	10	3						300
Lower Doctors Gorge	**W06**	214	2	39	22	2	5	12	3						300
Mid Waipara River	**W07**	151	6	32	16	34	48	9	4						300
Mid Waipara River	**W08**	97	8	26	15	47	6	4	2			2(fossils)	92(matrix)	1	300
Mid Waipara River	**W09**	82	3	12	15	60	6		3			96(silt)	23(matrix		300
Mid Waipara River	**W12**	75	7	1	21	152			4	1		23(silt)	16		300
Mid Waipara River	**W13**	70	3	2	27	185			1			4(silt)	8(matrix)		300

APPENDIX 2
SANDSTONE POINT COUNT DATA (cont.)

Location - Iron Creek	Sample	Quartz	Polycrystalline Quartz	K-Feldspar	Plag-Feldspar	Glauconite	Muscovite	Sed. Lithics	Chert	Micritic-Matrix	Spar-Calcite-Cement	others	Calcite-grains		**Total**
Iron Creek	**3**	221	21	26		2		29		1(epoxy resin)					300
Iron Creek	**4**	174	2	24		93		4				3			300
Iron Creek	**7**	104	28	7		63			1	32(calcite)	49(calcite)	16(H-O)			300
Iron Creek	**8**	185	1	40		64		10							300
Location Avoca-Broken River	**Sample**	Quartz	Polycrystalline Quartz	K-Feldspar	Plag-Feldspar	Glauconite	Muscovite	Volcanic Lithic	Sedim. Lithic	Plutonic lithic	Chert	others	Calcite	Sericite	**Total**
Kowhai Canyon	**AV1**	218	7	35	17	14	3	2	4						300
Kowhai Canyon	**AV2**	194	7	40	8	48	2		1						300

APPENDIX 2
SANDSTONE POINT COUNT DATA (cont.)

Location Castle Hill Basin	Sample	Quartz	Polycrystalline Quartz	K-Feldspar	Plag-Feldspar	Glauconite	Muscovite	Volcanic Lithic	Sedim. Lithic	Chert	Matrix	others	Calcite	Sericite	**Total**
Upper Broken River	**BR3**	229	15	24		1		4	12	1		14(silt)			300
Upper Broken River	**BR4**	207	7	18		48	1	1	3			15(silt)			300
Tims Stream	**TS-2**	207	10	24	2		1		3		47 (Silt)	6(sericite)			300
Tims Stream	**TS-3**	206	8	34			4				45(silt)	3(sericite)			300
Cuckoo Stream-Broken River headwaters	**BR1**	231	26	28	3			5	6	1					300
Cave Stream	**BR6a**	170	19	23		64	2	3	2		3	11		3	300
Whitewater Stream	**Ic3a**	198	1	42		37	7	7	3		2(sericite)	3			300
Whitewater Stream	**Ic3b**	165		28	1	101	1	2	2						300
Whitewater Stream	**Ic1**	155	2	10	31	9	3	1	1		42(calcite)	31(fossils)	15		300
Whitewater Stream	**Ic2**	112	57	10	24	93			1			3			300
Location - Malvern	**Sample**	Quartz	Polycrystalline Quartz	K-Feldspar	Plag-Feldspar	Glauconite	Muscovite	Volcanic Lithic	Sedim. Lithic	Chert-lithic	Matrix	others	Calcite		**Total**
Surveyors Gully-Malvern	**SGM-1**	220	15	20		13	12	5	11	3		1			300

APPENDIX 2
SANDSTONE POINT COUNT DATA (cont.)

Location - Mount Somers	Sample	Quartz	Polycrystalline Quartz	K-Feldspar	Plag-Feldspar	Glauconite	Muscovite	Volcanic Lithic	Sedim. Lithic	Plutonic lithic	Chert	others	Calcite	Sericite	**Total**
Mt Somers - Woolshed Creek	**WC1**	193	37	61	4	1		3	1						300
Mt Somers - coal mine	**CM1**	244	11	31	2			2	1					9	300
Mt Somers - silica sand quarry	**SQ1**	182	66	37	13						2				300
Mt Somers - silica sand quarry	**SQ2**	227	20	43	5			3	2						300
Mt Somers - Woolshed Creek	**WC6**	136	20	15		60		1	18		18			32	300
Mt Somers - silica sand quarry	**SQ3**	123	35	20		54		2	24					42	300
Mt Somers - Boyds Road	**BR1**	218	3	45	14	12	3	1			1			3	300
Mt Somers - Woolshed Creek	**WC3**	195	24	60	10			1	10						300

APPENDIX 2
SANDSTONE POINT COUNT DATA (cont.)

Quartz-Feldspar-Lithics results					Normalized values		
Mandamus		Total	Total	normalizing	Quartz	Feldspar	Lithics
Sample#	Quartz	Feldspar	Lithics	factor			
MGS1	223	26	3	252	88.49	10.32	1.19
CC1a	92	19	1	112	82.14	16.97	0.89
CC1b	85	21		106	80.19	19.81	
CC3	201	23		224	89.73	10.27	
CC4a	205	39	5	249	82.33	15.66	2.01
CC4b	223	30		253	88.14	11.86	
SB2	132	16	3	151	87.42	10.6	1.98
SB3	125	17	1	143	87.42	11.88	0.7
TPGC-1	104	23	3	130	80	17.7	2.3
5	184	41	2	227	81.06	18.06	0.88
8	160	29	1	190	84.21	15.26	0.53
11	94	15	4	113	83.2	13.27	3.53
15	184	41	3	228	80.7	17.98	1.32
17	167	32	4	203	82.26	15.76	1.98

APPENDIX 3
QUARTZ – FELDSPAR – LITHICS DATA
PROPORTIONS AS TOTAL NUMBERS AND NORMALIZED PERCENTAGES

Lower Waipara River		Total	Total	normalizing	Normalized values		
Sample#	**Quartz**	**Feldspar**	**Lithics**	**factor**	**Quartz**	**Feldspar**	**Lithics**
W01	206	71	21	298	69.13	23.83	7.04
W03	175	93	29	297	58.92	31.32	9.76
W04	203	56	19	278	73.03	20.14	6.83
W05	222	63	13	298	74.5	21.14	4.36
W06	216	61	15	292	73.97	20.9	5.13
W07	157	48	13	218	72.02	22.02	5.96
W08	105	41	6	152	69.08	26.97	3.95
W09	85	27	3	115	73.91	23.48	2.61
W12	82	22	5	109	75.23	20.19	4.58
W13	73	29	1	103	70.87	28.15	0.98

APPENDIX 3
QUARTZ – FELDSPAR – LITHICS DATA (cont.)
PROPORTIONS AS TOTAL NUMBERS AND NORMALIZED PERCENTAGES

Castle Hill Basin - Broken River		Total	Total	normalizing	Normalized values		
Sample#	Quartz	Feldspar	Lithics	factor	Quartz	Feldspar	Lithics
BR1	257	31	11	299	85.95	10.37	3.68
BR3	244	24	16	284	85.91	8.45	5.63
BR4	214	18	4	236	90.67	7.63	1.7
BR6a	189	23	5	217	87.1	10.6	2.3
Ic3a	199	42	10	251	79.3	16.7	4
Ic3b	165	29	4	198	83.33	14.65	2.02
Ic1	167	41	2	210	79.52	19.52	0.95
Ic2	169	34	1	204	82.84	16.66	0.5
TS-2	217	26	3	246	88.21	10.57	1.22
TS-3	214	34		248	86.29	13.71	

Avoca-Broken River		Total	Total	normalizing	Normalized values		
Sample#	Quartz	Feldspar	Lithics	factor	Quartz	Feldspar	Lithics
AV1	225	52	6	283	79.51	18.37	2.12
AV2	201	48	1	250	80.4	19.2	0.4
Iron Creek -Avoca							
Sample #							
3	242	26	29	297	81.5	8.75	9.75
4	176	24	4	204	86.3	11.75	1.95
7	132	7		139	95	5	
8	186	40	10	236	78.81	16.95	4.24

APPENDIX 3
QUARTZ – FELDSPAR – LITHICS DATA (cont.)
PROPORTIONS AS TOTAL NUMBERS AND NORMALIZED PERCENTAGES

Surveyor's Gully- Malvern		Total	Total	normalizing	Normalized values		
Sample#	**Quartz**	**Feldspar**	**Lithics**	**factor**	**Quartz**	**Feldspar**	**Lithics**
SGM-1	235	20	16	271	86.71	7.38	5.91
Mt.Somers - Woolshed Creek		**Total**	**Total**	**normalizing**	**Normalized values**		
Sample#	**Quartz**	**Feldspar**	**Lithics**	**factor**	**Quartz**	**Feldspar**	**Lithics**
WC1	230	65	4	299	76.92	21.74	1.34
CM1	255	33	3	291	87.63	11.34	1.03
SQ1	248	50	2	300	82.66	16.67	0.67
SQ2	247	48	5	300	82.33	16	1.67
SQ3	158	20	26	204	77.45	9.8	12.75
WC6	156	15	19	190	82.11	7.89	10
BR1	221	59	5	285	77.54	20.71	1.75
WC3	219	70	11	300	73	23.33	3.67

APPENDIX 3
QUARTZ – FELDSPAR – LITHICS DATA (cont.)
PROPORTIONS AS TOTAL NUMBERS AND NORMALIZED PERCENTAGES

APPENDIX 4
GLAUCONITE PROPERTIES – DATA

Glauconite properties		Mature	Nascent	micaceous
Location: Mandamus	Sample #	well rounded		glauconite
Mandamus River - section B	**TPGS-1**	24	1	3
Mandamus River - section B	**5**	34	3	14
Mandamus River - section B	**8**	60	1	2
Mandamus River - section B	**11**	21	1	1
Mandamus River - section B	**15**	27	13	5
Mandamus River - section B	**17**	40	5	2
Mandamus River	**MGS1**	31	11	1
Coal Creek - section A	**CC1a**	11	47	15
Coal Creek - section A	**CC1b**	18	29	11
Coal Creek	**CC3**	25		2
Coal Creek	**CC4a**	29	2	
Coal Creek	**CC4b**	5	4	
Western syncline limb - section C	**Sb2**	9	2	
Western syncline limb - section C	**SB3**	2	2	1

Glauconite properties		Mature	Nascent	Micaceous
Location Mid Waipara River	Sample #	well rounded		glauconite
Doctors Gorge	W03		3	
Doctors Gorge	W04		22	
Doctors Gorge	W06		2	
Mid-Waipara River	W07	7	22	5
Mid-Waipara River	W08	41	2	1
Mid-Waipara River	W09	54	3	
Mid-Waipara River	W12	146	1	1
Mid-Waipara River	W13	177		2

Glauconite properties		Mature	Nascent	micaceous
Locality: Castle Hill Basin		well rounded		glauconite
Broken River	**BR3**		1	
Broken River	**BR4**	46	1	1
Cave Stream	**BR6a**	64		
Whitewater Stream	**Ic3a**	16	14	7
Whitewater Stream	**Ic3b**	77	10	14
Whitewater Stream	**Ic1**	5	3	1
Whitewater Stream	**Ic2**	72	16	

APPENDIX 4
GLAUCONITE PROPERTIES – DATA (cont.)

Glauconite properties		Mature	Nascent	micaceous
Locality: Iron Creek	Sample#	well rounded		glauconite
Iron Creek	3	1	1	
Iron Creek	4	93		
Iron Creek	7	51	8	4
Iron Creek	8	30	21	12
Locality: Avoca	AV1		12	2
Avoca	AV2	44	2	
Locality: Malvern	SGM-1		13	

Glauconite properties		Mature	Nascent	Micaceous
Locality: Mount Somers	Sample#	well rounded		Glauconite
Boyds Road	BR1		3	8
Silica sand quarry	SQ3	1	49	
Woollshed Creek	WC6	6	49	3

APPENDIX 5
OPTICAL-SEM/CL IMAGES

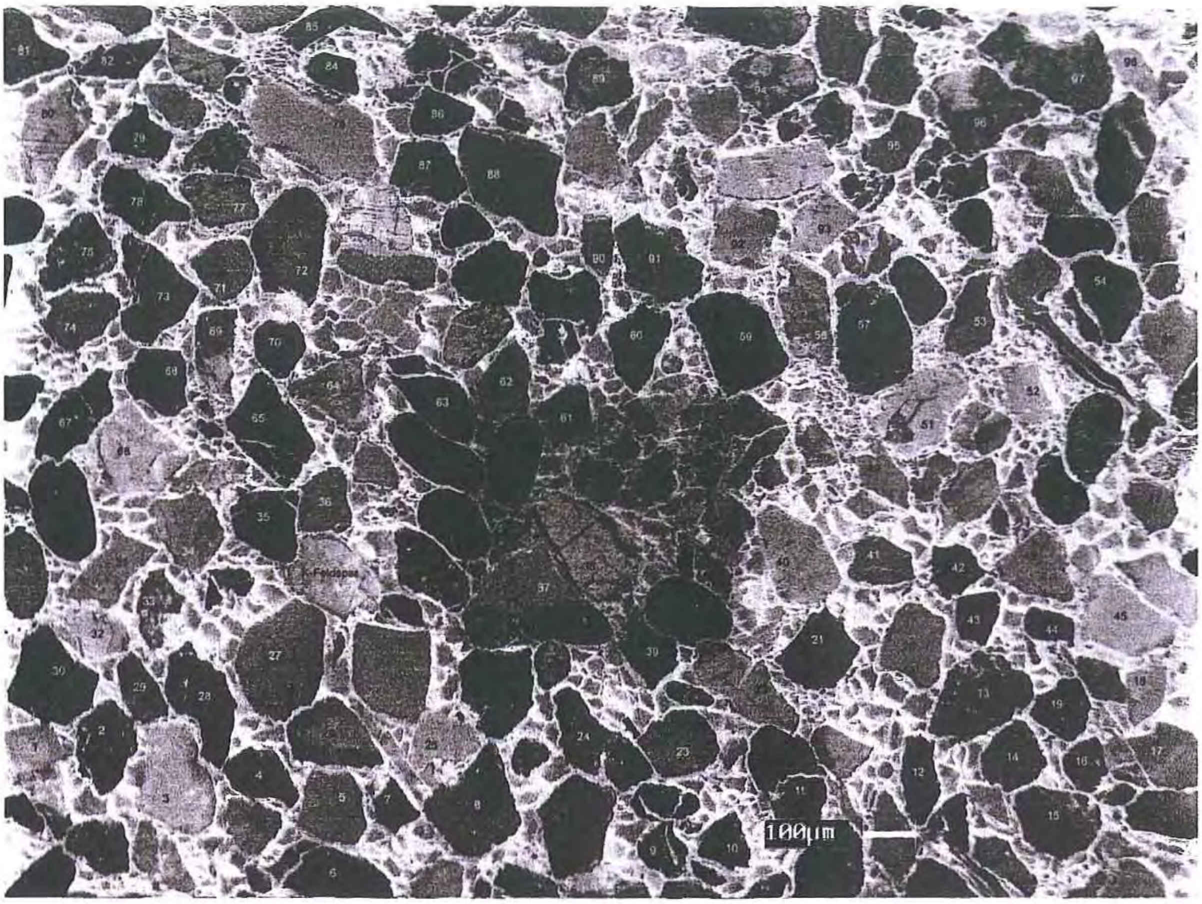

Figure 5.1: Sample TPGS-1, SEM-CL image of the Iron Creek Formation at Mandamus River (type section B).

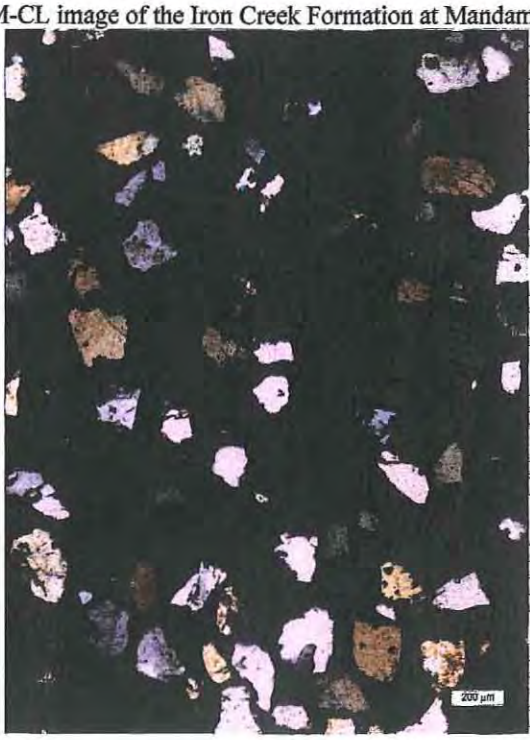

Figure 5.2: Sample TPGS-1, photomicrograph, cross polarized light.

Figure 5.3: Sample 11, SEM-CL image of the Iron Creek Formation at Mandamus River (type section B).

Figure 5.4: Sample 11, photomicrograph, cross polarized light.

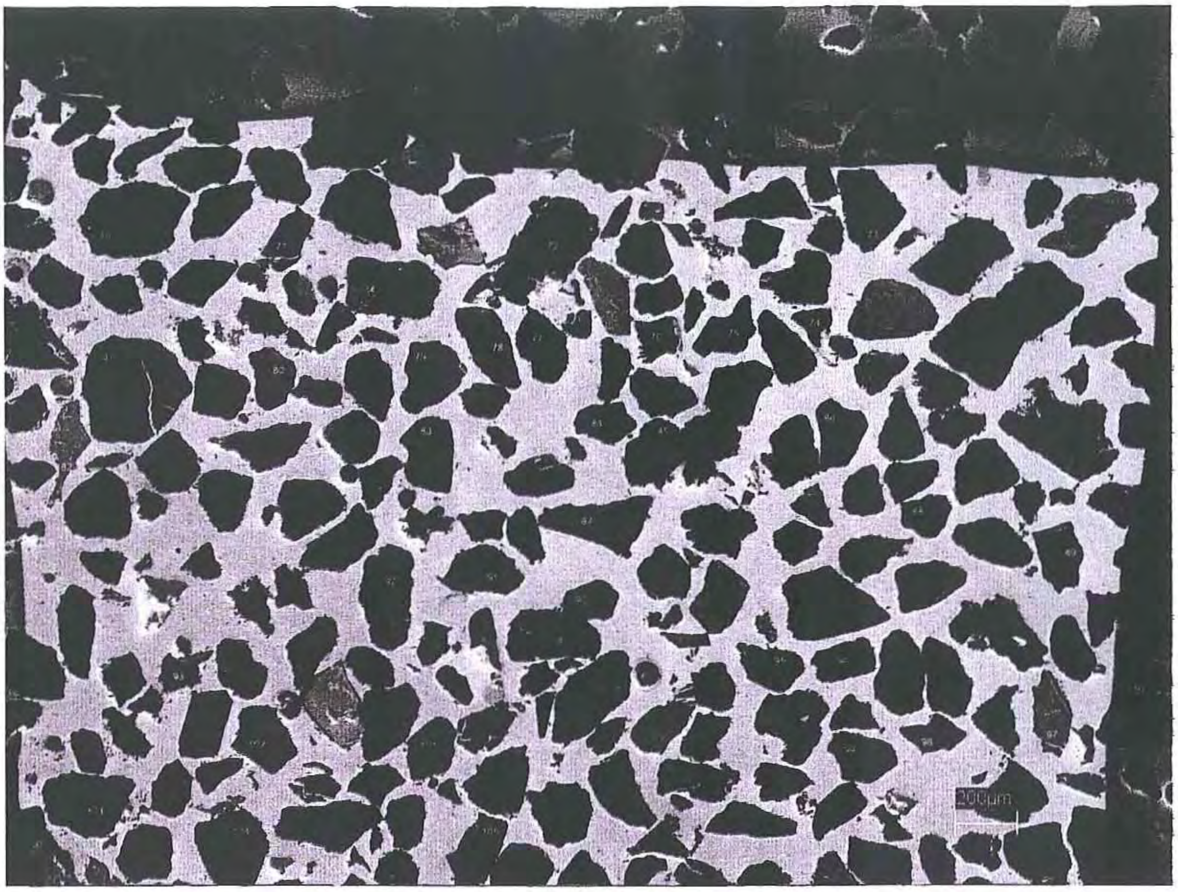

Figure 5.5: SEM-CL image of sample W01 from the Broken River Formation.

Figure 5.6 : Sample W01, petrographic photomicrograph, cross polarized light.

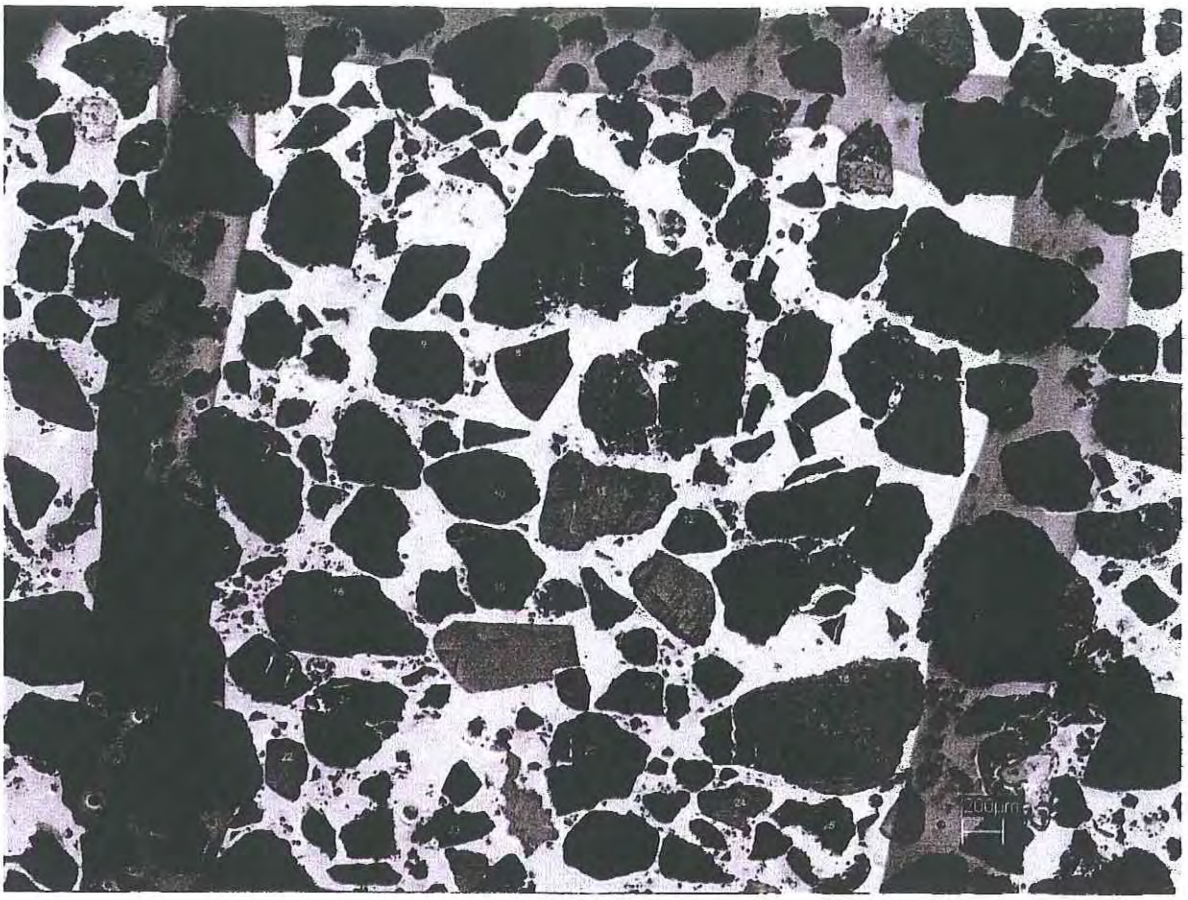

Figure 5.7: SEM-CL image of sample W03, from the Broken River Formation.

Figure 5.8: Sample W03, petrographic photomicrograph, cross polarized light.

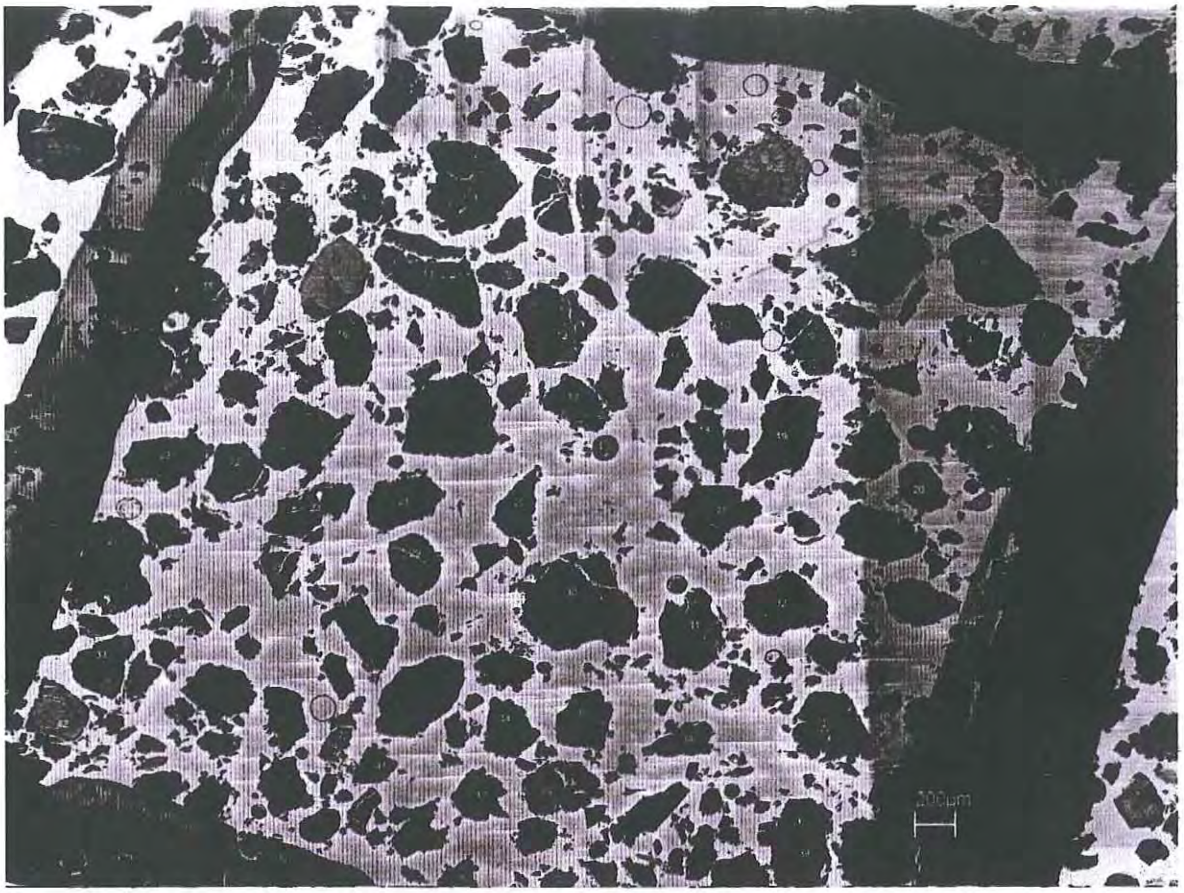

Figure 5.9: SEM-CL image of sample BR1 from the Broken River Formation, displaying equal quartz grains with healed microcracks of plutonic origin and dark CL grains with moderate extinction typical of metamorphic origin.

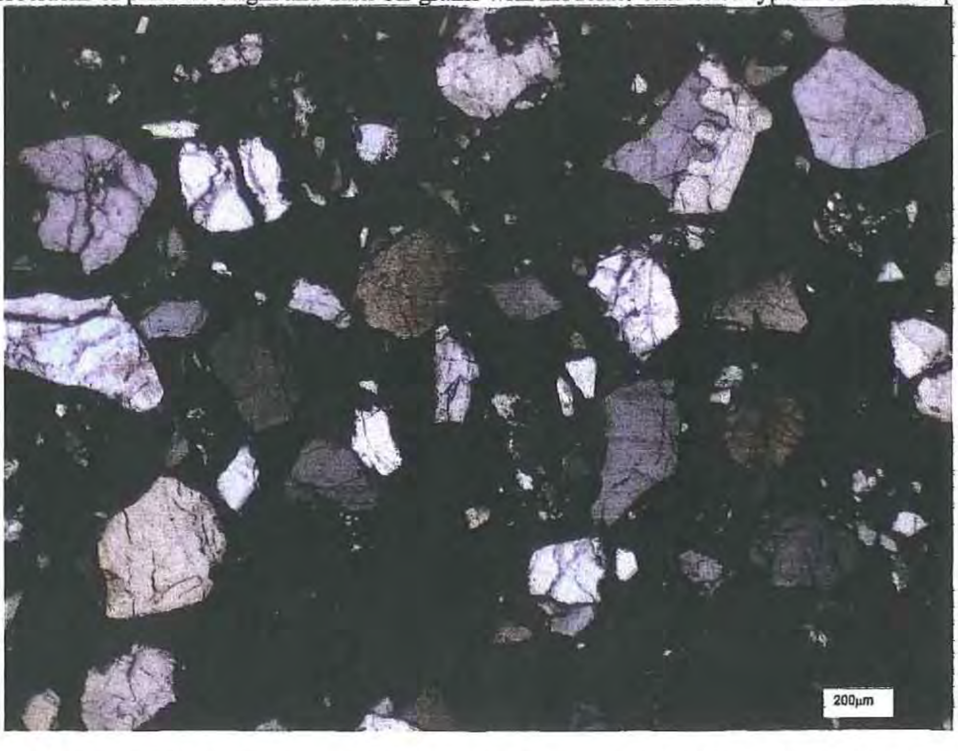

Figure 5.10: Sample BR1, petrographic photomicrograph (cross polarizedl light), grain 5 in the previous Image depicts healed microcracks while under the optical microscope reveals the left side of the grain (see top right corner) is quartz while the right lighter side is orthoclase feldspar. A characteristic plutonic quartz nucleated with a feldspar crystal indicative of the melt biding the two minerals.

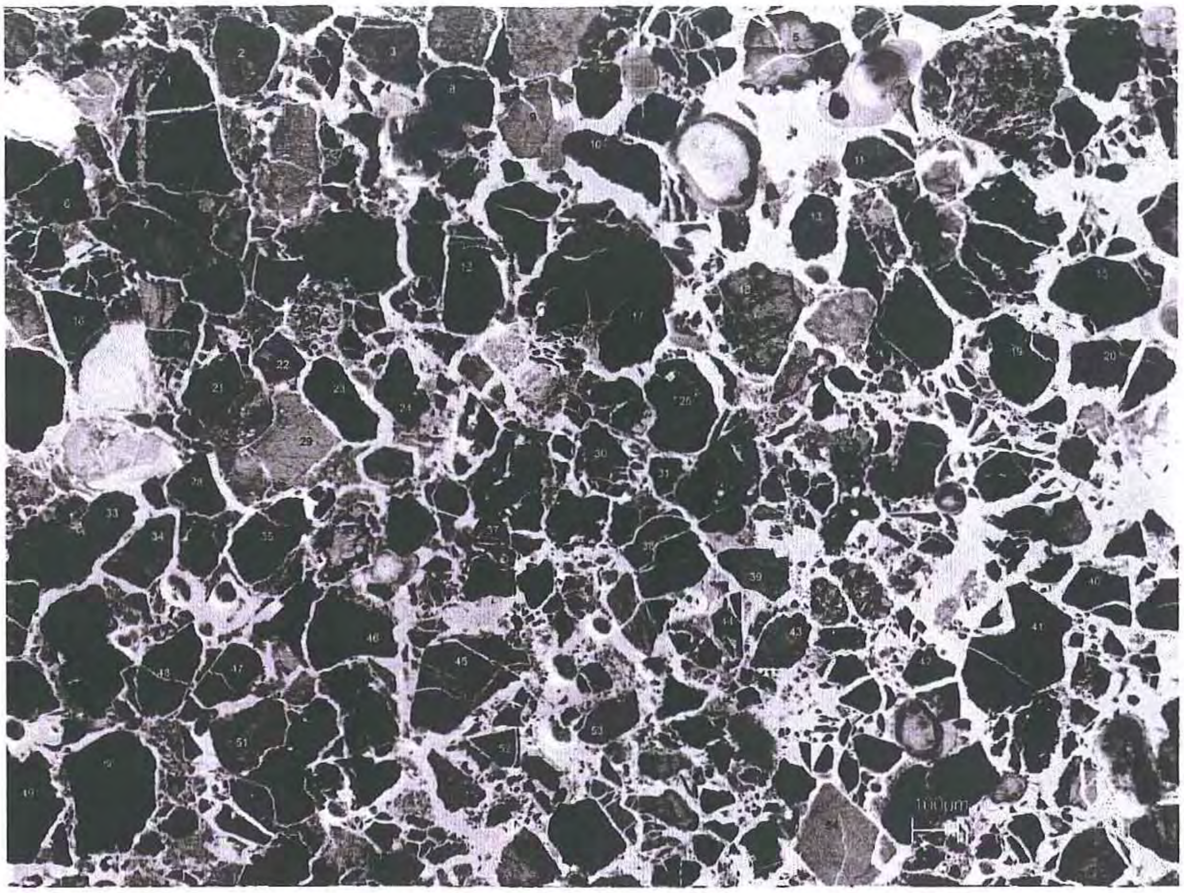

Figure 5.11: SEM-CL image of sample BR4 of the Broken River Formation in Broken River depicting almost equal Proportions of metamorphic versus plutonic quartz grains (see figure 5.28 & appendix 5 for further data).

Figure 5.12: Sample BR4, petrographic photomicrograph, cross polarized light.

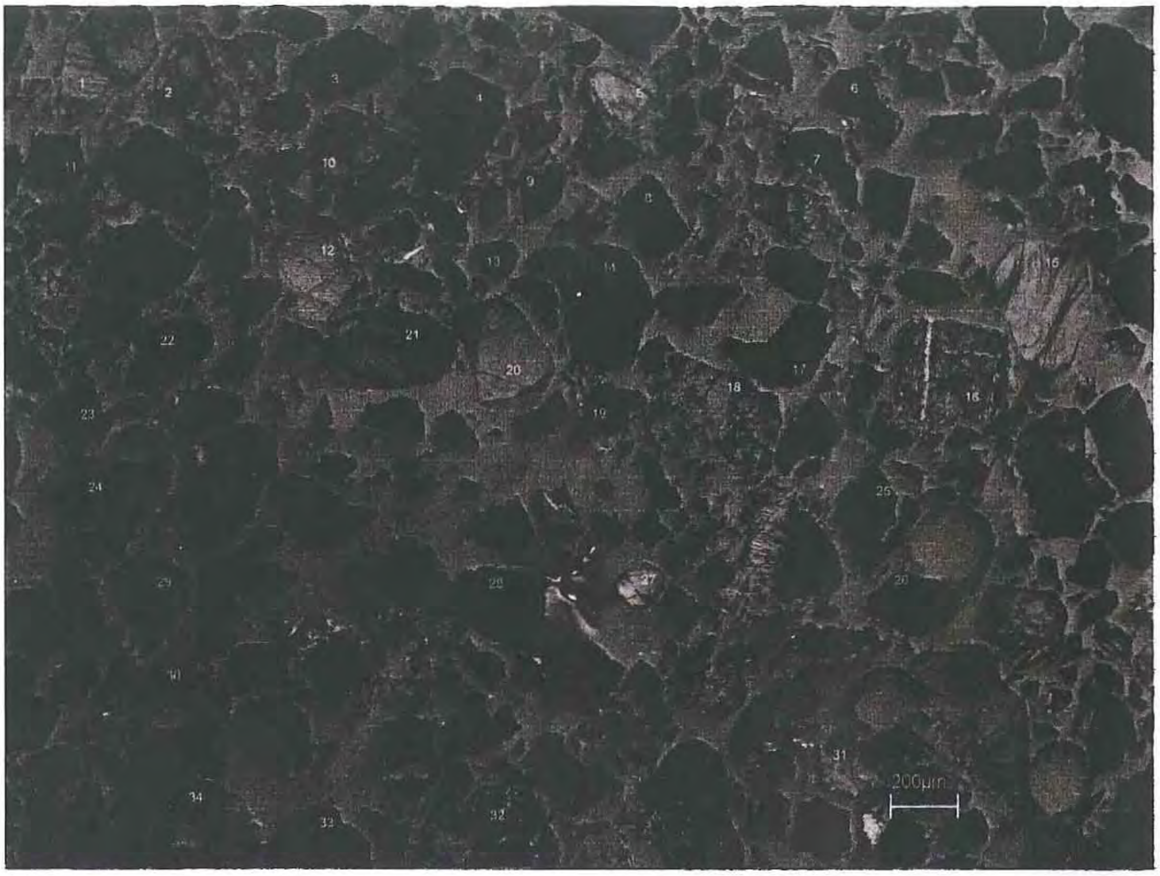

Figure 5.13: SEM-CL image of sample AV1 from Avoca showing abundant plutonic quartz grains with healed microcracks.

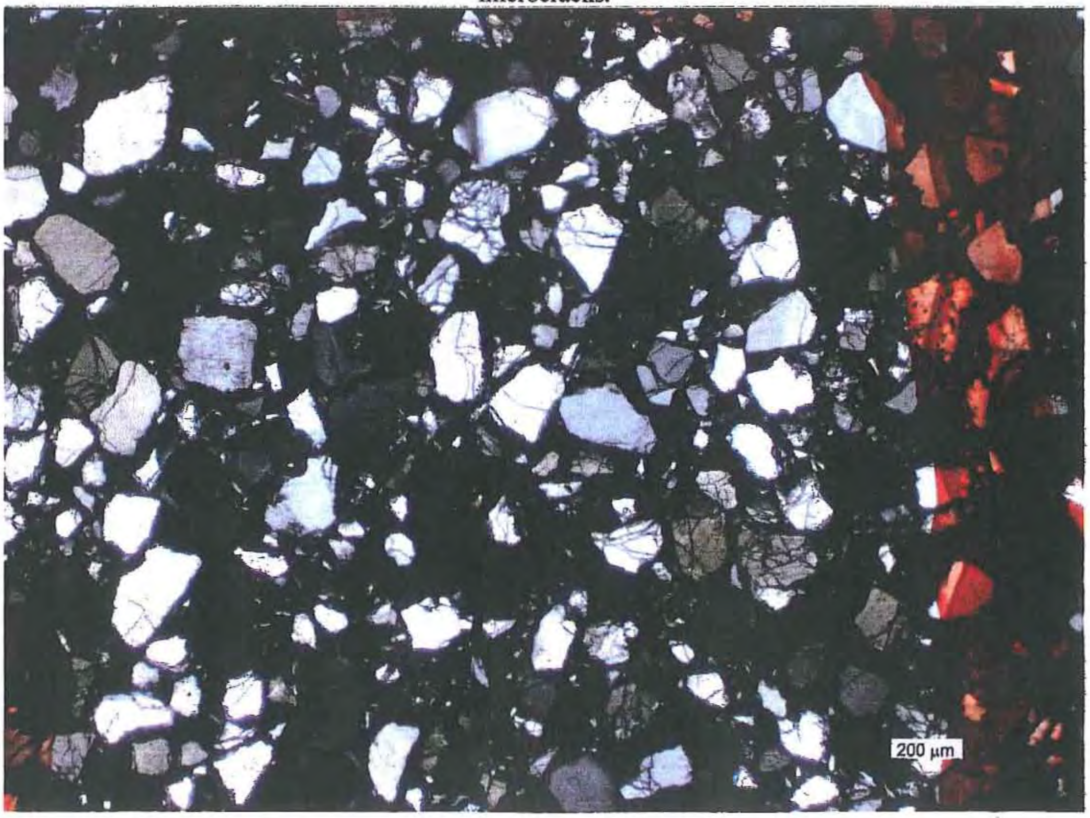

Figure 5.14: Optical petrographic micrograph of sample AV1 from Avoca.

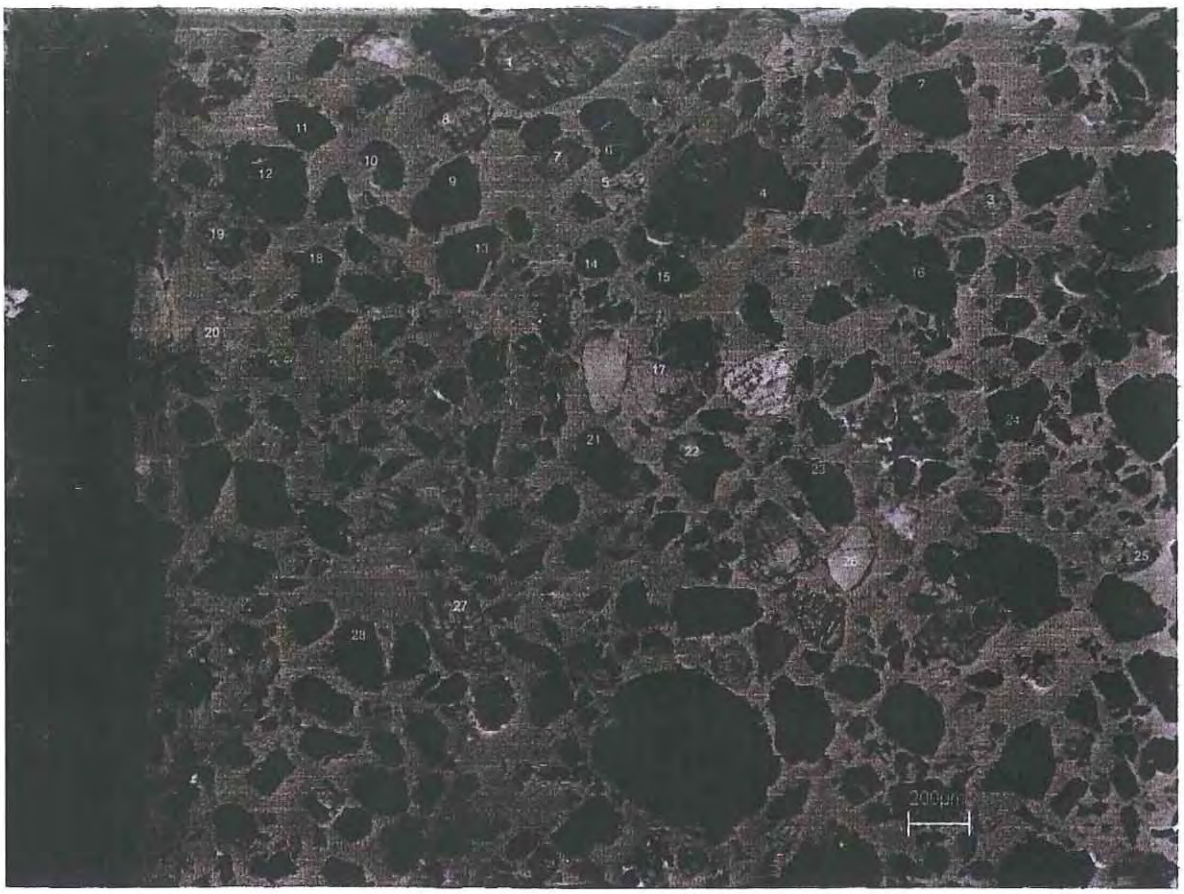

Figure 5.15: SEM-CL image of sample AV2 from Avoca showing plutonic grains with healed microcracks and metamorphic quartz grains with dark CL.

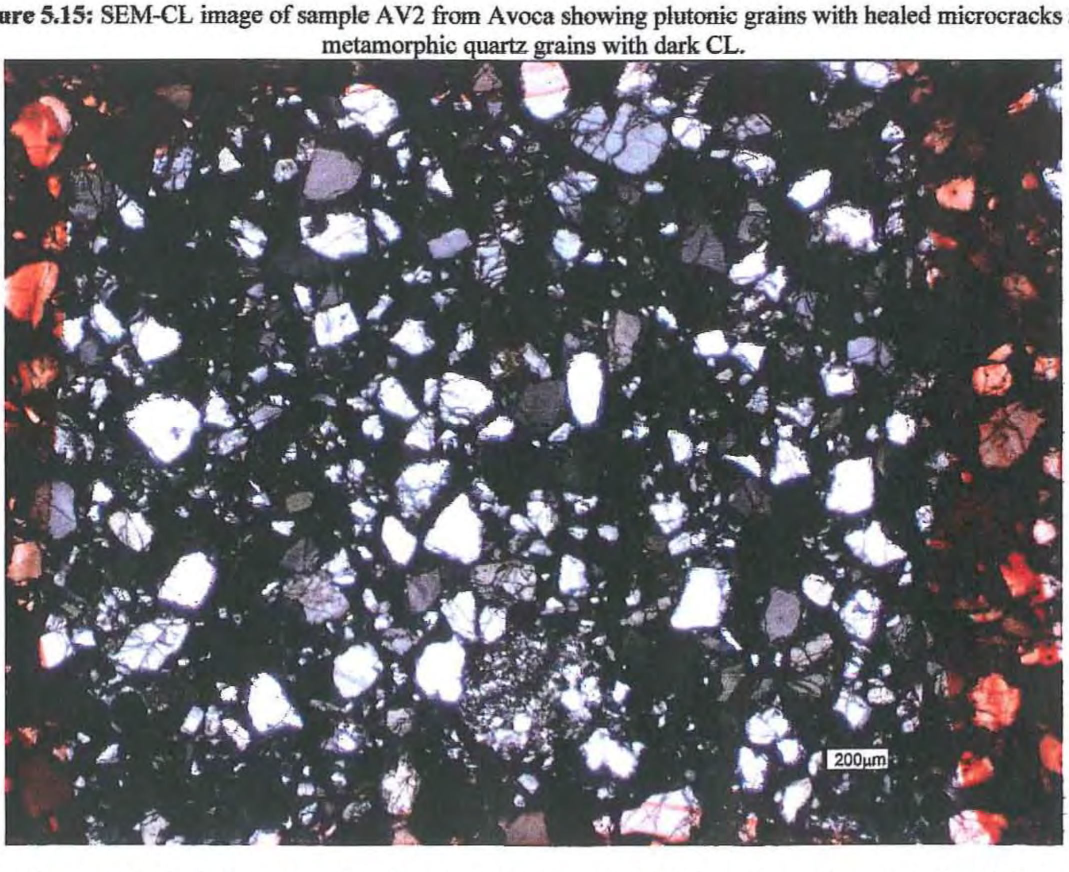

Figure 5.16: Optical petrographic micrograph from sample AV2 from Avoca (cross polarized light).

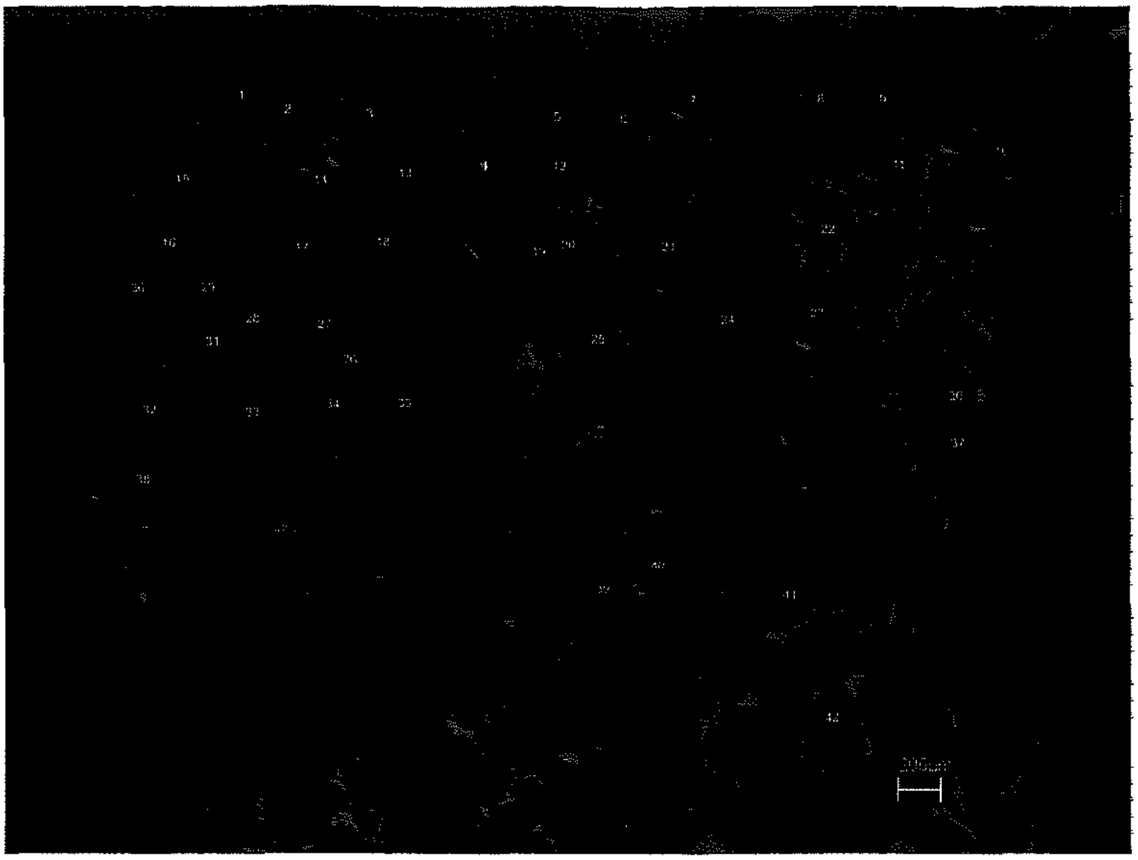

Figure 5.17: SEM-CL image of sample IC3 at Iron Creek (Charteris Bay Sandstone Member-Iron Creek Fm) with bimodal plutonic and metamorphic quartz grains.

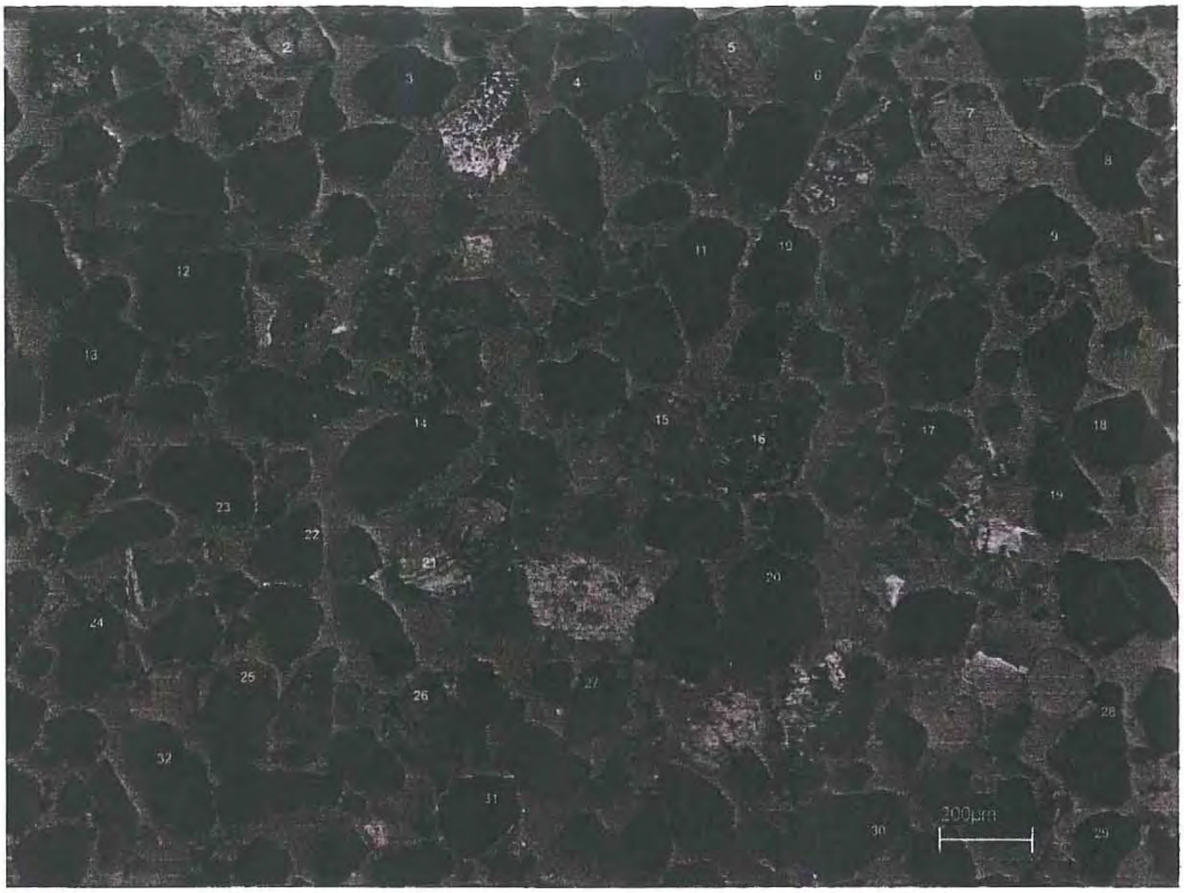

Figure 5.18: SEM-CL image of sample CM1 from Mount Somers Stour Coal Measures Member (coal mine).

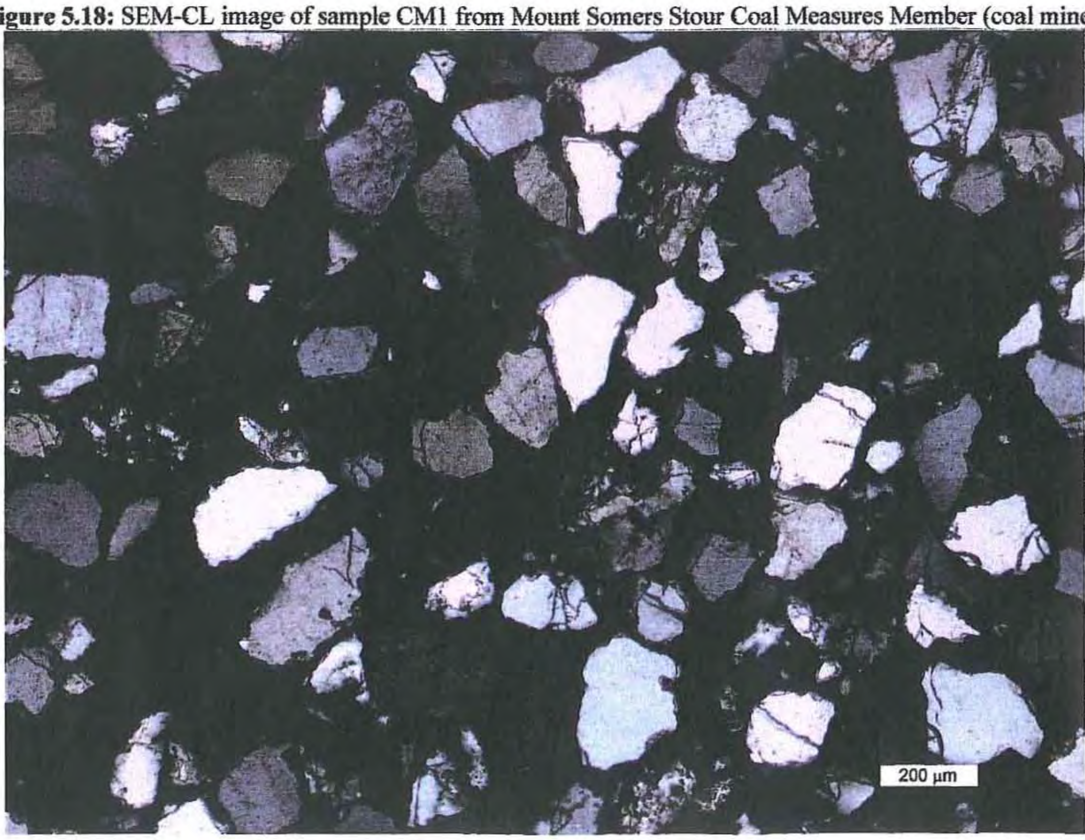

Figure 5.19: Optical petrographic micrograph of sample CM1.

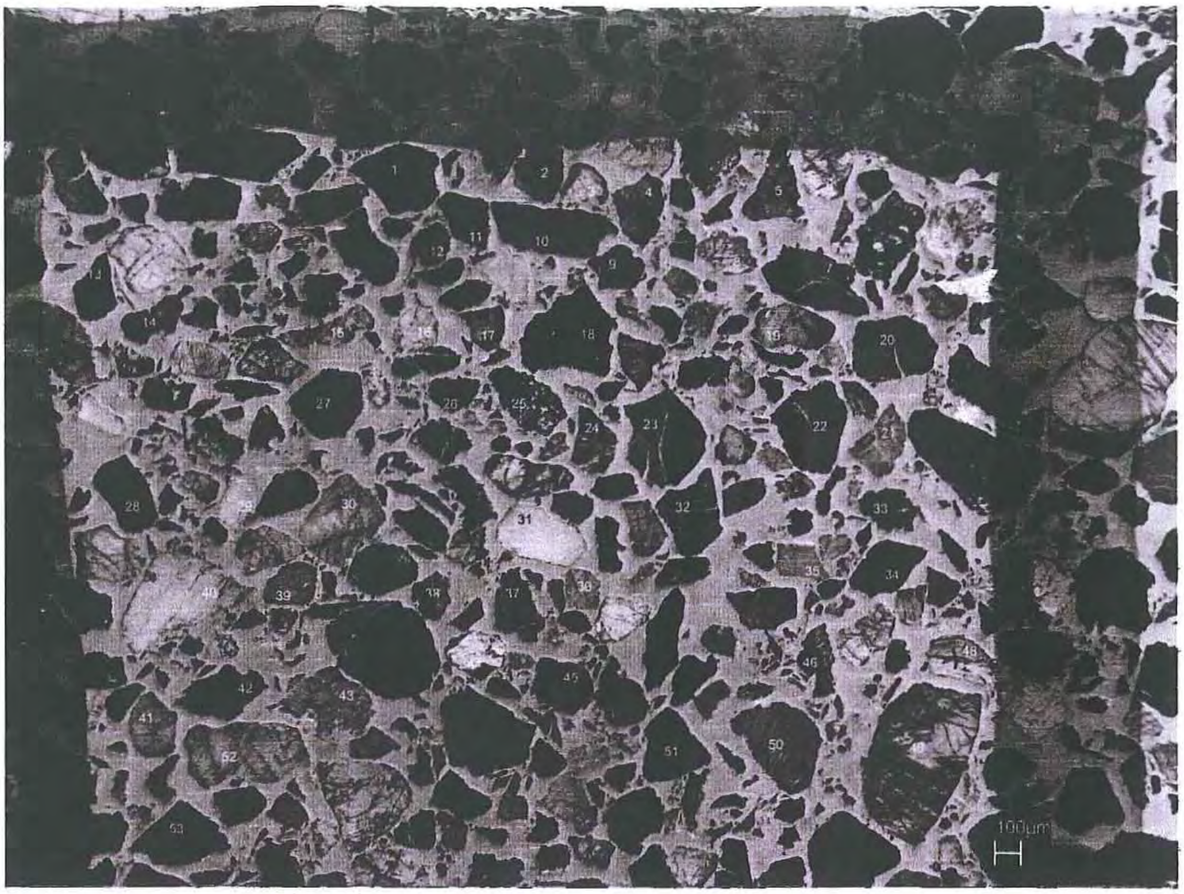

Figure 5.20: SEM-CL image of sample SQ2 from the Blondin Sand Member at the silica sand quarry.

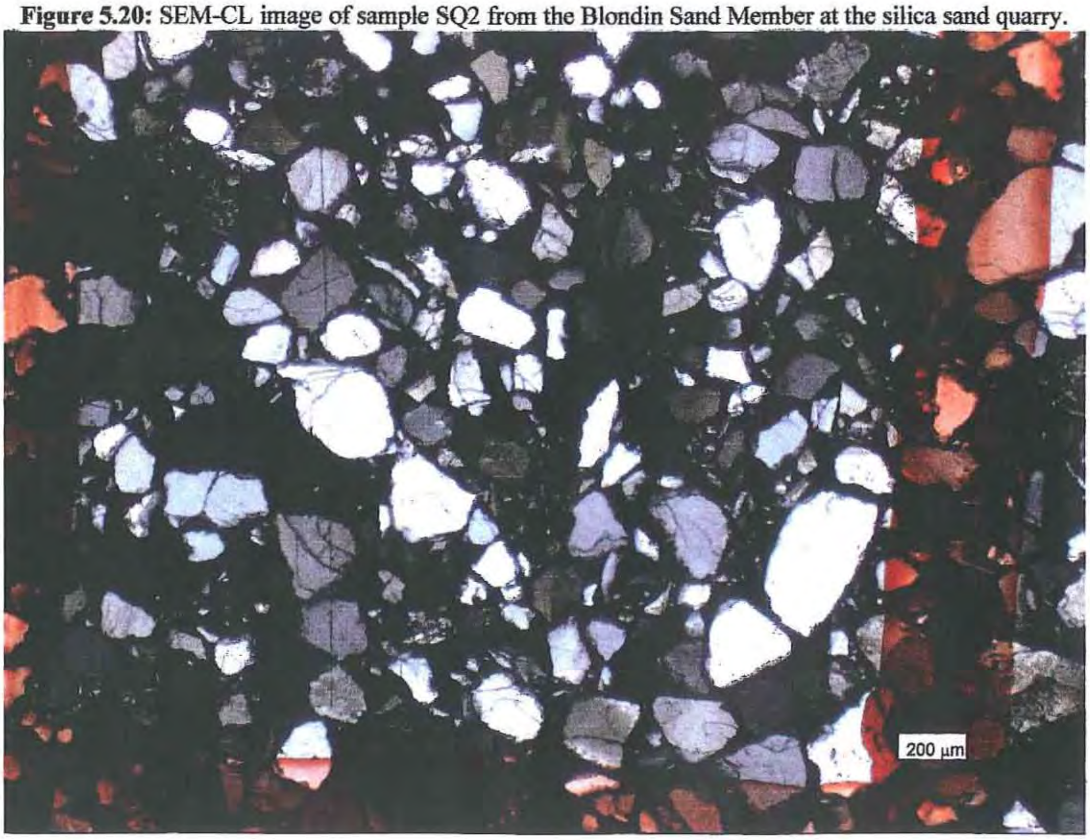

Figure 5.21: Optical petrographic micrograph of sample SQ2.

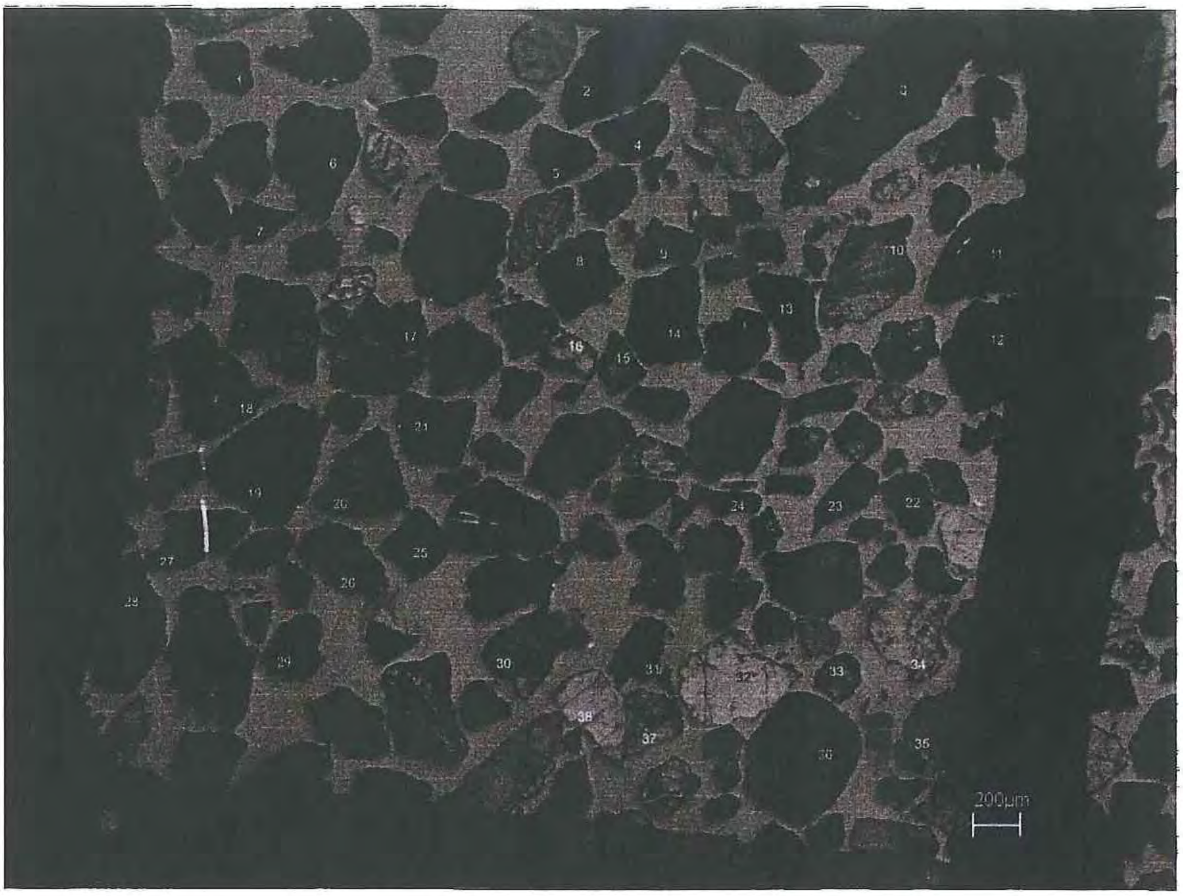

Figure 5.22: SEM-CL image of sample WC3 of Blondin Sand Member from Woolshed Creek.

Figure 5.23: Optical petrogrphic micrograph of sample WC3.

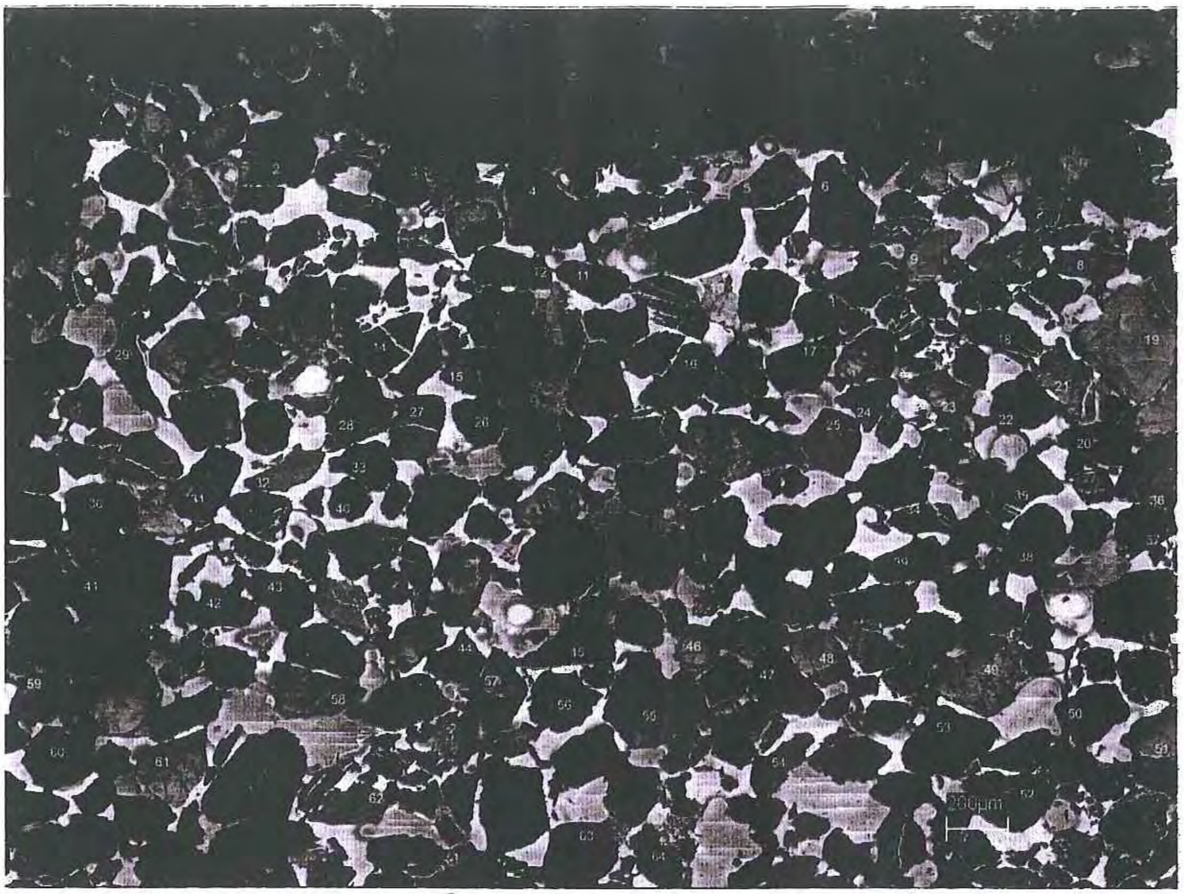

Figure 5.24: SEM-CL image of sample SGM1 from the Conway Formation.

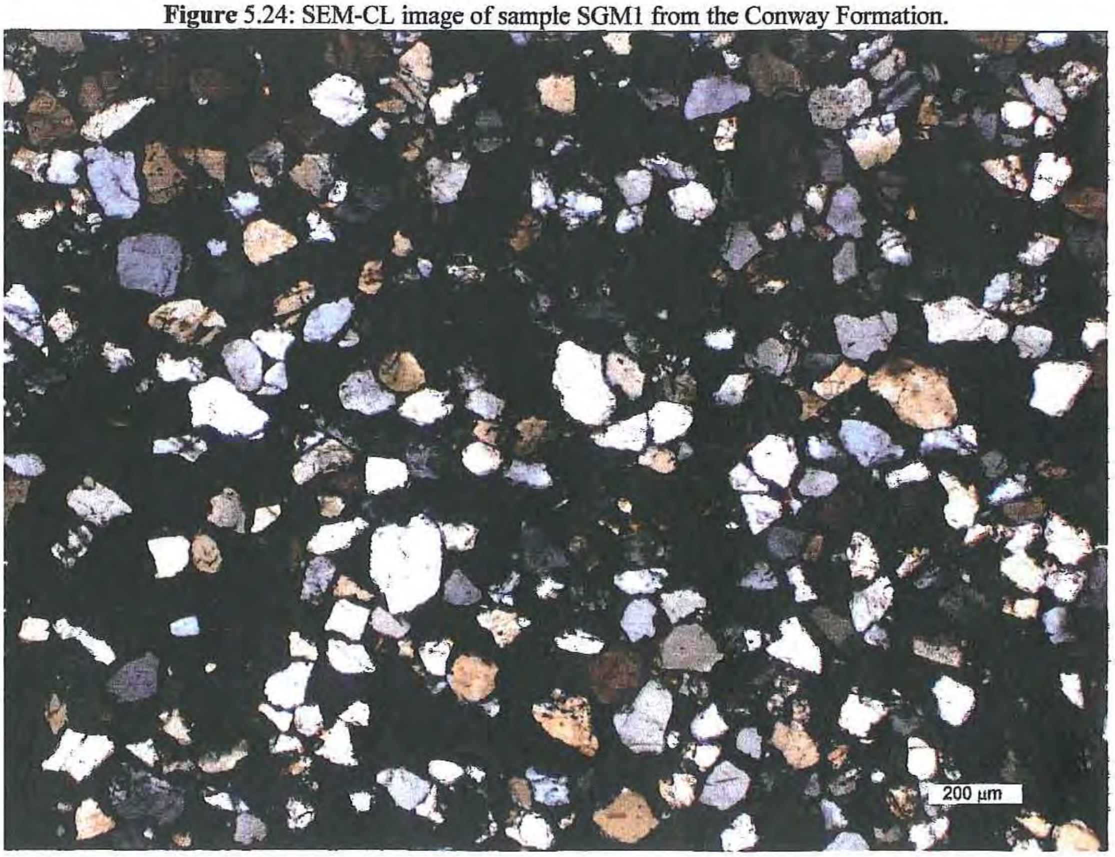

Figure 5.25: Optical petrographic micrograph of sample SGM1 from the Conway Formation.

APPENDIX 6
SEM-CL/OPTICAL MICROSCOPY DATA TABLE STRUCTURE

The usage of cathodoluminescence on quartz grains as a technique for provenance and basin analysis, involved direct grain to grain comparison of quartz with a petrological microscope and subsequent examination of CL features and characteristics with a Leica stereoscan scanning electron microscope.

After the direct grain to grain comparison using the CL features and petrologic features, the data was entered in to an excel spreadsheet. The white columns were common for all types of quartz and include features observed under the petrological microscope; such features include comments (quartz overgrowths, Deformation features, polycrystallinity), grain size, grain properties (shape and rounding) and fracture patterns observed under both microscopes.

The coloured cell blocks were devised to include expected signatures for each type of quartz based on optical microscopy and CL observation. Therefore the framework for quartz types was set based on the previous literature that given features observed under petrologic microscopes correspond to certain CL features and characteristics. The collection of data using this technique followed the flow chart devised by Mathias and Bernet (2005).

For example metamorphic quartz is ascertained by the presence of undulatory extinction sometimes polycrystallinity and the overall dark CL or mottled CL with the scanning electron microscope. Each grain was entered as a single digit initially in the columns common to all types of quartz and then in columns based on extinction patterns and then based on CL features and characteristics. Each grain was entered in each column based entirely on observation irrespective of the set coloured blocks to avoid bias.

Features such as healed microcracks, light to moderate CL intensity and/or patchy CL and straight extinction or weak undulose extinction correspond to plutonic quartz. In the case that a grain displayed all expected CL features typical of plutonic origin but displayed strong undulatory extinction an entry was made into the column of strong undulose extinction in the metamorphic quartz section. After that entry the entire row was coloured with a different colour, hence that grain was interpreted as a plutonic quartz grain that had undergone a period of deformation/metamorphism therefore deformed plutonic. The same principle in the structure of the CL/optical tables was maintained for grains that displayed CL features typical of volcanic origin but had weak or strong undulose extinction. At the end of the description of 105 quartz grains each column was totalled at the base of the table. All grains counted were set in categories at the base of the spreadsheet to their corresponding colour.

Cathodoluminescence-polarized microscope analysis
Sample# TPGS-1
Location Mandamus

	PLUTONIC QUARTZ							METAMORPHIC QUARTZ								VOLCANIC QUARTZ							Fracture patterns Optical/CL features				Grain properties: rounding			shape			grain size in microns					
Grain	homogeneous	patchy	Light CL	Moderate CL	Microcracks-Healed	weak undulose	straight extinction	mottled	dark	Moderate CL	strong undulose	weak undulose	poly-crystalline = <3	poly-crystalline>3	total poly-crystalline	homogeneous	zonation	Light CL	Moderate CL	Open Fractures	Quartz embayments	Straight extinction	Sub-parallel fractures	Dark Shear bands	Random oriented fractures	Grain boundaries	angular	subangular-subrounded	rounded	elongate	platy	spherical	<2000	<1000	<500	<250	<125	Comments
1																	1	1		1		1			1		1				1						1	
2								1		1	1																1			1						1		
3	1		1		1	1																	1					1			1					1		QO
4								1		1	1													1			1				1						1	
5																1			1			1	1					1			1						1	QO
6									1		1														1				1	1						1		QO
7									1			1											1				1				1						1	QO
8																1			1	1		1	1				1				1					1		
9									1			1																1				1					1	
10									1		1																1				1						1	
11	1			1			1																1					1				1					1	
12									1			1											1					1		1						1		
13								1		1	1														1			1				1				1		
14	1			1	1	1																	1					1				1					1	
15								1				1													1			1				1				1		QO
[illegible]																																						
17		1	1		1	1																	1	1			1					1				1		QO
18		1			1	1																	1		1		1			1							1	QO
19								1		1		1																1				1					1	QO
20		1	1			1																						1			1						1	
21									1		1		1														1					1				1		
[illegible]																																						
23								1				1																1				1					1	QO
24								1				1															1			1					1			
25	1		1		1		1																						1		1						1	
26																	1					1			1		1				1					1		QO
27								1			1			1														1				1			1			QO
28									1		1																1			1					1			Polygonized Qtz
29								1				1															1			1							1	
30								1			1			1													1				1					1		QO
31		1	1		1	1																			1		1			1						1		QO
32		1	1		1		1																		1			1			1						1	
33								1			1																1				1					1		
34		1	1		1	1																			1		1				1					1		QO
35									1			1											1		1		1				1					1		
36	1		1		1		1																					1			1						1	QO
37	1		1		1		1																					1		1						1		QO
38	1		1		1		1																					1		1					1			QO
39									1		1																1				1						1	QO
40		1	1		1	1																					1			1					1			QO
41	1			1	1	1																	1		1		1				1						1	
42									1			1															1				1						1	
43									1							1						1					1			1							1	QO
44									1			1															1			1							1	QO
45																1		1				1	1				1			1						1		QO
46		1	1		1	1																	1				1				1					1		QO
47		1	1		1	1																			1		1					1					1	QO
[illegible]																																						
49		1	1		1		1																		1		1			1							1	QO
50		1	1		1	1																					1			1							1	
51		1	1		1	1																						1			1					1		QO
52		1	1		1		1																				1			1						1		QO
[illegible]																																						
54								1			1																	1				1				1		Deformed lamellae
55								1			1														1		1					1				1		QO
56																1			1			1					1			1							1	
57									1		1																	1		1						1		
58		1	1		1	1																					1			1						1		
59									1			1																1		1						1		
60								1				1															1				1					1		
61																1			1			1					1			1							1	QO
62											1					1											1			1							1	
63																1			1			1							1	1						1		QO
64								1			1																1				1					1		
65									1			1													1		1			1						1		QO
66		1	1		1		1																				1			1						1		QO
67											1					1									1		1			1						1		Deformed lamellae
68									1		1																		1			1					1	
69								1				1															1			1						1		QO
70									1			1																	1			1					1	
71	1			1	1		1																					1				1					1	QO
72		1		1	1	1																						1		1						1		
73																1			1			1					1				1					1		
74									1			1																1				1				1	1	QO
75								1				1																1			1					1		QO
76		1	1		1		1																		1		1			1					1			QO
[illegible]																																						QO
78									1			1													1		1			1						1		
79									1			1															1				1					1		QO
80		1	1		1	1																					1			1					1			
81								1				1															1				1						1	
82									1			1													1		1			1						1		
83		1	1		1	1																					1				1					1		QO
84									1			1															1			1							1	
85									1			1															1			1							1	
86									1			1																1				1					1	
87									1			1													1		1				1						1	
88								1			1														1			1			1				1		1	
89								1			1														1				1			1					1	
90	1		1		1	1																	1				1			1							1	
91																1						1						1			1				1			
92		1	1		1		1																					1				1					1	
93		1	1		1		1																				1			1							1	
94								1			1		1															1				1				1		
95																1			1			1						1		1							1	
96								1			1																1				1					1		Polygonized Qtz
97								1			1																	1			1				1			
98	1		1		1	1																			1		1			1							1	
99									1		1														1		1				1					1		
100		1		1	1	1																			1			1		1					1			
101	1			1	1		1																1		1			1				1					1	
102	1			1	1		1																		1		1			1					1			
103									1		1																1				1						1	
104		1	1		1		1																				1			1						1		
105								1			1												1				1				1						1	
	13	26	29	10	39	21	17	27	27	4	29	26	2	2	0	12	2	2	7	2	0	12	16	2	30	0	63	36	6	45	37	23	0	0	13	44	48	

PLUTONIC QTZ : 36
DEFORMED PLUTONIC QTZ : 5
TOTAL : 41

METAMORPHIC QTZ Total: 60

VOLCANIC QTZ Total: 12
DEFORMED VOLCANIC QTZ Total : 2
TOTAL : 14

athodoluminescence-polarized microscope analysis
ample# 11
ocation Island Hills-Type section

	PLUTONIC QUARTZ							METAMORPHIC QUARTZ								VOLCANIC QUARTZ							Grain properties						rounding		shape			grain size in microns					Comments
rain	homogeneous	patchy	Light CL	Moderate CL	Microcracks -Healed	weak undulose	straight extinction	mottled	dark	Moderate CL	strong undulose	weak undulose	poly-crystalline = <3	poly-crystalline>3	total poly-crystalline	homogeneous	zonation	Light CL	Moderate CL	Open Fractures	Quartz embayments	Straight extinction	Parallel/Sub-parallel fracture	Dark shear bands	Random oriented fractures	Grain boundaries	angular	subangular-subrounded	rounded	elongate	medium	spherical	<2000	<1000	<500	<250	<125	
1		1		1	1		1																1						1			1		1				
2								1		1		1											1					1			1					1		
3									1			1																	1			1						1	
4								1	1			1											1						1		1					1		
5								1	1		1			1															1			1						1	
6									1			1																	1			1						1	
7									1			1																1				1						1	
8								1		1	1												1						1			1						1	
9								1	1		1												1						1			1					1		
10								1	1			1											1					1				1					1		
11																																						
12		1		1			1																					1				1						1	
13																	1		1			1					1					1						1	
14								1	1			1																	1			1						1	
15								1	1			1															1					1						1	
16									1			1																1				1						1	
17									1		1																		1			1			1			Polygonized
18																1			1		1	1					1					1				1		
19		1	1		1		1																1					1			1				1			
20								1			1																		1			1					1		
21									1		1			1												1			1			1					1		
22		1		1			1																			1			1			1			1			
23								1	1			1											1						1			1						1	
24								1	1			1											1						1			1					1		
25								1		1		1													1				1			1						1	
26									1			1															1				1							1	
27									1		1		1															1				1						1	
28		1		1			1																1						1			1						1	
29		1	1				1																1						1	1							1		
30		1		1	1	1																	1				1			1					1			
31		1					1																		1	1	1				1							1	
32		1		1			1																					1		1					1			
33									1			1																1			1							1	
34																																						Polygonized
35									1			1											1					1		1							1		
36									1		1																		1			1					1		
37									1			1														1		1				1						1	
38								1				1																	1			1					1		
39																																						
40								1	1			1														1	1				1					1		
41		1		1	1	1																			1				1			1			1			
42								1	1		1																		1			1					1		Polygonized
43									1			1																	1	1							1		
44		1	1		1		1																1					1			1					1		
45									1		1															1			1			1					1		
46		1		1	1		1																					1				1					1		
47		1		1	1		1																1				1			1						1		
48								1		1		1																	1			1						1	
49		1		1		1																					1				1							1	
50									1			1															1					1						1	
51									1			1																	1			1						1	
52								1	1		1		1															1				1						1	
53																																						
54									1			1																	1			1			1			
55									1			1																1				1					1		
56		1		1	1	1																	1						1	1					1			
57																																						
58									1		1																	1		1					1			Polygonized
59									1		1			1															1	1				1				Elong.host crystals cren.
60									1		1																		1	1				1				Polygonized, Def. bands
61		1		1	1	1																							1			1			1			
62									1			1																	1		1					1		
63									1		1			1												1			1			1		1				Recryst. Qtz
64	1			1			1																				1					1				1		
65									1			1																1			1					1		
66		1	1				1																						1			1			1			
67									1		1															1	1				1						1	
68									1			1														1		1				1					1	
69		1		1	1		1																					1		1						1		
70								1				1																	1			1					1		
71								1						1														1				1					1		Polyhedral,polygonal
72																																						
73									1			1																1				1					1		
74		1		1	1	1																							1			1					1		
75									1			1																1				1						1	
76																																						
77		1		1		1																			1	1					1					1		
78	1			1			1																				1				1							1	
79									1		1		1														1					1						1	
80								1			1		1																1		1						1		
81									1		1																1			1							1		
82								1				1															1				1					1			
83									1		1			1															1	1						1			Polygonized Qtz
84	1		1		1		1																				1			1								1	
85		1	1				1																						1			1					1		
86		1	1				1																				1				1						1		
87																1		1		1	1	1						1				1					1		
88		1		1	1		1																					1			1						1		
89									1			1																	1		1						1		
90								1				1																	1		1							1	
91									1		1		1																1		1							1	Polygonized Qtz
92									1		1																	1			1							1	
93									1		1												1						1			1		1				Polygonized Qtz
94										1	1																		1			1			1			Polygonized Qtz
95								1			1																1				1				1			Polygonized Qtz
96								1			1															1	1					1					1		
97		1		1	1		1																1			1		1			1					1		
98																																						
99		1		1		1																	1						1		1				1			
100									1		1												1		1			1		1						1		
101		1		1	1		1																					1		1					1			
102								1				1																	1			1					1		
103								1				1																	1			1						1	
104								1				1											1						1			1						1	
105									1		1			1														1			1					1		Polygonized Qtz
	3	33	7	25	16	10	23	35	48	5	30	38	5	7	0	2	1	1	2	1	2	3	23	0	5	13	24	31	50	19	26	60	0	6	19	45	35	

PLUTONIC QTZ : 29
DEFORMED PLUTONIC QTZ : 8
TOTAL PLUTONIC GRAINS : 37

METAMORPHIC QUARTZ Total: 84

VOLCANIC QUARTZ Total: 3

Cathodoluminescence-polarized microscope analysis
Sample# CC3
Location : Mandamus - Coal Creek

Grain	PLUTONIC QUARTZ							METAMORPHIC QUARTZ								VOLCANIC QUARTZ											Grain properties: rounding			shape			grain size in microns					Comments
	homogeneous	patchy	Light CL	Moderate CL	Microcracks -Healed	weak undulose	straight extinction	mottled	dark	Moderate CL	strong undulose	weak undulose	poly-crystalline = <3	poly-crystalline >3	total poly-crystalline	homogeneous	zonation	Light CL	Moderate CL	Open Fractures	Quartz embayments	Straight extinction	Parallel/Sub-parallel feature	Dark shear bands	Random oriented fractures	Grain boundaries	angular	subangular-subrounded	rounded	elongate	platy	spherical	<2000	<1000	<500	<250	<125	
1	1			1	1		1																						1	1				1				
2									1		1			1															1			1		1				Polygonal Qtz
3																1			1			1				1			1			1				1		
4								1			1															1	1				1						1	
5									1		1																		1	1				1				
6								1			1														1				1			1			1			
7									1		1				1														1	1					1			Crenulated-polygonized QTZ
8											1				1											1			1			1		1				Polygonal Qtz
9	1			1	1	1																							1		1				1			
10									1		1		1													1			1			1				1		
11									1		1		1													1			1			1				1		
12																1			1			1	1				1			1						1		
13								1				1																	1			1				1		
14									1		1				1														1			1		1				Polygonal Qtz
15									1		1															1	1					1				1		
16		1	1		1		1																						1		1				1			
17									1		1				1													1				1		1				Polygonal-Polyhedral Qtz
18									1		1				1														1			1	1					
19									1		1				1														1			1	1					
20	1		1		1		1																		1	1			1			1		1				
21								1			1														1	1		1				1			1			
22									1			1																	1			1				1		
23									1		1																		1			1				1		
24									1		1																	1				1			1			
25								1			1														1	1			1			1		1				
26									1		1				1														1			1		1				Polyhedral Qtz
27									1		1				1											1			1			1	1					Polyhedral Qtz
28								1													1	1							1			1		1				
29																1					1	1							1			1			1			
30	1			1	1		1																						1	1			1					
31									1		1		1																1		1					1		
32									1		1				1														1	1			1					Polygonized Qtz Crenulated -
33	1			1	1		1																						1			1				1		
34									1		1				1														1			1		1				Polyhedral Qtz
35	1			1	1		1																					1			1				1			
36	1			1	1		1																						1		1					1		
37									1		1				1														1			1	1					Polygonized- Crenulated Qtz
38	1			1	1		1																						1		1				1			
39									1		1				1														1	1				1				Recrystallised Qtz
40									1		1																		1			1				1		
41									1			1																1				1				1		
42																1			1			1					1				1						1	
43									1		1																1				1						1	
44									1			1																	1			1					1	
45									1			1																	1	1					1			
46									1			1																1			1					1		
47																																						
48	1			1	1		1																				1				1					1		
49								1			1																1			1							1	
50									1		1				1														1			1		1				Polyhedral Qtz
51									1			1													1				1			1				1		
52									1		1																1			1							1	
53																																						
54									1		1																		1			1			1			
55									1			1																1				1				1		
56	1			1	1	1																							1			1					1	
57									1			1																	1	1						1		
58								1				1															1				1						1	
59	1			1	1	1																							1			1				1		
60	1			1	1		1																						1			1				1		
61	1			1	1		1																						1			1				1		
62	1			1	1		1																					1			1				1			
63	1			1	1		1																						1			1					1	
64									1			1																	1			1				1		
65									1			1															1				1						1	
66									1			1															1				1						1	
67									1		1				1														1			1	1					Polygonized- Crenulated Qtz
68									1		1																		1	1					1			
69																1			1			1						1				1					1	
70	1			1	1		1																						1			1				1		
71									1		1				1													1				1				1		Polygonized Qtz
72	1			1	1		1																						1	1				1				
73	1		1		1		1																						1	1					1			
74	1			1	1		1																						1			1			1			
75																1			1			1							1		1					1		
76	1			1	1		1																					1				1			1			
77									1			1																1				1					1	
78									1		1																		1			1				1		
79									1		1																		1			1			1			
80									1		1																		1			1		1				
81	1			1	1	1																						1			1					1		
82									1		1																		1		1					1		
83									1		1																1				1					1		
84									1		1																1			1						1		
85									1		1																		1			1				1		
86									1			1																	1	1						1		
87																																						
88									1		1																		1			1					1	
89																																						
90								1				1															1				1					1		
91																																						
92									1		1																	1		1						1		
93									1			1																	1			1			1			
94									1		1																	1			1				1			
95									1			1															1				1					1		
96								1				1															1				1				1			
97																																						
98									1		1																		1	1						1		
99									1		1																1			1							1	
100									1		1																1			1						1		
101																																						
102									1		1																1					1					1	
103									1		1				1														1			1		1				
104	1			1	1	1																						1				1					1	
105	1			1	1	1											1											1			1					1		
TOTAL	26	5	3	28	31	7	21	14	57	0	50	20	3	1	16	6	1	0	5	0	2	7	1	0	5	10	21	18	66	23	24	58	7	17	23	41	17	

PLUTONIC QTZ : 24
DEFORMED PLUTONIC QTZ : 7
PLUTONIC QTZ TOTAL : 31

METAMORPHIC QTZ TOTAL : 67

VOLCANIC QTZ : 6
DEFORMED VOLCANIC QTZ : 1
VOLCANIC TOTAL : 7

Cathodoluminescence-polarized microscope analysis
Sample# CC4b
Location Mandamus - Coal Creek

	PLUTONIC QUARTZ							METAMORPHIC QUARTZ								VOLCANIC QUARTZ							Grain properties				rounding			shape			grain size in microns					Comments
Grain	homogeneous	patchy	Light CL	Moderate CL	Microcracks-Healed	weak undulose	straight extinction	mottled	dark	Moderate CL	strong undulose	weak undulose	poly-crystalline = <3	poly-crystalline>3	total poly-crystalline	homogeneous	zonation	Light CL	Moderate CL	Open Fractures	Quartz embayments	Straight extinction	Parallel-Subparallel feature	Dark shear bands	Random oriented fractures	Grain boundaries	angular	subangular-subrounded	rounded	elongate	platy	spherical	<2000	<1000	<500	<250	<125	
1																												1				1					1		
2		1	1			1																								1			1			1			
3	1		1				1																						1				1					1		
4																														1	1					1			
5																										1			1	1			1					Recrystallised Qtz
6																										1			1			1		1					
7																										1			1			1		1					
8		1		1			1																						1			1			1			
9		1	1		1	1																	1				1			1		1				
10																												1				1			1					
11																										1			1			1			1			Recrystallised Qtz
12		1	1				1																				1				1						1	
13																													1			1					1		
14																										1			1			1		1					
15																										1			1			1		1					Polygonized Qtz
16																														1			1			1			
17																														1			1			1			
18																														1			1	1						
19		1	1			1																						1			1					1		
20	1		1				1																					1				1				1		
21																														1			1					1	
22																														1			1					1	
23		1	1		1	1																				1				1						1	
24																													1				1				1		
25																									1				1			1		1					
26		1	1		1		1																1			1				1			1			
27																										1			1			1			1				
28																									1	1			1	1			1					Polygonized Qtz
29																									1	1	1				1					1		
30																									1	1			1			1				1		
31																									1	1			1			1		1					Polygonized Qtz
32		1	1				1																				1				1					1		
33																													1			1					1		
34		1		1		1																						1			1						1		
35																									1	1		1			1				1			
36																									1				1	1			1					Polygonized Qtz
37																									1	1			1			1		1					Polygonized Qtz
38																									1	1		1			1				1			
39																														1			1			1			Polygonized Qtz
40																														1		1			1					
41																									1			1		1				1					
42		1		1		1																							1		1			1					
43																									1				1			1		1					
44																														1			1					1	
45																												1				1						1	
46		1		1		1																					1				1						1	
47		1		1		1																						1			1					1		
48																														1		1			1					Polyhedral Qtz
49	1			1			1																1				1		1					1		
50																										1			1		1					1		
51	1			1			1																1			1		1					1			
52																									1				1			1		1					
53		1	1				1																						1			1					1		
54		1			1		1																					1		1					1			
55																												1				1					1		
56																														1			1				1		Qtz overgrowths
57											1						1		1										1		1						1		
58																														1			1	1						Recrystallised
59	1			1		1																					1				1					1		
60																										1			1			1				1		
61		1			1	1																								1		1					1		
62		1	1		1	1																							1			1				1		
63																													1				1				1		
64																													1			1					1		
65		1	1		1		1																						1			1				1		
66																													1			1				1			
67		1					1																				1				1					1		
68	1			1		1																			1	1				1					1		
69										1			1					1				1									1				1				1		
70											1						1	1		1	1				1			1			1			1					
71	1		1		1		1																			1				1					1		
72																														1	1						1		
73																														1			1			1			Recrystallised Qtz
74																														1		1					1			Polygonized Qtz
75																									1				1			1	1						Recrystallised Qtz
76											1						1	1										1			1				1				Deformation lamellae
77	1			1	1		1																			1				1					1		
78																														1	1						1		
79																														1		1						1	
80	1				1		1																			1				1					1		
81																													1				1				1		
82		1		1	1		1																1			1				1				1		
83																									1				1			1			1			Polygonized
84																									1				1			1	1						Polygonized
[illegible]																																						
86																														1			1				1		
87																									1				1			1		1					Polyhedral Qtz
88	1			1	1	1																							1			1				1		
[illegible]																																						
90		1		1	1	1																							1	1					1			
91		1		1	1		1																						1		1					1			
92		1		1	1	1																						1				1				1		
93		1		1	1		1																							1			1				1		
94																														1			1					1	Polygonized Qtz
95																														1		1				1			
96																														1			1			1			Polygonized Qtz
97																														1			1				1		Polygonized Qtz
[illegible]																																						
99		1		1	1	1																							1			1				1		
100																									1				1			1		1					
101																									1				1		1				1			
102																														1			1	1						Polyhedral Qtz
TOTAL	12	26	13	22	22	17	18	17	47	1	59	11	1	0	30	1	3	2	1	2	1	0				18	18	24	63	13	39	53	8	21	23	44	9	

PLUTONIC QUARTZ : 34
DEFORMED PLUTONIC QTZ : 6
TOTAL PLUTONIC GRAINS : 40

METAMORPHIC QTZ Total: 61

DEFORMED VOLCANIC QTZ : 4

Cathodoluminescence-polarized microscope analysis
Sample# MGS1
Location Island Hills-Coal Creek

Grain	PLUTONIC QUARTZ: homogeneous	patchy	Light CL	Moderate CL	Microcracks-Healed	weak undulose	straight extinction	METAMORPHIC QUARTZ: mottled	dark	Moderate CL	strong undulose	weak undulose	poly-crystalline = <3	poly-crystalline>3	total poly-crystalline	VOLCANIC QUARTZ: homogeneous	zonation	Light CL	Moderate CL	Open Fractures	Quartz embayments	Straight extinction	Parallel/Sub-parallel feature	Dark shear bands	Random oriented fractures	Grain boundaries	Grain properties – rounding: angular	subangular-subrounded	rounded	shape: elongate	platy	spherical	grain size in microns: <2000	<1000	<500	<250	<125	Comments
1																																						
2									1		1				1								1			1	1				1					1		
3																																						
4	1				1	1																	1			1			1		1			1				
5																																						
6									1		1															1			1		1			1				
7									1		1															1			1			1			1			
8									1		1				1								1	1		1			1			1		1				
9									1		1				1								1			1			1			1		1				
10																																						
11									1		1				1										1	1			1		1			1				Polygonized Qtz
12									1		1				1										1				1			1		1				Polyhedral Qtz
13									1		1				1										1				1			1		1				Polyhedral Qtz
14									1		1				1									1					1		1				1			
15																																						
16																																						
17									1		1				1														1		1		1					
18									1		1				1														1	1				1				Polyhedral Qtz recryst.
19									1		1				1														1			1		1				Polyhedral Qtz recryst.
20									1		1				1													1			1			1				Polygonized Qtz
21									1		1				1														1			1		1				Polygonized Qtz
22									1		1				1														1			1		1				Polyhedral Qtz recryst.
23									1		1				1													1				1		1				Polyhedral Qtz recryst.
24												1				1			1	1									1			1		1				
25																																						
26									1		1																		1					1				Polyhedral Qtz recryst.
27																																						
28											1												1					1		1				1				
29																																						
30															1													1						1				Polygonized Qtz recryst.
31																																						
32																																						
33									1		1																		1			1			1			
34									1		1																		1			1		1				
35									1		1																	1			1			1				
36		1		1		1			1		1																	1		1					1			
37									1		1																		1			1		1				
38									1		1																		1			1		1				
39											1					1			1	1							1			1				1				
40																																						
41																																						
42									1		1																		1			1				1		
43									1		1																		1			1		1				Polygonized Qtz recryst.
44																																						
45	1		1		1				1		1																		1			1			1			
46									1		1				1														1		1			1				Polygonized Qtz
47									1		1				1													1			1			1				Polyhedral Qtz
48									1		1				1														1			1			1			
49	1			1	1				1		1																	1		1				1				
50									1		1		1															1				1				1		
51									1		1				1														1		1				1			
52									1		1															1	1			1				1				
53									1		1				1											1			1			1		1				
54									1		1															1	1				1			1				Polygonized Qtz
55									1		1				1											1			1			1		1				Polygonized Qtz recryst.
56									1		1																	1		1				1				Polygonized Qtz
57									1		1			1												1		1			1			1				Polygonized Qtz
58									1		1				1											1			1			1		1				Recrystallised Qtz
59									1		1				1											1			1			1		1				Polyhedral Qtz
60																																						
61											1					1			1							1			1			1			1			
62		1		1	1	1																							1			1			1			
63									1		1		1															1			1				1			Polygonized Qtz
64									1		1	1														1		1		1				1				
65									1		1				1											1	1				1			1				Polygonized Qtz
66									1		1				1														1			1		1				Polygonized Qtz/ crenulated
67									1		1				1											1			1			1			1			
68									1		1				1											1			1			1			1			
69									1		1				1											1		1			1			1				Polyhedral Qtz
70									1		1			1											1				1		1			1				Polygonized Qtz
71																																						
72									1		1				1											1						1		1				Polygonized Qtz
73																																						
74									1		1				1										1	1			1			1		1				Polygonized Qtz
75									1		1				1										1	1			1		1			1				Crenulated Qtz
76																																						
77									1		1				1										1	1	1				1				1			Polygonized Qtz
78	1			1	1	1																			1				1		1			1				
79									1		1				1										1	1		1			1			1				Polyhedral Qtz
80	1			1	1		1																1						1			1		1				
81									1		1				1										1	1			1			1		1				Polygonized crenulated Qtz
82		1		1	1	1																			1			1			1			1				
83									1		1				1										1				1			1		1				Polyhedral Qtz
84								1			1														1	1			1			1		1				
85									1		1																	1		1					1			Polygonized Qtz
86									1		1				1										1	1			1			1		1				Polygonized Qtz
87								1			1														1	1			1			1		1				
88									1		1																		1	1				1				
89								1			1														1	1	1				1			1				
90	1			1	1		1																	1	1			1			1			1				
91									1		1				1										1				1			1	1					Polygonized Qtz
92		1		1	1		1																		1				1	1					1			
93									1		1		1												1				1		1			1				Polygonized Qtz
94									1		1				1										1				1		1			1				Elongated original crystals
95									1		1			1											1				1		1			1				Polygonized Qtz
96																																						
97									1		1				1										1	1		1			1			1				
98									1		1														1	1	1				1			1				Polygonized Qtz
99											1					1			1	1					1	1			1	1				1				
100		1		1	1	1																					1			1					1			
101									1		1				1										1	1	1				1				1			Polygonized Qtz
102								1			1				1										1			1		1				1				Elongated original crystals
103																																						
104									1		1				1														1			1		1				Polygonized Qtz crenulated
105									1		1				1										1	1			1			1		1				Polygonized Qtz crenulated
	17	14	4	23	27	7	3	7	64	0	92	3	3	3	44	4	0	0	4	3	0	0	10	3	33	42	13	30	61	19	39	43	8	76	18	3	0	

PLUTONIC QTZ : 10
DEFORMED PLUTONIC QTZ : 20
TOTAL: 30

METAMORPHIC QUARTZ Total: 71

DEFORMED QUARTZ Total: 4

Cathodoluminescence-polarized microscope analysis
Sample# 15
Location Mandamus

Grain	PLUTONIC QUARTZ: homogeneous	patchy	Light CL	Moderate CL	Microcracks -Healed	weak undulose	straight extinction	METAMORPHIC QUARTZ: mottled	dark	Moderate CL	strong undulose	weak undulose	poly-crystalline = <3	poly-crystalline>3	total poly-crystalline	VOLCANIC QUARTZ: homogeneous	zonation	Light CL	Moderate CL	Open Fractures	Quartz embayments	Straight extinction	Grain properties: Parallel/Sub-parallel feature	Dark shear bands	Random oriented fractures	Grain boundaries	rounding: angular	subangular-subrounded	rounded	shape: elongate	platy	spherical	grain size in microns: <2000	<1000	<500	<250	<125	Comments
1									1		1												1					1		1					1			Deformation lamellae
[illegible]																																						
3									1			1											1				1				1						1	
4									1																		1				1						1	QO
5									1		1																1			1						1		
6									1			1															1			1							1	
[illegible]																																						
8									1														1					1		1					1			
[illegible]																																						
12											1						1		1				1		1			1		1						1		
13									1							1						1			1			1				1				1		
14	1		1		1		1																				1					1				1		
15	1			1	1	1																			1			1		1						1		
16									1		1														1				1		1					1		QO
17																1			1			1			1				1			1					1	
18																1			1			1	1				1					1					1	QO
19	1			1	1	1																	1						1		1					1		
20	1		1		1		1																				1				1				1			
21								1			1												1		1			1				1					1	
22								1			1												1					1				1					1	
23									1		1																1			1							1	
24	1			1	1	1																			1			1		1						1		
25									1			1													1		1					1					1	QO
26									1		1														1				1			1				1		
27									1			1															1				1						1	
28									1			1											1				1				1					1		
29									1		1												1				1					1					1	
30									1			1											1				1				1					1		
31	1		1		1		1																		1			1				1				1		
[illegible]																																						
33									1		1														1		1				1						1	
[illegible]																																						
35								1				1											1				1				1						1	
36									1			1											1		1		1				1						1	
37									1			1													1		1				1					1		
38									1		1														1				1		1					1		
39	1		1		1	1																					1				1					1		
40									1			1											1		1		1				1					1		
41																1			1	1		1			1			1			1					1		
42	1			1	1		1																						1			1					1	
43	1		1		1		1																					1				1				1		
44									1		1																		1			1			1			
45									1			1																	1			1					1	
46	1		1		1	1																	1					1			1					1		
47									1		1														1				1			1				1		
48												1					1	1											1			1					1	
49									1		1														1		1				1					1		
50	1			1	1	1																					1				1						1	
51									1			1				1				1			1				1			1						1		Deformation lamellae
52									1		1												1		1				1		1						1	
53	1			1	1	1																							1			1					1	
54									1			1											1				1				1					1		
55									1			1																	1			1					1	
[illegible]																																						
57	1			1	1		1																							1						1		
58									1			1		1												1			1			1				1		
59									1			1															1				1						1	
[illegible]																																						
61									1		1																1			1							1	
62	1			1	1	1																							1	1						1		
63									1		1																1				1					1		
64								1			1																	1			1					1		
65									1		1																1				1						1	
66									1		1																	1				1					1	
67								1				1															1			1						1		QO
68									1		1														1		1				1					1		
69	1			1	1	1																					1			1						1		QO
70									1		1																1				1					1		QO
71									1		1																1			1						1		Deformation lamellae
72	1			1	1		1																						1			1			1			
73									1		1																1				1						1	
74								1			1		1															1				1				1		QO
75								1				1															1				1						1	QO
76								1				1															1				1					1		QO
[illegible]																																						
79								1			1																	1			1						1	
80									1				1													1		1			1						1	QO
81								1				1																1				1				1		
82																1			1			1						1				1					1	
83	1			1	1		1																						1		1				1			
84								1				1															1			1					1			
85								1			1																1			1						1		
86									1		1																1			1							1	
87	1			1	1		1																					1				1				1		
88								1				1																	1	1						1		
89									1			1																1				1					1	
90									1			1													1			1			1					1		
91									1		1		1													1			1		1					1		Polygonized Qtz
92								1			1																1				1						1	
93	1			1	1	1																						1			1					1		
94	1			1	1		1																					1		1						1		
95								1			1																1				1						1	
96	1			1	1	1																					1			1							1	
97									1			1																1			1					1		
98												1				1		1										1				1					1	
99																1			1	1		1			1		1					1					1	
[illegible]																																						
102									1		1																		1		1						1	
103									1		1																1			1						1		
104									1			1											1					1			1						1	
105									1		1																		1			1				1		
	25	7	8	24	34	15	10	22	50	0	45	29	3	1	0	6	3	2	6	3	0	6	20	0	30	5	46	35	23	24	47	34	0	0	8	55	42	

PLUTONIC QTZ : 21
DEFORMED QTZ : 13
TOTAL PLUTONIC 34

METAMORPHIC QTZ : 61

VOLCANIC QTZ : 5
DEFORMED VOLCANIC QTZ : 5
TOTAL VOLCANIC : 10

Cathodoluminescence-polarized microscope analysis
Sample# 5
Location Island Hills-Type section

Grain	PLUTONIC QUARTZ: homogeneous	patchy	Light CL	Moderate CL	Microcracks-Healed	weak undulose	straight extinction	METAMORPHIC QUARTZ: mottled	dark	Moderate CL	strong undulose	weak undulose	poly-crystalline = <3	poly-crystalline>3	total poly-crystalline	VOLCANIC QUARTZ: homogeneous	zonation	Light CL	Moderate CL	Open Fractures	Quartz embayments	Straight extinction	Grain properties: Parallel/Sub-parallel fracture	Dark Shear bands	Random oriented fractures	Grain boundaries	rounding: angular	subangular-subrounded	rounded	shape: elongate	platy	spherical	grain size in microns: <2000	<1000	<500	<250	<125	Comments
1									1		1												1	1				1			1					1		
2									1			1											1	1				1		1						1		
3									1		1												1	1			1				1						1	
4								1			1			1									1	1					1			1			1			
5									1		1												1	1		1			1			1				1		
6																	1		1	1		1	1			1	1			1						1		
7									1		1												1		1		1				1					1		
8		1					1																1						1			1					1	QO
9																	1		1	1		1	1				1			1								
10								1				1												1					1			1					1	QO
11									1		1													1					1			1				1		
12									1		1												1					1			1				1			
13									1		1												1					1				1			1			
14																	1	1		1		1	1				1				1						1	
15	1						1																1				1					1					1	
16	1			1		1																	1				1				1						1	
17					1												1	1				1							1	1	1			1				
18		1		1	1		1																1				1				1						1	
19																1			1	1		1	1						1			1					1	
20		1		1	1		1																1	1				1			1				1			DL
21		1		1		1																	1			1	1					1					1	
22									1			1											1			1	1				1						1	
23								1	1	1		1											1					1				1					1	
24								1			1															1		1				1			1			
25		1			1		1																													1		
26	1			1	1	1																	1				1			1						1		
27		1		1	1	1																	1				1				1				1			
28	1			1			1																1					1				1			1			DL
29		1	1		1		1																1					1				1			1			
30									1			1											1			1		1			1				1			
31	1			1	1	1																	1			1		1		1							1	
32	1			1	1		1																1					1				1					1	DL
33									1		1												1			1			1			1				1		
34									1		1												1				1			1							1	
35		1			1	1																	1				1					1					1	
36								1				1											1				1				1					1		
37	[illegible]																																					
38									1		1												1					1			1						1	
39		1		1	1		1																1						1			1					1	
40	1						1																1					1				1					1	
41																1	1		1	1		1	1					1				1					1	
42		1		1	1	1																	1					1				1				1		
43		1			1	1																	1						1			1				1		
44									1		1												1					1		1						1		
45								1		1	1												1					1			1					1		
46									1	1		1											1				1					1					1	
47									1		1																	1				1					1	
48		1				1																					1				1				1			DL
49									1			1											1				1			1							1	
50	[illegible]																																					
51									1		1				1								1						1	1					1			
52	1			1		1																	1				1				1					1		
53		1		1	1		1																1				1			1						1		
54									1		1												1						1	1							1	
55	1			1	1	1																	1						1		1						1	
56		1		1			1																1					1				1				1		
57									1		1												1					1				1			1			
58	[illegible]																																					
59									1		1												1						1			1				1		
60									1		1	1											1						1	1					1			DL
61									1		1																	1				1					1	
62									1		1																	1			1						1	
63								1	1		1																		1	1						1		
64	1	1		1			1																1			1	1				1						1	
65	1	1		1		1																				1	1			1							1	
66	1	1		1			1																1						1			1					1	
67								1	1		1												1			1			1			1					1	
68								1		1	1															1			1			1				1		
69								1		1	1															1		1		1						1		
70								1	1			1											1			1			1	1						1		
71									1			1														1		1								1		
72									1			1														1	1					1					1	
73	1	1		1			1																1			1			1			1				1		
74								1	1	1	1	1											1					1		1						1		
75								1	1		1															1		1		1						1		
76		1		1		1																							1			1				1		
77									1		1				1											1			1			1		1		1		
78									1		1				1											1			1			1						
79									1		1																	1				1					1	
80									1			1																	1			1				1		
81	1			1			1																					1		1					1			
82	[illegible]																																					
83								1				1																										
84	1																												1			1				1		
85	1			1			1																					1		1							1	
86				1			1																						1		1						1	QO
87									1		1	1											1						1			1				1		
88									1		1												1					1		1						1		
89									1		1	1											1						1	1							1	
90								1		1	1																1					1				1		
91								1		1	1			1												1	1				1					1		
92		1	1		1	1																						1			1					1		
93		1	1				1																				1				1				1			
94									1		1																1				1					1		
95									1		1																		1			1				1		
96								1		1	1																		1			1				1		
97		1		1	1		1																						1			1				1		
98								1		1	1	1											1						1			1				1		
99	1								1			1															1					1				1		
100	1			1			1																					1			1						1	
101				1			1																				1				1						1	
102		1		1			1																						1	1						1		
103	1								1				1																1	1						1		
104				1			1																						1			1					1	
105	[illegible]																																					
TOTAL	20	26	3	30	19	15	25	21	43	10	31	28	1	2	3	2	5	2	4	5	0	8	63	6	1	21	29	37	38	26	27	51	0	2	19	42	42	

PLUTONIC QTZ : 38
DEFORMED PLUTONIC QTZ : [illegible]
TOTAL : 43
METAMORPHIC QUARTZ Total: 56
VOLCANIC QUARTZ Total : 6

ation Upper Waipara
nple# W01

Grain	PLUTONIC QUARTZ							METAMORPHIC QUARTZ								VOLCANIC QUARTZ							Fracture patterns Optical/CL features				Grain properties: rounding			shape			grain size in microns					Comments
Grain	homogeneous	patchy	Light CL	Moderate CL	Microcracks-Healed	weak undulose	straight extinction	mottled	dark	Moderate CL	strong undulose	weak undulose	poly-crystalline = <3	poly-crystalline>3	total poly-crystalline	homogeneous	zonation	Light CL	Moderate CL	Open Fractures	Quartz embayments	Straight extinction	Sub-parallel fractures	Dark Shear bands	Random oriented fractures	Grain boundaries	angular	subangular-subrounded	rounded	elongate	platy	spherical	<2000	<1000	<500	<250	<125	
1									1			1																1				1				1		
2											1																1					1				1		
3	1			1	1	1																						1			1					1		
4	1			1	1		1																					1				1				1		
5									1		1																	1		1						1		
6								1			1																		1		1					1		
7									1			1				1											1					1				1		Deformation lamellae
8	1		1		1		1																				1					1				1		
9		1	1		1		1																		1		1				1					1		
10										1		1															1				1					1		
11																1			1			1					1				1					1		
12								1				1																1			1				1			
13																1			1			1					1				1					1		
14																1			1			1					1			1						1		
15									1		1			1													1				1					1		
16																																						Deformation lamellae
17								1			1																1				1						1	
18											1						1		1								1			1						1		
19											1					1		1							1		1			1					1			Deformation lamellae
20																																						
21		1	1		1		1																				1			1						1		
22	1		1		1		1																				1			1						1		
23									1		1																	1			1					1		
24	1		1		1		1																				1				1				1			
25								1			1																	1			1				1			
26	1	1		1	1	1																							1			1			1			Deformation lamellae
27										1		1															1					1				1		
28																1			1			1					1			1					1			
29																1		1				1						1		1						1		
30																																						Deformation lamellae
31									1		1																		1			1				1		
32																	1		1			1					1				1					1		
33								1			1																		1		1				1			
34									1			1															1				1					1		
35									1			1																	1		1				1			
36																1			1			1						1			1					1		
37	1		1		1		1																				1			1						1		
38									1		1																	1		1					1			
39																																						
40											1					1			1									1			1				1			Deformation lamellae
41									1		1		1															1			1					1		
42									1		1																		1			1				1		
43									1		1																		1		1					1		
44									1		1																	1				1				1		
45	1		1		1		1																						1		1				1			
46																																						
47									1		1																	1		1						1		
48												1				1			1									1			1				1			Deformation lamellae
49									1		1				1														1			1			1			Polygonal quartz
50	1			1	1		1																					1			1				1			
51									1		1																		1			1				1		
52									1			1																1				1				1		
53									1			1																		1	1					1		
54								1			1																	1			1				1			
55								1			1				1													1		1					1			
56																																						
57									1		1																	1			1					1		
58										1		1															1				1					1		
59	1			1	1		1																				1				1					1		
60																1			1			1					1				1					1		
61	1		1		1		1																				1				1					1		
62												1					1		1									1				1			1			Deformation lamellae
63								1				1															1				1					1		
64	1			1	1		1																				1			1						1		
65									1		1																	1		1					1			
66								1			1				1														1			1			1			Polyhedral quartz
67	1			1	1		1																						1			1				1		
68	1			1	1		1																						1			1				1		
69									1		1																1				1					1		
70																1			1			1					1					1			1			
71									1			1															1			1						1		
72								1			1																	1		1					1			
73										1	1																1			1					1			
74									1		1																1				1						1	
75									1		1																1				1					1		
76									1		1																1				1						1	
77									1							1						1						1			1					1		
78																																						
79								1			1		1																1		1					1		
80	1		1		1		1																					1				1				1		
81									1		1						1												1			1			1			Deformation lamellae
82	1		1		1		1																				1			1					1			
83								1									1		1			1					1			1					1			
84									1		1		1															1				1				1		
85									1		1		1																1			1				1		
86								1			1																	1				1				1		
87																																						
88									1							1						1							1			1					1	
89	1		1		1		1																				1			1						1		
90									1							1						1							1			1					1	
91									1		1																		1			1				1		
92									1			1																	1			1			1			
93	1		1		1		1																				1				1					1		
94																	1	1				1					1			1					1			
95									1		1																		1			1				1		
96									1		1																	1		1						1		
97																1		1				1					1			1					1			QO
98		1	1		1		1																				1				1					1		QO
99										1	1																	1				1				1		
100									1		1																	1		1						1		
101									1			1																	1			1				1		
102									1		1		1														1				1					1		
103										1	1																	1				1			1			
104									1		1																	1			1					1		
105	1			1	1		1			1		1															1			1					1			
Total	24	7	16	14	30	4	21	16	39	7	48	17	6	1	3	16	6	4	13			15			3		46	34	24	30	44	32			36	64	5	

PLUTONIC QUARTZ: 22
DEFORMED PLUTONIC QUARTZ: 8
TOTAL PLUTONIC QUARTZ: 30

METAMORPHIC QUARTZ: 54

VOLCANIC QUARTZ: 15
DEFORMED VOLCANIC QUARTZ: 6
TOTAL VOLCANIC QUARTZ: 21

Location Upper Waipara
Sample# W03

PLUTONIC QUARTZ | METAMORPHIC QUARTZ | VOLCANIC QUARTZ | Fracture patterns Optical/CL features | Grain properties

Grain	homogeneous	patchy	Light CL	Moderate CL	Microcracks-Healed	weak undulose	straight extinction	mottled	dark	Moderate CL	strong undulose	weak undulose	poly-crystalline = <3	poly-crystalline>3	total poly-crystalline	homogeneous	zonation	Light CL	Moderate CL	Open Fractures	Quartz embayments	Straight extinction
1																	1		1			1
2								1			1				1							
[illegible]																						
4								1			1				1							
5	1			1	1	1																
6								1														
7																1			1			1
8			1		1		1										1					
9	1		1		1		1															
10								1			1											
11	1		1		1		1															
12											1					1		1				
13											1											
14																						
15								1	1		1											
[illegible]																						
17																1		1				1
18								1			1											
19									1		1											
20											1		1									
21									1		1		1									
22																	1	1				1
23									1		1											
24	1		1		1		1															
25								1			1		1									
26	1		1		1		1															
27																1		1			1	1
28	1		1		1		1															
29											1					1						
30	1		1		1		1															
[illegible]																						
32	1		1		1		1															
33								1			1											
34										1	1											
35	1		1		1		1															
36												1										
37	1		1		1		1															
38								1			1											
[illegible]																						
40									1			1										
41								1			1											
42								1			1											
43								1			1				1							
44								1			1											
[illegible]																						
46										1		1										
47									1		1				1							
48	1		1		1		1															
49	1		1		1		1															
50									1		1											
51									1		1											
52									1		1											
53									1		1				1							
54											1					1			1		1	
55	1			1	1		1															
56								1				1	1									
57									1		1											
58										1	1		1									
59																1		1				1
60	1		1		1		1															
61								1			1											
62									1		1											
63								1			1											
64									1		1											
65																1		1				1
66								1				1										
[illegible]																						
68	1		1		1		1															
69	1			1	1		1															
70	1		1		1		1															
71								1			1											
72																1			1			1
[illegible]																						
74									1		1											
75	1		1		1	1																
76																1		1				1
[illegible]																						
78																	1		1			1
79																1			1			1
80									1		1				1							
81									1		1		1									
82									1		1											
83								1			1				1							
84									1		1											
85									1		1											
86																1			1			1
87																						
88	1			1	1		1															
89	1	1	1		1		1															
[illegible]																						
[illegible]																						
92	1		1		1		1															
93	1	1	1		1	1																
[illegible]																						
95									1		1											
96								1								1						1
97																1			1			1
98									1		1											
99									1		1				1							
100	1			1	1		1															
101	1			1	1	1																
102	1			1	1	1																
103												1				1			1			
104																1		1				1
105								1			1		1									
Total	30	8	23	14	37	5	26	29	23	5	51	7	8		13	16	4	8	9		2	16

Grain	Sub-parallel fractures	Dark Shear bands	Random oriented fractures	Grain boundaries	rounding: angular	subangular-subrounded	rounded	shape: elongate	platy	spherical	grain size in microns: <2000	<1000	<500	<250	<125	Comments
1					1			1					1			
2				1		1			1				1			
[illegible]																
4					1			1				1				crenulated quartz
5					1				1				1			
6					1				1			1				
7							1			1			1			
8					1				1				1			shallow plutonic
9						1		1					1			
10							1		1				1			
11						1		1				1				
12							1		1					1		
13						1			1				1			Polyhedral quartz
14					1			1						1		
15							1		1				1			
[illegible]																
17					1			1				1				
18						1		1				1				crenulated quartz
19					1			1					1			
20						1			1				1			
21							1		1				1			
22					1			1						1		
23					1			1					1			
24						1		1					1			
25					1			1					1			Polyhedral quartz
26					1				1					1		
27					1				1				1			
28					1		1							1		
29					1			1					1			
30						1			1				1			
[illegible]																
32							1		1				1			
33						1		1				1				Polygonized quartz
34							1			1		1				Polygonized quartz
35					1			1					1			
36					1				1					1		
37						1				1			1			
38						1		1				1				
[illegible]																
40						1				1		1				
41						1		1					1			
42					1			1					1			
43							1		1				1			crenulated quartz
44							1			1			1			
[illegible]																
46							1			1			1			
47					1				1					1		Polygonized quartz
48							1			1			1			
49							1		1				1			
50					1				1					1		
51	1					1				1			1			
52						1				1				1		
53							1			1		1				crenulated quartz
54							1			1			1			Deformation lamellae
55					1			1				1				
56							1		1			1				
57					1				1				1			
58					1				1				1			
59					1				1				1			
60					1				1				1			
61							1			1			1			Polygonized quartz
62					1				1					1		
63							1			1		1				
64							1		1				1			
65					1			1				1				
66							1			1		1				Deformation lamellae
[illegible]																
68					1				1				1			
69					1				1				1			
70					1			1					1			
71							1	1					1			
72							1	1					1			
[illegible]																
74					1				1				1			
75						1			1					1		
76					1				1				1			
[illegible]																
78						1			1					1		
79							1			1			1			
80					1				1				1			Polyhedral quartz
81					1				1				1			Polygonized quartz
82							1	1					1			
83						1			1		1					Polyhedral quartz
84					1				1				1			
85							1			1				1		
86						1			1				1			
87													1			
88					1			1								
89							1			1			1			
[illegible]																
[illegible]																
92					1					1				1		
93					1				1				1			
[illegible]																
95						1		1					1			
96							1			1				1		
97						1		1					1			
98					1			1				1				Polyhedral quartz
99					1			1				1				Polyhedral quartz
100							1			1			1			
101						1		1						1		
102							1			1			1			
103					1			1						1		Deformation lamellae
104							1			1			1			
105					1				1			1				
Total	1			1	44	24	37	35	41	25	1	21	63	18		

PLUTONIC QUARTZ: 26
DEFORMED PLUTONIC QUARTZ: 11
TOTAL PLUTONIC QUARTZ: 37

METAMORPHIC QUARTZ: 49

VOLCANIC QUARTZ: 15
DEFORMED VOLCANIC QUARTZ: 4
TOTAL VOLCANIC QUARTZ: 19

Location Upper Waipara
Sample# W04

Grain	PLUTONIC QUARTZ							METAMORPHIC QUARTZ								VOLCANIC QUARTZ							Fracture patterns Optical/CL features				Grain properties: rounding			shape			grain size in microns					Comments
Grain	homogeneous	patchy	Light CL	Moderate CL	Microcracks-Healed	weak undulose	straight extinction	mottled	dark	Moderate CL	strong undulose	weak undulose	poly-crystalline =<3	poly-crystalline>3	total poly-crystalline	homogeneous	zonation	Light CL	Moderate CL	Open Fractures	Quartz embayments	Straight extinction	Sub-parallel fractures	Dark Shear bands	Random oriented fractures	Grain boundaries	angular	subangular-subrounded	rounded	elongate	platy	spherical	<2000	<1000	<500	<250	<125	Comments
1									1							1						1							1			1			1			
2									1		1																1				1						1	
3	1		1		1		1																						1		1				1			
4									1		1				1													1			1				1			Polygonized quartz
5	1		1		1		1																				1				1						1	
6									1			1																	1			1				1		
7																1		1				1					1				1					1		
8									1		1		1														1			1					1			
9											1						1										1				1					1		Deformation lamellae
10	1			1	1		1																						1			1			1			
11									1		1		1																1		1				1			Crenulated quartz
12									1			1															1			1						1		
13	1	1	1		1		1	1																			1			1					1			
14	1		1		1		1																			1			1						1		
15									1			1													1			1			1					1		
16									1			1													1		1				1					1		
17									1		1																		1			1				1		
18									1		1																		1			1				1		
19									1							1						1					1				1					1		
20	1		1		1		1																			1				1				1			
21					1												1	1				1						1				1			1			shallow plutonic
22	1		1		1		1																					1			1				1		
23									1			1														1			1						1		
24	1		1		1		1																			1				1					1		
25		1		1	1		1																			1			1					1			
27									1			1															1			1					1		
28	1		1		1	1																				1			1					1			Deformation lamellae
29									1		1															1			1					1			
30								1			1																	1			1			1			
31	1		1		1		1																			1			1						1		
32									1			1														1			1						1		
33									1		1															1				1					1		
34	1		1		1		1																			1			1						1		
																																						Deformation lamellae
36								1											1			1							1			1			1			
37									1		1															1				1					1		
38									1		1															1				1					1		
39									1		1																	1			1				1		
40								1				1															1			1					1		
41									1			1															1				1				1		
42									1			1														1				1					1		
43									1		1															1			1					1			
44		1		1	1		1																			1				1					1		
45								1			1				1													1			1			1			Polyhedral quartz
46								1			1															1				1					1		
47	1		1		1		1																			1			1						1		
48									1			1																1			1				1		
49																	1					1					1				1				1			
50									1		1				1												1			1					1			crenulated quartz
51																													1			1			1			
52	1		1		1		1																			1				1					1		
53									1		1																	1	1					1			
54	1		1		1		1																			1			1					1			
55									1			1														1				1					1		
56									1			1														1			1					1			
58											1					1		1										1			1				1			
59	1		1		1		1																			1				1				1			
60								1			1																1			1				1			
61								1			1																	1			1				1		
62		1	1		1	1																				1			1					1			
63	1			1	1		1																			1			1					1			
64	1		1		1		1																			1				1				1			
65																1			1	1		1			1				1			1			1			
66									1		1																	1		1					1		
67	1		1		1		1																			1					1			1			
68	1		1		1		1																				1		1					1			
71								1				1												1						1	1					1			
72									1		1				1										1				1	1				1					crenulated quartz
74									1		1															1				1				1			
75									1		1				1													1	1					1			crenulated quartz
76									1		1				1									1			1		1					1			polygonized quartz
77								1													1							1		1					1		
78								1			1		1															1			1			1			
79	1			1	1		1																	1		1				1			1				
81									1			1	1													1					1			1			
82								1								1			1			1							1			1			1			
83									1			1															1		1					1			
84	1		1		1		1																				1		1						1		
85									1		1															1					1		1				
86								1											1	1		1					1			1				1				
87									1		1				1											1					1		1					Polygonized quartz
88								1			1				1													1			1			1			polyhedral quartz
89									1			1				1			1							1				1				1			Deformation lamellae
90								1			1													1				1			1			1			
91									1		1																	1	1					1			
92	1			1	1		1																			1			1					1			
93									1		1				1												1		1				1					polyhedral quartz
94									1		1				1												1		1					1			polyhedral quartz
95									1							1						1						1				1			1			
96									1		1												1			1				1			1			
97									1		1															1			1					1			
98	1		1		1	1																			1				1					1		
99								1			1				1										1			1			1			1			Polygonized quartz
100																1			1	1		1							1		1				1			
101									1		1															1			1					1			
																																						Deformation lamellae
103									1		1															1				1				1			
104									1		1															1			1					1			
Total	25	11	21	13	36	4	27	23	48		44	17	4		11	9	3	3	6	3		12		1	8		57	18	30	39	38	26		6	60	37	2	

PLUTONIC QUARTZ : 27
DEFORMED PLUTONIC QUARTZ : 9
TOTAL PLUTONIC QUARTZ : 36

METAMORPHIC QUARTZ : 64

VOLCANIC QUARTZ : 11
DEFORMED QUARTZ : 4
TOTAL VOLCANIC QUARTZ : 15

Location Upper Waipara
Sample# W06

Grain	PLUTONIC QUARTZ							METAMORPHIC QUARTZ								VOLCANIC QUARTZ						
	homogeneous	patchy	Light CL	Moderate CL	Microcracks-Healed	weak undulose	straight extinction	mottled	dark	Moderate CL	strong undulose	weak undulose	poly-crystalline = <3	poly-crystalline>3	total poly-crystalline	homogeneous	zonation	Light CL	Moderate CL	Open Fractures	Quartz embayments	Straight extinction
2	1			1	1		1															
3											1											
4									1		1											
5																1			1			1
6											1											
7											1											
8											1											
9									1		1											
10									1							1						1
12	1		1		1	1																
13	1		1		1		1															
14									1		1											
15									1		1											
16	1		1		1		1															
17	1		1		1	1																
18											1											
19	1		1		1	1																
20									1			1										
21																1		1				1
22											1											
23									1		1											
24									1													
25	1			1	1		1															
26									1		1											
27									1		1											
28									1		1											
29									1		1											
30	1		1		1		1															
31	1			1	1		1															
32									1		1											
33	1		1		1		1															
34									1		1											
35									1		1											
36	1			1	1		1															
37									1		1											
38	1			1	1																	
39									1		1											
40	1			1	1		1															
41									1		1											
42									1			1										
43									1			1										
44										1		1										
45									1		1											
47									1		1											
50																1			1			1
51																	1					1
52	1		1		1		1															
53	1		1		1		1															
56									1		1											
57								1			1											
58									1		1											
59	1		1		1		1															
60																1			1			1
61	1		1		1		1															
63								1											1			1
64											1					1			1			
65									1		1											
66									1		1											
68	1		1		1	1																
69	1				1	1																
70								1			1											
71									1		1											
72									1		1											
74									1		1											
75																	1	1				1
76									1		1											
77									1		1											
78									1		1											
79									1		1											
80								1			1											
81									1		1											
82									1		1											
84									1		1											
85									1		1											
86	1			1	1		1															
87										1	1											
88																	1	1				1
89									1		1											
90																1			1			1
91	1		1		1		1															
92									1			1										
94																	1		1			1
95									1							1						1
97									1							1						1
98																	1	1				1
99									1			1				1						
100	1			1	1	1																
101									1			1				1						
102	1	1	1		1		1															
104	1		1		1		1															
105									1			1										
Total	33	6	17	19	38	8	20	9	50	2	54	9				11	5		7			14

Grain	Fracture patterns Optical/CL features				Grain properties: rounding			shape			grain size in microns					Comments
	Sub-parallel fractures	Dark Shear bands	Random oriented fractures	Grain boundaries	angular	subangular-subrounded	rounded	elongate	platy	spherical	<2000	<1000	<500	<250	<125	
2						1				1				1		
3		1					1			1				1		
4						1			1					1		
5					1			1						1		
6						1			1					1		
7					1				1						1	
8					1				1						1	
9						1				1					1	
10					1					1				1		
12					1				1						1	
13							1			1			1			
14						1			1						1	
15					1				1						1	
16					1				1						1	
17					1				1					1		
18							1			1				1		
19					1				1					1		
20							1			1				1		
21	1				1				1					1		
22					1			1						1		
23					1				1						1	
24					1			1							1	
25					1				1						1	
26			1			1				1				1		
27						1				1					1	
28						1			1						1	
29							1			1			1			
30					1				1					1		
31			1		1				1					1		
32					1				1					1		
33							1			1			1			
34					1				1						1	
35							1			1					1	
36					1				1						1	
37						1			1						1	
38					1				1						1	
39					1				1					1		
40					1				1					1		
41					1			1						1		
42							1			1				1		
43							1			1				1		
44					1			1						1		
45					1				1					1		
47					1				1					1		
50				1		1				1				1		
51					1				1					1		
52					1				1					1		
53					1				1					1		
56					1				1						1	
57					1			1						1		
58							1			1				1		
59							1			1				1		
60							1			1					1	
61	1						1			1			1			
63					1				1					1		
64					1				1					1		
65							1			1					1	
66			1				1	1						1		
68					1			1						1		
69					1			1						1		
70						1				1				1		
71					1				1						1	
72							1			1					1	
74							1			1				1		
75						1				1				1		
76					1			1						1		
77					1				1					1		
78					1				1				1			
79					1				1						1	
80							1	1						1		
81					1				1						1	
82							1			1					1	
84					1				1						1	
85						1		1							1	
86						1			1					1		
87							1			1			1			
88					1			1					1			
89					1				1					1		
90					1			1							1	
91					1				1						1	
92					1				1					1		
94						1			1				1			
95							1	1						1		
97						1			1						1	QO
98					1				1						1	
99							1			1					1	Deformation lamellae
100							1			1					1	
101							1			1					1	Deformation lamellae
102					1				1					1		
104					1				1						1	
105						1			1						1	
Total	2	2	3	2	56	20	29	23	51	31			9	50	36	

PLUTONIC QUARTZ: 24
DEFORMED PLUTONIC QUARTZ : 14
TOTAL PLUTONIC QUARTZ : 38

METAMORPHIC QUARTZ : 61

VOLCANIC QUARTZ : 14
DEFORMED VOLCANIC QUARTZ : 3
TOTAL VOLCANIC QUARTZ : 17

Location Upper Waipara
Sample# W07

Grain	PLUTONIC QUARTZ							METAMORPHIC QUARTZ								VOLCANIC QUARTZ							Fracture patterns Optical/CL features				Grain properties: rounding			shape			grain size in microns					Comments
	homogeneous	patchy	Light CL	Moderate CL	Microcracks-Healed	weak undulose	straight extinction	mottled	dark	Moderate CL	strong undulose	weak undulose	poly-crystalline = <3	poly-crystalline>3	total poly-crystalline	homogeneous	zonation	Light CL	Moderate CL	Open Fractures	Quartz embayments	Straight extinction	Sub-parallel fractures	Dark Shear bands	Random oriented fractures	Grain boundaries	angular	subangular-subrounded	rounded	elongate	platy	spherical	<2000	<1000	<500	<250	<125	
1		1			1		1																				1				1					1		
2											1						1		1								1			1						1		
3									1		1																1				1					1		
4								1			1																1				1					1		
5									1			1																1				1					1	
6									1		1																		1			1				1		
7																																						
8								1			1													1			1				1					1		
9																1			1			1					1				1					1		
10																																						
11									1		1																		1			1				1		
12	1			1	1		1																				1			1						1		
13									1		1																	1			1				1			
14									1		1																1				1					1		
15									1		1																		1			1				1		
16								1			1																1			1							1	
17																	1	1				1					1				1					1		
18									1		1																1				1					1		
19	1		1		1	1																							1			1				1		
20									1		1																1				1					1		
21									1		1																1				1						1	
22								1			1			1														1			1					1		
23									1		1																		1		1					1		
24									1		1		1														1			1						1		
25	1		1		1	1																							1			1					1	
26									1		1				1														1			1				1		
27	1			1	1		1																				1			1						1		
28	1			1	1		1																						1			1				1		
29																1			1			1							1	1						1		
30											1						1	1											1			1				1		
31											1						1	1									1			1						1		
32																																						Deformation lamellae
33								1											1			1					1				1						1	
34																																						
35								1			1				1														1			1				1		
36									1		1																1					1					1	
37																											1				1					1		
38												1					1		1								1				1						1	
39									1		1																1				1						1	
40																1			1			1						1			1						1	
41											1						1		1										1	1						1		
42	1			1	1		1																				1				1						1	
43																																						
44								1			1																		1			1					1	
45									1		1			1														1		1							1	
46									1		1																		1	1						1		
47									1		1																1				1						1	
48																																						
49								1									1					1							1		1					1		
50								1			1																1				1						1	
51									1		1																1				1						1	
52									1			1																	1			1					1	
53								1			1																1			1						1		
54								1				1																	1			1				1		
55									1		1																		1	1							1	
56								1			1																1				1						1	
57											1					1			1									1		1						1		Deformation lamellae
58									1		1																1				1						1	
59	1			1	1	1																					1				1						1	
60										1	1													1			1				1						1	
61	1			1	1	1																					1				1						1	
62									1							1			1			1							1	1							1	
63											1					1			1										1	1						1		Deformation lamellae
64	1			1	1	1																					1				1						1	
65									1		1																		1			1					1	
66									1		1																1				1						1	
67									1		1																	1			1					1		
68									1		1																		1	1							1	
69	1		1		1		1																					1			1						1	
70									1		1																		1	1						1		
71									1		1																	1		1						1		
72	1			1	1		1																					1			1						1	
73								1			1		1															1			1						1	
74									1		1																	1			1						1	
75	1			1	1		1																				1				1						1	
76																																						
77								1																			1				1					1		
78																																						
79									1		1																		1	1						1		
80									1		1																	1		1						1		
81									1		1																1				1						1	
82								1			1																	1			1					1		
83									1		1																	1			1					1		
84								1			1								1			1					1			1						1		
85									1		1																		1			1					1	
86											1					1			1								1				1						1	
87	1			1	1		1																				1				1						1	
88									1		1																1			1						1		
89									1		1																1				1						1	
90									1		1																		1		1						1	
91																	1		1			1						1			1					1		
92								1											1			1							1			1				1		
93								1			1																		1			1				1		
94								1			1																	1		1						1		
95									1			1																1			1					1		
96								1			1																1				1					1		
97									1		1																		1			1					1	
98								1			1																		1			1				1		
99	1		1		1																						1			1						1		Deformation lamellae
100									1		1																1				1					1		
101																																						
102									1		1																	1				1					1	
103									1		1																		1			1					1	
104									1		1																1				1						1	
105									1		1		1																1		1					1		
TOTAL	19	5	4	19	24	7	9	25	45	1	73	5	3	3	2	7	8	3	14			10		2			51	21	33	28	54	23				57	47	

PLUTONIC QUARTZ : 15
DEFORMED PLUTONIC QUARTZ : 9
TOTAL PLUTONIC QUARTZ : 24

METAMORPHIC QUARTZ : 63

VOLCANIC QUARTZ : 10
DEFORMED VOLCANIC QUARTZ : 8
TOTAL VOLCANIC QUARTZ : 18

Location Castle Hill
Sample# BR1

PLUTONIC QUARTZ — METAMORPHIC QUARTZ — VOLCANIC QUARTZ — Fracture patterns Optical/CL features — Grain properties: rounding, shape, grain size in microns — Comments

Grain	homogenous	patchy	Light CL	Moderate CL	Microcracks-Healed	weak undulose	straight extinction	mottled	dark	Moderate CL	strong undulose	weak undulose	poly-crystalline = <3	poly-crystalline>3	sutural poly-crystalline	homogenous	zonation	Light CL	Moderate CL	Open Fractures	Quartz embayments	Straight extinction	Sub-parallel fractures	Dark Shear bands	Random oriented fractures	Grain boundaries	angular	subangular-subrounded	rounded	elongate	platy	spherical	<2000	<1000	<500	<250	<125	Comments
1									1		1																	1		1						1		Polygonized
2									1		1				1													1		1					1			
3								1			1			1														1			1					1		
4								1				1																1				1			1			
5			1		1		1																				1			1					1			quartz grown adjacent to feldspar
6																																						
7		1	1		1		1																					1				1				1		
8									1		1				1													1				1				1		
9								1				1													1			1			1				1			
10																1			1			1					1				1					1		
11											1																1			1						1		
12																																						
13									1		1														1			1			1			1				
14																1						1			1			1			1				1			
15								1			1																1				1					1		
16									1						1														1	1					1			
17									1			1																1			1					1		
18									1		1																1			1						1		
19	1		1		1	1																					1			1					1			
20																																						
21									1		1														1				1			1			1			
22									1		1																1				1					1		
23									1		1													1			1			1					1			
24								1			1		1															1			1				1			
25									1		1																	1		1					1			
26									1		1																1			1					1			
27									1		1				1													1	1						1			
28									1		1																1				1					1		
29	1			1	1		1																						1			1				1		
30																																						
31		1		1	1		1																					1			1				1			
32																1			1			1					1				1				1			
33		1	1		1	1																			1	1			1		1				1			
34																																						
35									1		1		1														1				1					1		
36									1		1																1			1						1		
37																																						
38	1			1	1	1																						1		1					1			
39									1		1																		1			1				1		QO
40								1			1		1																1			1				1		
41																																						
42	1		1		1		1																				1				1					1		
43									1			1																1		1					1			
44									1		1																	1				1			1			
45									1		1																1					1			1			
46									1		1																	1			1				1			
47	1		1		1	1																							1			1			1			
48									1		1																1				1					1		QO
49								1			1																	1		1					1			
50																1			1			1							1			1				1		
51									1		1																1				1				1			
52									1		1																1			1					1			
53									1		1				1												1				1					1		
54									1		1																	1		1					1			
55		1		1	1		1																					1		1					1			
56	1			1	1	1																							1		1				1			
57								1			1																1				1				1			
58									1		1																	1			1					1		
59																																						
60									1		1																		1		1					1		
61									1		1																1			1						1		
62																																						
63		1		1	1	1																					1				1					1		
64																																						
65																																						
66																	1		1			1					1				1				1			
67		1	1		1		1																						1			1		1				
68									1		1																	1		1					1			
69									1		1																1			1						1		
70								1			1																1				1					1		
71								1			1																	1				1			1			
72	1		1		1	1																							1	1					1			
73									1		1		1																1		1				1			
74																1			1			1					1				1					1		
75		1	1		1		1																				1				1					1		
76									1			1	1														1			1					1			
77											1						1		1								1				1					1		
78	1			1	1		1																				1					1		1				
79																																						
80																	1	1				1					1				1					1		
81	1			1	1	1																			1		1				1				1			
82									1		1																1				1					1		
83		1	1		1		1																					1				1			1			
84																																						
85		1		1	1		1																						1			1			1			
86											1						1	1									1			1						1		
87									1			1																1			1					1		
88																1			1			1					1			1					1			
89									1			1																1			1				1			
90	1		1		1	1																					1				1					1		
91																																						
92									1		1														1				1			1			1			
93								1			1																	1			1					1		
94									1		1		1																1			1			1			
95		1	1		1		1																					1		1						1		
96		1	1		1	1																					1					1			1			
97									1		1														1		1			1						1		
98									1		1		1																1			1				1		
99																																						
100								1			1																1			1					1			
101																																						
102																																						
103									1		1		1															1		1					1			
104		1		1	1		1																					1			1					1		
105																																						
	13	26	16	24	41	15	16	20	42		59	7	8	1	6	6	5	2	7			8		2	8	1	46	39	19	32	47	25		3	53	48		

PLUTONIC QUARTZ: 23
DEFORMED PLUTONIC QUARTZ: 18
TOTAL PLUTONIC QUARTZ: 41

METAMORPHIC QUARTZ: 64

VOLCANIC QUARTZ: 8
DEFORMED VOLCANIC QUARTZ: 2
TOTAL VOLCANIC: 10

ample# BR3
ocation Castle Hill Basin - Broken River

Grain	PLUTONIC QUARTZ							METAMORPHIC QUARTZ								VOLCANIC QUARTZ												Grain properties: rounding			shape			grain size in microns					Comments
Grain	homogeneous	patchy	Light CL	Moderate CL	Microcracks-Healed	weak undulose	straight extinction	mottled	dark	Moderate CL	strong undulose	weak undulose	poly-crystalline = <3	poly-crystalline>3	total poly-crystalline	homogeneous	zonation	Light CL	Moderate CL	Open Fractures	Deformation lamellae	Quartz embayments	Straight extinction	Parallel/Sub-parallel fracture	Dark Shear bands	Random oriented fractures	Grain boundaries	angular	subangular-subrounded	rounded	elongate	platy	spherical	<2000	<1000	<500	<250	<125	
1								1	1		1														1		1			1			1			1			
2									1			1																1					1			1			
3									1			1																	1		1							1		
4																																							
5								1	1		1																			1	1						1			
6								1			1			1														1				1						1		
7									1		1																		1		1						1			
8									1		1																1		1				1					1			
9									1		1		1															1				1						1		
10									1		1		1														1	1		1				1			1			
11	1		1		1		1																						1		1					1			
12									1			1																	1		1							1		
13								1							1															1			1			1			
14									1			1																	1				1					1		
15								1			1																	1			1						1			
16									1		1			1															1				1			1			
17									1		1																			1	1						1			
18									1		1																		1			1					1			
19									1		1														1					1		1					1			
20									1		1																		1		1						1			
21																																							
22									1			1																	1				1					1		
23	1			1	1		1																					1					1			1			
24																	1		1				1		1			1			1						1			
25									1		1																			1			1			1			
26		1	1		1		1																						1				1			1			
27								1				1																		1			1			1			
28									1		1																			1	1							1		
29	1		1		1		1																						1				1			1			
30									1		1															1		1					1			1			
31																1			1				1							1			1			1			
32								1				1																1			1						1			
33									1		1															1		1				1					1			
34		1		1	1		1										1												1				1				1		
35												1				1												1				1				1			Deformation lamellae
36									1		1			1														1			1						1			
37									1		1																			1			1			1			
38									1		1		1																	1			1			1			
39								1				1																	1				1					1		
40									1			1	1																1			1					1			
41		1	1		1		1										1												1			1					1			
42									1		1				1															1	1						1			
43									1			1																	1				1			1			
44									1			1																		1			1					1	
45									1		1																		1				1			1			
46	1		1		1		1																						1				1				1		
47									1		1		1																1		1						1			
48									1		1		1																1		1							1		
																																							Deformation lamellae
51		1		1	1	1																							1				1			1			
52									1		1																	1			1							1		
53	1		1		1		1																						1		1						1			
54									1		1																		1				1				1		
55	1			1	1		1																					1					1				1		
56	1		1		1	1																						1			1						1			
57									1			1														1				1			1			1			
58									1		1				1															1			1			1			
59								1				1																		1			1					1	
60	1		1		1		1										1													1			1			1			
61									1			1																1				1					1			
62																																							
63									1			1																		1		1						1		
64								1			1																		1				1			1			
65		1		1	1	1																							1		1							1		
66																																							
67									1		1																			1			1			1			QO
68	1			1	1		1																							1			1					1	
69																1		1					1						1			1						1		
70								1			1		1																1				1					1		
71								1			1															1				1			1			1			
72								1			1														1					1			1			1			
73									1		1				1															1			1			1			
74																																							
75																1			1				1							1		1					1			
76									1			1																	1				1			1			
77								1			1														1					1			1		1				
78									1		1																		1		1				1				
79																																							
80								1			1																	1					1			1			
81									1		1																			1			1				1		
82								1			1			1															1			1					1			
83									1		1																			1			1				1		
84								1											1				1					1			1						1			
85								1				1																	1			1					1			
86								1			1								1			1																	
87									1							1					1									1			1		1				
88	1		1		1		1																						1		1						1			
89								1			1																			1			1			1			
90	1		1		1		1																					1			1						1			
91		1	1		1	1																						1				1						1		
92									1		1		1															1					1			1			
93																																							
94												1					1		1										1		1				1				
95								1			1																			1			1			1			
96								1															1							1			1			1			
97																																							
98											1					1		1			1									1			1			1			
99		1		1	1		1																					1			1						1			
100								1															1						1		1							1		
101		1		1	1		1																						1		1						1			
102		1		1	1		1																							1			1				1		
103								1			1				1														1				1		1				
104	1			1	1		1																						1		1						1			
105								1			1				1															1			1			1			
	13	18	11	16	30	7	19	33	44	0	51	20	8	4	6	6	6	2	6	0	2	1	7	0	5	6	2	25	41	38	29	19	55	0	5	68	28	3	

PLUTONIC QUARTZ: 21
DEFORMED PLUTONIC QUARTZ: 10
TOTAL PLUTONIC: 31

METAMORPHIC QUARTZ: 62

VOLCANIC QUARTZ: 4
DEFORMED VOLCANIC QUARTZ: 8
TOTAL VOLCANIC: 12

Sample# BR4
Location Castle Hill Basin - Broken River

Grain	PLUTONIC QUARTZ: homogeneous	patchy	Light CL	Moderate CL	Microcracks-Healed	weak undulose	straight extinction	METAMORPHIC QUARTZ: mottled	dark	Moderate CL	strong undulose	weak undulose	poly-crystalline =<3	poly-crystalline>3	total poly-crystalline	VOLCANIC QUARTZ: homogeneous	zonation	Light CL	Moderate CL	Open Fractures	Deformation lamellae	Quartz embayments	Straight extinction	Parallel/Sub-parallel fracture	Dark Shear bands	Random oriented fractures	Grain boundaries	Grain properties: rounding: angular	subangular-subrounded	rounded	shape: elongate	platy	spherical	grain size in microns: <2000	<1000	<500	<250	<125	Comments
1											1						1		1										1		1					1			
2		1		1	1		1																							1			1				1		
3																													1				1				1		
4	1		1		1		1																						1		1					1			
[redacted]																																							
6																												1					1				1		
7								1															1							1	1						1		
8									1			1																		1			1				1		
9	1		1		1	1																								1	1						1		
10																									1				1		1					1			
11		1		1	1	1																								1		1					1		
12																														1	1					1			
13																														1			1				1		
[redacted]																																							
15																												1					1				1		
16																												1				1						1	
17																													1				1				1		
18		1		1	1		1																					1					1			1			
19																														1			1				1		
20											1						1		1									1			1						1		
21																										1		1			1						1		
22								1	1																			1				1						1	
23									1			1																	1		1						1		
24											1						1		1										1		1						1		
25											1						1		1						1				1				1			1			
26	1		1		1		1										1											1			1						1		
27		1	1		1	1			1																			1			1							1	
28									1										1				1					1				1						1	
29	1		1		1		1																						1			1					1		
30									1																					1			1				1		
31	1				1		1																					1				1						1	
32									1		1																		1				1				1		
[redacted]																																							
34		1		1	1		1																					1			1						1		
35									1							1				1			1							1	1					1			
36		1	1		1	1																							1			1					1		
37												1				1			1	1						1	1		1		1						1		
38	1			1	1	1																							1				1			1			
39		1		1	1	1																							1		1						1		
40									1		1																	1			1						1		
41											1						1		1	1	1								1				1			1			
42																1			1				1					1				1						1	
43																	1	1					1						1				1				1		
44									1			1																1			1						1		
45	1			1	1	1																							1			1				1			
[redacted]																																							
47									1																				1		1						1		
48								1			1																			1			1				1		
49											1																	1				1				1			
50									1		1																			1			1			1			
[redacted]																																							
52	1			1	1	1																						1				1					1		
53		1		1	1		1																							1		1					1		
54	1		1		1	1																						1				1				1			
55								1																						1			1				1		
56								1								1							1					1				1					1		
57																1			1				1						1			1					1		
58								1				1																		1			1					1	
59	1			1	1	1																							1			1					1		
60	1		1		1		1																						1			1					1		
61								1				1																		1			1				1		
62		1	1		1	1																						1			1						1		
63								1																					1		1					1			
64		1	1		1		1																					1				1					1		
65								1																					1			1					1		
66								1				1																	1			1					1		
67												1																		1			1				1		
68	1		1		1		1																					1				1					1		
69																	1		1				1							1		1				1			
70								1			1																		1		1						1		
71								1			1																			1	1						1		
72									1		1																			1			1				1		
[redacted]																																							
74		1	1		1		1										1												1			1						1	
75									1		1																			1			1					1	
76																														1			1					1	
77											1						1		1											1	1					1			
78		1		1	1		1																					1			1							1	
79								1			1																			1			1				1		
80											1						1		1	1	1									1			1			1			
[redacted]																																							
82																												1				1						1	
83																														1			1				1		
[redacted]																																							
85																	1		1				1						1		1					1			
[redacted]																																							
87									1		1																			1			1				1		
88								1																						1			1					1	
[redacted]																																							
90									1			1																		1	1					1			
91	1		1		1	1																							1		1					1			
92								1				1																1			1					1			
93	1		1		1		1																					1			1								
94																												1									1		
95									1		1																	1				1						1	
96									1		1																		1				1			1			
97																												1				1						1	
98								1															1						1			1					1		
99									1		1																			1		1					1		
100																												1				1						1	
101								1															1					1			1						1		
102								1			1																			1		1					1		
[redacted]																																							
104	1		1		1	1																								1			1					1	
105																													1				1				1		
	20	18	19	18	38	14	14	25	31	0	49	17	2	0	0	5	13	1	13	4	2	0	11	0	2	2	1	35	36	34	34	38	33	0	0	24	64	17	

PLUTONIC QUARTZ : 27
DEFORMED PLUTONIC QUARTZ : 11
TOTAL PLUTONIC QUARTZ: 38

METAMORPHIC QUARTZ : 46

VOLCANIC QUARTZ : 7
DEFORMED VOLCANIC QUARTZ : 12
TOTAL VOLCANIC QUARTZ : 19

Location Castle Hill Basin - Whitewater stream
Sample# IC2

PLUTONIC QUARTZ — METAMORPHIC QUARTZ — VOLCANIC QUARTZ — Fracture patterns Optical/CL features — Grain properties: rounding, shape, grain size in microns — Comments

Grain	homogeneous	patchy	Light CL	Moderate CL	Microcracks-Healed	weak undulose	straight extinction	mottled	dark	Moderate CL	strong undulose	weak undulose	poly-crystalline =<3	poly-crystalline>3	total poly-crystalline	homogeneous	zonation	Light CL	Moderate CL	Open Fractures	Quartz embayments	Straight extinction	Sub-parallel fractures	Dark Shear bands	Random oriented fractures	Grain boundaries	angular	subangular-subrounded	rounded	elongate	platy	spherical	<2000	<1000	<500	<250	<125	Comments
1									1		1																	1			1				1			
2																1			1			1							1			1				1		
3	1			1	1	1																								1							1	
4	1		1		1		1																				1				1						1	
5									1			1																1			1				1			
6									1		1																	1			1					1		
7								1			1																		1			1				1		
8																1			1	1		1			1				1			1				1		
9									1		1																1				1						1	
10									1		1														1		1				1					1		
11	1		1		1	1																					1				1					1		
12									1		1																		1			1					1	
13									1		1																	1		1							1	
14								1			1																		1			1		1				
15									1		1				1														1			1	1					
16		1		1	1			1			1																					1						
17								1			1																	1				1			1			
18								1				1																	1			1				1		
19									1		1																		1			1			1			
20									1		1																	1		1					1			
21									1		1																1			1					1			
22								1			1				1													1				1				1		
23									1		1				1														1			1	1					
24		1			1	1		1																														
25									1		1		1														1					1				1		
26	1		1		1						1																											
27									1		1																1				1				1			
28									1		1																1				1					1		
29									1		1																1				1					1		
30									1		1			1															1			1			1			
31									1			1																	1			1			1			
32									1		1				1														1			1		1				
33									1		1				1														1			1		1				
34									1		1			1														1			1					1		
35									1		1																		1			1		1				
36									1		1																		1			1			1			
37																1			1			1					1					1			1			
38									1		1		1																1			1			1			
39									1		1																		1			1			1			
40									1		1																		1			1			1			
41									1		1																		1			1			1			
42									1		1				1														1			1		1				Polygonized quartz
43									1			1																	1			1			1			
44	1			1	1	1																							1			1			1			
45									1		1																		1			1			1			
46									1		1																		1			1			1			Polygonized quartz
47	1			1	1	1																		1			1			1					1			
48									1		1																1				1				1			
49								1			1		1																1			1			1			
50																1			1			1					1				1					1		
51									1		1				1														1			1		1				crenulated quartz
52									1		1																1				1				1			
53									1		1																		1			1		1				
54									1		1																	1			1					1		
55									1		1				1														1		1			1				crenulated quartz
56									1		1																1			1						1		
57									1		1													1				1			1			1				
58									1		1																	1				1			1			
59									1		1		1																1			1				1		
60									1		1																		1			1			1			
61									1		1																		1			1				1		
62									1		1				1														1			1		1				polyhedral quartz
63									1		1																	1			1					1		
64									1		1																		1			1				1		
65									1		1																1				1					1		
66								1			1																	1			1					1		
67	1			1	1	1																						1			1				1			
68	1			1	1	1																					1				1					1		
69	1			1	1						1																											
70	1			1	1		1																				1				1				1			
71								1			1																		1		1				1			
72									1		1		1																1			1		1				
73									1		1																		1			1			1			
74									1		1		1																1			1			1			
75									1		1				1														1			1			1			Polyhedral quartz
76									1		1																		1			1				1		
77									1		1																	1			1					1		
78									1			1															1					1				1		
79	1			1	1						1																											
80									1		1															1			1			1			1			
81												1				1			1					1					1			1			1			Deformation lamellae
82									1		1																	1				1			1			
83	1			1	1	1																			1	1			1			1			1			
84									1		1																		1			1			1			
85	1			1	1		1																						1			1		1				
86									1		1				1														1			1			1			Polyhedral quartz
87	1		1		1		1																					1			1				1			
88									1		1																		1			1			1			
89									1		1																		1	1						1		
90									1		1				1														1			1		1				Polyhedral quartz
91		1		1	1		1	1																														QO
92	1			1	1		1																				1				1					1		
93		1		1	1		1	1																														
94																1			1			1							1			1		1				
95	1		1		1		1																					1		1				1				QO
96											1					1			1					1				1		1					1			QO
97									1		1		1																1		1				1			
98									1		1																	1		1						1		
99									1		1																		1			1				1		
100									1			1																	1			1			1			
101																1			1			1								1		1			1			
102		1		1	1			1			1																											
103									1			1																	1	1						1		
104	1			1	1		1																					1			1				1			
105	1			1	1		1																					1			1				1			
TOTAL	18	5	5	18	23	8	10	13	66		73	8	7	2	12	8			8	1		6		5	3	2	24	23	56	12	34	60	2	15	48	35	5	

PLUTONIC QUARTZ: 16
DEFORMED PLUTONIC QUARTZ: 8
TOTAL PLUTONIC QUARTZ : 24

METAMORPHIC QUARTZ : 74

VOLCANIC QUARTZ: 6
DEFORMED VOLCANIC QUARTZ: 2
TOTAL VOLCANIC QUARTZ : 8

Location Castle Hill Basin - Whitewater stream
Sample# IC4

Grain	PLUTONIC QUARTZ							METAMORPHIC QUARTZ								VOLCANIC QUARTZ							Fracture patterns Optical/CL features				Grain properties: rounding			shape			grain size in microns					Comments
Grain	homogeneous	patchy	Light CL	Moderate CL	Microcracks-Healed	weak undulose	straight extinction	mottled	dark	Moderate CL	strong undulose	weak undulose	poly-crystalline = <3	poly-crystalline>3	total poly-crystalline	homogeneous	zonation	Light CL	Moderate CL	Open Fractures	Quartz embayments	Straight extinction	Sub-parallel fractures	Dark Shear bands	Random oriented fractures	Grain boundaries	angular	subangular-subrounded	rounded	elongate	platy	spherical	<2000	<1000	<500	<250	<125	Comments
1									1		1																1				1					1		QO
3	1			1	1		1																				1			1						1		
4									1		1																	1				1			1			Polygonized quartz
5									1		1																	1			1					1		
6									1		1																1				1					1		
7									1			1	1														1				1					1		
8									1		1																		1			1				1		
9									1		1																	1			1					1		
10									1		1														1	1		1			1					1		
11									1		1																		1			1				1		
12	1		1		1		1																				1					1				1		
13									1																		1			1					1			
14										1	1																		1			1			1			
15									1		1		1															1			1					1		
16									1		1		1															1			1					1		
17									1		1																1				1					1		
18											1					1			1										1		1				1			Deformation lamellae
19		1		1	1	1																						1			1					1		
20									1																		1				1						1	
21								1				1															1				1					1		QO
22									1		1																		1			1				1		
23	1			1	1		1																					1			1				1			
24																1			1			1						1				1					1	
25									1			1																1			1					1		
26								1			1																1				1						1	
27								1				1																1			1					1		
28									1			1																	1			1					1	
29									1		1																		1			1			1			
30									1		1																		1			1				1		
31											1						1	1							1		1				1				1			QO
32										1	1																1				1				1			
33											1					1	1		1									1				1			1			
34											1						1	1											1			1				1		
35	1			1	1		1																						1			1			1			
36								1			1																1				1					1		
37	1			1	1	1																						1			1					1		
38																1			1			1							1	1					1			QO
39											1						1		1									1			1					1		
40									1		1																		1		1					1		
41								1				1																	1			1					1	
42									1		1																	1			1					1		
43								1			1																1				1				1			
44								1			1																1				1				1			
45		1		1	1		1																				1				1					1		complex sheared quartz
46									1		1																	1				1				1		
																																						Deformation lamellae
48									1		1				1														1	1					1			Polyhedral quartz
49								1				1															1			1						1		
50								1			1																		1		1					1		
51									1		1																	1			1					1		
52									1			1																	1	1					1			
53									1		1																1			1						1		
54										1	1																		1			1				1		
55																1			1			1						1				1				1		
56		1		1	1	1																							1	1					1			
57									1			1																1				1			1			
58									1		1																		1		1					1		
59	1		1		1		1																						1			1				1		
60											1						1		1									1				1				1		
61									1		1																		1			1				1		
62	1			1	1		1																				1				1					1		
63									1		1																	1			1					1		
64	1			1	1		1																				1					1			1			
65	1		1		1		1																						1			1			1			
66									1		1																		1			1				1		
67	1			1	1	1																							1			1				1		
68									1			1																	1			1					1	
69										1	1																	1			1					1		
70								1								1			1			1							1			1			1			
71									1		1																		1			1			1			
73									1		1																		1			1				1		
75									1		1																	1		1						1		
76									1		1																		1	1						1		
77									1		1																		1			1				1		
78											1					1		1											1	1						1		
79										1	1																		1		1				1			
80								1			1								1			1						1				1				1		
81								1			1																		1			1					1	
82	1			1	1	1																							1			1				1		
																																						Deformation lamellae
84	1			1	1		1																						1			1				1		
85	1			1	1	1																					1				1						1	
86								1											1			1							1			1			1			
88									1			1															1			1							1	
89									1							1						1							1			1					1	
90								1			1																	1			1					1		
91									1		1		1																1			1				1		
92											1					1			1										1			1				1		
94											1					1			1										1	1					1			Deformation lamellae
96								1			1																		1			1					1	
97									1		1																1			1						1		
98									1		1													1					1			1				1		
99									1		1																1				1						1	
100								1			1													1					1			1				1		
101									1		1																		1			1			1			
																																						Deformation lamellae
103	1		1		1		1																						1		1				1			
105									1		1																		1	1					1			
	22	5	5	22	27	7	12	18	45	5	68	11	5		1	10	5	3	12			7		3	3	1	28	27	50	16	42	46			32	59	14	

PLUTONIC QUARTZ: 17
DEFORMED PLUTONIC QUARTZ: [illegible]
TOTAL PLUTONIC QUARTZ: 27

METAMORPHIC QUARTZ: 62

VOLCANIC QUARTZ: 7
DEFORMED VOLCANIC QUARTZ: 9
TOTAL VOLCANIC QUARTZ: 16

Location Avoca
Sample# AV1

Grain	PLUTONIC QUARTZ homogeneous	patchy	Light CL	Moderate CL	Microcracks-Healed	weak undulose	straight extinction	METAMORPHIC QUARTZ mottled	dark	Moderate CL	strong undulose	weak undulose	poly-crystalline = <3	poly-crystalline>3	total poly-crystalline	VOLCANIC QUARTZ homogeneous	zonation	Light CL	Moderate CL	Open Fractures	Quartz embayments	Straight extinction	Fracture patterns Optical/CL features Sub-parallel fractures	Dark Shear bands	Random oriented fractures	Grain boundaries	Grain properties rounding angular	subangular-subrounded	rounded	shape elongate	platy	spherical	grain size in microns <2000	<1000	<500	<250	<125	Comments
1	1		1		1		1																				1			1					1			
2																																						
3									1		1																1			1						1		
4												1				1			1						1		1			1					1			Deformation lamellae
5											1						1	1										1				1			1			
6								1			1																1				1					1		
7												1				1			1								1			1					1			
8									1		1																1			1						1		
9	1			1	1		1																				1				1						1	
10								1			1																	1			1				1			
11									1		1		1															1				1					1	
12																1		1				1				1	1				1					1		
13									1		1																	1			1						1	
14									1		1														1			1		1				1				Polygonized
15	1		1		1	1																			1			1		1					1			
16																																						
17									1			1															1				1					1		
18	1		1		1		1																				1			1					1			
19											1																	1			1					1		
20	1		1		1		1																					1		1					1			
21	1		1		1	1																						1		1					1			
22									1		1																		1			1				1		
23	1			1	1		1																				1				1					1		
24																									1			1			1				1			
25																																						
26																1			1			1						1				1				1		
27																																						
28	1		1		1	1																							1			1			1			
29																													1			1				1		
30																												1			1					1		
31	1		1		1		1																				1				1					1		
32																												1		1						1		Polyhedral
33																													1			1				1		
34	1		1		1	1																					1			1					1			
35	1		1		1		1																					1							1			
36																												1								1		
37																			1									1			1					1		
38																									1		1			1							1	
39																											1				1					1		
40																1						1						1			1					1		
41																																						
42																																						Deformation lamellae
43																									1			1				1				1		
44																																						
45											1					1			1										1			1				1		
46																			1			1	1					1			1					1		
47												1					1		1									1			1					1		Deformation lamellae
48												1				1		1										1				1				1		
49	1		1		1		1																						1			1					1	
50																						1							1			1				1		
51												1				1		1										1		1							1	Deformation lamellae
52																											1			1						1		
53																									1			1		1					1			
54																																						
55																												1		1						1		Polygonized
56																									1		1			1					1			
57																																						
58																1			1			1					1			1						1		
59	1		1		1		1																						1			1			1			
60	1			1	1		1																				1				1					1		
61								1			1																		1			1				1		
62																																						Deformation lamellae
63	1		1		1		1																						1			1				1		
64									1		1																1				1					1		
65									1		1				1														1			1				1		Polygonal
66																																						
67								1			1								1			1					1				1					1		
68									1		1																1				1					1		
69									1		1	1																	1			1				1		
70								1			1		1																1			1				1		
71																																						
72	1			1	1		1																					1		1						1		
73								1											1			1		1	1			1			1					1		
74											1					1			1									1			1					1		Deformation lamellae
75								1				1															1			1					1			
76											1																1			1					1			
77	1			1	1	1																					1				1					1		
78		1		1	1	1		1																			1				1					1		
79																1			1			1							1			1					1	
80		1		1	1		1	1																				1			1					1		
81																1			1			1							1			1					1	
82	1			1	1		1																					1			1					1		
83	1		1		1		1																				1			1						1		
84									1		1														1			1			1				1			
85									1		1		1												1			1			1					1		
86								1			1																	1		1					1			
87												1					1	1										1		1					1			
88	1		1		1	1																						1			1					1		
89		1		1	1		1	1																			1				1					1		
90																												1		1					1			
91									1		1				1	1						1							1	1					1			
92	1			1	1	1																						1		1					1			crenulated
93																												1		1						1		
94	1		1		1		1										1										1			1						1		
95								1			1																1			1					1			
96											1					1			1								1				1					1		
97									1		1					1						1					1				1					1		
98									1		1																1				1					1		
99	1		1		1		1																					1			1					1		Deformation lamellae
100									1																				1			1			1			
101	1		1		1		1																				1			1						1		
102	1		1		1		1																				1			1					1			
103									1				1												1				1			1			1			
104		1		1	1		1	1																			1				1					1		
TOTAL	34	9	28	14	43	8	21	32	22	0	51	12	4	0	4	17	4	6	14	0	0	13	1	1	15	1	42	42	21	36	42	27	0	2	30	63	10	

PLUTONIC QUARTZ: 29
DEFORMED PLUTONIC QUARTZ: 14
TOTAL PLUTONIC QUARTZ: 43

METAMORPHIC QUARTZ: 38

VOLCANIC QUARTZ: 13
DEFORMED VOLCANIC QUARTZ: 10
TOTAL VOLCANIC QUARTZ: 23

Location Avoca
Sample# AV2

	PLUTONIC QUARTZ							METAMORPHIC QUARTZ								VOLCANIC QUARTZ							Fracture patterns Optical/CL features				Grain properties rounding			shape			grain size in microns					Comments
Grain	homogeneous	patchy	Light CL	Moderate CL	Microcracks-Healed	weak undulose	straight extinction	mottled	dark	Moderate CL	strong undulose	weak undulose	poly-crystalline = <3	poly-crystalline>3	total poly-crystalline	homogeneous	zonation	Light CL	Moderate CL	Open Fractures	Quartz embayments	Straight extinction	Sub-parallel fractures	Dark Shear bands	Random oriented fractures	Grain boundaries	angular	subangular-subrounded	rounded	elongate	platy	spherical	<2000	<1000	<500	<250	<125	
1	1		1		1	1																			1				1	1				1				
2									1		1																1				1					1		
3	1		1		1		1																					1		1						1		
4									1		1																1			1						1		
5	1		1		1	1																							1			1					1	
6									1		1														1			1			1					1		
7	1		1		1	1																							1			1					1	
8	1		1		1		1																					1				1				1		
9																1			1			1						1			1					1		
10								1			1																		1			1					1	
11								1			1																1			1						1		
12								1			1																	1			1					1		
13																	1		1			1						1			1					1		
14	1		1		1		1																						1			1					1	
15																	1		1			1							1			1					1	
16									1		1																1				1					1		
17	1		1		1		1																					1			1					1		
18									1		1																1				1					1		
19	1		1		1		1																				1				1					1		
20																1		1				1							1		1					1		
21								1			1							1				1					1			1					1			
22								1			1																	1			1					1		
23								1			1																1				1					1		
24									1		1																1				1					1		
25	1		1		1		1																						1			1				1		
26	1		1		1		1																						1		1					1		
27																																						
28																	1		1			1							1			1				1		
29								1											1			1		1				1				1				1		
30									1		1																1			1					1			
31									1		1																		1			1				1		
32											1					1			1									1			1					1		
33												1				1			1								1				1					1		
34									1			1																1			1						1	
35																																						
36									1		1				1														1	1					1			
37	1		1		1		1																						1			1				1		
38									1		1																1			1						1		
39									1		1														1				1			1				1		
40									1		1																	1			1					1		
41									1		1					1						1						1			1					1		
42												1					1		1										1			1				1		
43									1		1														1			1			1					1		
44								1											1			1							1			1				1		
45																																						
46											1					1			1						1		1			1						1		
47									1		1														1		1				1					1		
48	1		1		1		1																				1			1						1		
49									1		1					1						1			1			1		1						1		
50	1		1		1		1																					1				1				1		
51								1			1																		1			1					1	
52									1		1																1				1					1		
53	1		1		1		1																						1			1				1		
54									1			1													1				1			1				1		
55								1				1													1		1				1					1		
56	1		1		1		1																		1			1			1					1		
57									1							1						1			1				1			1				1		
58	1			1	1	1																						1			1						1	
59	1			1	1	1																					1				1						1	
60																																						
61								1			1														1		1				1						1	
62	1		1		1		1																				1				1					1		
63									1		1														1			1		1						1		
64									1			1													1				1			1				1		
65									1		1																	1			1					1		
66									1							1						1					1			1						1		
67									1							1						1							1			1				1		
68									1							1						1			1			1			1					1		
69									1		1																1				1					1		
70									1		1																	1		1					1			
71	1		1		1		1																					1				1				1		
72									1		1														1		1				1					1		
73																																						
74	1		1		1	1																					1			1						1		
75									1		1																	1			1						1	
76											1					1			1								1				1					1		Deformation lamellae
77	1		1		1		1																						1			1				1		
78									1		1														1		1				1					1		
79	1		1		1		1																				1			1						1		
80	1		1		1		1																					1			1				1			
81								1			1														1		1				1					1		
82	1		1		1		1																						1			1					1	
83									1		1														1		1				1					1		
84																																						
85									1		1																1			1						1		
86																																						
87																																						
88																1			1			1					1				1					1		
89	1		1		1	1																					1				1					1		
90								1			1													1			1			1					1			Polygonized
91																1			1			1					1				1					1		
92																																						
93	1			1	1	1																						1		1							1	
94	1		1		1		1																				1				1					1		
95									1							1						1						1			1				1			
96	1		1		1		1																				1			1						1		
97	1			1	1		1																				1			1						1		
98	1			1	1		1																					1		1						1		
99	1		1		1		1																		1			1			1				1			
100		1	1		1		1	1																				1			1					1		
101									1		1																1				1						1	
102	1		1		1	1																					1				1					1		
103																1			1			1							1			1				1		
104	1		1		1		1																				1				1					1		
105	1		1		1		1																				1			1						1		
TOTAL	42	2	37	6	44	9	26	15	35	0	46	6	0	0	1	16	4	2	14	0	0	18	0	2	21	0	47	32	26	29	50	26	0	1	10	79	15	

PLUTONIC QUARTZ: 35
DEFORMED PLUTONIC QUARTZ: 9
TOTAL PLUTONIC QUARTZ: 44

METAMORPHIC QUARTZ: 38

DEFORMED VOLCANIC QUARTZ: 5
VOLCANIC QUARTZ: 18
TOTAL VOLCANIC QUARTZ: 23

Location Iron Creek
Sample# IC3

PLUTONIC QUARTZ (columns 2–8) · METAMORPHIC QUARTZ (columns 9–16) · VOLCANIC QUARTZ (columns 17–23)

Grain	homogeneous	patchy	Light CL	Moderate CL	Microcracks-Healed	weak undulose	straight extinction	mottled	dark	Moderate CL	strong undulose	weak undulose	poly-crystalline = <3	poly-crystalline>3	total poly-crystalline	homogeneous	zonation	Light CL	Moderate CL	Open Fractures	Quartz embayments	Straight extinction
1	1			1	1		1															
2	1			1	1		1															
3									1		1											
4	1			1	1		1															
5	1		1		1		1															
6									1		1											
[redacted]																						
8									1			1										
9									1		1											
10									1		1											
11									1		1											
12											1						1		1			
13									1		1		1									
14									1		1											
15	1			1	1	1																
16									1		1											
17	1			1	1		1															
18								1											1			1
19								1			1											
20									1		1											
21									1		1											
22									1		1											
23											1					1			1			
24									1		1											
25	1		1		1		1															
26									1		1											
27									1			1										
28									1		1											
29									1		1											
30									1		1											
31																1			1			1
32									1		1											
33									1		1				1							
34								1			1											
35											1											
36									1		1											
37	1		1		1		1															
[redacted]																						
40	1		1		1		1															
41									1		1											
42									1		1				1							
43									1		1											
44									1		1											
45											1					1		1				
46									1		1		1									
[redacted]																						
49									1		1											
50									1		1											
[redacted]																						
52									1		1											
53									1		1											
54	1		1		1		1															
55									1		1											
56									1		1											
[redacted]																						
58									1		1											
59									1		1											
60	1		1		1		1															
61									1		1											
62									1		1											
63	1			1	1		1															
64									1			1										
65	1			1	1		1															
66	1		1		1		1															
67									1		1											
68	1		1		1	1																
69									1		1											
70								1			1											
71	1			1	1	1																
[redacted]																						
73	1			1	1	1																
74	1		1		1		1															
75									1		1											
76									1		1											
77									1		1											
[redacted]																						
79									1		1											
80								1			1											
81									1		1											
82									1		1											
83									1		1		1									
84									1		1											
85									1		1											
86									1		1											
87																1		1				1
88									1		1											
89								1			1											
90									1		1											
91									1		1											
92	1			1	1		1															
93									1		1											
[redacted]																						
95									1		1											
96									1		1											
97																1		1				1
98									1		1											
99																1		1				1
100	1		1		1		1															
101	1		1		1		1															
102									1							1						1
[redacted]																						
105									1													
TOTAL	29	4	16	17	33	4	17	9	59		75	3	4	0	2	7	1	4	4	0	0	6

PLUTONIC QUARTZ: 21
[redacted]
TOTAL PLUTONIC QUARTZ: 33

METAMORPHIC QUARTZ: 63

VOLCANIC QUARTZ: 6
DEFORMED VOLCANIC QUARTZ: 3
TOTAL VOLCANIC QUARTZ: 9

Fracture patterns Optical/CL features · Grain properties: rounding, shape, grain size in microns · Comments

Grain	Sub-parallel fractures	Dark Shear bands	Random oriented fractures	Grain boundaries	angular	subangular-subrounded	rounded	elongate	platy	spherical	<2000	<1000	<500	<250	<125	Comments
1						1			1					1		
2						1			1					1		
3						1				1				1		
4					1				1					1		
5					1			1					1			
6						1			1					1		
[redacted]																
8					1				1					1		
9					1			1						1		
10						1			1					1		
11					1				1					1		
12		1			1				1					1		
13						1		1					1			
14					1			1						1		
15			1		1				1					1		
16					1				1						1	
17					1				1						1	
18							1			1				1		
19					1				1					1		
20			1			1			1					1		
21					1				1					1		
22						1			1					1		
23							1			1				1		
24						1			1					1		
25			1				1			1				1		
26					1				1					1		
27			1		1				1					1		
28						1			1					1		
29					1			1						1		
30						1		1						1		
31					1				1					1		
32					1			1						1		
33						1				1			1			Polyhedral
34					1			1					1			
35							1			1				1		
36			1				1			1				1		
37			1		1			1					1			
[redacted]																
40							1			1			1			
41					1			1					1			
42					1			1					1			Polyhedral
43					1				1					1		
44					1			1						1		
45			1		1			1						1		
46			1				1			1				1		
[redacted]																
49			1				1			1			1			
50			1				1			1			1			
[redacted]																
52					1			1					1			
53					1			1					1			
54							1			1				1		
55							1			1			1			
56					1			1						1		
[redacted]																
58			1		1			1					1			
59			1				1			1		1				
60							1			1			1			
61			1			1			1					1		
62					1			1						1		
63			1		1			1					1			
64			1		1			1						1		
65					1			1						1		
66					1			1						1		
67					1			1					1			
68	1				1			1					1			
69	1				1			1					1			
70			1		1			1					1			polygonized
71			1				1			1				1		
[redacted]																
73			1			1		1						1		
74			1		1			1					1			
75			1		1			1					1			
76					1				1					1		
77					1				1				1			
[redacted]																
79			1				1	1				1				
80						1				1			1			
81							1			1			1			
82			1			1		1					1			
83			1				1			1			1			
84					1				1					1		
85						1			1					1		
86			1		1			1					1			
87			1			1				1				1		
88							1		1					1		
89			1			1			1					1		
90					1			1					1			
91						1			1				1			
92					1			1					1			
93					1			1					1			
[redacted]																
95			1		1			1						1		
96						1		1					1			
97			1				1			1			1			
98			1			1			1				1			
99							1	1					1			
100					1			1					1			
101					1				1				1			
102					1				1				1			
[redacted]																
105					1			1					1			
TOTAL	0	3	36	1	59	22	24	48	32	25	0	2	49	52	2	

Cathodoluminescence-polarized microscope analysis
Sample# 4 Formation : Iron Creek Greensand
Location Iron Creek

	PLUTONIC QUARTZ							METAMORPHIC QUARTZ								VOLCANIC QUARTZ							Grain properties				rounding			shape			grain size in microns					Comments
Grain	homogeneous	patchy	Light CL	Moderate CL	Microcracks -Healed	weak undulose	straight extinction	mottled	dark	Moderate CL	strong undulose	weak undulose	poly-crystalline = <3	poly-crystalline>3	total poly-crystalline	homogeneous	zonation	Light CL	Moderate CL	Open Fractures	Quartz embayments	Straight extinction	Parallel/Sub-parallel features	Dark shear bands	Random oriented fractures	Grain boundaries	angular	subangular-subrounded	rounded	elongate	platy	spherical	<2000	<1000	<500	<250	<125	
1		1	1		1		1																				1			1						1		QO
2																1			1			1				1			1						1		
3									1		1																	1		1					1		QO
[illegible]																																						
5									1		1																1					1				1		
6									1			1															1			1						1		
[illegible]																																						
8									1		1																1			1						1		
9								1			1																		1			1						1	QO
10	1		1		1		1																					1			1					1		
11																1			1			1						1			1				1		
12	1		1		1		1																			1				1					1		
13									1			1																1		1					1			
14									1		1												1	1	1			1					1			
15									1		1																1			1						1		
16									1		1																	1			1					1	QO
17	1		1		1		1																					1			1				1		
18									1		1			1												1			1			1			1			
19								1			1																1					1				1		
20	1		1		1		1																			1				1					1		
21								1			1																	1		1						1		
22	1			1	1		1																			1				1					1		
23									1		1																	1				1				1		
24								1				1																1				1				1		
25									1		1																	1				1				1		
26									1		1																		1			1			1			
27									1		1																1				1					1		
28								1																1			1		1						1		
29																1			1			1				1			1						1		
[illegible]																																						
31									1			1															1				1				1			
[illegible]																																						
33	1		1		1		1																			1			1					1			
34									1		1																1			1						1		
[illegible]																																						
[illegible]																																						
37									1		1																	1				1				1		
38								1			1		1															1			1					1		
39									1			1															1					1					1	
40									1			1																1		1							1	
41									1		1																	1				1				1		
42									1		1			1																1		1					1		
43	1			1	1	1																					1				1					1		
44									1		1												1	1	1					1				1		
45								1				1																	1			1				1		
46	1			1	1		1																			1				1					1		
47									1			1															1			1						1		
48								1				1																1				1				1		
49									1		1																	1				1				1		
50									1		1																		1			1				1		
51	1			1	1		1																						1			1				1		
52									1		1																1				1					1		
53									1		1																		1			1				1		QO
[illegible]																																						
[illegible]																																						
56									1		1																		1			1			1			
57									1		1																	1			1					1		
58	1		1		1		1																					1			1			1			
59									1			1															1				1					1		
60									1		1			1														1					1				1		
61	1		1		1		1																					1	1					1			QO
62									1		1																	1				1					1	QO
63	1			1	1	1																						1				1				1		
64	1		1		1	1																								1		1					1		
65									1			1															1				1					1		
66	1		1		1		1																					1			1				1		
[illegible]																																						
68	1		1		1		1																			1					1			1		QO
69									1			1																	1	1						1		
[illegible]																																						
71									1		1																1				1					1		
72	1		1		1		1																1		1				1					1		
73									1		1												1				1			1			1			
74									1			1																	1			1				1		
75								1			1														1			1			1					1		
76	1		1		1																				1		1				1					1		
77	1			1	1		1																				1		1					1			
78	1			1	1		1																			1			1					1			
79	1		1		1		1																1			1				1				1		QO
[illegible]																																						
81	1		1		1	1																		1			1			1				1			
82								1			1																	1				1			1			
83									1		1																	1				1				1		
84									1		1																1			1					1			
85									1		1		1														1				1				1			Polygonized Qtz
86	1			1	1		1																			1			1						1		
87												1						1		1										1				1					1		
88									1		1		1														1				1					1		
89	1			1	1	1																					1				1					1		
90	1			1	1	1																						1			1					1		
[illegible]																																						
[illegible]																																						
93											1					1		1												1				1				1		
94	1		1		1	1																						1				1			1		QO
95									1		1												1	1	1			1						1		
96											1					1		1						1				1			1			1			
97									1		1												1		1				1					1		
98									1		1																1			1						1		QO
99									1		1																	1			1					1		QO
100	1		1		1		1																				1			1					1		QO
101									1		1																1			1					1			
102	1		1		1	1																						1		1					1			
103									1		1		1														1				1					1		QO
104	1			1	1		1																				1				1				1		QO
105	1		1		1		1																				1		1					1				QO
	35	8	24	18	43	10	24	17	46	0	53	15	4	3	0	3	4	0	6	0	0	3	0	0	15	4	43	39	23	30	33	42	0	0	29	70	6	

PLUTONIC QTZ : 29
DEFORMED PLUTONIC QTZ : 13
TOTAL PLUTONIC : 42

METAMORPHIC QTZ: 57

VOLCANIC QTZ : 3
DEFORMED VOLCANIC QTZ : 3
TOTAL VOLCANIC QTZ : 6

Location Mount Somers - Coal Mine
Sample# CM1

Grain	PLUTONIC QUARTZ: homogeneous	patchy	Light CL	Moderate CL	Microcracks-Healed	weak undulose	straight extinction	METAMORPHIC QUARTZ: mottled	dark	Moderate CL	strong undulose	weak undulose	poly-crystalline = <3	poly-crystalline>3	total poly-crystalline	VOLCANIC QUARTZ: homogeneous	zonation	Light CL	Moderate CL	Open Fractures	Quartz embayments	Straight extinction	Fracture patterns Optical/CL features: Sub-parallel fractures	Dark Shear bands	Random oriented fractures	Grain boundaries	Grain properties, rounding: angular	subangular-subrounded	rounded	shape: elongate	platy	spherical	grain size in microns: <2000	<1000	<500	<250	<125	Comments
1											1						1		1				1				1			1						1		
2	1		1		1		1																				1			1						1		
3								1			1																		1			1				1		Deformation lamellae
[illegible]																																						Deformation lamellae
[illegible]																																						Deformation lamellae
6												1															1				1					1		
7	1		1		1		1																				1			1						1		
8												1															1				1					1		
9								1				1															1				1					1		
10											1																1			1						1		
11											1						1	1									1			1						1		
[illegible]																																						
13											1																1			1						1		
14											1						1		1									1		1					1			Deformation lamellae
15											1						1		1			1					1				1					1		
16											1						1		1								1			1					1			Deformation lamellae
17											1						1	1								1		1			1				1			Deformation lamellae
18												1				1		1									1				1					1		Deformation lamellae
19												1				1			1								1			1						1		Deformation lamellae
20										1	1																	1				1			1			
21											1						1	1		1						1	1				1				1			
22	1		1		1		1																				1				1					1		
23	1		1		1	1																							1			1				1		
24								1				1															1		1							1		
25	1		1		1		1																					1			1					1		
26		1	1		1		1																					1			1					1		
27								1			1																1			1						1		
28								1			1																1				1					1		
29								1			1																	1			1					1		
30												1					1	1										1		1						1		
31									1		1																	1				1				1		
32																1		1				1						1		1						1		
[illegible]																																						Deformation lamellae
34	1		1		1		1																				1				1					1		
35																	1		1			1						1				1				1		
36											1					1		1											1			1				1		
37											1						1	1									1			1						1		Deformation lamellae
38								1			1																	1			1					1		
39																	1	1				1					1			1						1		
40								1			1																1			1					1			
41									1		1																1			1						1		
42											1						1	1									1				1					1		
43											1						1	1									1				1					1		Deformation lamellae
44											1						1	1									1			1					1			
[illegible]																																						
46											1					1			1						1				1	1						1		
47											1						1		1									1			1					1		
48																1		1				1						1			1					1		
49	1		1		1		1																						1		1					1		
50											1						1		1								1				1					1		
51												1					1	1									1					1			1			
52	1			1	1	1																										1			1			Deformation lamellae
53								1			1																1				1					1		
54											1						1	1									1			1					1			
55																	1	1				1						1				1				1		
56									1		1																	1		1						1		
57												1				1		1											1			1				1		
58																1		1				1			1		1			1						1		
59																1			1			1			1			1		1					1			Deformation lamellae
60																	1	1				1					1				1					1		
61								1			1																1				1				1			
62								1			1	1															1				1					1		Deformation lamellae
63									1		1																	1		1						1		
64												1				1			1									1			1					1		
65											1					1			1									1			1					1		Deformation lamellae
66									1		1																1				1					1		
67																1		1				1					1			1					1			
[illegible]																																						
69																1		1				1			1		1				1					1		
70																1		1				1			1		1				1					1		
71	1		1		1		1																						1			1				1		
72												1					1		1								1				1					1		
73																1			1			1							1			1			1			
74	1			1	1	1																					1				1					1		
75									1		1																1				1					1		
76									1		1																1			1					1			
77																1		1				1					1				1					1		
78												1					1	1									1				1					1		
79																	1	1				1						1		1					1			
80		1		1	1		1																				1				1					1		
81								1			1																1				1					1		
82																1		1				1					1			1						1		
[illegible]																																						Deformation lamellae
[illegible]																																						
85	1		1		1	1																					1				1					1		
86																1		1				1					1			1						1		
87	1		1		1		1																					1			1					1		
[illegible]																																						
89									1		1																1			1					1			
90								1			1					1						1					1				1					1		
91								1			1													1			1				1					1		
92									1		1																		1	1					1			
93									1		1																1				1					1		
94								1			1													1			1			1						1		
95											1					1		1					1				1				1				1			Deformation lamellae
96											1					1		1					1				1				1						1	
97								1			1			1														1		1					1			
98								1			1													1			1				1				1			
99											1					1		1									1				1					1		Deformation lamellae
100								1				1																1		1						1		
101												1					1	1									1				1				1			
102								1			1																		1			1				1		
103								1			1																1			1						1		
104											1						1	1									1					1			1			
105											1														1		1				1					1		
TOTAL	18	3	17	6	23	4	10	21	14	1	55	18	0	1	0	22	27	32	14	1		16	3	3	6	2	67	26	12	37	51	16	0	0	25	79	1	

PLUTONIC QUARTZ : 14
DEFORMED PLUTONIC QUARTZ : 9
TOTAL PLUTONIC QUARTZ : 23

TOTAL METAMORPHIC QUARTZ : 55

VOLCANIC QUARTZ : 18
DEFORMED VOLCANIC QUARTZ : 29
TOTAL VOLCANIC QUARTZ : 47

Location Mount Somers - Silica Sand Quarry
Sample# SQ1

Grain	PLUTONIC QUARTZ							METAMORPHIC QUARTZ								VOLCANIC QUARTZ							Fracture patterns Optical/CL features				Grain properties rounding			shape			grain size in microns					Comments
	homogeneous	patchy	Light CL	Moderate CL	Microcracks-Healed	weak undulose	straight extinction	mottled	dark	Moderate CL	strong undulose	weak undulose	poly-crystalline =<3	poly-crystalline>3	total poly-crystalline	homogeneous	zonation	Light CL	Moderate CL	Open Fractures	Quartz embayments	Straight extinction	Sub-parallel fractures	Dark Shear bands	Random oriented fractures	Grain boundaries	angular	subangular-subrounded	rounded	elongate	platy	spherical	<2000	<1000	<500	<250	<125	
2									1		1																1				1					1		
3								1			1																1				1					1		
4																																						Deformation lamellae
5								1			1																1			1					1			
6									1		1																1				1			1				crenulated quartz
7											1						1	1										1			1				1			
8									1		1			1													1				1				1			Polygonized quartz
9									1		1																1				1					1		
10											1					1			1								1			1						1		Deformation lamellae
11									1		1																1				1					1		
12									1		1														1		1				1				1			
13	1			1	1		1																					1			1				1			
14									1		1																	1		1					1			quartz overgrowths
15											1				1													1		1				1				
16								1			1																	1		1					1			
17	1		1		1	1																						1		1					1			
18																1			1			1			1		1				1				1			
19											1		1															1				1				1		
20									1		1																1			1					1			
21											1																1			1					1			
22																																						quartz overgrowths
23											1																	1			1			1				Polygonized quartz
24	1		1		1		1																					1				1		1				
25									1		1																1				1				1			quartz overgrowths
26	1		1		1	1																					1				1				1			
27																1		1		1		1			1				1			1			1			
28									1		1																	1		1						1		
29									1		1																1			1						1		
30											1					1			1								1				1				1			
31											1														1			1				1		1				
32									1		1																1			1				1				
33									1		1																1			1						1		
34									1		1		1														1				1				1			
35									1		1																	1			1					1		
36											1					1			1									1		1				1				Deformation lamellae
37									1		1																1			1					1			
38											1					1			1								1				1					1		Deformation lamellae
39											1					1			1								1			1						1		Deformation lamellae
40	1		1		1		1																				1			1						1		
41								1			1																1			1					1			Deformation lamellae
42												1					1			1								1			1					1		
43									1		1				1												1			1				1				Crenulated quartz
44								1			1																	1		1					1			
45																1			1			1			1		1				1					1		
46								1				1															1				1					1		
47									1		1				1												1			1					1			
48																																						
49		1	1		1	1																					1				1				1			
50									1			1															1				1					1		
51									1		1				1												1				1				1			Polygonized quartz
52								1			1																1				1					1		
53									1		1				1													1			1					1		Polygonized quartz
54								1				1															1			1				1				
55									1		1				1														1			1	1					Recrystalized quartz
56	1		1		1		1																				1				1					1		
57								1				1															1				1					1		
58											1						1		1								1				1					1		Deformation lamellae
59																	1	1				1							1			1				1		
60																1			1			1					1			1					1			
61								1			1																1				1					1		
62											1					1			1										1			1				1		Deformation lamellae
63																																						
64											1					1			1	1																		Deformation lamellae
65																	1	1				1						1				1				1		
66																	1	1				1					1			1					1			
67																	1		1			1					1				1				1			
68									1		1																1			1					1			
69																																						Deformation lamellae
70											1					1			1									1				1			1			
71									1		1																1				1				1			
72									1		1																		1	1						1		
73	1			1	1		1																					1			1					1		
74																	1		1			1						1			1					1		
75									1		1																1				1					1		
76									1		1																1				1				1			
77									1		1																	1				1				1		
78									1		1																1			1					1			
79											1						1		1								1			1				1				Deformation lamellae
80								1			1																		1			1				1		
81									1		1																1			1					1			
82								1			1													1					1			1		1				Deformation lamellae
83								1			1																1			1					1			
84											1						1		1					1			1			1					1			Deformation lamellae
85	1			1	1		1																		1		1				1					1		
86																																						Deformation lamellae
87		1						1											1			1					1			1					1			
88																																						
89	1		1		1		1																					1			1					1		
90									1		1				1														1			1	1					Polyhedral quartz-schist
91																																						
92											1					1			1								1			1						1		Deformation lamellae
93																1			1			1					1			1						1		
94																1			1			1					1				1					1		
95																																						
96											1					1			1									1			1					1		Deformation lamellae
97																																						
98								1			1																		1			1		1				Deformation lamellae
99											1						1	1											1			1				1		
100																1		1				1						1		1				1				
101								1			1																1				1					1		
102								1			1																1			1					1			
103									1		1																1			1						1		
104								1			1																		1			1				1		
105	1		1		1		1																					1				1				1		
TOTAL	17	6	17	5	22	3	8	19	36	1	76	5	2	1	7	17	11	7	21	3	0	13	0	2	6	0	63	29	12	37	46	21	2	14	40	48	0	

PLUTONIC QUARTZ : 11
DEFORMED PLUTONIC QUARTZ : 11
TOTAL PLUTONIC QUARTZ : 22

TOTAL METAMORPHIC QUARTZ : 64

VOLCANIC QUARTZ : 12
DEFORMED VOLCANIC QUARTZ : 17
TOTAL VOLCANIC QUARTZ : 29

Location Mount Somers - Silica Sand Quarry
Sample# SQ2

Grain	PLUTONIC QUARTZ							METAMORPHIC QUARTZ								VOLCANIC QUARTZ							Fracture patterns Optical/CL features				Grain properties rounding			shape			grain size in microns					Comments
	homogeneous	patchy	Light CL	Moderate CL	Microcracks-Healed	weak undulose	straight extinction	mottled	dark	Moderate CL	strong undulose	weak undulose	poly-crystalline = <3	poly-crystalline>3	total poly-crystalline	homogeneous	zonation	Light CL	Moderate CL	Open Fractures	Quartz embayments	Straight extinction	Sub-parallel fractures	Dark Shear bands	Random oriented fractures	Grain boundaries	angular	subangular-subrounded	rounded	elongate	platy	spherical	<2000	<1000	<500	<250	<125	
1									1																			1				1				1		Polygonized quartz
2																																						
3																	1	1				1							1			1				1		Quartz overgrowths
4																																						
5	1			1	1		1																				1				1				1			
6	1		1		1		1																					1		1					1			
7																																						
8																																						
9									1																			1			1					1		
10									1							1				1		1					1			1					1			
11																																						
12								1																					1			1					1	Deformation lamellae
13																											1			1						1		
14																												1			1					1		
15	1		1		1		1																				1			1					1			
16	1		1		1		1																					1			1					1		
17																																						
18														1													1				1				1			Polygonized quartz
19											1						1	1										1				1			1			
20											1					1		1		1					1			1				1			1			
21																																						
22											1														1			1			1				1			Deformation lamellae
23																																						
24	1		1		1	1																			1		1				1					1		
25								1			1				1													1		1					1			
26								1																				1			1					1		
27											1					1			1									1				1			1			
28	1		1		1	1																						1		1						1		
29																1		1				1							1	1						1		
30	1		1		1		1																					1				1			1			
31																1						1							1	1					1			
32	1		1		1	1																			1			1		1					1			
33																																						
34									1							1			1			1					1				1				1			
35	1		1		1		1																				1			1						1		
36																1		1		1		1						1				1					1	
37								1																			1				1				1			
38											1						1	1											1			1					1	Deformation lamellae
39											1					1			1										1			1				1		Deformation lamellae
40	1		1		1		1																		1		1				1				1			
41																																						
42									1		1																1				1					1		
43	1		1		1	1																						1			1				1			
44											1					1		1										1				1				1		Quartz overgrowths
45									1		1																		1			1				1		
46								1			1																	1			1					1		
47																																						
48																																						
49								1																				1		1				1				
50											1						1	1										1			1				1			Deformation lamellae
51											1					1		1									1				1					1		
52	1		1		1	1																						1		1					1			
53								1				1															1				1				1			
54	1		1		1	1																			1			1			1				1			
55											1					1		1										1				1				1		Deformation lamellae
56											1						1		1									1			1						1	
57	1		1		1		1																				1				1				1			
58								1										1				1						1			1				1			
59																	1	1				1					1			1					1			
60											1					1			1								1				1				1			
61	1		1		1		1																					1				1				1		
62	1		1		1		1																				1				1						1	
63									1		1																1				1					1		
64									1		1		1												1	1		1				1			1			
65																																						
66																																						
67								1			1		1																1			1			1			
68									1		1																	1			1					1		
69									1		1																1				1						1	
70									1		1																1				1				1			
71																						1	1	1					1			1			1			
72											1					1			1								1					1				1		
73											1					1			1								1			1						1		Deformation lamellae
74									1		1																	1				1				1		
75									1		1																	1		1						1		
76									1		1																		1			1				1		
77																1			1			1							1			1			1			
78																1		1				1		1				1				1			1			
79									1		1			1															1			1		1				Polyhedral quartz
80									1		1		1														1				1				1			
81								1			1	1	1																1			1			1			
82									1		1																		1	1				1				
83								1			1														1			1		1						1		
84									1		1																1				1					1		
85	1		1		1	1																					1				1					1		
86																																						
87								1			1																1				1						1	
88									1		1																1				1					1		
89									1		1																1					1				1		
90	1			1	1		1																		1		1				1				1			
91											1					1			1									1				1				1		
92																																						
93																																						
94	1			1	1	1																					1				1				1			
95																																						
96								1			1																1				1					1		
97									1		1				1														1	1				1				Polygonized quartz
98								1			1						1		1								1				1					1		
99																																						
100																	1	1		1		1			1			1				1				1		
101	1		1		1	1																					1				1				1			
102											1						1		1								1								1			
103	1		1		1	1																			1		1							1				
104	1		1		1		1										1								1		1				1			1				
105																											1			1						1		Polygonized quartz
TOTAL	38	3	29	12	41	12	13	18	25		66	2	3	2	2	18	12	15	11	4		12	1	2	13	0	44	46	15	25	49	30	0	6	44	46	9	

PLUTONIC QUARTZ : 22
DEFORMED PLUTONIC QUARTZ : 19
TOTAL PLUTONIC QUARTZ : 41

METAMORPHIC QUARTZ : 37

VOLCANIC QUARTZ : 11
DEFORMED QUARTZ : 16
TOTAL VOLCANIC QUARTZ : 27

Location Woolshed Creek - Mount. Somers
Sample# WC1

Quartz types (PLUTONIC QUARTZ / METAMORPHIC QUARTZ / VOLCANIC QUARTZ)

Grain	Plutonic: homogeneous	Plutonic: patchy	Plutonic: Light CL	Plutonic: Moderate CL	Plutonic: Microcracks-Healed	Plutonic: weak undulose	Plutonic: straight extinction	Metamorphic: mottled	Metamorphic: dark	Metamorphic: Moderate CL	Metamorphic: strong undulose	Metamorphic: weak undulose	Metamorphic: poly-crystalline = <3	Metamorphic: poly-crystalline>3	Metamorphic: total poly-crystalline	Volcanic: homogeneous	Volcanic: zonation	Volcanic: Light CL	Volcanic: Moderate CL	Volcanic: Open Fractures	Volcanic: Quartz embayments	Volcanic: Straight extinction
1									1		1			1								
2																1			1			1
3								1		1	1											
4											1					1			1			
5								1			1											
6								1											1		1	1
7												1				1			1			
8											1					1			1			
9									1		1											
10											1					1			1			
11																1			1			1
12								1			1				1							
13											1					1			1			
14										1	1											
15									1							1						1
16																	1	1				1
17											1					1			1			
18									1		1											
19									1		1				1							
20	1		1		1	1																
21									1		1				1							
22												1					1		1			
23																1		1			1	1
24																						
25									1							1						
26									1		1				1							
27											1				1							
28									1						1		1	1				1
29																						
30								1									1		1			1
31	1		1		1		1															
32									1		1				1							
33																1		1				1
34											1					1			1			
35									1		1				1							
36									1		1				1							
37									1		1											
38									1		1											
39									1		1				1							
40																						
41	1		1		1	1																
42																	1	1		1		1
43									1		1				1							
44												1					1	1				
45									1		1											
46									1		1											
47								1			1		1									
48	1		1		1		1															
49								1										1				1
50									1			1										
51								1				1										
52																						
53																	1	1				1
54									1		1		1									
55								1										1				1
56									1			1	1									
57								1											1			1
58																						
59									1							1						1
60												1				1			1			
61	1			1	1		1															
62																1		1				1
63									1							1						1
64								1			1											
65																	1	1				1
66											1					1		1				
67											1					1		1				
68																1			1			1
69																1		1				1
70																	1	1				1
71																1		1				1
72								1			1											
73								1										1				1
74									1		1											
75									1							1						1
76								1			1											1
77									1							1						1
78								1			1											
79											1						1		1			
80									1							1						1
81								1				1				1						
82																						
83								1			1											
84												1					1		1			
85									1							1						1
86									1		1											
87	1			1	1	1																
88											1					1					1	
89									1		1		1									
90									1		1				1							
91									1							1						1
92								1			1											
93																						
94								1			1											
95								1			1											
96																1		1				1
97								1				1										
98																	1	1				1
99								1										1				1
100																1		1				1
101									1							1						1
102																						
103									1							1						1
104	1			1	1		1															
105																1		1				1
TOTAL	14	1	10	5	15	3	4	23	34	2	52	10	4	1	12	34	12	22	17	1	3	36

Fraiture patterns Optical/CL features; Grain properties (rounding / shape / grain size in microns)

Grain	Sub-parallel fractures	Dark Shear bands	Random oriented features	Grain boundaries	angular	subangular-subrounded	rounded	elongate	platy	spherical	<2000	<1000	<500	<250	<125	Comments
1					1			1					1			schistose
2							1			1				1		
3					1				1					1		
4					1			1					1			Deformation lamellae
5					1			1					1			Polyhedral
6					1				1					1		
7					1				1				1			Deformation lamellae
8		1			1				1				1			Deformation lamellae
9					1				1					1		
10					1				1					1		Deformation lamellae
11						1			1					1		
12						1			1					1		Polyhedral
13					1				1					1		Deformation lamellae
14					1				1					1		
15						1		1						1		
16					1			1					1			
17					1				1				1			Deformation lamellae
18						1		1				1				polygonized
19						1				1				1		
20						1		1					1			
21					1			1					1			Polyhedral
22					1				1					1		
23						1				1		1				
24																Deformation lamellae
25						1		1					1			
26					1				1			1				Polyhedral
27					1			1				1				Polyhedral
28							1			1		1				
29																
30						1				1				1		
31					1			1					1			
32							1			1		1				schistose
33			1		1				1				1			
34					1			1					1			Deformation lamellae
35						1			1			1				Polyhedral
36					1			1								Polyhedral
37						1		1					1			
38							1			1				1		
39					1			1				1				Polyhedral
40																
41						1		1				1				
42			1		1				1				1			
43					1			1					1			Polyhedral
44						1		1				1				Deformation lamellae
45						1				1		1				
46						1			1				1			
47					1			1					1			
48							1			1		1				
49						1		1						1		
50						1			1					1		
51						1		1						1		
52																
53					1					1			1			
54						1		1					1			
55						1			1				1			
56					1			1					1			
57					1				1					1		
58																Polygonized
59			1		1				1					1		
60			1			1		1				1				
61					1			1					1			
62					1			1						1		
63					1			1					1			
64					1			1						1		
65					1			1						1		
66						1			1					1		Deformation lamellae
67					1			1					1			Deformation lamellae
68							1			1		1				Deformation lamellae
69						1				1				1		
70					1				1					1		
71						1				1				1		
72		1			1			1					1			
73					1			1					1			
74							1			1			1			Polygonized
75					1				1					1		
76						1		1					1			
77					1			1					1			
78							1		1				1			
79					1			1				1				Deformation lamellae
80						1				1				1		
81					1			1						1		Deformation lamellae
82																
83						1			1					1		
84					1			1				1				Deformational lamellae
85			1		1				1					1		
86						1		1						1		
87						1		1						1		
88					1				1				1			Deformation lamellae
89						1				1				1		
90						1		1				1				Polyhedral quartz
91						1			1					1		
92					1			1						1		
93																
94		1			1			1						1		
95						1		1					1			Deformation lamellae
96						1			1					1		
97					1			1						1		
98						1		1						1		
99					1			1					1			
100					1				1					1		
101					1				1					1		
102																Deformation lamellae
103					1				1					1		
104					1				1					1		
105					1			1				1				
TOTAL		3	5		60	37	8	51	38	16		20	37	47		

PLUTONIC QUARTZ: 7
DEFORMED PLUTONIC QUARTZ: 8
TOTAL PLUTONIC: 15

METAMORPHIC QUARTZ: 38

VOLCANIC QUARTZ: 36
DEFORMED VOLCANIC QUARTZ: 16
TOTAL VOLCANIC QUARTZ: 52

Location Woolshed Creek
Sample# WC3

	PLUTONIC QUARTZ							METAMORPHIC QUARTZ								VOLCANIC QUARTZ							Fracture patterns Optical/CL features				Grain properties rounding			shape			grain size in microns					Comments
Grain	homogeneous	patchy	Light CL	Moderate CL	Microcracks-Healed	weak undulose	straight extinction	mottled	dark	Moderate CL	strong undulose	weak undulose	poly-crystalline = <3	poly-crystalline>3	total poly-crystalline	homogeneous	zonation	Light CL	Moderate CL	Open Fractures	Quartz embayments	Straight extinction	Sub-parallel fractures	Dark Shear bands	Random oriented fractures	Grain boundaries	angular	subangular-subrounded	rounded	elongate	platy	spherical	<2000	<1000	<500	<250	<125	
1											1					1		1										1				1				1		
2																											1			1				1				Deformation lamellae
3								1			1				1												1			1			1					Schistose-crenulated
4																											1				1					1		
5																											1				1					1		
6																											1				1				1			Deformation lamellae
7																			1			1					1				1						1	
8																											1				1				1			Polygonized
9											1					1		1									1			1						1		Deformation lamellae
10	1		1		1	1																					1			1					1			
11									1																			1		1				1				Polyhedral
12									1																		1				1				1			Polyhedral
13	1		1		1		1																				1			1					1			
14																1		1				1					1			1					1			Deformation lamellae
15																						1					1				1					1		
16											1						1	1										1			1					1		
17																													1			1			1			Polyhedral
18															1												1			1				1				Polyhedral
19																1			1			1						1				1			1			Deformation lamellae
20												1					1	1							1		1				1				1			
21									1		1					1											1				1					1		Deformation lamellae
22																											1			1						1		Deformation lamellae
23																		1				1					1			1						1		
24									1			1				1											1			1						1		
25	1		1		1	1																					1				1					1		Deformation lamellae
26	1			1	1		1																					1		1					1			
27	1			1	1	1																					1			1					1			
[illegible]																																						[illegible]
29																													1			1				1		
[illegible]																																						
31																												1		1						1		
32	1		1		1		1																						1			1			1			
33																		1				1							1			1				1		
34	1		1		1	1																						1			1				1			
35	1		1		1		1																						1			1				1		
36																													1			1		1				Schistose-crenulated
37	1		1		1																						1				1					1		
38																1						1			1		1			1					1			
39																													1			1			1			
40	1			1	1	1																							1			1			1			
41																	1	1				1						1			1			1				
[illegible]																																						
43																												1			1					1		Deformation lamellae
44																						1					1			1					1			
45																						1			1		1			1					1			
46												1				1		1									1			1					1			
47	1		1		1		1																				1			1					1			
48	1		1		1		1																				1			1				1				
49											1						1	1						1				1			1				1			
50																	1		1			1							1			1		1				
51																													1			1			1			
52	1		1		1		1																						1		1					1		
53																						1					1			1				1				
54																						1					1				1				1			
55	1		1		1		1																					1			1					1		
56								1			1							1			1							1			1				1			Deformation lamellae
57																											1			1				1				Polyhedral
58																	1					1	1				1				1				1			
59											1					1			1								1				1					1		
60																											1			1					1			
61																												1			1					1		
62																											1				1				1			Polyhedral
63																											1			1				1				Polygonized
[illegible]																																						
65																											1				1				1			Polyhedral
66	1		1		1		1																					1			1					1		
67																													1			1				1		
68																1		1				1	1		1		1			1						1		
69																											1			1				1				
70																												1		1				1				Polygonized
71											1						1		1		1						1			1					1			
[illegible]																																						
73	1		1		1	1																					1			1					1			
74																1						1					1			1					1			
75												1					1	1										1		1				1				Deformationl lamellae
76	1		1		1		1																				1			1					1			
77																											1			1						1		
78																											1				1					1		Polygonized
79	1		1		1	1																			1				1			1				1		
80																1						1			1		1				1					1		
81																			1			1		1			1			1						1		
82	1		1		1		1																				1				1					1		
83											1					1			1										1			1				1		
84								1			1								1		1						1				1					1		
85																													1			1			1			Polygonized
[illegible]																																						
87											1					1		1									1			1					1			
88																													1			1				1		
89	1		1		1		1																						1	1					1			
90	1		1		1		1																				1				1				1			
91	1		1		1		1																				1				1					1		
92																													1	1						1		
93																												1			1				1			Polyhedral
94																													1			1				1		
[illegible]																																						
96	1		1		1		1																		1		1			1					1			
97																											1			1					1			
98																												1			1					1		
99																											1			1					1			
100																	1					1					1			1					1			
101												1				1		1										1			1					1		Deformation lamellae
102																												1			1					1		
103																											1			1						1		
104																						1					1				1					1		
105											1					1		1									1				1					1		
TOTAL	27	3	25	5	30	7	16	32	24	0	56	6	2	1	10	18	10	25	8	0	3	20	2	2	7	0	63	21	21	45	40	20	1	15	44	44	1	

PLUTONIC QUARTZ: 23
DEFORMED PLUTONIC QUARTZ: 7
TOTAL PLUTONIC QUARTZ: 30

METAMORPHIC QUARTZ: 38

DEFORMED VOLCANIC QUARTZ: 17
VOLCANIC QUARTZ: 20
TOTAL VOLCANIC QUARTZ: 37

Location Malvern
Sample# SGM1

	PLUTONIC QUARTZ							METAMORPHIC QUARTZ								VOLCANIC QUARTZ						
Grain	homogeneous	patchy	Light CL	Moderate CL	Microcracks-Healed	weak undulose	straight extinction	mottled	dark	Moderate CL	strong undulose	weak undulose	poly-crystalline = <3	poly-crystalline>3	total poly-crystalline	homogeneous	zonation	Light CL	Moderate CL	Open Fractures	Quartz embayments	Straight extinction
1	1		1		1		1															
2									1		1											
3									1		1											
4									1		1											
5	1		1		1		1															
6	1			1	1	1																
7	1		1		1	1																
8	1			1	1		1															
9	1		1		1		1															
10	1		1		1		1															
11									1		1											
12	1			1	1		1															
13																						
14									1			1										
15	1			1	1		1															
16																						
17	1			1	1	1																
18									1		1											
19																	1	1				1
20								1											1			1
21	1		1		1		1															
22	1			1	1		1															
23								1											1			1
24								1			1											
25	1			1	1		1															
26								1			1											
27																						
28											1						1		1			
29								1			1											
30									1		1					1						1
31								1			1											
32											1					1			1			1
33									1		1											
34									1		1											
35									1		1											
36	1		1		1		1															
37																						
38									1		1											
39									1		1											
40									1		1											
41	1			1	1	1																
42																						
43	1		1		1		1															
44																						
45									1		1											
46	1		1		1		1															
47									1		1											
48	1		1		1		1															
49	1		1		1		1															
50																						
51	1		1		1		1															
52								1			1											
53																						
54									1		1											
55								1			1											
56									1		1											
57	1		1		1		1															
58								1			1											
59																						
60	1			1	1		1															
61	1		1		1		1															
62	1		1		1		1															
63	1		1		1		1															
64									1							1						1
65									1		1											
66	1		1		1		1															
67																						
68	1		1		1		1															
69	1			1	1		1															
70								1			1											
71									1		1											
72	1		1		1		1															
73		1		1	1		1	1														
74									1		1											
75	1			1	1		1															
76									1							1						1
77								1											1			1
78																	1	1				1
79									1		1											
80											1							1	1			
81								1				1										
82																						
83									1		1											
84									1							1						1
85	1		1		1		1															
86		1		1	1		1	1														
87									1		1											
88		1		1	1		1	1														
89																						
90									1		1		1									
91								1			1											
92																	1		1			1
93	1			1	1		1															
94									1		1											
95									1			1										
96								1			1											
97											1					1			1			
98	1		1		1		1															
99									1		1		1									
100	1		1		1	1																
101																1			1			1
102																						
103																1			1			1
104																	1		1			1
105								1				1										
TOTAL	44	5	26	23	49	5	32	20	31		50	4	2			8	6	3	12			14

	Fracture patterns Optical/CL features				Grain properties: rounding			shape			grain size in microns					Comments
Grain	Sub-parallel fractures	Dark Shear bands	Random oriented fractures	Grain boundaries	angular	subangular-subrounded	rounded	elongate	platy	spherical	<2000	<1000	<500	<250	<125	
1						1			1					1		
2						1				1				1		
3					1				1					1		
4						1			1					1		
5					1			1						1		
6					1				1					1		
7					1			1							1	
8						1		1						1		
9					1			1						1		
10					1			1						1		
11						1		1						1		
12						1		1						1		
13																
14			1		1			1						1		
15					1				1					1		
16																Deformation lamellae
17							1			1				1		
18					1			1					1			Polygonized
19					1				1				1			
20						1		1						1		
21					1				1					1		
22					1				1					1		
23					1				1					1		
24					1				1					1		
25					1				1					1		
26							1			1				1		
27																
28					1				1					1		Deformation lamellae
29					1			1					1			
30							1			1				1		
31					1			1						1		
32					1			1						1		
33							1			1				1		
34			1		1			1						1		
35					1				1					1		
36					1				1					1		
37																
38							1			1				1		
39					1			1						1		
40							1			1					1	
41						1			1				1			
42																
43					1				1					1		
44																
45					1			1					1			
46							1			1					1	
47						1		1					1			
48					1				1					1		
49					1				1				1			
50																
51					1			1						1		
52						1		1					1			
53																Deformation lamellae
54					1			1						1		
55					1				1				1			
56					1					1				1		
57					1					1					1	
58					1			1						1		
59																
60					1				1					1		
61					1				1					1		
62					1			1						1		
63						1			1					1		
64					1				1					1		
65						1			1					1		
66						1		1						1		
67																
68					1			1						1		
69						1				1				1		
70						1		1					1			
71							1			1				1		
72					1			1						1		
73						1			1					1		
74					1				1					1		
75					1			1							1	
76					1				1					1		
77						1				1				1		
78						1			1					1		
79			1			1		1					1			
80						1			1					1		
81			1			1		1						1		
82																
83					1			1							1	
84					1			1						1		
85					1				1					1		
86							1			1				1		
87					1			1						1		
88					1				1					1		
89																Deformation lamellae
90							1			1				1		
91							1	1						1		
92					1			1						1		
93					1				1					1		
94						1		1						1		
95					1				1					1		
96					1				1					1		
97							1	1					1			Deformation lamellae
98						1			1					1		
99						1		1						1		Polyhedral
100					1			1						1		
101					1				1					1		
102																
103					1				1					1		
104							1			1				1		
105					1				1					1		
TOTAL			5		64	26	15	44	43	18	0	0	13	86	6	

PLUTONIC QUARTZ: 37
DEFORMED PLUTONIC QUARTZ: [illegible]
TOTAL PLUTONIC QUARTZ: 49

METAMORPHIC QUARTZ: 38

VOLCANIC QUARTZ: 14
DEFORMED VOLCANIC QUARTZ : 4
TOTAL VOLCANIC QUARTZ: 18